ABSTRACT

KARAHAN TOPRAKCI, HATICE AYLIN. Piezoresistive Properties of Polyvinyl Chloride Composites. (Under the direction of Dr. Tushar K. Ghosh and Dr. Richard J. Spontak.)

Textile based sensors provide an interface between the user and the electronic system by converting any type of physiological or environmental signal into electrical signals. Common applications include health monitoring, rehabilitation, multimedia, and surveillance.

In this research we demonstrate fabrication of piezoresistive sensors on textile fabrics through application of a screen-printed conductive nanocomposite layer of plasticized poly(vinyl chloride) (PVC), and carbon nanofiber (CNF). In order to understand the behavior of conductive plastisol, morphological, mechanical and electrical properties of composite films were investigated for different molecular weights of PVC. Homogeneous filler dispersion and good filler/polymer interphase were observed without any dominant filler orientation. Mechanical and electrical properties were found to be affected by CNF, plasticizer content and matrix molecular weight. CNFs were found to provide substantial bridging in the matrix and enhance strength. These nanostructured composite sensors were found to be sensitive under different levels of strain which can be monitored by change in electrical resistance.

Finally, we demonstrate the fabrication of piezoresistive sensors on textile fabrics through application of a screen-printed conductive nanocomposite layer of conductive plastisol. Conductive plastisol was found to show good adhesion to fabric with homogeneous CNF distribution. As in composite films, samples were found to show negative piezoresistance at different levels of strain. Strain level and filler concentration were found to affect the piezoresistive behavior and sensitivity of the printed sensors.

Pizoresistive Properties of Polyvinyl Chloride Composites

by
Hatice Aylin Karahan Toprakci

A dissertation submitted to the Graduate Faculty of
North Carolina State University
in partial fulfillment of the
requirements for the degree of
Doctor of Philosophy

Fiber & Polymer Science

Raleigh, North Carolina

2012

APPROVED BY:

_____	_____
Dr. Tushar K. Ghosh Chair of Advisory Committee	Dr. Richard J. Spontak
_____	_____
Dr. Hoon Joo Lee	Dr. Paul Franzon

DEDICATION

I dedicate this dissertation;

To my wonderful family, this accomplishment was impossible without their endless support, prayers and inspiration.

To the memory of my grandmother, Ayse Demirel, who emphasized the importance of education and helped me throughout her life and taught me whatever she knew without any expectation. She is the meaning of patience in my life.

To my parents, Hicran and Erdogan Karahan, who have been my role-model for hard work, tolerance, personal sacrifices, and have always encouraged me to think in a different and constructive way to follow my dreams.

To my sister, Aysen Karahan, who has been my endless support from the day I learnt to stand on my feet and has been my role-model for rationale thinking and imagination. She is the meaning of trust in my life.

To my husband, Ozan Toprakci, whom I grew-up with and has always been there to lighten the pressure on me by his amazing music and sense of humor. He is the meaning of love, fun and enjoyment in my life.

BIOGRAPHY

Hatice Aylin Karahan Toprakci was born in Izmir, Turkiye, as a second daughter of Hicran and Erdogan Karahan. She graduated from Afyon Science High School in 1999. She completed her Bachelor of Textile Engineering degree in 2004 at Ege Univeristy. After that she started to work as a research assistant for her Master of Science (M.S.) degree in the same university and graduated in 2007. Following her M.S. in 2007, she worked as a laboratory manager assistant in Gamateks, Turkey. In 2008 she joined North Carolina State University to pursue her Ph.D. in 'Fiber & Polymer Science' with a minor in 'Materials Science & Engineering'.

ACKNOWLEDGMENTS

I express my gratitude to my advisor, Dr. Tushar K. Ghosh for letting me work with him on this amazing project. Under his tutelage, I took a leap forward in the world of science. From him, I learnt the art of conducting scientific investigation. He has been the cardinal support system for me in terms of knowledge and patience throughout my project. I thank him from the bottom of my heart for his motivation and encouragement.

I extend my gratitude to Dr Richard J. Spontak. Under his mentorship, I have learnt to view things in a scientific light. His methodical guidance has always been and will always remain a source of inspiration for me. His novel ideas and his all-out encouragement played an overwhelming role in shaping my scientific outlook for the rest of my life.

I am grateful to Dr. Hoon Joo Lee, Dr. Paul D. Franzon, and Dr. Alexander Deiters for their willingness to be on my committee.

I am grateful to Dr. Russell E. Gorga and Dr. Wendy Krause for letting me use their DMA and rheometer facility. I would also like to thank Nags for helping me out with the DMA and rheology measurements. In addition, I thank Mr. Chuck Mooney and Ms. Birgit Anderson for their assistance with SEM and FTIR analysis respectively. Furthermore, I thank Mr. Hai Bui and Mr. Dzung Nguyen (Win) for their prompt assistance whenever required. Moreover, I am thankful to Ms. Angie Brantley, Ms. Traci Figura and Ms. Vicky Stockdale for making my stay here smooth and hurdle free through their help and cooperation by ensuring that I don’t miss any deadlines.

I would like to thank National Science Foundation for financial support of the project and National Education Ministry of Turkish Republic for partial funding for my study.

I would like to thank Showa Denko Corporation for vapor grown carbon nanofibers and Solvay Company for polyvinyl chloride resins.

I would also like to thank my lab mates Saral and Krishna in Dr. Ghosh's research group for their friendship, motivation and words of encouragement. Special note of thanks to Polymer Morphology Group for their constant support.

I would like to thank my friends Elif and Derya and other friends and teachers in Turkey for their endless support and making my stay here at Raleigh so lovely and memorable.

I would also like to thank Partha for his friendship, support, positive energy, respect and prayers.

I also would like to thank Marie Skłodowska Curie whose life helped me to understand the meaning of dedication to science.

I would like to thank to Fikret Kizilok, who has been always with me with his amazing music.

Finally, I would like to thank my family, Hicran, Erdogan, Aysen Karahan and Ozan Toprakci. This accomplishment would not have been possible without their unconditional love, support and prayers.

TABLE OF CONTENTS

LIST OF TABLES

LIST OF FIGURES

CHAPTER 1. INTRODUCTION

Recently, increasing demand of mobile devices opened a new era for wearable electronics. Textiles constitute an ideal choice as platforms for wearable devices, since they are flexible, lightweight, and can be worn everywhere in many forms. This class of textiles with electronic capabilities has been referred to as electronic textiles (e-textiles). Depending on the type and application, e-textiles may be capable of sensing, data processing, actuation, and energy storage or generation. Among all these, textile-based sensing has become an active area of research in the emerging field of e-textiles. Textile based sensors provide an interface between the user and an electronic system by converting physiological or environmental signals into electrical signals. Truly, wearable garments may be capable of monitoring variables such as strain, pressure, temperature, displacement, humidity, *etc.*, and can be used in many applications including medical rehabilitation, health monitoring, communication, entertainment, sports, space, firefighting, security, and surveillance.

Textile based strain sensors can be fabricated by using different materials, among which conductive polymer composites seem to have great potential. Poly(vinyl chloride) (PVC) is a promising material for forming textile-compatible conducting polymer composites for many of these applications. PVC is a product of polymerization of vinyl chloride [CH_2=CHCl]. It is one of the most consumed thermoplastics, with a wide range of applications ranging from construction supplies to textiles because of its unique properties such as strength, lightweight, ease of processing-blending, low flammability, chemical stability, and low cost. PVC based products can either be made from pure PVC or with various additives, such as plasticizers,

colorants, modifiers, fillers [1-3]. Depending on the composition and mechanical properties, PVCs can be classified into two main categories as rigid and plasticized PVCs. While, unplasticized PVCs are known as rigid PVCs; plasticized ones are referred as flexible PVCs [1,2]. Plastisol is a multiphase, paste-like composition obtained by the suspension of PVC resin in a suitable plasticizer with other additives such as thermal stabilizers and fillers [4-6]. Plasticizer is the key component of the plastisol and it determines both processing (viscosity, glass transition temperature, *etc.*) and end-use properties (*i.e.*, flexibility) of the composition. Plasticizer characteristics, such as, polarity, molecular weight, chain length and linearity, viscosity, weight fraction, *etc.* can be used to tune these properties [7]. An effective plasticization is achieved when a homogeneous distribution of the plasticizer within the resin occurs thereby reducing the interaction between the polymer chains so that they can move easily. Phthalates, sebacates, phosphates and epoxies, are the common plasticizers for PVC [1,5,7-9].

Polymer nanocomposites (PNCs) are relatively new and promising class of materials with at least one nanoscale component. Nanofillers with relatively high surface area and aspect ratio can have profound effects on the mechanical, electrical and thermal properties of the composites even at very low concentrations. The PNCs can be formed using nanoparticles in the form of fibers, tubes, spheres, or platelets in order to obtain desired properties with any of thermoplastic, thermosetting, or elastomer resins as the matrix material [10,11]. Carbon nanofiber (CNF) is one of the common nanofillers used for nanocomposites, because of its high surface area, superior electrical [12], thermal [13], mechanical [14] properties and relatively lower cost (compared with carbon nanotubes).

The research presented here, is aimed at development of textile based piezoresistive sensors with tunable electrical and mechanical properties. This innovative approach includes use of conductive plastisol composite whose properties can be controlled by tailoring the system components and other parameters.

The dissertation is organized in different chapters each of which represents an article. All chapters, with the exception of 1 and 7, is written in the form of review or research articles. A short description of each is provided below.

Chapter 1. Introduction to conductive and piezoresistive composites and outline of the thesis

Chapter 2. Includes review of the recent literature on conductive polymer composites with particular focus on piezoresistive polymer composites.

Chapter 3. Includes a detailed review of textile based sensors (TBS). Various TBSs are classified based on their working principles, advantage, and limitations.

Chapter 4. Describes the fabrication and mechanical characterization of carbon nanofiber-filled polyvinyl chloride (PVC) composites.

Chapter 5. Detailed account of fabrication and electrical properties of carbon nanofiber-filled polyvinyl chloride (PVC) composites are explored here.

Chapter 6. Describes piezorestive sensing characteristics of printed textile fabrics.

Chapter 7. Includes summary of the present study and recommendations for future work.

References

[1] Titow WV. PVC technology. London ; New York: Elsevier Applied Science, 1984.

[2] Wilkes CE. PVC handbook. Munich ; Cincinnati, Ohio: Hanser, 2005.

[3] Nass LI. Encyclopedia of PVC. New York: Marcel Dekker, 1998.

[4] Nakajima N, Harrell ER. Rheology of PVC plastisol: Particle size distribution and viscoelastic properties. J Colloid Interface Sci 2001;238:105-15.

[5] Grossman RF. Handbook of vinyl formulating. Hoboken, N.J.: Wiley-Interscience, 2008.

[6] Cadogan DF, Howick CJ. Plasticizers. John Wiley & Sons Inc., 2000.

[7] Wypych G. Handbook of plasticizers. Toronto; New York: ChemTec Pub.; William Andrew Pub, 2004.

[8] Ritchie PD. Plasticisers, stabilisers and fillers. London, Iliffe Books for the Plastics Institute, 1972.

[9] Edenbaum J. Plastics additives and modifiers handbook. New York: Van Nostrand Reinhold, 1992.

[10] Koo JH. Polymer nanocomposites : processing, characterization, and applications. New York: McGraw-Hill, 2006.

[11] Advani SG. Processing and properties of nanocomposites. Singapore: World Scientific Publishing, 2007.

[12] Lozano K, Bonilla-Rios J, Barrera EV. A study on nanofiber-reinforced thermoplastic composites (II): Investigation of the mixing rheology and conduction properties. J Appl Polym Sci 2001;80:1162-72.

[13] Lozano K, Barrera EV. Nanofiber-reinforced thermoplastic composites. I. Thermoanalytical and mechanical analyses. J Appl Polym Sci 2001;79:125-33.

[14] Kuriger RJ, Alam MK, Anderson DP, Jacobsen RL. Processing and characterization of aligned vapor grown carbon fiber reinforced polypropylene. Composites Part A 2002;33:53-62.

CHAPTER 2. PIEZORESISTIVE BEHAVIOR OF POLYMER COMPOSITES

Abstract

Polymers are preferred in many applications because of their desirable properties, such as strength, toughness, lightweight and facile process ability. However the vast majority of the polymers are electrically insulating and used extensively as electrical insulators. In order to expand their applications, electrical conductivity is engendered by incorporating various conductive fillers including nanoparticles into their structure. Polymeric nanocomposites that are filled with conducting nanoparticles have received great attention with regard to their functional structures. Lower percolation threshold and improved mechanical properties are the most important contributions of nanofillers which are stemmed from their high aspect ratio and high surface area. They have wide range of applications including static electricity discharging, electromagnetic interference shielding, conducting adhesives, self-regulating heaters and piezoresistive sensors.

Piezoresistance is referred to a change in resistance due to applied strain or temperature. In general, the behavior is attributed to change in dimensions and/or material properties. Since most of the polymeric composites are not very rigid structures, any external factor can lead to change in dimensions, filler-filler relative distances and resistance of the composite. By monitoring the change in resistance, magnitude of the external factor can be determined which is basically mechanism of the piezoresistive sensing.

2.1 Polymer Based Electronics (Organic Electronics)

Polymer based electronics, also known as organic electronics, are fabricated from polymeric materials including conductive polymers and plastics with molecular level functionality, satisfied physical, chemical, mechanical and electrical characteristics. Since organic structures present weak intermolecular interaction, they show high flexibility in the solid state in addition to toughness, low temperature processing, and especially low cost. The main difficulties of organic electronics, however, are their low carrier mobility that prevents their use under high-frequency and their unstable structure, which may lead to rapid degradation of electronic properties under environmental exposure [1-3]. But these disadvantages can be overcome through the help of organic chemistry which enables the formation of organic molecules with desired properties or by addition of organic/inorganic materials. Polymers can be used to fabricate a wide variety of electronic components such as conductors, resistors, semiconductors, insulators mainly based on their varying electrical conductivity [3,4]. Electrical as well as other characteristics of polymers can be modified by the addition of any filler, additive or reactants. [3-5]. Polymers can be found in different forms and structures like pure materials (homopolymers), blends of different polymers, short-chain oligomers, longer-chain polymers, precursors to polymers, inorganic polymers, conjugated organic molecules, or conductive filler containing (organic–inorganic) composites [5,6]. Depending on the dominant properties of the organic polymer, main applications include switching devices [7], low-end smart cards, and radio-frequency identification tags (RFIDs) [3,4,8], organic light emitting diodes (OLEDs), LCDs, thin film transistors, organic field-

effect transistors (OFETs), solar cells and sensors [1,3,4,9,10]. Especially sensor applications are of increasing importance because of their wide range of usage for many areas.

2.2 Electrically Conducting Polymers

Most polymers are insulating and are used extensively as electrical insulators. However, there are two major classes of conducting polymers that have been developed over the last fifty years and are currently used in many applications. They include intrinsically conducting polymers and conducting polymer composites. A major breakthrough in the area of conductive polymers,the discovery that polyacetylene could be easily oxidized (by electron acceptors) or reduced (by donors) in 1971 [11], lead to an entirely new field of intrinsically conductive polymers. In conducting polymer composites, an electrically conducting phase is dispersed in sufficient quantity in a polymeric matrix to form a conductive composite.

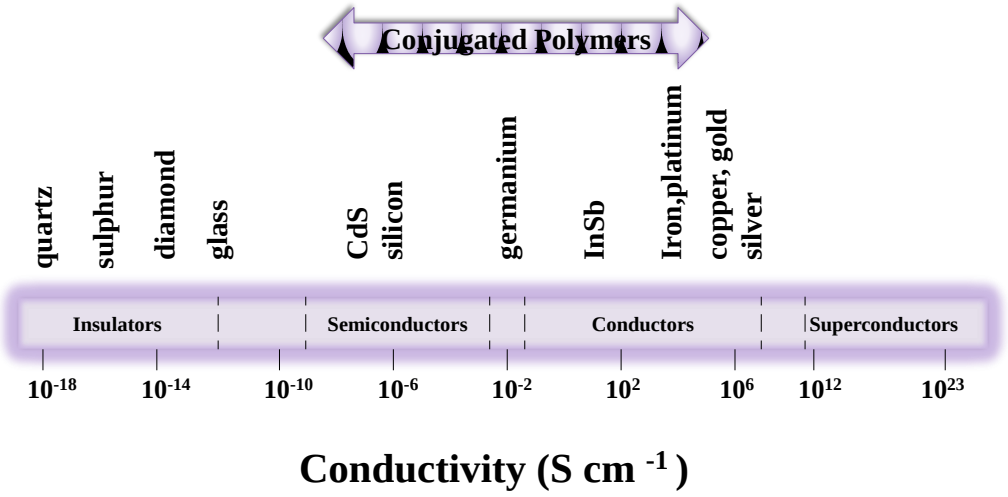

Figure 2.1 Classification of materials based on their conductivity [12]

Conductive polymers which show electrical conductivity in the range of semiconductors and conductors (Fig. 2.1 and Fig. 2.2) are emerging as the basis of a number of new technologies, including static electricity discharging, electromagnetic interference shielding, conducting adhesives, self-regulating heaters and piezoresistive sensors.

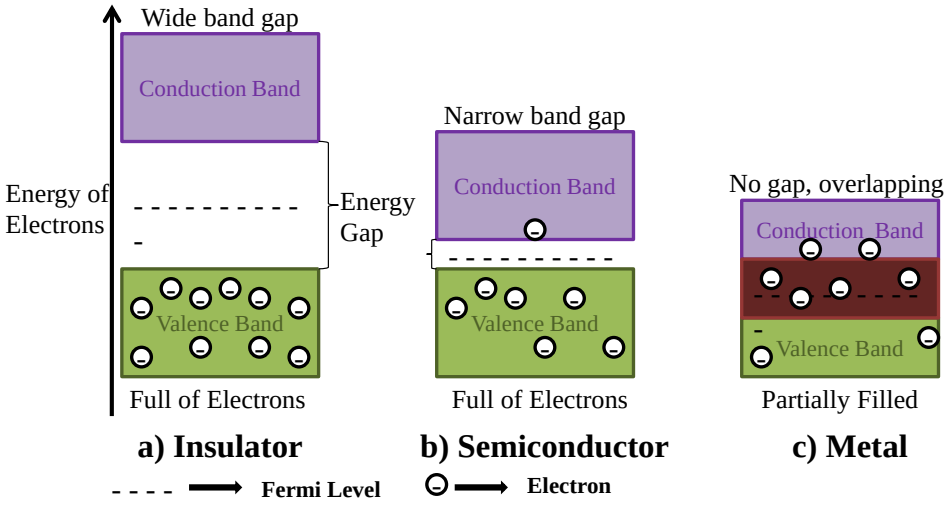

Figure 2.2 Band theory model for (a) insulators (b) semiconductors and (c) metals [12]

The constant of proportionality is the electrical resistance (R) for the material;

$$V = IR \qquad \text{Equation (2.1)}$$

In SI units, voltage is expressed in volts (V), resistance in Ohms (Ω) and current in amperes (A). Another formulation of Ohm's law is expressed as:

$$J = \sigma E \qquad \text{Equation (2.2)}$$

where, J is the current density in unit area (A m^{-2}), σ is the conductivity E is the electric field or electrical potential gradient and is used to express the voltage drop (V) through the length (L) of the material.

$E = V/L$ Equation (2.3)

Conductivity (σ) can also be formulated as a function of conductance (G, Ω^{-1}), in general,

$G = I/V$ Equation (2.4)

$G = \sigma EA/V$ Equation (2.5)

$\sigma = GL/A$ Equation (2.6)

Since conductance (G) is the reciprocal of resistance (R) it can be written as a function of resistivity:

$\rho = RA/L$ Equation (2.7)

Polymers are different from metals in theory in terms of their electrical behavior. Unlike metals, most polymeric materials are insulating. Since electrons are located in covalent bonds in polymers, they cannot move as in metals. In polymers electrical conductivity can be attained through the addition of organic or inorganic conductive fillers or by producing a polymer with special structure which are called intrinsically conducting polymers (ICP), consisting of conjugated bonds [12,13].

2.2.1 Intrinsically Conducting Polymers (ICPs)

Intrinsically conducting (IC) polymers are materials which possess both polymer and metal properties. They behave like a polymer in terms of their basic chemical, physical and mechanical characteristics (flexibility, elasticity, toughness, malleability) and like a metal in

terms of their electrical properties [14]. Most polymers are "saturated" and act as electrical insulators because all available electrons in their structure, which can carry electrical current, are located in the σ-bonds. On the other hand conjugated structure of IC polymers give rise to electrons that are able to move more easily along the polymer backbone, because π-electrons are less strongly bound than the σ-electrons [15,16]. Other effects of π-electrons (conjugated structure) can be observed on some electronic properties such as low energy optical transitions, low ionization potentials, and high electron affinities which are mainly caused by the less chemically stable structure of the polymers. In other words, these polymers can be oxidized or reduced more easily and more reversibly than conventional polymers [14-16]. Excitation of a polymer (addition or removal of electrons) which leads it to behave like a metal can be obtained by visible photons, electron donating or accepting chemicals and so on [15,16]. Discovery of this effect in doped polyacetylene was first reported in 1977 by Chiang *et al.* [17]. Dopant is an element which is added to ICPs in low concentrations in order to enhance their optical/electrical properties. Doping is a process for increasing the carrier concentration and mobility in which conjugated polymer is exposed to a doping agent in the gas or solution phase, or by electrochemical oxidation or reduction. Electrical properties of these ICPs can be changed from an insulator to conductor by controlling the doping level [14,15]. The key properties of a conjugated polymer in relation to its potential as a precursor to a conducting composition are ionization potential, electron affinity, band gap, and band width [15,16]. ICPs can be in polyaromatic and linear forms. Polyaniline, polypyrole, polythiophene are polyaromatic; polyacetylene, polythiazyl are linear ICPs.

ICPs are potential materials for all types of applications which require conductivity, because they are flexible, relatively lightweight compared to standard metals, do not corrode and they can be easily controlled during chemical processing. They can be used in different forms from films to coatings, and as nanofibers. While in some applications such as electromagnetic radiation shielding, batteries, conductive adhesives-printing, antistatic clothing, active electronics they are preferred for their conductivity; for some applications such as electrical displays, chemical, biochemical and thermal sensors the main reason is their electroactivity [14].

2.2.2 Conducting Polymer Composites (CPCs)

Polymer composites represent a convenient route to multi-functional materials. Conducting polymer composites (CPCs) are systems consisting of at least one polymeric matrix with at least one type of conducting phase (organic/inorganic fillers). In general, composites often offer significant alternatives to single-phase materials not only for their easy processing, lower cost, light weight structure but also for superior physical and chemical properties such as high strength, chemical resistance. Electrically conducting polymer composites are ideal for many applications including static electricity discharging, electromagnetic interference shielding, conducting adhesives, self-regulating heaters and piezoresistive sensors. For obvious reasons, there has been a rapid increase in the number of publications in this area in recent years and a number of good reviews of literature have been published. The focus of this comprehensive review is polymer composites as it relates to textile sensors. The review is done in two parts. In the first part, basic terms and definitions, mechanisms and parameters

are explained; the second part of the study is dedicated to piezoresistive behavior of CPCs under different external conditions.

2.2.2.1 Mechanism of electrical conduction and percolation behavior in conducting polymer composites

Mechanism of electrical conduction in conductive polymer composite has been studied extensively. Based on the composition of the composite different mechanisms of conduction such as electron tunneling, electron hopping, ionic transport, field emission, band type conduction and simple inter-aggregate conduction by contact have been suggested. While conduction by contact is ohmic, electron tunneling shows non-ohmic behavior [13,18,19].

As the fraction of conducting phase of the composite increases, the composite generally undergoes from insulator to conductor transition. This transition has been generally analyzed within the framework of effective media and percolation theories. The clearly delineated transition from insulating to conducting behavior is referred to as the percolation threshold. The fundamental reason for this transition is the existence of aggregates (or islands) of conducting particles in the heterogeneous mixture of materials. Below the critical content of conducting particles, conduction throughout the material cannot take place. Above this threshold, sufficient conducting pathways throughout the composite are set up such that the bulk conductivity increases dramatically.

Conductivity of the composite is directly related with the conduction mechanism of the fillers and “interparticle charge transfer” that mainly depends on the number of contact points in the composite and is affected by many factors, such as filler, matrix, and component properties,

processing conditions (fiber-matrix interface, alignment of filler, anisotropy, applied pressure, shear, and fiber breakage) [13].

Percolation is a standard model to describe the spatial distribution of species within disordered systems [20,21]. It was firstly developed by Flory (1941) and Stockmayer (1943) to describe the formation of large molecules from small branching molecules. In the mathematics, percolation was introduced by Broadbent and Hammersley (1957). Their approach was mainly based on the spread of hypothetical fluid particles through a random medium. It can be used to explain different physical phenomena in diverse research topics including, electrical conductivity, magnetism, electrochemistry, and molecular transport [20,21].

Percolation can be described in terms of either the structural or the dynamic properties of a system. From the structural perspective, it occurs when geometric features composed of large clusters (of size p) approach p_c, the critical cluster size. At small values of cluster size, flocs or individually separated particles exist. However, as p is increased, the physical cluster size increases and at p_c sufficiently large flocs starts to form a continuous network and connect opposite edges of the specimen [20-22]. From the dynamical aspect, any deterministic parameter (*i.e.*, a site or bond) is designated as a physical property such as conductivity or elasticity [22]. In that sense, percolation depends on the bond structure and bond density in the network. Two sites are called connected if there is at least one path between them. As seen in Fig. 2.3d a set of connected sites bounded by vacant bonds forms a cluster. This transition point in the network structure from a disconnected structure to a connected one; is called the percolation concentration [20,21].

According to percolation theory, the bulk conductivity (σ) of a percolating composite with volume concentration, Φ, of the conducting phase behaves as a power law of the form [19,20] where σ_o is a constant of proportionality, and Φ_c is the critical volume fraction of the filler at the percolation threshold.

$$\sigma = \sigma_0(\Phi - \Phi_c)^t \qquad \text{Equation (2.8)}$$

The exponent t is characteristic of the transition from dispersed filler particles to networked particles, and is assumed to be universal, *i.e.*, material independent. In three-dimensional systems, t is around 2 when describing electrical conductivity [13,23].

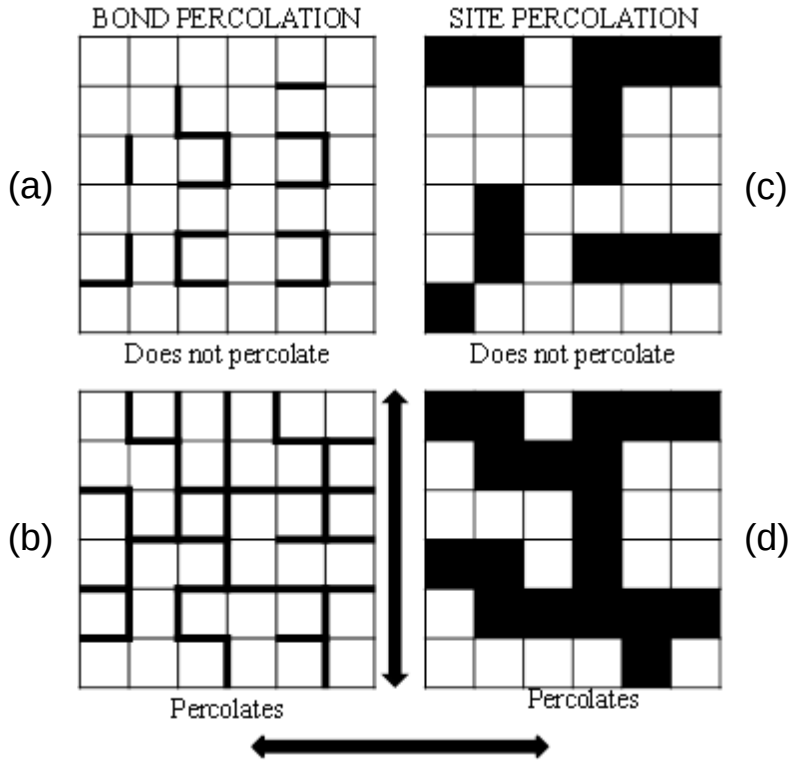

Figure 2.3 Bond (a, b) and site (c, d) percolation

Although, percolation theory is the basic phenomena accepted for the conductivity in composites, there are other conditions before and after percolation threshold which required to be explained simply.

Depending on the filler or matrix properties and filler concentration, fillers have mainly two positions in the matrix:

- Separated by a distance (highly separated (x_a), closely separated (x_b))
- Direct contact (direct contact one continuous network (x_c), direct contact many networks (x_d)).

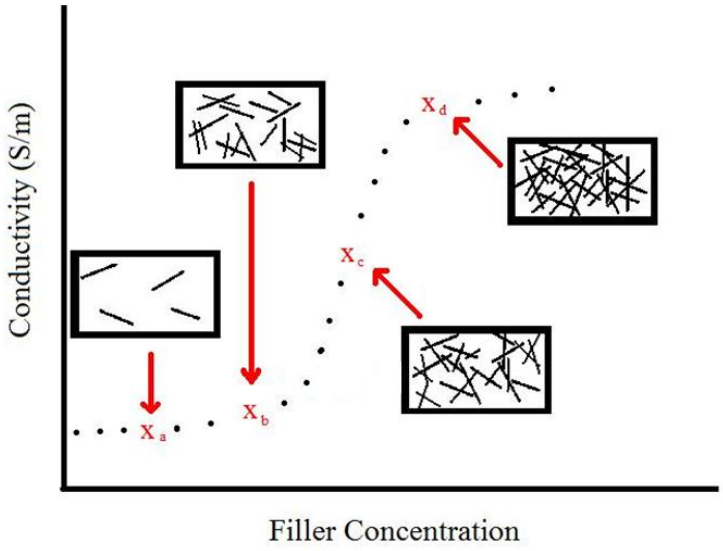

Figure 2.4 General behavior of a composite material conductivity *vs.* filler concentration

As shown in Fig. 2.4, at low filler concentrations x_a, conductivity is governed by the insulating polymeric matrix because of inadequate amount of filler. At this level, fillers are highly separated and can be found individually dispersed or in the form of flocks. Since the

distance between the fillers is not enough to transfer charges, they can only inject some carriers into the polymeric matrix and do not change the conductivity of the system significantly [19,24].

For the filler concentration designated as x_b in the Fig. 2.4, although fillers/flocks are theoretically separated from each other and filler concentration is less than the concentration required to establish conducting networks, the composite may show some level of conductivity that can be explained by quantum mechanical model [24-27]. When the movement of an electron is evaluated according to the classical physics, we will face with two cases. Basically, if it has enough kinetic energy, it can pass a barrier, or if the energy is not enough to overcome the barrier, it won't pass. On the other hand, from the quantum mechanics perspective; electrons can be expressed as waves under specific circumstances. A wave can cross (or tunnel) a potential energy barrier even if it does not have enough energy, because when a wave come across a potential barrier, it does not immediately lose all its energy but starts to diminish exponentially and small fraction of electrons can penetrate (tunnel) to the conduction band of the neighboring conductive filler and creates current flow. This phenomenon is called electron tunneling and it presents the ability of a particle to cross a potential energy barrier and forming a tunneling-percolation system with the help of other conducting fillers in the vicinity. The rate of the tunneling in a composite is directly affected by the energy of the electrons, thickness, electrical characteristics of the barrier and applied voltage. The ability of an electron to tunnel a gap, under a given electric field, increases exponentially with a decrease in the gap size. The gap size between fillers/flocks has to be sufficiently close for interacting with each other's with a threshold particle-particle distance

of ~10 nm or less (in the range of Å). Another important factor is the applied voltage. Voltage dependence of the current intensity is given as,

$$J = AV^n \exp\left(\frac{B}{U}\right) \qquad \text{Equation (2.9)}$$

where $A, n, \frac{B}{U}$ are the constants. Eq. (2.9) shows that under higher voltage, current density increases and more electrons can tunnel through the insulating gap [13]. Since, the mechanism of conductivity based on electron tunneling is not same as the one observed in metals, it is expected to show different I-V behavior. While linear I-V relationship is obtained for the composites with continuously contacting fillers; nonlinear I-V curve is obtained for the composites with closely separated fillers/flocks [19,24,28-30]. Besides non-ohmic I-V character, temperature and pressure dependency of the composite resistance can be some of the other hints which indicate electron tunneling as a dominant mechanism in the system. Especially, thermal fluctuations are important factors for lowering the potential barrier [13,24].

The mechanism of conduction changes from electron tunneling to direct inter-particle/aggregate conduction in the case of increase in the concentration designated as x_c in Fig 2.4, known as percolation threshold as mentioned previously [13,19].

The conductivity of the composite at concentrations above percolation threshold (x_c) as designated x_d in Fig. 2.4, is determined by the filler properties and theoretically it approaches the conductivity of the filler particle since the connected filler pathways span the composite. Fig. 2.4 also shows that conductivity does not change a lot in this region as in percolation region, and becomes almost flat. The conduction mechanism is affected by: e the charge, n

the carrier concentration and μ the mobility of the carriers ($\sigma = en\mu$). Although carrier concentration increases, mobility of the carriers show slow decrease because of increasing interface/surface area between matrix and fillers [19,24,31].

2.2.2.2 Factors affecting the conductivity in conducting polymer composites

Although conductivity phenomenon occurs to some extent in almost every composite containing conducting particle, every composite shows different electrical behavior mainly because of its components. Filler and matrix polymer properties, processing conditions are factors that have direct effect on the dominant mechanism of conductivity.

A) Filler properties

Composites are complex systems with at least two different components. Since fillers are the charge carriers in the system, their properties directly affect the electrical properties of the system. Filler type [32,33], dimension (diameter, length, *etc.*), shape (tube, cylinder, *etc.*), geometry [34], surface properties, compatibility with matrix [35,36], purity [37], concentration [38,39], production process (*i.e.*, vapor grown CNF shows better conduction), tendency to disperse or aggregate, and their orientation [40,41] are important factors that have strong influence on electrical properties of the composites.

Different types of metallic, organic and inorganic fillers have been reported in the literature. These include silver [42], nickel [43], copper [44], ICPs [45], carbon fibers (CF) [32,46,47], carbon black (CB) [33,46], graphite [32,48], graphite nanosheets (GN) [48], carbon nanofibers, (CNF) [33,49], carbon nanotubes (CNTs) [33], and mixture of some of these materials [32,45,50]. In addition to these particles, continuous fibers have also been used in

different forms such as laminates or woven fabrics [51,52]. Metallic fillers are one of the oldest materials used in CPCs because of their excellent electrical and thermal conductivity. However, for CPCs, generally carbonaceous fillers are preferred because of their relatively low cost and ease of processing as well as light weight and chemical and corrosion resistance [51]. The main difference in the electrical behavior of a CPC is caused from the inherent conductivity of the filler particles. Typically, CPCs have conductivity between polymer and filler. Even if two fillers belong to the same group, they can show different electrical properties. Since carbonaceous fillers are generally produced from artificial materials, their properties including fine structure, filler length, diameter, wall thickness, structural defect ratio are directly related with raw material and processing conditions such as pressure, temperature and time. All these variables have effects on the growth mechanism of carbon layers [53,54].

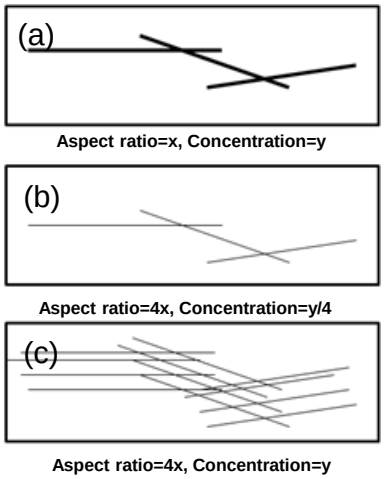

Figure 2.5 Fillers with different aspect ratios (a and b, c), fillers with different aspect ratio and same concentration (a and c)

In all fillers mentioned above; if we assume fillers made from the same material, continuous fillers are expected to show the higher conductivity than the chopped ones. As known for the conductivity in a system consisting chopped/loose fillers, can be obtained by contacts between fillers. On the other hand for the continuous fillers, even single filament might be enough to transfer charge from one end to another because of being a network itself.

Filler geometry (dimension, shape, *etc.*) is another important factor that determines charge transport throughout the CPCs. The aspect ratio or the ratio of the length to the diameter for fibers or ratio of diameter to thickness for platelets and flakes is considered a key dimensional characteristic of particles. Aspect ratios of the fillers can change from 1 (spheres) to 100s; while low aspect ratio indicates short, thick fillers; high aspect ratio indicates long, thin/narrow fillers. In general, the percolation threshold is lower for high aspect ratio particles [55-57]. Particles with a higher aspect ratio present higher probability to span the composite boundary at a lower concentration (see Fig 2.5 and 2.6).

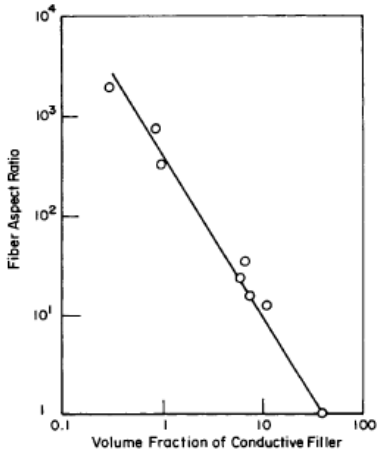

Figure 2.6 Effect of filler aspect ratio on the critical filler concentration [58]

In addition to aspect ratio, shape of the filler also affects the percolation behavior of the composite. While spheres/particles have to be packed closely and form continuous conductive chains of a network [59]; higher aspect ratio particles such as fibers, wires, tubes, sheets just need to come to close proximity to each other along their length in order to set up a conducting pathway [34]. While percolation threshold of carbon black composites have been reported to be in the range of 25-60 wt% depending on the intrinsic conductivity and the structure [59-61], CNF filled composites have been shown to have a lower percolation threshold in the range of 0.68-6.3 wt% [39,49,62]. CNTs showed even lower values of PT within the range of 0.1-2 wt% because of their relatively higher aspect ratios ranging between 100 and 5000 [63-66]. Another important parameter, the surface area of the fillers, differentiates the particles with same aspect ratio. As shown in Fig. 2.7, although all three CB particles have aspect ratio of 1, they have different surface areas which affect their filler-filler and filler-matrix interaction and number of the contact points. Generally, higher structures lead to lower percolation threshold because of their higher potential of forming contacts throughout the composite [67].

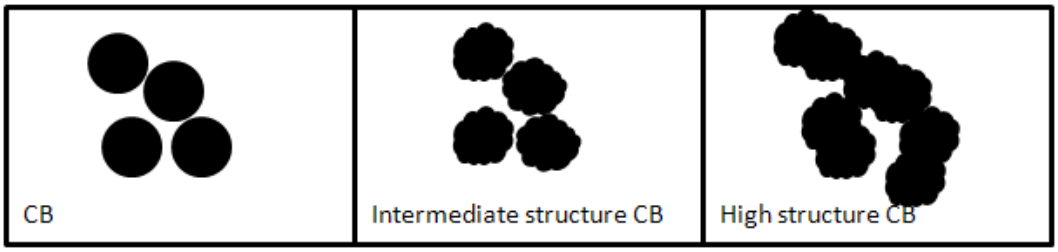

Figure 2.7 Carbon black with different structures

Flandin *et al.*, used carbon fiber (CF), carbon black (low and high structure) with an ethylene–octene elastomer in order to compare the effect of filler aspect ratio on percolation threshold. While low structure carbon black (LSCB) showed percolation threshold around 40% v/v, the high structure carbon black (HSCB) had a lower threshold of 15% v/v, and the same for CF was 10% v/v (see Fig. 2.8) [67].

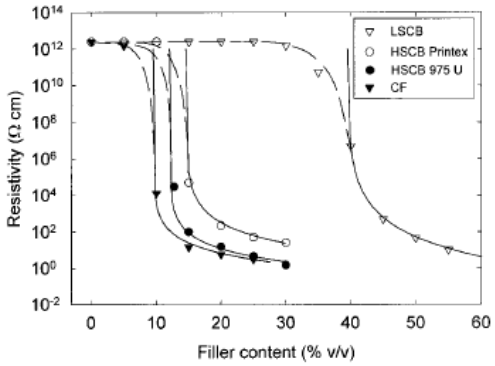

Figure 2.8 Effect of concentration for different fillers [67]

Li *et al.*, used different fillers fabricated by different methods including spraying carbon black (4.87 m^2 g^{-1}), semi-reinforcement furnace black (13.55 m^2 g^{-1}), fast extruding furnace black (FEF, 33.38 m^2 g^{-1}), high abrasion furnace black (HAF, 68.36 m^2 g^{-1}), and conductive carbon black (CCB, 981.62 m^2 g^{-1}) with increased high surface areas as shown inside the parentheses. Polymeric matrix was ethylene-propylene-diene rubber (EPDM) and EPDM/CCB composites showed the highest conductivity because of its larger surface area [61].

In another study with CB/PE, CF/PE and CNT/PE composites, Zhu *et al.*, reported lower percolation threshold for particles with increasing aspect ratio, see Fig. 2.9 [68].

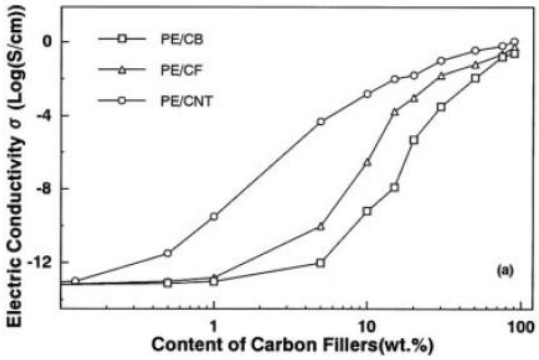

Figure 2.9 Effect of filler type and concentration on conductivity [68]

Filler concentration is a measure of the amount of filler in the composite and is generally expressed in weight percent (wt%), volume percent (v%), or parts per hundred (pph). In addition to intrinsic filler properties (*i.e.*, conductivity) and geometry, filler concentration is the most important parameter influencing conductivity of a CPC. Filler concentration has the most influence on filler-filler and filler/polymer interspacing and interaction. In general, the conductivity-concentration relation can be divided into three main regions, see Fig. 2.4 [19,24,59].

1) The region between bulk polymer and the threshold concentration,

2) A transition region from insulating to conducting phase which shows significant increase in conductivity, and

3) Conducting region

In the first region, fillers are highly separated and can be found individually dispersed or in the form of flocks. Since at this concentration, fillers are not close enough, conductivity does not change significantly. On the other hand, in the second region, abrupt change is observed with increasing concentration. In this region particles start to come close and form a

continuous network throughout the composite and conductivity of the composite increases dramatically. In the third region conductivity of the composite does not change significantly. Although different CPCs have different percolation threshold, all of them show characteristic conductivity behavior for composites [13,18,19,38,59,69].

Filler surface property is another important factor in determining the conductivity of the CPC. Since there are significant structural differences between filler and matrix materials including density, surface energy, and stiffness; it is not always easy to process and obtain optimum composite properties However, this can be overcome by additional processing such as modification of the surface characteristics of the filler. Surface properties and surface chemistry of the components are extremely important, because materials get in contact at the outer boundary of a material [35,70]. Different physical and/or chemical modifications have been carried out for fillers including heat treatment [36,71,72], grafting [73], electrochemical deposition [74] and acid treatments by sulfuric and/or nitric acid in order to:

- enhance the cleanness, degree of purity [74],
- remove structural defects [74],
- increase the effective surface area [34,75],
- increase surface functionality [73],
- decrease surface energy [36],
- increase conductivity of the filler [72],
- enhance the filler-matrix interaction (bondability, compatibility, *etc.*) and to control the interface properties [73,76,77].

Heat treatment of fillers is an effective way to remove structural defects and polar functional groups, improvement of the graphitic structure/crystallinity and electrical properties. On the other hand, heat treatment may reduce specific surface area, length and aspect ratio of the filler through removal of pore volume and this might lead to increase in percolation threshold of a CPC. In order to minimize these disadvantages of heat treatment, optimization of the process is strongly advised [36,71,72].

Grafting has been used for functionalization of surface by chemically bonding different structures and increasing the interaction between filler and matrix [73,76,77]. While strength and modulus of the composites showed significant increase [77], electrical conductivity is decreased because of the grafted layer. As shown in Fig. 2.10 grafted layer tend to wrap the filler and hinder the charge transport by increasing the filler-filler distance [73,76,77], and can even change the mechanism of conductivity from linear (ohmic) to nonlinear (non-ohmic) [73].

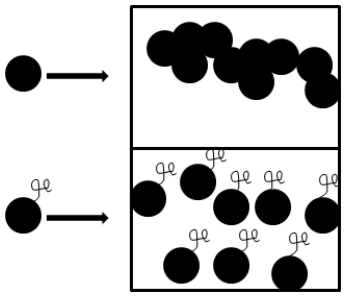

Figure 2.10 Effect of surface functionalization on filler dispersion

Acidic pretreatment can also be effective as a surface modification method. It is a chemical oxidative pre-treatment that causes etching of the filler surface and generally carried out at

high temperatures. The treatment is used for increasing the surface area of the filler, removal of impurities, exfoliation of nanofillers and functionalization of filler surface by imparting oxygen containing groups such as carboxyl and hydroxyl. All of these not only affect the geometry and electrical properties of the fillers but also dispersability, adhesion behavior of fillers in the matrix and electrical, mechanical properties of the composites [33,74,75,78]. Since carbonaceous fillers are inert structures, strong acids such as nitric and/or sulfuric acid, hydrochloric acid or strong bases such as ammonium hydroxide/hydrogen peroxide are required in order to modify the properties [74,75,78]. It is also one of the common ways to obtain expanded graphite which shows activated surface and multi-pores with a higher volume expansion ratio. The process not only increases the filler-polymer interaction and dispersion rate but also lowers percolation threshold because of expanded filler structure [34,75]. In addition, nitric acid has been used to remove the amorphous carbon from CNFs and thereby increasing the filler conductivity [74].

B) Matrix properties

Polymer type is another factor which plays a significant role on the conductivity of CPCs. In the literature, different polymers and polymer blends have been used including elastomeric, amorphous, semi-crystalline, liquid crystalline, thermoplastic, thermosetting polymers. In all these groups of polymers, epoxy [79-81], polyethylene (PE) [82,83], polypropylene (PP) [84], polyvinyl chloride (PVC) [85], polycarbonate (PC) [62], polystyrene (PS) [86,87], polyamide (PA) [88], poly(methacrylate) (PMA) [89], polyacrylonitrile (PAN) [90], polydimethylsiloxane (PDMS) [91] are the commonly investigated ones.

The electrical conductivity of the CPC is significantly influenced by the polymer's electrical behavior, filler-matrix interaction. The filler-matrix interaction in turn determines filler dispersion in the matrix and is directly affected by the molecular weight [89,92], and crystallinity [92] of the matrix polymer. In addition, polarity and surface tension of the matrix polymer are also important [19,54,93].

Molecular weight of a matrix polymer is directly related to the number of the repeat units in a polymer chain which determines the physical properties such as glass transition temperature (T_g), melting point (T_m), chain mobility, melt viscosity, entanglement ratio, average diameter of random coils (average radius of gyration) [89]. As known, polymer chains can entangle with fillers and minimize the movement of other chains in the vicinity or restrict the fillers. This behavior is affected by the radius of gyration of a polymer and higher molecular weight polymers might have more impact because of their relatively high radius of gyration [89]. In order to minimize the percolation threshold; filler geometry, filler-filler distance and average diameter of the random coil should be taken into consideration [89]. Effect of the molecular weight on electrical conductivity was studied by many authors. In these studies, different molecular weights of PS, PE [92], vinyl acetate (EVA) copolymers [54,94], poly(methylmethacrylate) (PMMA) and polyvinyl chloride–vinyl acetate copolymer (PVC–VA) [94], polyethylene oxide (PEO) were used with a conducting filler. The outcomes showed that, highest percolation threshold was observed for highest molecular weight because higher chain entanglement ratio and lower chain mobility make it difficult to spread on filler and minimize the percolating network formation [54,92,94]. Another effect of molecular weight is reflected by the melt viscosity [54,94]. As reported by Huang, higher

molecular weight leads to higher melt viscosity resulted high shearing during mixing and this is an undesired effect for the dispersion of carbon black and formation of the conducting network [54,94]. In addition to that, high viscosity requires higher shear mixing which might lead to breakage of the fibrous fillers and decrease in the aspect ratio [95].

Crystallinity of a polymer determines the ratio of structural order which affects the physical and mechanical properties. When the issue is the CPCs, crystallinity of the polymer has some influences on the electrical conductivity of the system basically resulting from dispersion of fillers [96]. Tiong *et al.*, used amorphous PS, low density polyethylene (LDPE) with low crystallinity, high density polyethylene (HDPE) with high crystallinity and CNFs as conducting filler. While CNFs dispersed well in LDPE, and PS; agglomeration was observed for HDPE. Different types of dispersion characteristics lead to different percolation behavior. PS/CNF nanocomposites had the lowest and HDPE/CNF nanocomposites had the highest percolation concentration [96]. On the other hand, Wessling *et.al.,* reported relatively low percolation threshold for PE than amorphous PS [92]. Furthermore, Huang *et.al.,* used CB and three different vinyl acetate (EVA) copolymers with different crystallinity [54]. The lowest percolation threshold was found for the polymer with the highest crystallinity. It was concluded that crystalline polymers restricted the fillers into the amorphous region and increase the contact rate.

In addition to dispersion of fillers, another result of filler-matrix interaction is the nucleation. As previously reported by many authors, CNTs behave as nucleating agents for some semicrystalline polymers and change the shape of crystallites and orientation of the crystal growth [96,97] which might influence the electrical behavior of the system.

Polarity and surface tension of the polymer are other important factors for the electrical behavior of polymers and the CPCs. Since polarity and surface tension of a polymer can be affected by many criteria including chemical structure, amount of end groups, density, molecular weight, morphology of the polymer, components of the system, processing temperature; different polymers show different adhesion and electrical behavior as mentioned previously. While acrylonitrile butadiene rubber (NBR), a polar polymer, has a volume resistivity of 1010 ohm cm; non polar polymer ethylene-propylenediene monomer rubber (EPDM) showed around 1018 ohm cm [98]. In addition to these, polarity and surface tension are important factors for CPCs, especially for the behavior of intermolecular attraction between the polymer chains, filler-matrix interaction and spreading tendency of polymer onto the fillers. Polymer adhesion is of critical importance for filler dispersion, filler to filler distance and the interface layer on the filler. As reported by Miyasaka *et al.*, polymers with higher surface tension and polarity lead to higher percolation threshold. Because, higher amount of surface-active, polar segments are preferentially adsorb on the filler surface which generally leads to a better dispersion [99]. Yamamoto *et al.*, also reported similar behavior. While, polymers with low surface tensions PVA and PMMA were found to form cupper sulfide (CuS) aggregates; PAN resulted with a homogeneous filler distribution because of its high surface tension. This behavior leads to higher conductivity for CuS-PVA and -PMMA composites and lower for CuS-PAN composite [100]. On the other hand, Sau *et al.*, reported a lower percolation concentration for a polar polymer (*i.e.*, NBR) compared to a non-polar polymer (*i.e.*, EPDM) [98].

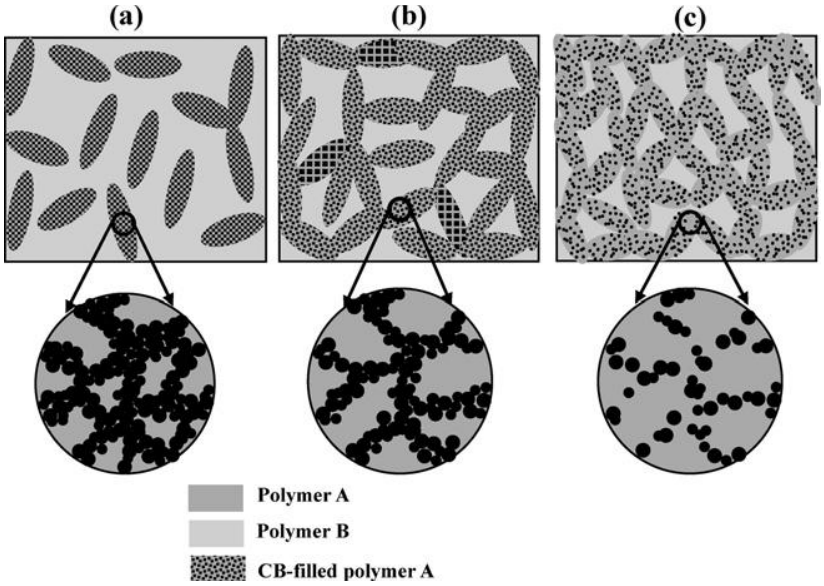

Figure 2.11 Selective localization of CB in a polymer blend [101]

In addition to single polymeric systems, polymer blends can be effectively used in order to lower the percolation threshold (see Fig. 2.11). In these systems, generally two different polymers are used with different degree of crystallinity which induces phase separation and forces fillers to migrate into one phase and lowers the percolation threshold [102-106].

C) Process parameters

Processing is as important as the inherent properties of filler and matrix; since it determines the dispersion, distribution, alignment, orientation, aspect ratio, filler-filler distance, filler concentration, and homogeneity of the CPCs. Processing should be determined by considering the end use of the CPC. If the composite is designed just for electrical applications, the process should focus on optimization of percolation behavior and lowering the threshold concentration. On the other hand, if the CPC is designed to be used for any type of electronic application requires high mechanical durability and stability; filler dispersion

and interface properties of the composite become significant. In the second case, optimization requires attention because in order to obtain a good dispersion, harsh processing conditions and longer processing time might be needed which influence the aspect ratio of the fillers and percolative behavior. However, dispersion mechanism is not governed only by processing but also type of the components and their physical properties (cluster size, purity, surface properties of filler, polymer surface tension, *etc.*) are of importance. If the fillers form strong agglomerates due to Van der Waals forces and physical entanglements it might be difficult obtain satisfied results [40,93,95,107].

For the production of CPCs, various methods can be used including melt mixing [40,107], in-situ polymerization [73], solution casting [57,108]. The common process in each method is the mixing which aims blending of the components. Depending on the filler concentration, viscosity of the mix and polymer processing conditions, it can be carried out by many different methods such as traditional (direct) mixing [109], high-shear mixing, ultrasound mixing, melt mixing and chaotic mixing which can be combined with another mixing or shaping process such as injection molding, extrusion or hot pressing [40,93,95].

Solution Processing: Solution processing is one of the common methods used for the preparation of CPCs because of its simple procedure. Process starts with the dispersion of filler in the solvent or polymer solution by any type of mixing (magnetic stirring, ultrasonication [110], high shear mixing and followed by pouring the solution on a plate and evaporation of the solvent under predetermined conditions. Since the properties of polymer solution changes for various solvents, type and amount of solvent are of significance in terms of solubility degree of the polymer and conductivity of the system [80,93,108,111,112].

Although solution processing has some drawbacks from the environmental aspects and industrial applicability, it leads to lower percolation thresholds since solvent decreases the viscosity of the system and enhances the dispersability of the filler [80,93,112,113].

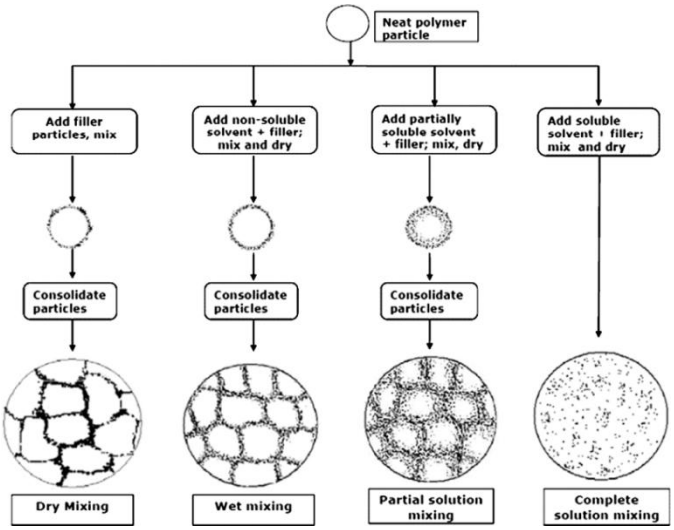

Figure 2.12 Effect of solvent on the formation of conducting network [57]

Sharma *et al.*, studied the effect of solvent type on the electrical behavior of MWCNT filled epoxy composites. They used dimethyl formamide (DMF) and N-methyl pyrrolidone (NMP) as solvents. Although both solvents lead to similar percolation behavior, samples prepared with DMF showed better dispersion, interface and higher electrical conductivity than that using NMP. In addition samples prepared with NMP, were found to have aggregates with porosity. DMF was found an effective solvent in terms of filler dispersability and filler-matrix interaction [108]. Another interesting study was carried out by Yunusa *et al.* [57]. They have designed a mixing process based on the solubility parameter and swelling ratio of the polymers. They have used polymer compositions of poly(acrylonitrile butadiene styrene)

and poly(styrene butadiene styrene) block copolymers and various solvents including; 1,1,1-trichloroethane, toluene, acetone, isopropyl alcohol. As shown in Fig. 2.12, depending on the solubility and swelling ratio of the polymer, different morphologies and lower percolation values can be obtained.

Melt mixing: As in all type of mixing techniques, the aim of the melt mixing is to provide homogeneous filler dispersion in a molten polymer. Needless to say that this process is used for thermoplastic polymers and basically consists of three steps including, incorporation of filler and matrix, deagglomeration, and distribution of the filler. Deagglomeration of fillers is the most important step of processing and its deagglomeration mode generally based on rupture or erosion mechanism. To have a homogeneous dispersion and to balance the agglomeration and deagglomeration; filler structure, polymer melt behavior, applied hydrodynamics have to be taken into consideration [40,107].

Melt mixing can be carried out under normal conditions if the fillers can easily disperse in the molten polymer. On the other hand, for the composites consisting of a polymer with high viscosity and highly agglomerated fillers; mixing conditions should be changed. Since some fillers, *i.e.* CNTs, show strong attractive van der Waals forces and they have the tendency to form agglomerates. In such cases, lower flock size, and high-shear mixing is required to obtain good dispersion [40,86]. Pegel *et al*. investigated the effect of mixing type, time and speed on the electrical behavior of multi walled carbon nanotube/polycarbonate composites. Mixing time, temperature and speed were found important in terms of CNT dispersability and electrical behavior [40], resistivity increases with mixing time because of homogeneous dispersion and breakage of fillers which was also reported in previous studies [86,114-116].

Viscosity of a filled matrix is determined by filler and matrix. Since carbonaceous and metallic fillers are solid, rigid structures and generally not affected by temperature changes, polymer properties become more important in terms of the viscosity of the system. Generally, any increase in the temperature leads to a reduction in the viscosity of the polymer and lowers the shear effects on fillers which trigger the aggregate and conductive network formation [93,117-119].

In-situ polymerization: Another way to produce CPC is the in-situ polymerization. It has been used for various types of polymers from thermosetting to thermoplastic and fillers including CB [87], CNF [73], and CNT [120]. Process consists of filler dispersion in the monomer liquid/monomer solution and followed by polymerization or curing. In the first step, low molecular weight and low viscosity monomers are adsorbed to the surface of the fillers that contributes proper filler wetting. In the second step, polymerization takes place which can be initiated by an initiator, heat or radiation. Since polymerization is a sensitive process, any change in the conditions might cause extreme change in filler dispersion, polymer absorption by the filler surface, filler-filler distance, filler orientation and conductivity of the system. By this method, aspect ratio of the fillers are retained and perfect dispersion with better filler matrix interaction can be obtained even at high filler loadings because of the grafted polymer onto the surface of the filler [73,87,93,111,112,121]. However, some critical factors have to be taken in to consideration. First of all, proper dispersion of the filler in the monomer liquid/monomer solution should be provided [87,111,121], because, once the polymerization starts, polymer settling is triggered and that might affect the viscosity of the medium which has an important role for the filler dispersion.

In addition to that side product formation is another important point which might influence the total volume and properties of the system, so additional steps might be required in order to remove these undesired products from the system [121]. It was reported by Arlen *et al*., that the success of the process in terms of filler dispersion and electrical behavior not only depend on the polymerization but also on the surface properties of the fillers and interface properties. While good dispersion and strong interface can be obtained by in situ polymerization, it was also noted that strong interface hinders the charge transfer from filler to filler and lowers the conductivity of the system [73]. Since polymerization is effected by the materials in the medium; filler concentration might affect the distribution of molecular weight of the polymer. At high concentrations, fillers restrict the macromolecular chains and prevent the interaction between polymer chains. As reported by Li *et al*., any increase in the CB fraction leads to decrease in the molecular weight of the polymer which did not affect the general percolation behavior of the CPC [87].

D) Other factors

In addition to filler characteristics, polymer properties and processing conditions, other factors such as additives and environmental factors can affect the resistivity by changing filler dispersion, filler-matrix interaction and filler-filler distance. While some systems only consist of matrix and filler, some systems require extra additives to obtain desired morphology and properties such as viscosity, flexibility *etc*. Additives can be in the form of plasticizers [122], blowing agents [123], surfactants [110], cross-linker, initiator [124] and so on. Since they change the physical and chemical composition of the composite, it is very much possible to observe a change in the electrical properties of the system depending on the

amount of additives. In addition to additives, external mechanical effects and environmental conditions were found to affect the conductivity of the system. Although other factors mentioned above affects conductivity without changing the filler-filler distance, environmental factors such as temperature, pressure, vibration, and ambient atmosphere were found effective under certain conditions which are going to be evaluated in the following chapter dealing with piezoresistive behavior of the composites.

2.3 Piezoresistivity and Piezoresistive Composites

Piezoresistivity is a material property that involves change in electrical resistance due to applied mechanical stresses. It was first reported in 1856 by William Thomson (Lord Kelvin) who observed the resistance change in iron and copper as a result of applied strain [125]. Application of this discovery has been in practice as strain gauges and thermo resistors since early 1900's. These devices are made from pure metals or metal alloys. In 1950's, piezoresistive behavior of silicon and germanium semiconductors was discovered by Smith [126] while working in the Bell Laboratories. It opened a new era in piezoresistive sensors.

To illustrate the concept of piezoresistivity consider a prismatic bar of uniform rectangular cross-section. The resistance R of the conductor can be expressed as,

$$R = \frac{\rho L}{A} \qquad \text{Equation (2.10)}$$

where ρ is the specific resistance or resistivity, L is the length, and A (= w x t) is the cross-sectional area of the conductor, see Fig. 2.13.

Differentiating Eq. (2.10) we obtain:

$$dR = \frac{\rho}{A}dL + \frac{L}{A}d\rho + \frac{\rho A}{L^2}dA \qquad \text{Equation (2.11)}$$

Dividing the Eq. (2.11) by resistance R,

$$\frac{dR}{R} = \frac{dL}{L} + \frac{d\rho}{\rho} + \frac{dA}{A} \qquad \text{Equation (2.12)}$$

The terms dA⁄A represents fractional change in area, dL/L represents fractional change in length in the long-direction, and $d\rho/\rho$ represents fractional change in resistivity of the conductor resulting from applied force along the longitudinal direction. The relative change in length, or the axial strain:

$$\varepsilon_{axial} = \frac{\Delta L}{L} \qquad \text{Equation (2.13)}$$

Lateral strain:

$$\varepsilon_{lateral} = \frac{\Delta W}{W} = \frac{\Delta H}{H} \qquad \text{Equation (2.14)}$$

If the Poisson ratio is now expressed in terms of axial and lateral strain:

$$\nu = -\frac{\varepsilon_{lateral}}{\varepsilon_{axial}} \qquad \text{Equation (2.15)}$$

Now the relative resistance change can be written as a function of the strain and resistivity;

$$\frac{\Delta R}{R} = (1 + 2\nu)\varepsilon_{axial} + \frac{\Delta \rho}{\rho} \qquad \text{Equation (2.16)}$$

The relative change in resistance expressed in Eq. (2.16) clearly has two components described as geometric and electronic.

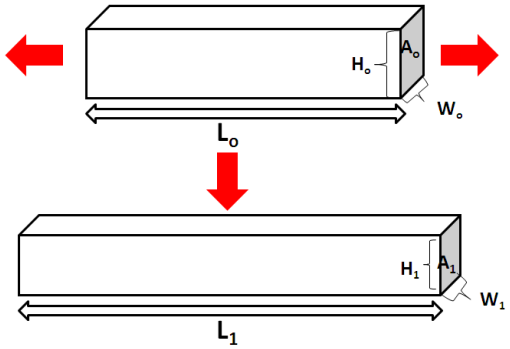

Figure 2.13 Piezoresistance caused from dimensional change [127]

The terms $(1+2v)\varepsilon_{axial}$, and $(\frac{\Delta\rho}{\rho})$ represent the geometric and material (or inherent) components of piezoresistivity, respectively. In semiconducting materials (e.g. silicon, germanium) the fractional change in resistivity, $(\frac{\Delta\rho}{\rho})$, is the predominant source of piezoresistive behavior. For metals, on the other hand, the fractional change in resistivity is nearly insignificant compared to the fractional change in resistance due to deformation or geometrical change.

The Gauge Factor (K) of a piezoresistive material is defined as the fractional change in resistance (Δ R/R) per unit strain, ε . It is expressed as [127];

$$\mathrm{K} = \frac{\left(\frac{\Delta R}{R}\right)}{\varepsilon_{axial}} = (1+2v) + \frac{\frac{\Delta\rho}{\rho}}{\varepsilon_{axial}} \qquad \text{Equation (2.17)}$$

In metals, the change in inherent resistivity is negligible and GF can be reduced to:

$$K_{metals} = \frac{\left(\frac{\Delta R}{R}\right)}{\varepsilon_{axial}} \simeq (1+2v) \qquad \text{Equation (2.18)}$$

For metals, the Poisson's ratio is generally in the range of between 0.3-0.4, and GF is around 2. If a semiconductor material is exposed to strain, symmetry of the crystal lattice is

degenerated and as a result the carrier mobility and resistance change [126,127]. Electrical sensitivity in the atomic state and generation of high resistance difference makes semiconductors very favorable materials for piezoresistive sensors. They generally show relatively high GFs, around two orders of magnitude more than metals. Since the geometrical component ($\nu \simeq 0.28$) of the GF is not as high as the material component, it can be neglected and GF can be written as [127]:

$$K_{semiconductors} = \frac{\left(\frac{\Delta R}{Ro}\right)}{\varepsilon_{axial}} \simeq \frac{\frac{\Delta \rho}{\rho}}{\varepsilon_{axial}} \qquad \text{Equation (2.19)}$$

For conducting composites, mechanism of piezoresistance is different. Although change in the geometry of the composite due to applied strain may be significant, the most important factor is the change in conducting network structure. The change in network structure may be due to a combination of change in inter-particle separation, and reorientation of filler particles [128,129].

$$GF_{composites} = \frac{\left(\frac{\Delta R}{Ro}\right)}{\varepsilon_{axial}} \simeq \frac{\frac{\Delta \rho}{\rho}}{\varepsilon_{axial}} \qquad \text{Equation (2.20)}$$

For composites, change in electrical resistance can be caused by external factors including mechanical (tensile, compression, bending), thermal or environmental. In all cases resistance change is governed by change structure of the composite involving change in filler-filler distance and number of the contact points and/or density of contact points. When any such external stimulus is applied, it may lead to the breakdown of the filler junctions; or the reformation of the conducting network by rotation, alignment and translation of the fillers [67,130]. If the dominant behavior is the filler separation, resistance will increase this behavior is referred as positive piezoresistance. On the other hand, if fillers get closer and

form new conducting networks, resistance will decrease which is referred as negative piezoresistance. Dominant mechanism depends on many structural and external factors such as polymer type, filler type, concentration, geometry [130], filler orientation-dispersion [131], amplitude, direction and type of external factor [130], measurement configuration.

2.3.1 Application of Piezoresistive Composites

Piezoresistive polymer composites can be used in different forms such as coating, printed layer, film and bulk form in many areas from civil engineering to textiles as self-monitoring sensory materials [52] because of their ability to reflect the magnitude of external factors in terms of change in resistance. These composites can be used as strain, pressure, temperature and gas sensors and can be produced easily with relatively lower cost [128].

Strain Sensors: Strain sensors are a widely used tool in a variety of applications including monitoring processes, infrastructure, and human health. Varieties of strain sensors used today include types of strain gauges, fiber optic sensors, *etc*. Most of these sensors, however, are rigid and are not suitable for monitoring large strains (>5%). High sensitivity of flexible carbonaceous polymer composites to mechanical strain makes them particularly suitable for sensor applications for detection of strain, force and pressure in applications that require flexibility, conformability, and ability to measure high strains. For a sensitive and effective sensor, strain and resistance ranges should be determined carefully in terms of linearity.

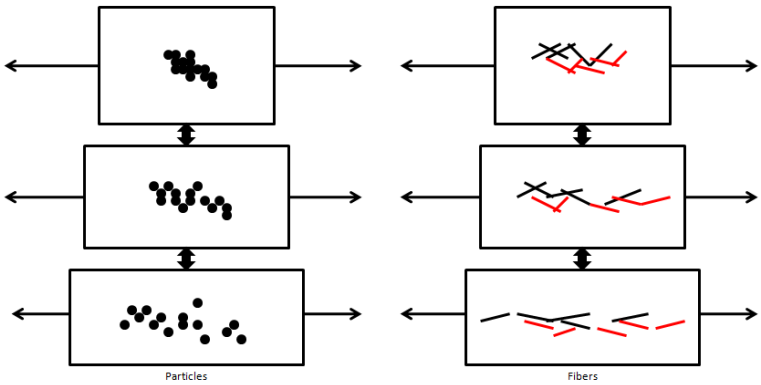

Figure 2.14 Positive piezoresistance

As shown in Fig. 2.14 application of unidirectional strain leads to filler separation and decrease in the resistance. Filler separation degree is directly related with the magnification of the strain/stress. On the other hand, when aligned continuous fibers or laminates are used as filler as shown in Fig. 2.15; filaments or laminates come closer under strain and leads to decrease in resistance. However if applied strain increased and elastic limits of the composite is exceeded, filler-matrix debonding, filler breakage, might occur and resistance will increase [132-134]. In addition to filament based composites, some authors reported negative response for CB [67] and nickel/carbon fiber [135] filled polymer composites. This behavior was attributed to the filler alignment during loading process as shown in Fig. 2.15.

As mentioned earlier, piezoresistive behavior in CPCs is measured with deformation of the composite in different modes. The response is not only governed by polymer and filler properties but also testing conditions. While, magnitude of the applied strain gives us the total deformation in the composite system; strain rate gives us the deformation at a given time. Since the viscoelastic response of the composite is affected by strain rate, filler configuration, filler-filler distances and piezoresistive response might also be affected.

Generally, a higher strain and strain rate can lead to higher change in resistance because of higher deformation of the composite [118,136-138].

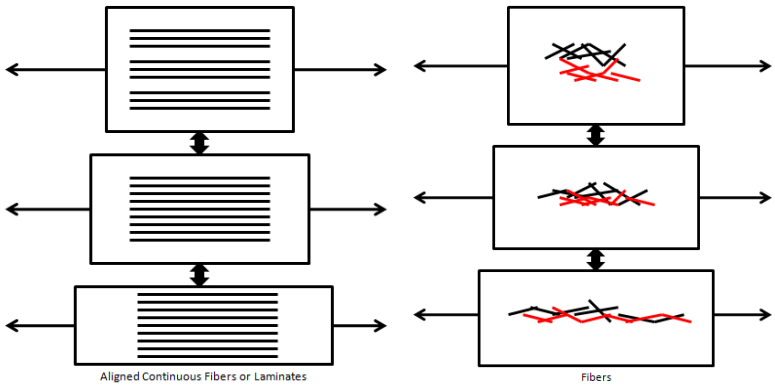

Figure 2.15 Negative piezoresistance

Kost *et al*. compared the effect of strain rate on the piezoresistive behavior of 10 wt% CB filled silicone rubber composites. As shown in Fig. 2.16, both magnitude of the strain and strain rate were found to influence the response of the composite. 2 mm/min strain rate lead to higher change in resistance when compared with 0.01 mm/min [136].

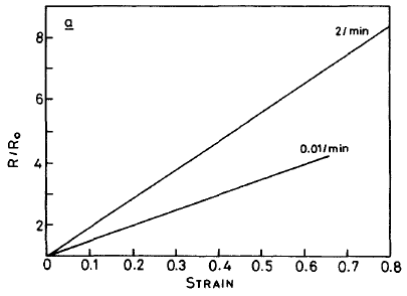

Figure 2.16 Effect of strain and strain rate on 10 wt% CB filled silicone rubber composites [136]

Similar study was carried out by Pramanik *et al*. with CB and short carbon fiber (SCFs) filled nitrile-rubber composites at higher strain values. As shown in Fig. 2.17, strain and strain rate were significant parameters in terms of the resistivity change because of their effect on filler configuration in the elongation process [137].

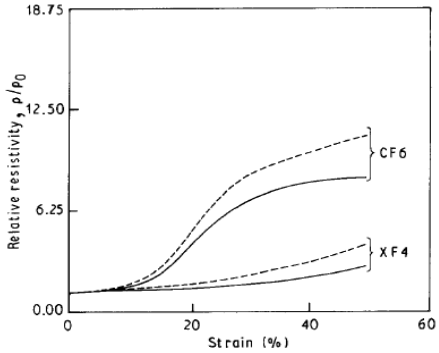

Figure 2.17 Effect of strain rate on the relative resistivity of different nitrile-rubber composites CF6 (SCF) and XF4 (SCF+CB): (- - -) 0.04 min^{-1} and (__) 0.02 min^{-1} [137]

Das *et al*., investigated the effect of magnitude of strain and strain rate on the piezoresistive behavior and repeatability of CB and SCF filled ethylene-vinyl acetate (EVA) composites.

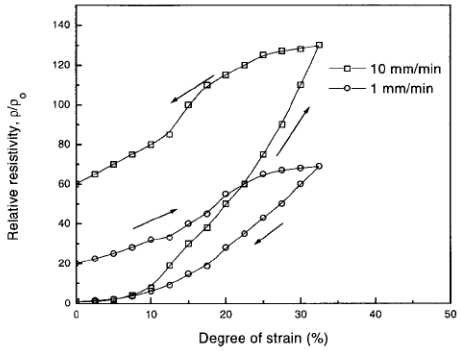

Figure 2.18 Effect of strain and strain rate on electrical resistivity during loading and unloading cycle of SCF/EVA composites [118]

As shown in Fig. 2.18 and 2.19 both CB and SCF filled composites showed higher sensitivity under higher strain and strain rate which is assumed to be caused from the higher separation ratio. On the other hand, composites showed irreversible behavior between loading and unloading cycles [118].

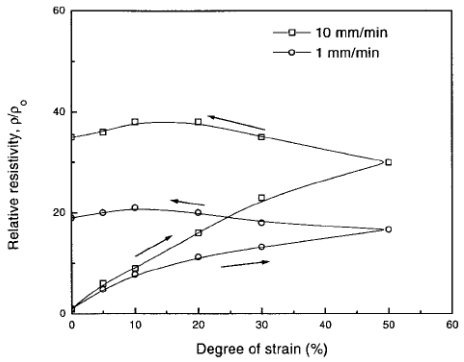

Figure 2.19 Effect of strain and strain rate on electrical resistivity during loading and unloading cycle of CB/EVA composites [118]

In addition to short fiber and particle filled composites, Boschetti-de-Fierro *et al*. investigated the electromechanical response of unidirectional and bi-directional continuous carbon fiber/epoxy composites under different magnitudes of strain.

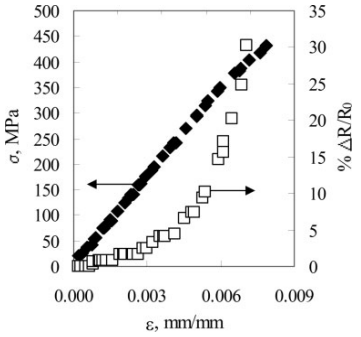

Figure 2.20 Piezoresistive behavior of unidirectional continuous carbon fiber reinforced epoxy [0°] [52].

As shown in Fig. 2.20, filler orientation is of significance in terms of piezoresistive response. Although both composites showed increase in resistance by the increase in strain; unidirectional continuous fiber reinforced epoxy showed increase in two steps and bi-directional one showed step-wise increase. The region which showed the highest increase was reported to be caused from the fracture of the fibers in the structure [52].

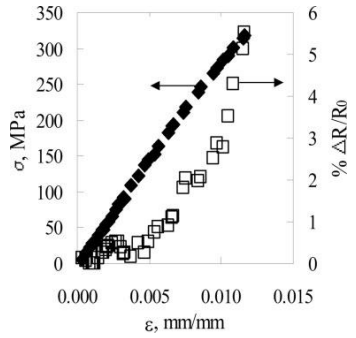

Figure 2.21 Piezoresistive behavior of cross-ply [0°/90°] continuous carbon fiber reinforced epoxy [52]

Pressure Sensors: Piezoresitive pressure sensors are devices that undergo change in resistance under applied pressure. The response is assumed to be caused from the different compressability of filler and polymeric matrix under pressure. Because of this difference as compression applied to CPC, fillers either separate or approach each others. In order to differentiate positive and negative relationship between pressure and resistance for pressure sensors, two acronyms; positive pressure coefficient (PPC) and negative pressure coefficient (NPC) can be used. As shown in Fig. 2.22, type of the piezoresistive behavior is directly related with the filler geometry and magnitude of the pressure [130,139,140].

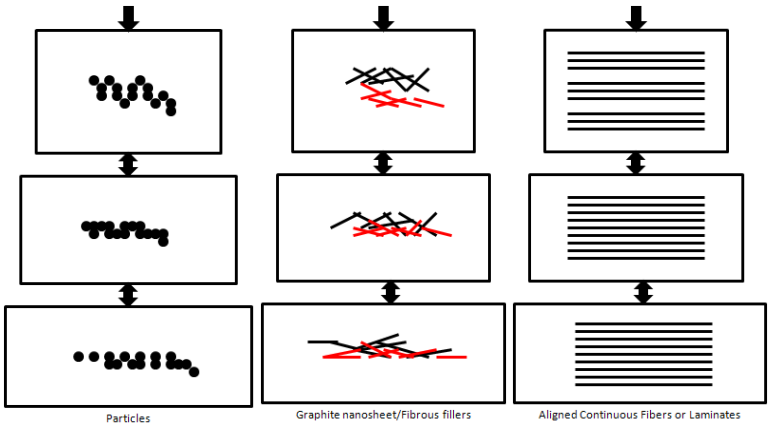

Figure 2.22 Positive piezoresistance for different types of fillers under compression

While for fillers such as graphite nanosheets it is easier to increase the number of the points by applying pressure, this might adversely affect the CB particles. Since nanosheets have higher surface area, formation of the new networks can be dominant during the pressure application [139].

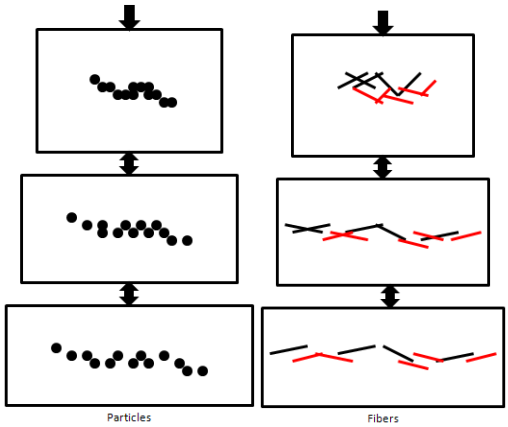

Figure 2.23 Negative piezoresistance for different types of fillers under compression

On the other hand, network formed by CB, can easily be destructed by the compression because of their spherical shape [141]. But, degree of resistance change is affected by the applied pressure. Pressure affects the filler configuration, filler to filler distances and piezoresistive response throughout the composite. The change in the resistance depends on the magnitude of the compression. Generally, at lower pressures, reformation of conducting networks dominates. However, at higher compression, resistance change can be higher because of higher dimensional change of the composite which leads to higher filler separation [54,103,130,141-143]. As reported by many authors, even if sample showed NPC, with the increase in the magnitude of the pressure, particle separation or destruction of the network even filler breakage might dominate and resistance will increase, see Fig. 2.22. On the other hand, type of the pressure coefficient not only depends on the magnitude of the pressure but also to the filler geometry and concentration [34,131,142,144]. As reported by Vidhate *et al*., at concentrations above the percolation threshold, increase in the compression stress was not found effective for resistance change [142].

Wang *et al*., studied the effect of magnitude of the compression on the piezoresistive behavior of carbon black filled silicone rubber composite. As shown in Fig. 2.24, increase in the pressure lead to increase in conductivity which was attributed to the higher rate of breakdown of conducting network under higher pressure values [141].

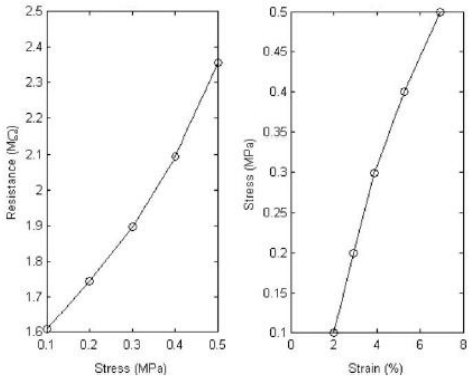

Figure 2.24 Effect of pressure on the piezoresistive behavior of CB filled rubber composites [141]

Similar behavior is reported for Sn-Pb/PE composites by Wu *et al*. As shown in Fig. 2.25, higher compression stresses lead to higher filler separation and breakdown of the conducting network [54].

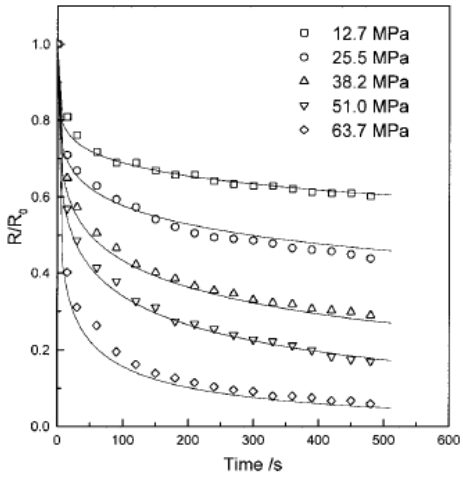

Figure 2.25 Time dependence of piezoresistance for the sample (vol 30%) of Sn–Pb/PE under various stresses [54]

Temperature Sensors: In addition to mechanically driven piezoresistance, thermally driven polymer expansion can lead to piezoresistive response in CPCs. Generally, increased temperature gives rise to expansion of the polymer and destruction of the conducting network by increasing filler-filler distance [138]. Similar to the designation for strain sensors, for temperature sensors, positive and negative piezoresistance is designated by positive temperature coefficient (PTC) and negative temperature coefficient respectively. The type of the piezoresistive behavior (PTC ot NTC) is directly related with the polymer physical-chemical properties, filler geometry, content, aspect, heating-cooling rate, number of the heating-cooling cycles (thermal history) [145-147].

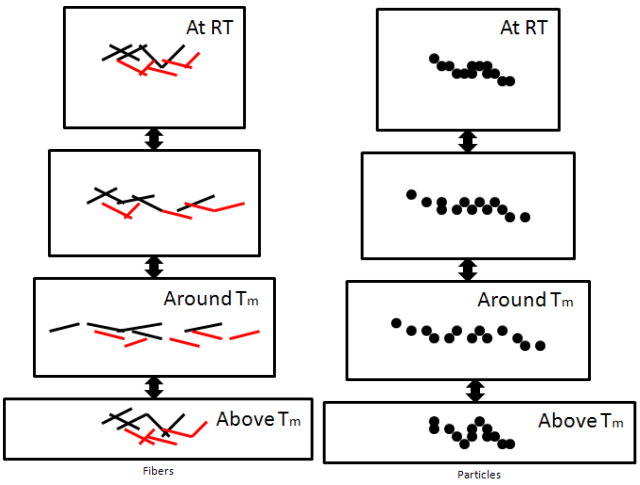

Figure 2.26 Positive and negative piezoresistance for different types of fillers under temperature effect

However thermal properties of the polymeric matrix are more pronounced and main reason is given as the higher thermal expansion coefficient of matrix than that of fillers'. Even if same amount of heat is transferred to two different CPC, the response can be different because of

the different expansion ratios of the polymers [145-147]. As reported by many authors, a PTC phenomenon is generally observed around the melting temperature (T_m) of the semicrystalline polymers. As shown in Fig. 2.26, with the increase in the temperature, thermal expansion of the polymer takes place and molecular movement increases; this leads to destruction of the conducting network and increase in the resistance [68,118,146-149]. On the other hand, except some special cases [118,150], NTC behavior is generally observed in the melt state of the polymer which is caused from the low viscosity of the polymer and reconnection/agglomeration tendency of the conducting filler [146,147].

Feng *et al*., studied the effect of temperature change on the resistivity of CB filled ethylen-tetratluoro ethylene (ETFE) composites. As shown in Fig. 2.27, normalized resistivity is not affected up to 60°C which is caused from the lower expansion rate of polymer far below its melting point. After 60°C, increase in the normalized resistivity becomes noticeable and huge jump is seen around melting point of the polymer [138].

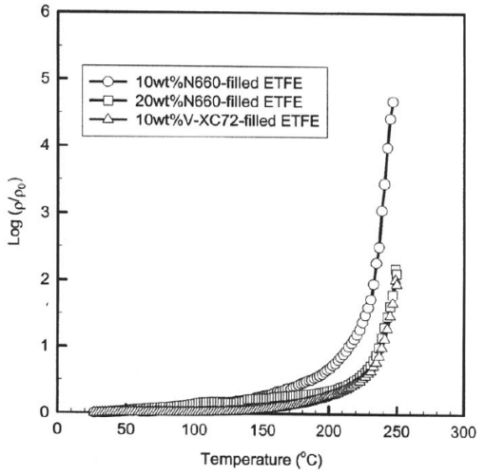

Figure 2.27 Piezoresistive behavior of CB/ETFE composites under various temperatures [138]

Gas Sensors: In addition to strain, pressure and temperature sensing ability of the CPCs, it was also reported by many authors that they are suitable materials for gas/ vapor sensors because of their ability to give measurable response about vapor type and concentration by change in resistance. The mechanism of the piezoresistance in this instance is similar to temperature sensors and shown in Fig. 2.28. When a CPC is exposed to vapor, gas molecules diffuse into the composite and lead to swelling of the polymeric matrix and decrease the system viscosity. Increase in the volume and decrease in the viscosity of the polymer affect the movement and distribution of polymer-filler and generally result with an increase in the filler-filler distance and composite resistance which is named as positive vapor coefficient (PVC) [87,151-156]. At a given time, resistance generally increases up to a peak value and followed by a decrease probably caused from the reformation of the conducting network which is named as negative vapor coefficient (NVC) [87,151].

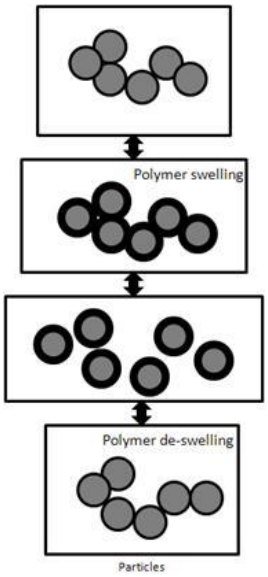

Figure 2.28 Positive and negative piezoresistance for particles under vapor effect

Type and magnitude of the piezoresistance depend on polymer-vapor interaction which is affected by both structural and environmental factors including; polymer type, crystallinity, filler type, dispersion, geometry, concentration, vapor type, pressure, and concentration, exposure time, composite processing [87,151-153,155,156].

2.3.2 Factors Affecting the Piezoresistance

Factors that influence piezoresistive behavior of CPCs can be divided into two groups as external and structural. While external factors are related with the environmental conditions, testing conditions such as rate and magnitude and exposure time of strain, pressure, temperature, type and concentration of vapor as summarized in the previous section; structural factors are related with the composition of the CPC such as filler and matrix properties and going to be explained in the following section.

2.3.2.1 Filler properties

Piezoresistance in CPCs is directly related with the filler-filler separation and number of the contact points; type of the fillers are extremely important in terms of piezoresistive behavior. Different types of metallic, organic and inorganic fillers were reported in the literature for piezoresistive composites including nickel [157], ICPs [27,158,158-160], carbon fibers [67,161-163], carbon black [67], graphite [131], graphite nanosheets [131], CNF [164], CNT [165] and mixture of some of these materials. It was also reported that different fillers show different electrical, mechanical and piezoresistive behavior mainly caused from their

geometry, specific surface area, interaction with matrix and distribution in the composite [67,131,140,166].

Many studies were carried out in order to discriminate the effects of fillers on piezoresistance. Fladin *et al*., used carbon fiber (CF), low structure carbon black (LSCB), and high structure carbon black (HSCB) with an ethylene–octene elastomer. While CF and LSCB showed positive piezoresistance, HSCB showed negative piezoresistance under low strain values. In addition to that, CF and LSCB containing composites did not show reversible mechanical and electrical behavior under repeated cycling. This behavior was assumed to be caused from the lower filler-matrix interaction and more interfacial disruption for composites containing CF and LSCB compared to HSCB [67]. Moreno *et al*. used poly (styrene–ethylene/butylene–styrene) (SEBS) as a matrix material; carbon black (CB) and graphite (GP) as conducting fillers. Piezoresistance was evaluated in terms of strain and pressure. While CB/SEBS showed an abrupt decrease at very low compressive strain, CB/SEBS showed more linear behavior.

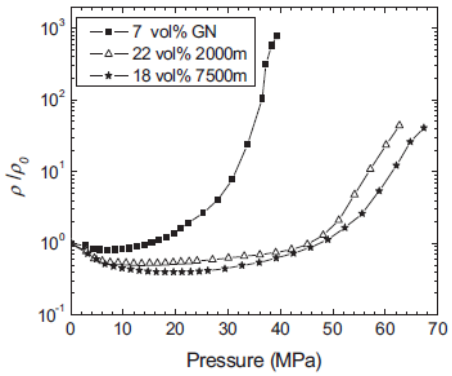

Figure 2.29 Piezoresistive behavior of HDPE/conventional graphite composites and HDPE/GN nanocomposite [131]

On the other hand, both the fillers showed similar trend under tensile strain. However, CB/SEBS was found to show higher change in resistance [166]. Lu *et al*., investigated the piezoresistive behavior of the high density polyethylene (HDPE) composites filled with graphite nanosheets (GN) and two different type of natural graphite powder. Piezoresistive behavior is tested under compression. As can be seen from Fig. 2.29, all three samples showed NPC for lower compression values which is followed by PPC. While graphite containing fillers showed higher NPC at lower compression values, GN containing composites were found to present higher PPC at high compression values which are assumed to be caused from the differences in filler aspect ratio and concentration [131]. As previously stated high aspect ratio and discontinuous fillers show larger sensitivity to mechanical effects [162]. Lu *et al*., used multiwalled carbon nanotube (CNT) and carbon black (CB) with poly (dimethylsiloxane) (PDMS) and investigated the piezoresistive behavior of these composites under tensile strain [165]. While 18 wt% CNT/PDMS composite had a GF 12.4, CB/PDMS sample showed a GF around 7.4 at the same concentration as shown in Fig. 2.30.

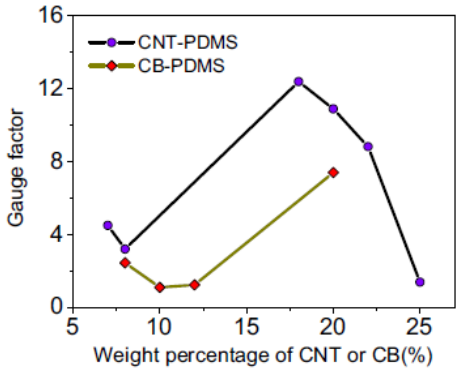

Figure 2.30 Gauge factor of CNT/PDMS and CB/PDMS composites [165]

Another comprehensive study was carried out by Zhang *et al*. They have used tin-lead (Sn±Pb) alloy powder, copper (Cu) powder, aluminum (Al) powder and carbon black (CB) as conducting fillers and polyethylene (PE), polystyrene (PS) and four different epoxy resins as matrixes. Piezoressitive behavior was evaluated under uniaxial pressures [140].

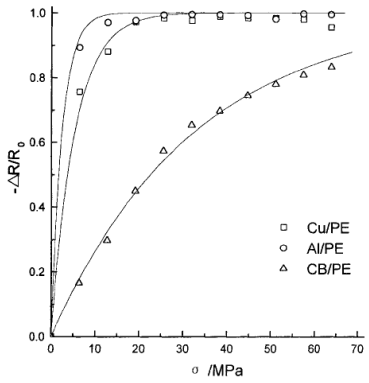

Figure 2.31 Fractional resistance change of (Φ=30%) of Cu/PE, Al/PE, and CB/PE composites under uniaxial pressure [140]

Regardless of the filler and polymer type, composites showed PPC. However, Al filled composite showed higher sensitivity in terms of resistance change followed by Cu and CB as shown in Fig. 2.31. This behavior is attributed to the differences in potential barrier height which is a constant used for transmission capability of electrons through the composite. In the same study they have also investigated the piezoresistive behavior of Sn-Pb fillers with different filler diameter as 0.1 and 0.5 μm. Composite filled with higher particle diameter was found to be more sensitive to pressure changes even at lower values (see Fig. 2.32). This is probably caused by the number of the fillers and contact points. Since concentration is same for both composites, the number of the fillers and contact points are higher for the

lower diameter filler, and it is not easy to destruct the network as easy as the composite with higher diameter filler [140].

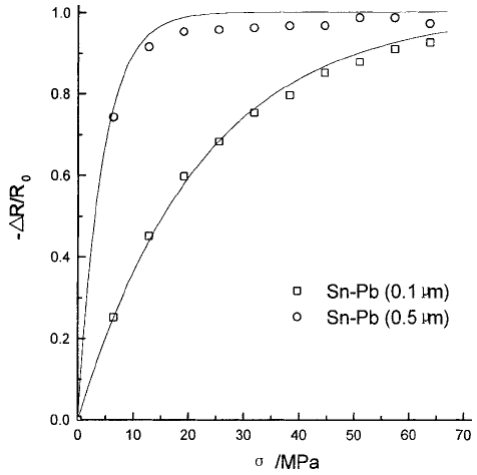

Figure 2.32 Fractional resistance change of (Φ=30%) of Sn-Pb/PS composites under uniaxial pressure [140]

In addition to fibrous and mostly spherical particle fillers, Gordon *et al*. evaluated the unidirectional piezoresistive behavior of single and two lamina carbon fiber epoxy composites under tensile strain. While single lamina showed positive piezoresistance with the GF of +2; two-lamina composite showed negative piezoresistance with the GF of -6. Reason was assumed to be caused by the change in the number of the contact points under strain. In the case of single lamina, dominant mechanism was reported to be the breakage of the conducting network with the effect of strain. On the other hand, for two-lamina composite, laminates come closer under tension and formation of new conducting network was achieved. For both composites, behavior was found linear and reversible which is caused form the continuous nature of the fillers [167]. In order to compare the fillers, another study

was carried out by Shui *et al*. They have used polyether sulfone (PES) as a matrix, and CF and carbon filament as filler with the diameters of 0.1 μm and 10 μm respectively. Carbon filament containing composite was found to show more linear piezoresistance with less noise. However, CF containing composites showed higher change in resistance at similar strain values. Robust structure of CF gives rise to separate easily [163].

Zhu *et al*., investigated the effect of filler type on the temperature dependent electrical behavior of CPCs [68]. In the study they have used carbon black (CB), vapor-grown carbon fiber (CF), and carbon nanotube (CNT) with polyethylene (PE). Charge transport mechanism was found to be depended on the filler type and geometry. CB was reported to be the most sensitive filler in terms of resistance change. As shown in Fig. 2.33, while CB and CF containing composites showed NTC before the melting temperature of the polymer, CNT/PE composites did not show any significant change in the resistance because polymer expansion was not sufficient to destruct the conducting network.

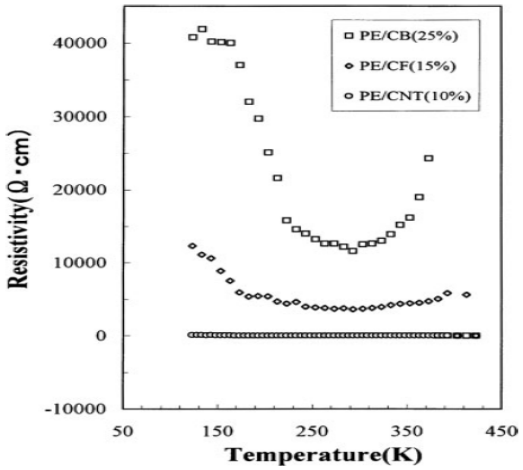

Figure 2.33 Temperature dependence of resistivities for the PE/CB, PE/CF, and PE/CNT composites with the indicated carbon contents [68].

Because of their limitations mentioned above, metallic fillers are not commonly preferred for piezoresistive composites. However different metallic fillers were reported in the literature including Ni [149,157,168], Ni coated Ag [149], Zn [169], Sn-Pb alloy, copper, aluminum [140], with the aim of using as a strain or compression sensor. As in all types of fillers, inherent conductivity and filler geometry are the most important factors for the conducting network formation and piezoresistive behaviour. Since all metals have different nature and conductivity, they will show different piezoresistive behavior. Zhang *et al.*, used copper and aluminum as fillers and PE, PS, epoxy as matrixes. According to their outcomes, Al filled composite showed higher sensitivity than that of Cu's under pressure and this was attributed to the differences in potential barrier height of two different metals [140]. Since metallic fillers are under risk of oxidation, they can be coated by other materials in order to prevent oxidation and enhance the electrical properties. Kchit and Bossis, used two different silicone with two different metallic fillers; nickel and nickel coated silver and observed negative piezoresistance with the effect of pressure [149]. Another study with Ni and elastomeric matrixes was carried out by Bloor *et al*. and samples were found to show negative piezoresistance under strain, pressure and bending. The highest magnitude of the resistivity change was reported around 1014 under pressure [157]. Abyaneh and Kulkarni, reported Zn–PDMS composites which showed negative pressure coefficient (NPC) under compression. The resistivity change was given about seven orders of magnitude around 4MPa with a good repeatability [169].

Unlike metallic fillers, ICPs are rarely used for the piezoresistive sensors because of their insoluble, instable and brittle structure. Polypyrrole (PPy) [159] and polyaniline (PANI) [27,158,160] are the most used ICPs for CPCs and piezoresistive composites.

Brady *et al*., developed PPy coated polyurethane (PU) foam which can be used as a pressure sensor. Conducting PU foam was found to show good stability against mechanical effects occurred during washing and reported to be used as a textile based pressure sensor. As shown in Fig. 2.34, resistance increased by the compression and magnitude of the change in resistance depends on the applied pressure [159].

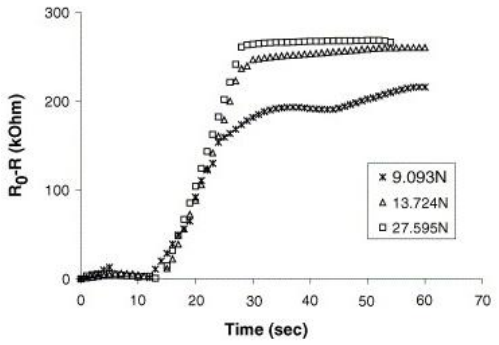

Figure 2.34 Normalised (R_0 − R) trace of PPy coated PU foam under different pressure values [159]

Dopant materials are of importance in terms of electrical properties of the ICPs. In order to investigate the dopant factor, Kar *et al.*, prepared PANI by two different dopants; HCl or dodecyl benzene sulfonic acid (DBSA) and mixed both PANIs with styrene–butadiene–styrene (SBS) elastomeric matrix. Although both composites reported to be used as piezoresistive pressure sensors because of their NPC behavior; some distinctions were

demonstrated in terms of piezoresistive sensitivity and morphology. As shown in Fig. 2.35, while DBSA doped PANI showed more uniform morphology, HCl doped PANI showed phase segregation which was assumed to be the reason for more sensitive piezoresistive behavior [160].

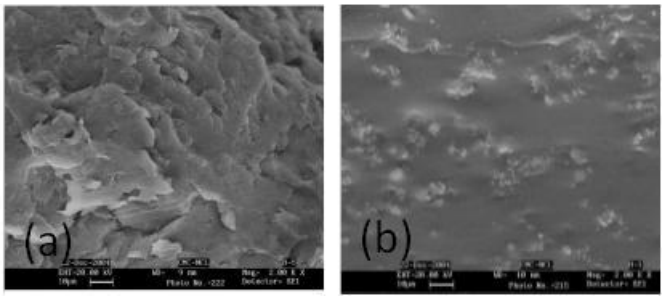

Figure 2.35 SEM images of PANI: (a) DBSA doped and (b) HCl doped [160]

Kalasad *et al*. designed conducting composite with PANI and cis-1,4-polyisoprene and investigated the effect of compression and temperature on the conductivity of the samples.

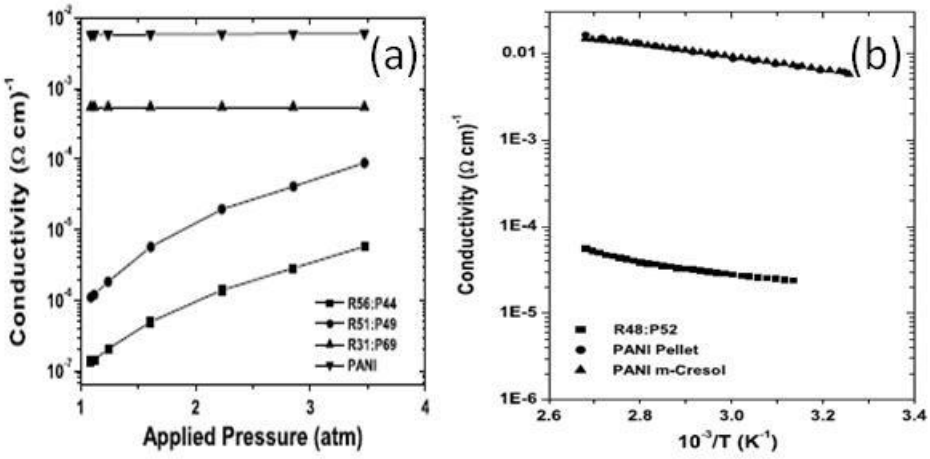

Figure 2.36 Change in conductivity with the effect of (a) compression and (b) temperature [27]

As shown in Fig. 2.36, increase in the applied pressure leads to NPC. On the other hand, increase in the temperature give rise to PTC which was attributed to the water decrease in the water content in PANI [27].

Castro *et al*. designed DBSA-doped polyaniline and poly(n-butyl methacrylate) composite and evaluated the piezoresistive behavior under tensile strain at different PANI concentrations. As reported, samples with PANI content (4 and 5 wt%) close to percolation concentration showed positive piezoresistance and were found more sensitive piezoresistive behavior than higher PANI containing samples (10 and 15 wt%) [158].

Carbon fibers are one of the most used conducting materials used for piezoresistive composites in the form of filament/continuous [163], short [67,118,162], chopped fiber [52], laminates [52,133] or woven fabrics [52]. Wang *et al.* investigated the piezoresistive behavior of short carbon fiber filled epoxy composites under tension and compression. While positive piezoresistance was observed for the samples under tension; compressed samples showed negative piezoresistance. Gauge factors were reported as 6-23 under tension and 29-31 under compression [162]. Das *et al*., used short CF, ethylene-propylene-diene rubber (EPDM), ethylene-vinyl acetate copolymer (EVA). According to their outcomes, polymer type, filler concentration, degree of strain and strain rate are of importance in terms of piezoresistive behavior of the composites [118]. Shui *et al*., used CF and carbon filament in order to compare the piezoresistive behavior of two different fillers with the diameters of 0.1 μm and 10 μm, respectively. Carbon filament containing composite was found to show more linear piezoresistance with less noise [163]. In addition to fibers and filaments, some studies are carried by using continuous carbon fiber laminates [133]. In order to determine the

piezoresistance in different directions, they have used different electrode configurations for various current introductions. Depending on the measurement configuration, while unidirectional composites showed positive GF -89 to +20.5; multidirectional laminates showed GF -7.1 to 11.19 [133]. Another interesting study was carried out by Boschetti-de-Fierro *et al.*, they have used chopped, unidirectional and bi-directional continuous carbon fiber. As reported, chopped fiber was found to show a linear piezoresistive behavior [52].

2.3.2.2 Filler concentration

As mentioned earlier, filler concentration is extremely important for obtaining a conducting system. Since filler-filler and filler/polymer interspacing and interaction ratio directly affected by filler concentration, piezoresistive behavior of the CPC is also affected [140,158,165,168,170,171]. Based on percolation theory, piezoresistive behavior can be evaluated in main three regions as shown in Fig. 2.37.

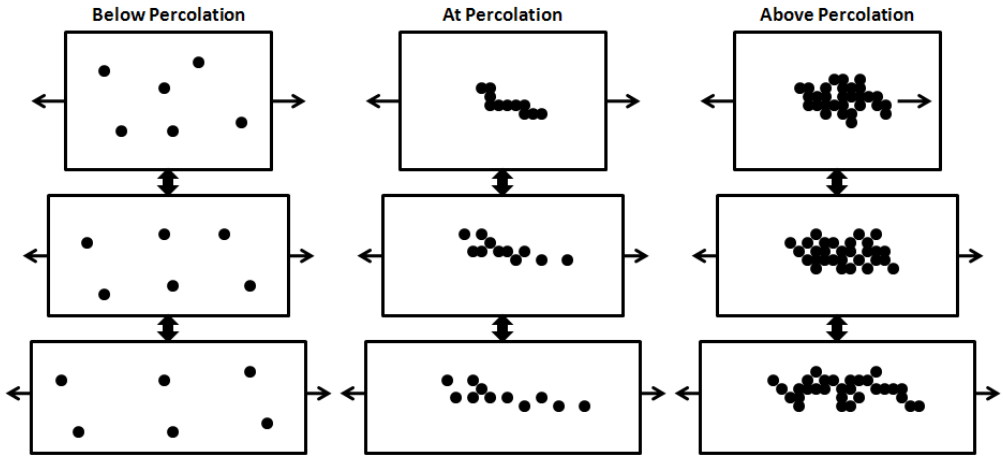

Figure 2.37 Effect of filler concentration on piezoresistive behavior of CPCs under strain

If the filler concentration is far below the percolation threshold, resistance of the composite will be more close to resistance of the polymeric matrix so even if there is a change in the resistance, determination of low value signal can be difficult. When the filler concentration is far above the percolation threshold, very low resistance output can be affected by the contact resistance [165] or it can be difficult to break-down the conducting network under low strain or pressure values [140,170-172]. However, piezoresistive behavior in percolation region was reported to show better piezoresistive behavior than other regions. Since percolation threshold is the concentration at which conducting network starts to form, composite is more sensitive to any external effect and any change in the filler-filler distance or resistance can be determined easier with a higher sensitivity [131,158,171].

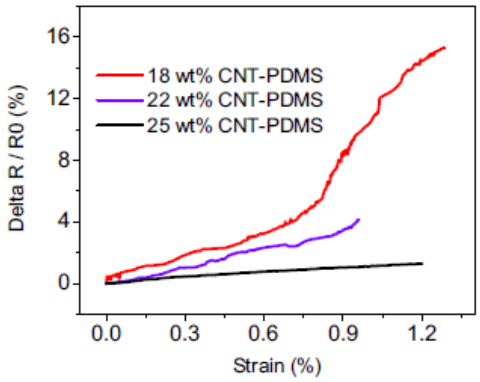

Figure 2.38 Piezoresistive behavior of CNT filled PDMS composites at different filler contents [165]

Lu *et al*., investigated the effect of filler concentration on piezoresistive behavior of CNT-PDMS composites under different strain values. As shown in Fig. 2.38, 18 wt% CNT containing composite, which is closer to percolation threshold, was found more sensitive to

strain change than the others. This was assumed to be caused from the dominant mechanism of destruction of conducting network which is more dominant at relatively lower concentrations of CNT [165]. Similar behavior was also observed for ICP filled CPCs. Castro *et al*., studied the response of the PANI/PBMA composites under different strain values at different PANI concentrations. As shown in Fig. 2.39, lower filler containing composites are more sensitive in terms of resistance change. On the other hand, at higher concentrations separation of conducting phase is more difficult than low concentrations [158].

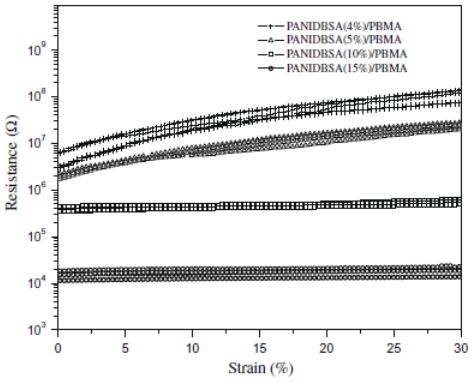

Figure 2.39 Piezoresistive behavior of PANI/PBMA composites at different filler contents [158]

Beruto *et al*., investigated the piezoresistive behavior of graphite filled silicone composites in the range of percolation region (25–35%) under compression. As shown in Fig. 2.40, although all the composites showed NPC, and reached a stable regime after some time, magnitude of the resistance change depends on filler concentration and decreases after percolation threshold. In addition to this, filler concentrations below percolation threshold

require higher compression values in order to show the same resistance mainly because of higher filler-filler distance [171].

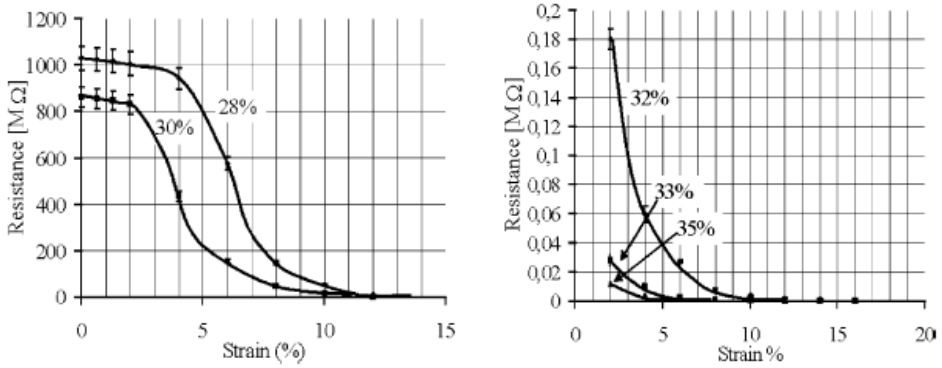

Figure 2.40 Piezoresistive behavior of graphite/silicone composites at different concentrations under compression [171]

Lu *et al*., investigated the piezoresistive behavior of graphite nanosheet filled high density polyethylene (GN/HDPE). As shown in Fig. 2.41, all composites showed the similar behavior, NPC followed by PPC.

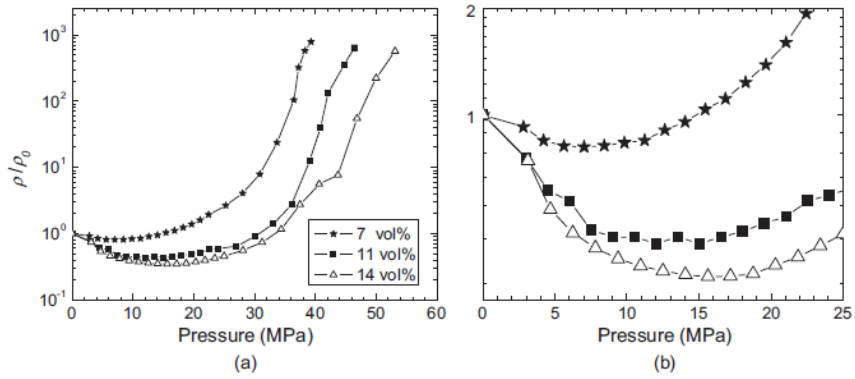

Figure 2.41 Piezoresistive behavior of HDPE/GN composites at different concentrations under compression [131]

However lower filler containing composites were found to show dominant mechanism of filler separation from lower compression values when compared with higher filler containing composites which is a result of higher filler-filler distance. Similar results were also reported by Chen *et al*., with graphite nanosheet and silicone rubber composites that lower filler concentration lead to higher sensitivity in terms of resistance change as given in Fig. 2.42 [144]. Luheng *et al*., prepared carbon black filled silicone rubber composites with different filler contents and investigated the piezoresistive behavior under compression [170,172]. As shown in Fig. 2.43 and 2.44, piezoresistive behavior is affected by the filler concentration. Although all three samples showed NPC at the beginning with the increase of the magnitude of the compression, their behavior changed to PPC at a critical pressure.

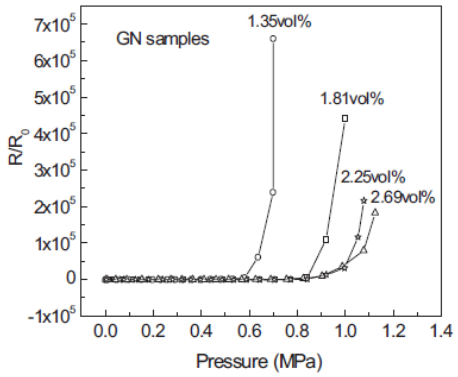

Fiure 2.42 Piezoresistive behavior of graphite nanosheet/silicone rubber composites at different concentrations under compression [144]

As shown in Fig. 2.43 and 2.44, critical pressure is affected by filler concentration. Higher filler concentration leads to higher critical pressure.

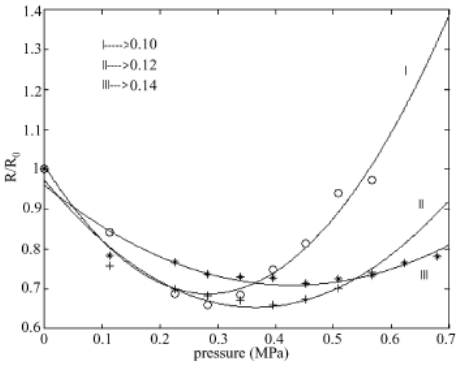

Figure 2.43 Piezoresistive behavior of carbon filled silicone rubber composites at different filler contents [172]

Because, increase in the filler amount decreases the filler-filler gap and requires higher values in order to break the conducting network. In addition to this, low filler content leads to more sensitive CPCs in terms of resistance change [170,172].

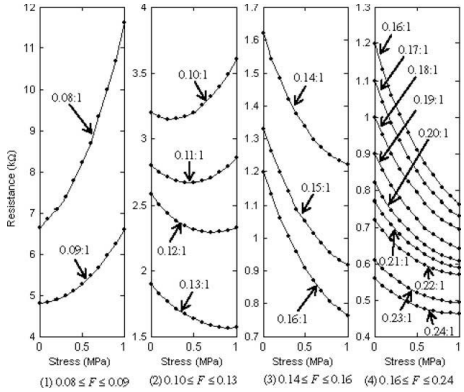

Figure 2.44 Effect of filler concentration on piezoresistive behavior of CB/silicone rubber composites [170]

Wang and Ding also obtained lower sensitivity for the lower concentrations of filler for carbon black-silicone rubber composites under compression (see Fig. 2.45). All the

composites showed NPC at the beginning followed by a constant-stable resistance which is probably caused from the high amount of the filler. Unlike the composites loaded with low amount of filler, dominant mechanism is not the breakage of the conducting network and filler separation is more difficult [173,174].

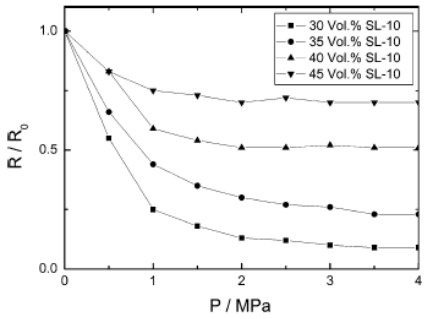

Figure 2.45 Piezoresistive behavior of CB/SR composites at different filler loading [173]

In addition to pressure and strain effects, Lu *et al*., investigated the effect of filler concentration on piezoresistance of MWCNT-PDMS composites under different temperatures [165].

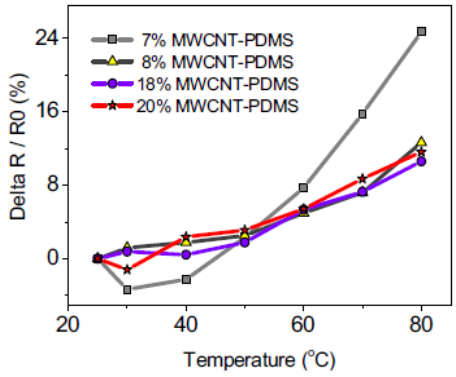

Figure 2.46 Changing of relative resistance for different MWCNT-PDMS composites at different temperatures [165]

As shown in Fig. 2.46, at higher temperatures, lower filler concentration leads to higher change in resistance. On the other hand, for higher filler concentrations, filler separation and reformation of conducting networks occur together and affects the rate of the change in resistance [165].

2.3.2.3 Matrix properties

Polymer properties such as molecular weight [89,92], crystallinity [92], polarity and surface tension [19,54,93] are of importance in terms of filler-matrix interaction, filler dispersion and filler-filler distance. Although these criteria seem to only affect the electrical behavior of the composite, they also affect the response of the polymer under different external factors. Depending on the type of the external factor, some polymer properties govern the mechanism of piezoresistance. While for strain and pressure sensing, mechanical and elastic properties of the polymers come forward; for temperature sensors thermal properties such as thermal expansion coefficient, of the polymer is taken into consideration. On the other hand for gas sensors glass transition- melting temperature, solubility and swelling degree of the polymer in a specific vapor become the deterministic polymer property [161].

The role of the polymeric matrix for pressure and strain sensors stem from different elongation and compressibility of fillers and polymers. Generally, fillers are stiffer than polymers and their movement and orientation in the composite might be affected by the polymer. At that point compressibility and modulus of the polymer come forward. Since, the response of a soft and stiff polymer under same strain or pressure is not same; difference in viscoelastic properties might affect the movement and orientation of the fillers in the matrix

[130]. While stiff/brittle polymers might restrict the filler movement, elastomeric polymers give more chance of rotation and orientation by the effect of polymer chain orientation [138]. Another important point to be taken into consideration is the effect of polymer type on the percolation behavior of the composite. Since percolation region is the most sensitive region in terms of the piezoresistive behavior, sensors are generally chosen from this region. Depending on the content of the filler throughout the composite, composites might show different piezoresistive behavior. As shown in Fig. 2.29 [131] and Fig. 2.42 [34] even if the same filler was used, percolation threshold was reported to be higher for HDPE than silicone rubber which might stem from polymer type and processing. While HDPE showed both NPC and PPC; silicone rubber showed PPC even at lower compression values [34,131].

Kchit and Bossis investigated the effect of polymeric matrix type on the piezoresistaive character of nickel coated silver containing composites. They have used commercial elastomer silicones RTV141 and silicone RTV1062 [149].

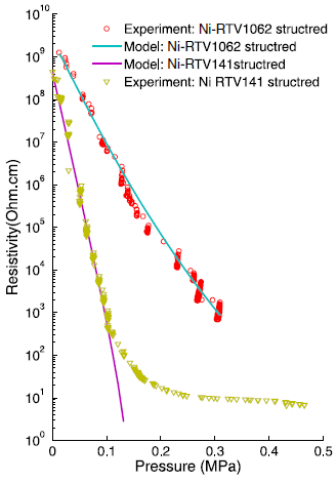

Figure 2.47 Piezoresistance of composites with the same volume fraction (30%) [149].

As shown in Fig. 2.47 RTV141 was found to be more sensitive under the same compression values and this was attributed to the distinction in the energy adsorption property of the polymer on conducting filler [149].

Dong *et al*., used poly(methyl methacrylate) (PMMA), poly(butyl methacrylate) (PBMA) and poly (2-ethylhexylmethacrylate) (PEHMA) and investigated the effect of type of polymeric matrix on the piezoresistive behavior of CB filled composites under different vapor exposure. As shown in Fig. 2.48, PEHMA was found to be the most sensitive composite in terms of resistance change and followed by PBMA and PMMA. This behavior was attributed to the difference in the viscosity and T_g of the polymers. These properties not only affect the dispersability of the filler in the matrix during processing but also diffusion of solvent vapor. Polymers with lower viscosity or T_g lead to higher solvent diffusion and higher sensitivity with lower response time [161].

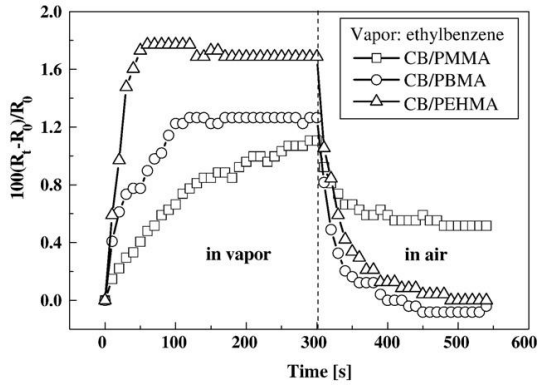

Figure 2.48 Piezoresistive behavior of CB filled polymethacrylate composites under the exposure of ethyl benzene vapor [161].

Zhu *et al*., used low-molecular-weight polyethylene (LMWPE) and high-molecular-weight polyethylene (HMWPE) as polymeric matrix and CB as filler and investigated the piezoresistive behavior under different temperatures for different ratios of LMWPE/HMWPE blends. As shown in Fig. 2.49, CB/LMWPE and CB/HMWPE showed different piezoresistance. While 100% LMWPE showed increase in resistance with the increase in the temperature; HMWPE did not show any significant change [68].

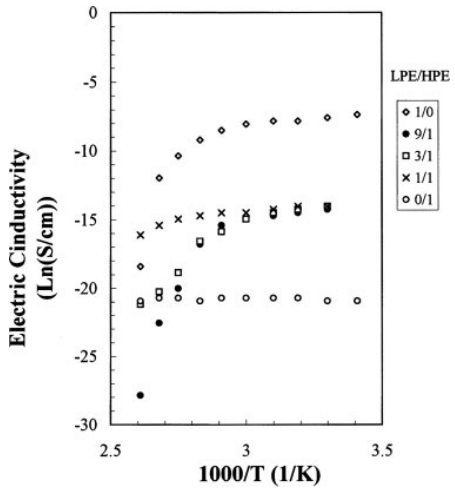

Figure 2.49 Piezoresistive behavior of CB (13 wt%) filled LMWPE/HMWPE composites [68]

Conclusions

This review study provides detailed overview about the basic concepts of conductive and piezoresistive polymer composites in order to develop a background for textile based piezoresistive sensors that have attracted considerable scientific and commercial interest because of their potential for health monitoring, posture monitoring, rehabilitation, *etc*.

Conductive polymer composites are alternative materials for piezoresistive sensors because of their tunable properties. They present superior piezoresistive sensing character compared with traditional metal and semiconductor sensors in terms of their flexible and lightweight structure. In addition to these, easy processing, lower cost, high strength, chemical resistance are the reasons for increasing demand to these materials. They can be used for many applications including strain, pressure and temperature sensors. Piezoresistive response is basically affected by two factors as external and structural. While external factors are testing and environmental conditions; structural factors are determined by the composition of the composites. Although various conductive materials can be used for piezoresistive sensors, nanofillers have become promising materials for obtaining relatively lower percolation threshold and higher sensitivity in terms of piezoresistive response. However they have some challenges during processing such as filler dispersion. In order to achieve the best piezoresistive response, material composition, processing and testing conditions are the most important parameters that should be taken into consideration.

References

[1] Forrest S, Burrows P, Thompson M. The dawn of organic electronics. IEEE Spectrum 2000;37:29-34.

[2] Forrest SR. The path to ubiquitous and low-cost organic electronic appliances on plastic. Nature 2004;428:911-8.

[3] Berggren M, Nilsson D, Robinson ND. Organic materials for printed electronics. Nat Mater 2007;6:3-5.

[4] Forrest SR, Thompson ME. Introduction: Organic electronics and optoelectronics. Chem Rev 2007;107:923-5.

[5] Gilleo K. Polymer thick film. New York: Van Nostrand Reinhold, 1996.

[6] Shaw JM, Seidler PF. Organic electronics: Introduction. IBM J Res Dev 2001;45:3-9.

[7] Jakobsson FLE, Crispin X, Colle M, Buchel M, de Leeuw DM, Berggren M. On the switching mechanism in Rose Bengal-based memory devices. Org Electron 2007;8:559-65.

[8] Dimitrakopoulos CD, Malenfant PRL. Organic thin film transistors for large area electronics. Adv Mater 2002;14:99.

[9] Mitzi DB, Chondroudis K, Kagan CR. Organic-inorganic electronics. IBM J Res Dev 2001;45:29-45.

[10] Burgi L, Pfeiffer R, Mucklich M, Metzler P, Kiy M, Winnewisser C. Optical proximity and touch sensors based on monolithically integrated polymer photodiodes and polymer LEDs. Org Electron 2006;7:114-120.

[11] Shirakaw H, and Ikeda S. Infrared spectra of poly(acetylene). Polym J 1971;2:231.

[12] Pionteck J. Handbook of antistatics. Toronto: Chem Tec Pub 2007.

[13] Gul VE. Structure and properties of conducting polymer composites. Netherlands: VSP, 1996.

[14] Koul S, Chandra R, Dhawan SK. Conducting polyaniline composite for ESD and EMI at 101 GHz. Polymer 2000;41:9305-9310.

[15] Kroschwitz JI. Electrical and electronic properties of polymers : a state-of-the-art compendium. New York: Wiley, 1988.

[16] Rupprecht L. Conductive polymers and plastics in industrial applications. Norwich, NY: Plastics Design Library, 1999.

[17] Chiang CK, Fincher CR, Park YW, Heeger AJ, Shirakawa H, Louis EJ et al. Electrical-Conductivity in Doped Polyacetylene. Phys Rev Lett 1977;39:1098-1101.

[18] Wang M. Carbon black : science and technology. New York: Dekker, 1993.

[19] White JR. Short fibre-polymer composites. Cambridge, England: Woodhead Pub, 1996.

[20] Stauffer D. Introduction to percolation theory. London ; Washington, DC: Taylor & Francis, 1992.

[21] Sahimi M. Applications of percolation theory. London ; Bristol, PA: Taylor & Francis, 1994.

[22] Sahimi M. Flow and transport in porous media and fractured rock : from classical methods to modern approaches. Weinheim ; New York: VCH, 1995.

[23] Clerc JP, Podolskiy VA, Sarychev AK. Precise determination of the conductivity exponent of 3D percolation using exact numerical renormalization. Eur Phys J B 2000;15:507-516.

[24] Sichel EK. Carbon black-polymer composites : the physics of electrically conducting composites. New York: M. Dekker, 1982.

[25] Sheng P. Fluctuation-induced tunneling conduction in disordered materials. Phys Rev B 1980;21:2180-2195.

[26] Toker D, Azulay D, Shimoni N, Balberg I, Millo O. Tunneling and percolation in metal-insulator composite materials. Phys Rev B 2003;68:041403.

[27] Kalasad MN, Gadyal MA, Hiremath RK, Ikram IM, Mulimani BG, Khazi IM et al. Synthesis and characterization of polyaniline rubber composites. Composites Sci Technol 2008;68:1787-1793.

[28] Strumpler R, Glatz-Reichenbach J. Conducting polymer composites. J Electroceram 1999;3:329-346.

[29] Balberg I. Tunneling and nonuniversal conductivity in composite materials. Phys Rev Lett 1987;59:1305-8.

[30] Balberg I. A comprehensive picture of the electrical phenomena in carbon black-polymer composites. Carbon 2002;40:139-43.

[31] Jana PB, Chaudhuri S, Pal AK, De SK. Electrical conductivity of short carbon fiber-reinforced polychloroprene rubber and mechanism of conduction. Polym Eng Sci 1992;32:448-56.

[32] Thongruang W, Balik CM, Spontak RJ. Volume-exclusion effects in polyethylene blends filled with carbon black, graphite, or carbon fiber. J Polym Sci Pt B-Polym Phys 2002;40:1013-1025.

[33] Park J, Kim D, Kim S, Kim P, Yoon D, DeVries KL. Inherent sensing and interfacial evaluation of carbon nanofiber and nanotube/epoxy composites using electrical resistance measurement and micromechanical technique. Compos Pt B-Eng 2007;38:847-861.

[34] Chen L, Chen G, Lu L. Piezoresistive behavior study on finger-sensing silicone rubber/graphite nanosheet nanocomposites. Adv Funct Mater 2007;17:898-904.

[35] Pantea D, Darmstadt H, Kaliaguine S, Summchen L, Roy C. Electrical conductivity of thermal carbon blacks, influence of surface chemistry. Carbon 2001;39:1147-1158.

[36] Zeng Y, Liu P, Du J, Zhao L, Ajayan PM, Cheng H. Increasing the electrical conductivity of carbon nanotube/polymer composites by using weak nanotube-polymer interactions. Carbon 2010;48:3551-3558.

[37] Ismagilov ZR, Shalagina AE, Podyacheva OY, Ischenko AV, Kibis LS, Boronin AI et al. Structure and electrical conductivity of nitrogen-doped carbon nanofibers. Carbon 2009;47:1922-1929.

[38] Costa P, Silva J, Sencadas V, Costa CM, van Hattum FWJ, Rocha JG et al. The effect of fibre concentration on the alpha to beta-phase transformation, degree of crystallinity and electrical properties of vapour grown carbon nanofibre/poly(vinylidene fluoride) composites. Carbon 2009;47:2590-2599.

[39] Hammel E, Tang X, Trampert M, Schmitt T, Mauthner K, Eder A et al. Carbon nanofibers for composite applications. Carbon 2004;42:1153-8.

[40] Pegel S, Poetschke P, Petzold G, Alig I, Dudkin SM, Lellinger D. Dispersion, agglomeration, and network formation of multiwalled carbon nanotubes in polycarbonate melts. Polymer 2008;49:974-84.

[41] Vaddiraju S, Cebeci H, Gleason KK, Wardle BL. Hierarchical multifunctional composites by conformally coating aligned carbon nanotube arrays with conducting polymer. ACS Appl Mater Interfaces 2009;1:2565-72.

[42] Jiang HJ, Moon KS, Li Y, Wong CP. Surface functionalized silver nanoparticles for ultrahigh conductive polymer composites. Chem Mat 2006;18:2969-73.

[43] Mrozek RA, Cole PJ, Mondy LA, Rao RR, Bieg LF, Lenhart JL. Highly conductive, melt processable polymer composites based on nickel and low melting eutectic metal. Polymer 2010;51:2954-8.

[44] Gelves GA, Lin B, Sundararaj U, Haber JA. Electrical and rheological percolation of polymer nanocomposites prepared with functionalized copper nanowires. Nanotechnology 2008;19:215712.

[45] Yao Q, Chen L, Zhang W, Liufu S, Chen X. Enhanced thermoelectric performance of single-walled carbon nanotubes/polyaniline hybrid nanocomposites. ACS Nano 2010;4:2445-51.

[46] Wen S, Chung DDL. Pitch-matrix composites for electrical, electromagnetic and strain-sensing applications. J Mater Sci 2005;40:3897-903.

[47] Ting JM, Lake ML. Vapor-grown carbon-fiber-reinforced carbon composites. Carbon 1995;33:663-7.

[48] Lu W, Lin H, Chen G. Nonuniversal transport behavior in heterogeneous high-density polyethylene/graphite nanosheet composites. J Polym Sci Pt B-Polym Phys 2006;44:1846-52.

[49] Palmeri MJ, Putz KW, Brinson LC. Sacrificial bonds in stacked-cup carbon nanofibers: biomimetic toughening mechanisms for composite systems. ACS Nano 2010;4:4256-64.

[50] Ma P, Liu M, Zhang H, Wang S, Wang R, Wang K et al. Enhanced electrical conductivity of nanocomposites containing hybrid fillers of carbon nanotubes and carbon black. ACS Appl Mater Interfaces 2009;1:1090-6.

[51] Bhattacharya SK, Chaklader ACD. Review on metal-filled plastics 1. electrical-conductivity. Polym Plast Technol Eng 1982;19:21-51.

[52] Boschetti-de-Fierro A, Pardey R, Savino V, Mueller AJ. Piezoresistive behavior of epoxy matrix-carbon fiber composites with different reinforcement arrangements. J Appl Polym Sci 2009;111:2851-8.

[53] Endo M, Kim YA, Hayashi T, Nishimura K, Matusita T, Miyashita K et al. Vapor-grown carbon fibers (VGCFs) - Basic properties and their battery applications. Carbon 2001;39:1287-97.

[54] Huang JC, Wu CL. Processability, mechanical properties, and electrical conductivities of carbon black-filled ethylene-vinyl acetate copolymers. Adv Polym Technol 2000;19:132-9.

[55] Xanthos M. Functional fillers for plastics. Weinheim: Wiley-VCH, 2010.

[56] Lee BO, Woo WJ, Park HS, Hahm HS, Wu JP, Kim MS. Influence of aspect ratio and skin effect on EMI shielding of coating materials fabricated with carbon nanofiber/PVDF. J Mater Sci 2002;37:1839-43.

[57] Balogun YA, Buchanan RC. Enhanced percolative properties from partial solubility dispersion of filler phase in conducting polymer composites (CPCs). Composites Sci Technol 2010;70:892-900.

[58] Bigg DM. The effect of compounding on the conductive properties of EMI shielding compounds. Adv Polym Technol 1984;4:255-66.

[59] Kraus G, Svetlik JF. Electrical conductivity of carbon black-reinforced elastomers. J Electrochem Soc 1956;103:337-42.

[60] Cheng HKF, Sahoo NG, Pan Y, Li L, Chan SH, Zhao J et al. Complementary effects of multiwalled carbon nanotubes and conductive carbon black on polyamide 6. J Polym Sci Pt B-Polym Phys 2010;48:1203-12.

[61] Li Z, Zhang J, Chen S. Effect of carbon blacks with various structures on electrical properties of filled ethylene-propylene-diene rubber. J Electrostatics 2009;67:73-5.

[62] Higgins BA, Brittain WJ. Polycarbonate carbon nanofiber composites. Eur Polym J 2005;41:889-93.

[63] Musumeci AW, Silva GG, Liu J, Martens WN, Waclawik ER. Structure and conductivity of multi-walled carbon nanotube/poly(3-hexylthiophene) composite films. Polymer 2007;48:1667-78.

[64] Kim B, Lee J, Yu IS. Electrical properties of single-wall carbon nanotube and epoxy composites. J Appl Phys 2003;94:6724-8.

[65] Kodgire PV, Bhattacharyya AR, Bose S, Gupta N, Kulkarni AR, Misra A. Control of multiwall carbon nanotubes dispersion in polyamide6 matrix: An assessment through electrical conductivity. Chem Phys Lett 2006;432:480-5.

[66] Spitalsky Z, Tasis D, Papagelis K, Galiotis C. Carbon nanotube-polymer composites: Chemistry, processing, mechanical and electrical properties. Prog Polym Sci 2010;35:357-401.

[67] Flandin L, Chang A, Nazarenko S, Hiltner A, Baer E. Effect of strain on the properties of an ethylene-octene elastomer with conductive carbon fillers. J Appl Polym Sci 2000;76:894-905.

[68] Zhu D, Bin Y, Matsuo M. Electrical conducting behaviors in polymeric composites with carbonaceous fillers. J Polym Sci Pt B-Polym Phys 2007;45:1037-44.

[69] Yamanaka S, Fukuda T, Sawa G, Ieda M, Ito M, Seguchi T. Effect of filler concentration on electrical-conductivity and ultralow-frequency dielectric-properties. IEEE Trans Dielectr Electr Insul 1995;2:54-61.

[70] Ebnesajjad S. Surface treatment of materials for adhesion bonding. Norwich, NY, U.S.A.: William Andrew Pub, 2006.

[71] Lee S, Da S, Ogale AA, Kim M. Effect of heat treatment of carbon nanofibers on polypropylene nanocomposites. J Phys Chem Solids 2008;69:1407-10.

[72] Howe JY, Tibbetts GG, Kwag C, Lake ML. Heat treating carbon nanoribers for optimal composite performance. J Mater Res 2006;21:2646-52.

[73] Arlen MJ, Wang D, Jacobs JD, Justice R, Trionfi A, Hsu JWP et al. Thermal-electrical character of in situ synthesized polyimide-grafted carbon nanofiber composites. Macromolecules 2008;41:8053-62.

[74] Cortes P, Lozano K, Barrera EV, Bonilla-Rios J. Effects of nanofiber treatments on the properties of vapor-grown carbon fiber reinforced polymer composites. J Appl Polym Sci 2003;89:2527-34.

[75] Zheng W, Wong SC. Electrical conductivity and dielectric properties of PMMA/expanded graphite composites. Composites Sci Technol 2003;63:225-35.

[76] Sung JH, Kim HS, Jin HJ, Choi HJ, Chin IJ. Nanofibrous membranes prepared by multiwalled carbon nanotube/poly(methyl methacrylate) composites. Macromolecules 2004;37:9899-902.

[77] Kim H, Park BH, Yoon J, Jin H. Thermal and electrical properties of poly(L-lactide)-graft-multiwalled carbon nanotube composites. Eur Polym J 2007;43:1729-35.

[78] Datsyuk V, Kalyva M, Papagelis K, Parthenios J, Tasis D, Siokou A et al. Chemical oxidation of multiwalled carbon nanotubes. Carbon 2008;46:833-40.

[79] Barrau S, Demont P, Peigney A, Laurent C, Lacabanne C. DC and AC conductivity of carbon nanotubes-polyepoxy composites. Macromolecules 2003;36:5187-94.

[80] Choi YK, Gotoh Y, Sugimoto KI, Song SM, Yanagisawa T, Endo M. Processing and characterization of epoxy nanocomposites reinforced by cup-stacked carbon nanotubes. Polymer 2005;46:11489-98.

[81] Kotaki M, Wang K, Toh ML, Chen L, Wong SY, He CB. Electrically conductive epoxy/clay/vapor grown carbon fiber hybrids. Macromolecules 2006;39:908-11.

[82] Bin YZ, Kitanaka M, Zhu D, Matsuo M. Development of highly oriented polyethylene filled with aligned carbon nanotubes by gelation/crystallization from solutions. Macromolecules 2003;36:6213-9.

[83] Zhang QH, Rastogi S, Chen DJ, Lippits D, Lemstra PJ. Low percolation threshold in single-walled carbon nanotube/high density polyethylene composites prepared by melt processing technique. Carbon 2006;44:778-85.

[84] Lee J, Yang S, Jung H. Carbon nanotubes-polypropylene nanocomposites for electrostatic discharge applications. Macromolecules 2009;42:8328-34.

[85] Shekhar S, Prasad V, Subramanyam SV. Transport properties of conducting amorphous carbon-poly(vinyl chloride) composite. Carbon 2006;44:334-40.

[86] Xu YJ, Higgins B, Brittain WJ. Bottom-up synthesis of PS-CNF nanocomposites. Polymer 2005;46:799-810.

[87] Li JR, Xu JR, Zhang MQ, Rong MZ. Carbon black/polystyrene composites as candidates for gas sensing materials. Carbon 2003;41:2353-60.

[88] Meincke O, Kaempfer D, Weickmann H, Friedrich C, Vathauer M, Warth H. Mechanical properties and electrical conductivity of carbon-nanotube filled polyamide-6 and its blends with acrylonitrile/butadiene/styrene. Polymer 2004;45:739-48.

[89] Du FM, Scogna RC, Zhou W, Brand S, Fischer JE, Winey KI. Nanotube networks in polymer nanocomposites: rheology and electrical conductivity. Macromolecules 2004;37:9048-55.

[90] Guo H, Rasheed A, Minus ML, Kumar S. Polyacrylonitrile/vapor grown carbon nanofiber composite films. J Mater Sci 2008;43:4363-9.

[91] Niu X, Peng S, Liu L, Wen W, Sheng P. Characterizing and patterning of PDMS-based conducting composites. Adv Mater 2007;19:2682.

[92] Wessling B. Electrical conductivity in heterogeneous polymer systems (v) .1. further experimental-evidence for a phase-transition at the critical volume concentration. Synth Met 1991;41:1057-62.

[93] Al-Saleh MH, Sundararaj U. A review of vapor grown carbon nanofiber/polymer conductive composites. Carbon 2009;47:2-22.

[94] Sumita M, Abe H, Kayaki H, Miyasaka K. Effect of melt viscosity and surface-tension of polymers on the percolation-threshold of conductive-particle-filled polymeric composites. J Macromol Sci -Phys 1986;B25:171-84.

[95] Zhang W, Dehghani-Sanij AA, Blackburn RS. Carbon based conductive polymer composites. J Mater Sci 2007;42:3408-18.

[96] Tjong SC, Liang GD, Bao SP. Effects of crystallization on dispersion of carbon nanofibers and electrical properties of polymer nanocomposites. Polym Eng Sci 2008;48:177-83.

[97] Lu K, Grossiord N, Koning CE, Miltner HE, van Mele B, Loos J. Carbon nanotube/isotactic polypropylene composites prepared by latex technology: morphology analysis of cnt-induced nucleation. Macromolecules 2008;41:8081-5.

[98] Sau KP, Chaki TK, Khastgir D. Carbon fibre filled conductive composites based on nitrile rubber (NBR), ethylene propylene diene rubber (EPDM) and their blend. Polymer 1998;39:6461-71.

[99] Miyasaka K, Watanabe K, Jojima E, Aida H, Sumita M, Ishikawa K. Electrical conductivity of carbon polymer composites as a function of carbon content. J Mater Sci 1982;17:1610-6.

[100] Yamamoto T, Kubota E, Taniguchi A, Dev S, Tanaka K, Osakada K et al. Electrically conductive metal sulfide polymer composites prepared by using organosols of metal sulfides. Chem Mat 1992;4:570-6.

[101] Xu H, Dang Z, Shi D, Bai J. Remarkable selective localization of modified nanoscaled carbon black and positive temperature coefficient effect in binary-polymer matrix composites. J Mater Chem 2008;18:2685-90.

[102] Gubbels F, Jerome R, Teyssie P, Vanlathem E, Deltour R, Calderone A et al. Selective localization of carbon-black in immiscible polymer blends - a useful tool to design electrical conductive composites. Macromolecules 1994;27:1972-4.

[103] Wu GZ, Asai S, Sumita M, Yui H. Entropy penalty-induced self-assembly in carbon black or carbon fiber filled polymer blends. Macromolecules 2002;35:945-51.

[104] Zhang Q, Xiong H, Yan W, Chen D, Zhu M. Electrical conductivity and rheological behavior of multiphase polymer composites containing conducting carbon black. Polym Eng Sci 2008;48:2090-7.

[105] Li Y, Shimizu H. Conductive PVDF/PA6/CNTs nanocomposites fabricated by dual formation of cocontinuous and nanodispersion structures. Macromolecules 2008;41:5339-44.

[106] Thongruang W, Spontak RJ, Balik CM. Bridged double percolation in conductive polymer composites: an electrical conductivity, morphology and mechanical property study. Polymer 2002;43:3717-25.

[107] Buschow KHJ. Encyclopedia of materials : science and technology. 2001.

[108] Sharma SC, Sheshadri TS, Krishna M, Murthy HNN, Jose J. Influence of solvents on the mwcnt/adhesive grade epoxy nanocomposites preparation. J Reinf Plast Compos 2009;28:2805-12.

[109] Diez-Pascual AM, Naffakh M, Gomez MA, Marco C, Ellis G, Teresa Martinez M et al. Development and characterization of PEEK/carbon nanotube composites. Carbon 2009;47:3079-90.

[110] Geng Y, Liu MY, Li J, Shi XM, Kim JK. Effects of surfactant treatment on mechanical and electrical properties of CNT/epoxy nanocomposites. Compos Pt A-Appl Sci Manuf 2008;39:1876-83.

[111] Tang WZ, Santare MH, Advani SG. Melt processing and mechanical property characterization of multi-walled carbon nanotube/high density polyethylene (MWNT/HDPE) composite films. Carbon 2003;41:2779-85.

[112] Coleman JN, Khan U, Blau WJ, Gun'ko YK. Small but strong: A review of the mechanical properties of carbon nanotube-polymer composites. Carbon 2006;44:1624-52.

[113] Choi Y, Sugimoto K, Song S, Endo M. Production and characterization of polycarbonate composite sheets reinforced with vapor grown carbon fiber. Compos Pt A-Appl Sci Manuf 2006;37:1944-51.

[114] Lozano K, Bonilla-Rios J, Barrera EV. A study on nanofiber-reinforced thermoplastic composites (II): Investigation of the mixing rheology and conduction properties. J Appl Polym Sci 2001;80:1162-72.

[115] Kharchenko SB, Douglas JF, Obrzut J, Grulke EA, Migler KB. Flow-induced properties of nanotube-filled polymer materials. Nat Mater 2004;3:564-8.

[116] Lee S, Jeon Y. Effects of mixing on electrical properties of carbon nanofiber and polymer composites. J Appl Polym Sci 2009;113:2980-7.

[117] Li L, Chung DDL. Effect of viscosity on the electrical-properties of conducting thermoplastic composites made by compression molding of a powder mixture. Polym Compos 1993;14:467-72.

[118] Das NC, Chaki TK, Khastgir D. Effect of processing parameters, applied pressure and temperature on the electrical resistivity of rubber-based conductive composites. Carbon 2002;40:807-16.

[119] Feller JF. Conductive polymer composites: Influence of extrusion conditions on positive temperature coefficient effect of poly(butylene terephthalate)/poly(olefin)-carbon black blends. J Appl Polym Sci 2004;91:2151-7.

[120] Jiang XW, Bin YZ, Matsuo M. Electrical and mechanical properties of polyimide-carbon nanotubes composites fabricated by in situ polymerization. Polymer 2005;46:7418-24.

[121] Twardowski T. Introduction to nanocomposite materials: properties, processing, characterization. DEStech Publications, Inc., 2007.

[122] Koscho ME, Grubbs RH, Lewis NS. Properties of vapor detector arrays formed through plasticization of carbon black-organic polymer composites. Anal Chem 2002;74:1307-15.

[123] Motlagh GH, Hrymak AN, Thompson MR. Improved through-plane electrical conductivity in a carbon-filled thermoplastic via foaming. Polym Eng Sci 2008;48:687-96.

[124] Tang Q, Lin J, Wu J. The preparation and electrical conductivity of polyacrylamide/graphite conducting hydrogel. J Appl Polym Sci 2008;108:1490-5.

[125] Thomson W. On the electro-dynamic qualities of metals: Effects of magnetization on the electric conductivity of nickel and of iron. Proc R Soc Lond 1856;8:546-550.

[126] Smith CS. Piezoresistance effect in germanium and silicon. Physical Review 1954;94:42-9.

[127] Sun Y. Strain effect in semiconductors: theory and device applications. New York: Springer Dec. 2009, 2009.

[128] Harsányi G. Sensors in biomedical applications : fundamentals, technology & applications. Lancaster, Pa.: Technomic Pub Co, 2000.

[129] Cochrane C, Koncar V, Lewandowski M, Dufour C. Design and development of a flexible strain sensor for textile structures based on a conductive polymer composite. Sensors 2007;7:473-92.

[130] Zheng Q, Zhou JF, Song YH. Time-dependent uniaxial piezoresistive behavior of high-density polyethylene/short carbon fiber conductive composites. J Mater Res 2004;19:2625-34.

[131] Lu JR, Weng WG, Chen XF, Wu DJ, Wu CL, Chen GH. Piezoresistive materials from directed shear-induced assembly of graphite nanosheets in polyethylene. Adv Funct Mater 2005;15:1358-63.

[132] Chung DDL. Structural health monitoring by electrical resistance measurement. Smart Mater Struct 2001;10:624-36.

[133] Angelidis N, Wei CY, Irving PE. The electrical resistance response of continuous carbon fibre composite laminates to mechanical strain. Composites Part A: Applied Science and Manufacturing 2004;35:1135-47.

[134] Wang S, Chung DDL. Negative piezoresistivity in continuous carbon fiber epoxy-matrix composite. J Mater Sci 2007;42:4987-95.

[135] Shui XP, Chung DDL. A new electromechanical effect in discontinuous-filament elastomer-matrix composites. Smart Mater Struct 1997;6:102-5.

[136] Kost J, Narkis M, Foux A. Effects of axial stretching on the resistivity of carbon-black filled silicone-rubber. Polym Eng Sci 1983;23:567-71.

[137] Pramanik PK, Khastagir D, Saha TN. Effect of extensional strain on the resistivity of electrically conductive nitrile-rubber composites filled with carbon filler. J Mater Sci 1993;28:3539-46.

[138] Feng JY, Chan CM. Effects of strain and temperature on the electrical properties of carbon black-filled alternating copolymer of ethylene-tetrafluoroethylene composites. Polym Eng Sci 2003;43:1064-70.

[139] Zheng Q, Song YH, Yi XS. Piezoresistive properties of HDPE/graphite composites. J Mater Sci Lett 1999;18:35-7.

[140] Zhang XW, Pan Y, Zheng Q, Yi XS. Piezoresistance of conductor filled insulator composites. Polym Int 2001;50:229-36.

[141] Wang L, Ding T, Wang P. Effects of instantaneous compression pressure on electrical resistance of carbon black filled silicone rubber composite during compressive stress relaxation. Composites Sci Technol 2008;68:3448-50.

[142] Vidhate S, Chung J, Vaidyanathan V, D'Souza N. Time dependent piezoresistive behavior of polyvinylidene fluoride/carbon nanotube conductive composite. Mater Lett 2009;63:1771-3.

[143] Gau C, Ko HS, Chen HT. Piezoresistive characteristics of MWNT nanocomposites and fabrication as a polymer pressure sensor. Nanotechnology 2009;20:185503.

[144] Chen L, Lu L, Wu D, Chen G. Silicone rubber/graphite nanosheet electrically conducting nanocomposite with a low percolation threshold. Polym Compos 2007;28:493-8.

[145] Hirano S, Kishimoto A. Effect of heating rate on positive-temperature-coefficient-of-resistivity behavior of conductive composite thin films. Appl Phys Lett 1998;73:3742-4.

[146] Di WH, Zhang G, Xu JQ, Peng Y, Wang XJ, Xie ZY. Positive-temperature-coefficient/negative-temperature-coefficient effect of low-density polyethylene filled with a mixture of carbon black and carbon fiber. J Polym Sci Pt B-Polym Phys 2003;41:3094-101.

[147] Di WH, Zhang G. Resistivity-temperature behavior of carbon fiber filled semicrystalline composites. J Appl Polym Sci 2004;91:1222-8.

[148] Hindermann-Bischoff M, Ehrburger-Dolle F. Electrical conductivity of carbon black-polyethylene composites - Experimental evidence of the change of cluster connectivity in the PTC effect. Carbon 2001;39:375-82.

[149] Kchit N, Bossis G. Piezoresistivity of magnetorheological elastomers. J Phys -Condes Matter 2008;20:204136.

[150] Xiang Z, Chen T, Li Z, Bian X. Negative temperature coefficient of resistivity in lightweight conductive carbon nanotube/polymer composites. Macromol Mater Eng 2009;294:91-5.

[151] Chen SG, Hu JW, Zhang MQ, Li MW, Rong MZ. Gas sensitivity of carbon black/waterborne polyurethane composites. Carbon 2004;42:645-51.

[152] Dong XM, Fu RW, Zhang MQ, Zhang B, Rong MZ. Electrical resistance response of carbon black filled amorphous polymer composite sensors to organic vapors at low vapor concentrations. Carbon 2004;42:2551-9.

[153] Castro M, Lu J, Bruzaud S, Kumar B, Feller J. Carbon nanotubes/poly(epsilon-caprolactone) composite vapour sensors. Carbon 2009;47:1930-42.

[154] Tsubokawa N, Shirai Y, Okazaki M, Maruyama K. A novel gas sensor from crystalline polymer-grafted carbon black: responsibility of electric resistance of composite from crystalline polymer-grafted carbon black against solvent vapor. Polym Bull 1999;42:425-31.

[155] Chen JH, Tsubokawa N. Novel gas sensor from polymer-grafted carbon black: Vapor response of electric resistance of conducting composites prepared from poly(ethylene-block-ethylene oxide)-grafted carbon black. J Appl Polym Sci 2000;77:2437-47.

[156] Arshak K, Moore E, Lyons GM, Harris J, Clifford S. A review of gas sensors employed in electronic nose applications. Sens Rev 1 June 2004;24:181,198(18).

[157] Bloor D, Donnelly K, Hands PJ, Laughlin P, Lussey D. A metal-polymer composite with unusual properties. J Phys D-Appl Phys 2005;38:2851-60.

[158] Del Castillo-Castro T, Castillo-Ortega MM, Herrera-Franco PJ. Electrical, mechanical and piezo-resistive behavior of a polyaniline/poly(n-butyl methacrylate) composite. Compos Pt A-Appl Sci Manuf 2009;40:1573-9.

[159] Brady S, Diamond D, Lau KT. Inherently conducting polymer modified polyurethane smart foam for pressure sensing. Sens Actuator A-Phys 2005;119:398-404.

[160] Radhakrishnan S, Kar SB. Role of non-linear processes in conducting polymer blends for piezo-sensors Part 2: Studies on polyaniline/SBS blends. Sens Actuator A-Phys 2005;120:474-81.

[161] Dong XM, Luo Y, Xie LN, Fu RW, Zhang MQ. Conductive carbon black-filled polymethacrylate composites as gas sensing materials: Effect of glass transition temperature. Thin Solid Films 2008;516:7886-90.

[162] Wang XJ, Chung DDL. Short-carbon-fiber-reinforced epoxy as a piezoresistive strain sensor. Smart Mater Struct 1995;4:363-7.

[163] Shui XP, Chung DDL. A piezoresistive carbon filament polymer-matrix composite strain sensor. Smart Mater Struct 1996;5:243-6.

[164] Paleo AJ, Hattum FWJ, Rocha JG, Lanceros-Mendez S. Piezoresistive polypropylene/carbon nanofiber composites as mechanical transducers. Microsyst Technol 2012;18:591-597.

[165] Lu J, Lu M, Bermak A, Lee Y. Study of Piezoresistance Effect of carbon nanotube-pdms composite materials for nanosensors. New York, USA: IEEE, 2007.

[166] Estrada Moreno IA, Diaz Diaz A, Mendoza Duarte ME, Ibarra Gomez R. Strain effect on the electrical conductivity of CB/SEBS and GP/SEBS composites. Macromol Symp 2009;283-84:361-8.

[167] Gordon DA, Wang SK, Chung DDL. Piezoresistivity in unidirectional continuous carbon fiber polymer-matrix composites: single-lamina composite versus two-lamina composite. Compos Interfaces 2004;11:95-103.

[168] Ausanio G, Barone AC, Campana C, Iannotti V, Luponio C, Pepe GP et al. Giant resistivity change induced by strain in a composite of conducting particles in an elastomer matrix. Sens Actuator A-Phys 2006;127:56-62.

[169] Abyaneh MK, Kulkarni SK. Giant piezoresistive response in zinc-polydimethylsiloxane composites under uniaxial pressure. J Phys D-Appl Phys 2008;41:135405.

[170] Luheng W, Tianhuai D, Peng W. Influence of carbon black concentration on piezoresistivity for carbon-black-filled silicone rubber composite. Carbon 2009;47:3151-7.

[171] Beruto DT, Capurro M, Marro G. Piezoresistance behavior of silicone-graphite composites in the proximity of the electric percolation threshold. Sens Actuator A-Phys 2005;117:301-8.

[172] Wang Luheng, Ding Tianhuai, Wang Peng. Effects of conductive phase content on critical pressure of carbon black filled silicone rubber composite. Sens Actuator A-Phys 2007;135:587-92.

[173] Wang P, Ding T. Creep of electrical resistance under uniaxial pressures for carbon black-silicone rubber composite. J Mater Sci 2010;45:3595-601.

[174] Wang P, Ding T. Conductivity and piezoresistivity of conductive carbon black filled polymer composite. J Appl Polym Sci 2010;116:2035-9.

CHAPTER 3. TEXTILE BASED SENSORS

Abstract

This review study provides detailed overview about textile based sensors which are capable of sensing fundamental signals related to physiological and mechanical activities, including vital signs, of a human body with no discomfort to the subject. Second section is an overview about sensors and mechanism of sensing. In the third section, textile based sensors are classified according to their sensing mechanism such as capacitive, inductive, piezoelectric, optical, chemical and piezoreistive. In this section there is a focus on piezoresistive textile based sensors. Although newer concepts and applications of textile based sensors are developing at a very fast rate, this review includes the most important contributions in this area.

3.1 Introduction

Recent efforts in integrating electronic functionality in fibers and textiles have led to an entirely new field of research and product development dubbed as electronic textiles or e-textiles. Electronic textiles are functional textiles which offer aesthetic appearance as conventional textiles with the additional electronic functionality. Although research in the field of e-textiles started at the end of 1960s; the most important contributions have been made in the last two decades, in parallel with the advances in polymer-based flexible electronics and optics. In addition, design and development of functional polymers and

fibers have played a significant role in this development [1-3]. Electronic textiles include wearable-instrumented garments capable of sensing fundamental signals related to physiological and mechanical activities, including vital signs, of a human body with no discomfort to the subject are crucial to many applications including biomedicine, rehabilitation, and haptic interfaces.

Textiles (garments and others products) constitute an obvious choice as multifunctional platforms because of many reasons, including, flexibility, lightweight, conformability, *etc.* Off-the-shelf electronic systems are often not ideal for integration in textiles because of their incompatible properties, such as bulk, rigidity, *etc.* and associated problems with wearability and lack of durability to washing, perspiration, *etc.* [2-6].

E-textiles can be classified according to their functions as passive smart, active smart textiles, and very smart. Passive smart textiles are mainly composed of sensory element which can only sense the changes in the environment. Active smart textiles have ability to sense and react. The third generation of the smart textiles has the ability of sensing, reacting and adapting to the environment [7-9]. Depending on the type and function of adapted/integrated electrical-electronic system, e-textiles may be capable of sensing, data processing, actuation, and energy storage or generation; integrated sensing capability with flexibility and environmental stability is a key element for future e-textile products. Ideal textile based sensors should be able to provide an interface between user and the electronic system by converting any type of physiological or environmental signal into electrical signals [1,2,10-20]. Such sensors can be readily used in many applications such as sports [21], medicine [12,14,18,22-26], communication [27], entertainment, and protection [15].

Although textile based sensors have many potential advantages over traditional semi-conductor based electronics, the flexibility of the textile substrate as well as number of other factors related to the application environment bring about a number of critical issues to be considered. Obviously, placement of a sensor is important for the reliability of the obtained data [4,5]. Sensors should be placed in/onto the best locations. While sensors which sense breathing or heart rate are generally placed around the chest [19,28], sweat sensors are located around the sweating area [20,29,30]. Even if sensors are located properly, if the garment is not well-fitted, sensory systems might easily move relative to any reference and the reliability and reproducibility of the data become questionable. Since textiles are layers between us and environment, we should also consider the environmental effects like temperature, humidity, pressure, macro and micro climate around us for the accuracy of a textile based sensor. Both outer environment and body conditions can easily affect the results. In that sense, sensor materials and systems should be compatible with the environment and/or resistive to the environmental conditions. In addition to all these technical requirements, they should be simple, can be used easily, and care/maintenance process should not be complex, difficult and the most important point is the economical affordably of the system [2].

3.2 Principles of Sensing

Sensors are transducers that are capable of converting mechanical, chemical, optical, and other forms of stimuli into electrical signals. In other words, sensors are able to measure and convert the quantity of physical variable into an electrical signal [10,31]. Depending on the

system, common physical variable or stimulus can be any kind of condition in the form of force, temperature, length, strain, pressure, time, resistance, capacity, frequency, velocity, acceleration; and output signal can be voltage or current [10,31].

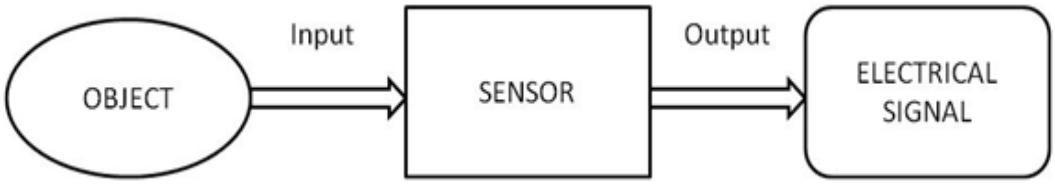

Figure 3.1 Mechanism of sensors

Sensors are used as a part of a system and can be located at any place in the system depending on the requirements and accuracy of the signals. Since the outputs of most sensors are relatively weak, and noisy, often it is necessary to amplify, condition and/or modify the output, through the help of conditioners, processors, filters, amplifiers, *etc.*, in order to generate useful information [10,31,32]. Ideally, sensors should be sensitive to the input stimulus, and should not influence the measured variable. May be the most important criteria is the sensor sensitivity which is the indication of change in the sensor's output as a function of input [10,31,32].

Sensors can be classified in a number of ways; such as contact/noncontact sensors, depending on the distance to the object; absolute/relative sensors depending on the chosen reference; and active/passive sensors depending on the requirement of external power, and finally based on the type of measured property. However, in a fundamental sense, the most useful classification can be based on the principle of sensing [10,31,32]. The principles discussed

here are not comprehensive by any means, but the following constitute the more relevant categories to the current topic.

3.2.1 Capacitive Sensors

Capacitive sensors are used for detection or monitoring of motion, proximity, position, flow, pressure, thickness, health monitoring, and electric field and so on. Changes in the system are followed by change in capacitance which is the ratio of the total charge to the potential difference for a given capacitor. A capacitor basically consists of a pair of conductors/metal plates separated by a dielectric material. Any change in the conductor area-size, distance or dielectric constant of the material directly affects the capacitance. In a capacitive sensory system, one of the conductor/metal plates is the sensor and the target is the other conductor/metal plate. In this case, a capacitive sensor system measures the current between a sensor and a material in terms of capacitance/electric field changes. If the sizes of the sensor and material are constant, any change in capacitance gives the change in distance [33].

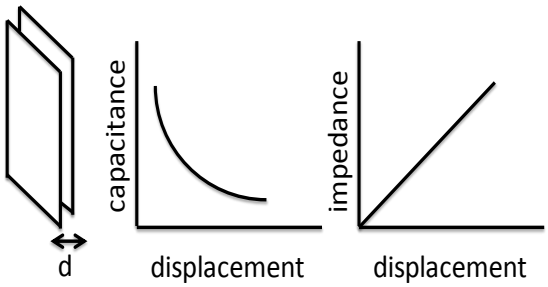

Figure 3.2 Capacitive sensor based on spacing variation [33]

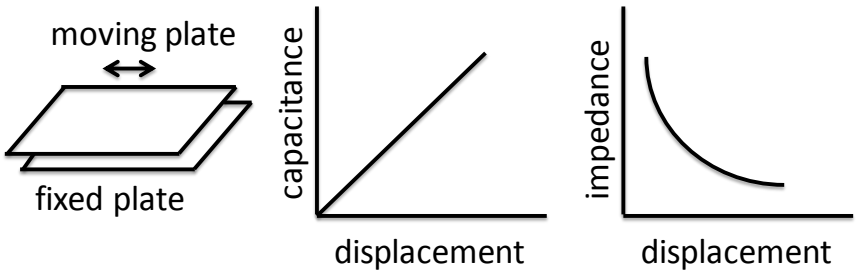

Figure 3.3 Capacitive sensor based on area variation [33]

Capacitive sensors could be either contact or non-contact type and are composed of a probe and a driver. While a probe is in charge of creating the sensing area; driver controls, and measures the sensing current. They are generally used to determine position of a conducting material or thickness, density of a non-conducting material. Recently, capacitive touch sensors become very popular for mobile devices, cell phones and mp3 players [10,32,33].

3.2.2 Inductive Sensors

Inductive sensors are generally used for determination of position, proximity in order to detect metallic materials in a non-contact mode. They can also be used to detect defects in conducting materials because of their ability to sense the structural changes of the material [10,32]. They operate according to the principle of inductance which is a characteristic of opposing any change in current.

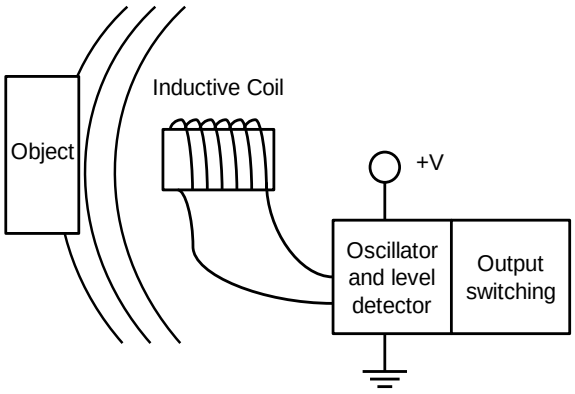

Figure 3.4 Inductive sensor and sensing mechanism

As shown in Fig. 3.4 an inductive sensor basically has four components: inductive coil, oscillator, detection circuit, and output circuit. Inductive sensors emit electromagnetic field generated by the oscillator, which penetrates and induces current in the material. Induced current creates its electromagnetic field which can be measured as a change in the field through the help of an induction loop/probe [10,32]. As shown in Fig. 3.4, if the target approaches to the inductive coil, an oscillator and a detection coil start to generate a magnetic field which induces Eddy currents. Eddy currents lead to generation of a magnetic field and affect the amplitude of the field produced by the sensor [10,32]. Type/structure of material, size of sensor and material, distance between them is of significance in terms of the obtained data [10,32].

3.2.3 Piezoelectric Sensors

Piezoelectric sensors are active sensors and used to determine pressure, acceleration, force or strain with the help of piezoelectric materials which can generate an electric potential when any mechanical stress is applied or conversely show mechanical deformation when electric

field is applied. This phenomenon is called piezoelectric effect and basically caused bythe change in polarization which is basically deformation of the crystal lattice and displacement of the ions in unit cells under any mechanical stress.

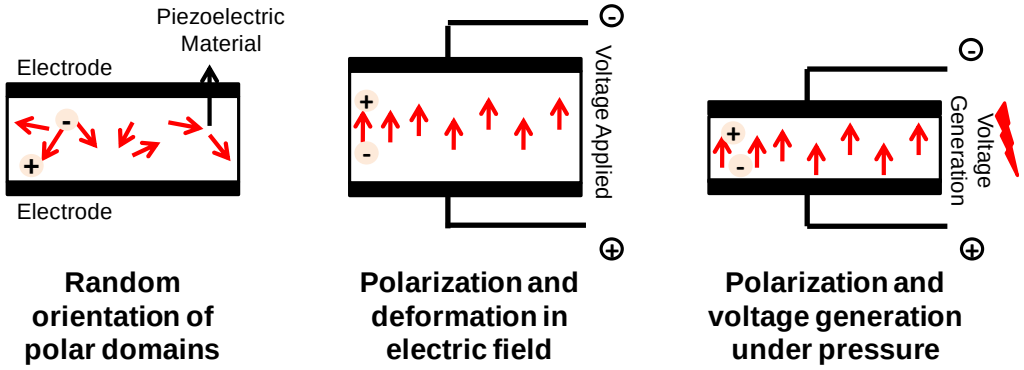

Figure 3.5 Mechanism of piezoelectric sensing

Quartz, tourmaline and some other piezoelectric ceramics are the common piezoelectrics which are insulating materials in the form of single crystals without center of symmetry in their crystalline structure [34-37].

3.2.4 Optical Sensors

Optical sensors are equipments with the ability of converting light rays into electronic signals. In other words, they measure the quantity of light as a function of intensity, phase, polarization, or wavelength and convert these variables into an understandable form. They have wide range of applications from daily life to aerospace applications in the form of temperature, pressure, and strain sensors because of their high performance even under harsh environments. They can perform in two different modes as intrinsic and extrinsic.

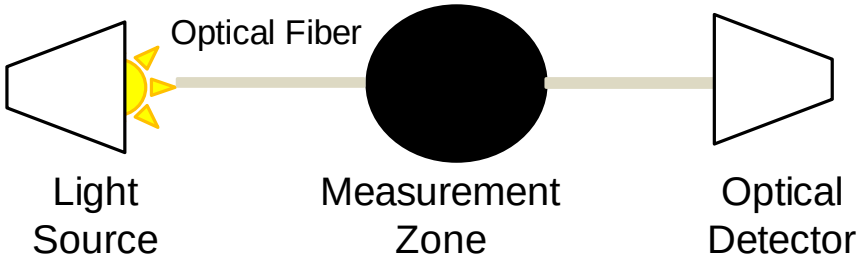

Figure 3.6 Mechanism of optical sensors

While intrinsic sensors are used for determining the change within the fiber; extrinsic ones are used for determining the change in the outside region of the fiber. They have many advantages mainly stemmed from their physical and structural properties such as light weight, small size with high sensitivity, electrical and chemical passiveness, excellent transmission properties, multiplexing capability, wide dynamic range, large bandwidth, and resistance to temperature, vibration and shock, *etc*. [38-40].

3.2.5 Chemical Sensors

A chemical sensor is a device used in order to transform chemical data into electrical signal. As shown in Fig. 3.7 they generally consist of two main parts such as active sensing layer and transducer. Signal generation takes place at the active layer by interaction of analyte and sensor. Any variation occurred in physical or chemical properties after interaction can be monitored by a transducer with different mechanisms including electrochemical, optical, mass, and thermal. Chemical sensors generally function with host-guest mechanism, so that; they must be specific to the sample.

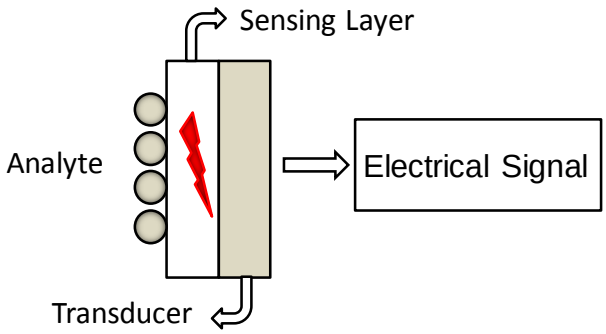

Figure 3.7 Mechanism of chemical sensors [41]

They can be work in contact and non-contact mode depending on the application which is a very wide range of including pH, concentration, color measurement of the materials [10,41,42].

3.2.6 Piezoresistive Sensors

Piezoresistive sensors are commonly used to determine the applied strain or pressure on a material by monitoring change in electrical resistance of the material.

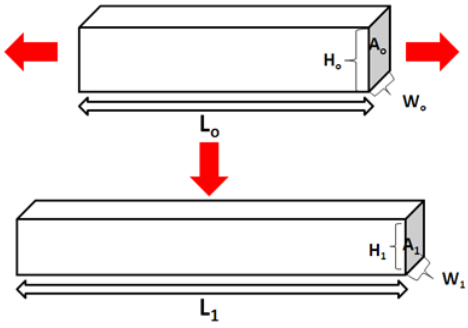

Figure 3.8 Mechanism of piezoresistive sensors

If we apply stress on a piezoresistive material in the form of stretching or compressing; change in the geometry/ dimensions of the material will cause a change in electrical resistance which is basically caused by the change in carrier density [32,43]. Generally metal alloys and semiconductors such as germanium and silicon [44] are used for the piezoresistive sensors. However, piezoresistive effect has been also observed for multicomponent systems as conducting composites as reviewed in Chapter 2 [45,46].

3.3 Textile Based Sensors

3.3.1 Textile Based Capacitive Sensors

As mentioned earlier, capacitive sensors measure the input stimulant through change in capacitance. A capacitor consists of a pair of conductors separated by a dielectric. A textile capacitive sensor consists of some sort of polymer (or fibrous) dielectric with textile electrodes onto the surface [11,47]. Conducting electrodes can be formed in many ways including weaving [11], knitting [47], embroidering onto the fabric by conductive yarns [21], or printing with a conducting material [11]. Textile based capacitive sensors has been proposed for the determination of;

- touch [11,47,48],
- proximity [47],
- load transfer, pressure [11,48],
- health monitoring, respiration monitoring [19],
- muscle activity and motion detection [21],
- sweat-rate [20],

- activity recognition of body posture, arm movement, chewing, swallowing, speaking, and head motions [49].

Sergio *et al.* designed a system for mapping applied pressure and imaging the shape of the area over which pressure is applied.

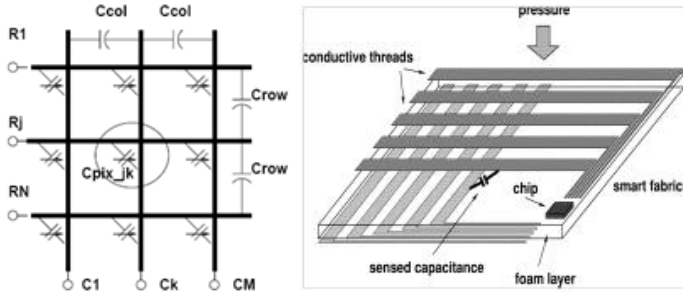

Figure 3.9 Diagram of the capacitor array [11,48]

The capacitive textile sensor is made of conducting fibers arranged in interlaced rows and columns on the opposite sides of piece elastic foam acting as the dielectric (see Figs. 3.9 and 3.10).

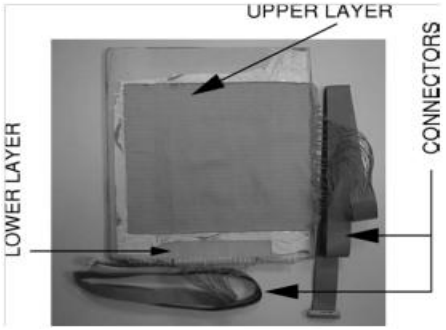

Figure 3.10 Smart fabric [48]

The change in capacitance depends on the magnitude of the applied pressure. In order to determine the pressure distribution, every row and column is scanned and signals are processed and turned into the image as shown in Fig. 3.11. While the system is advantageous in determining the distribution of pressure, it has the disadvantage of being very sensitive due to the structure of the foam layer [11,48].

Figure 3.11 Palm of a hand [11]

Wijesiriwardana *et al.*, used metal and conducting fibers, which is chemically CuS bonded polyester, for electrodes and polyester fabric as the dielectric [47].

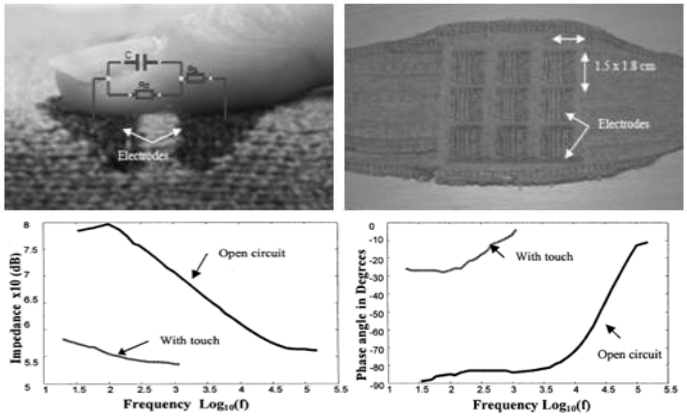

Figure 3.12 (a) Amplitude spectra of an electrode pair (b) phase spectra of an electrode pair [47]

This system reported to be a candidate for applications such as touch, proximity and position sensors. As shown in Fig. 3.12, two different configurations were used for the electrodes. In the first configuration, electrodes were designed to close the circuit when touched by a finger. The other system consists of parallel-plate electrode pads with an elastic dielectric [47].

Another interesting design of a textile based capacitive pressure sensor for tracking muscle activity and motion of the upper arm has been proposed by Meyer *et al.* The device consists of three layers including electrodes (1, 3), spacer fabric (2) and shielding layer (4). Electrodes are formed by embroidered silver coated yarn and separated by the compressible spacer fabric. In order to prevent crosstalk, the shielding layers are located on both sides of the sensory system [21].

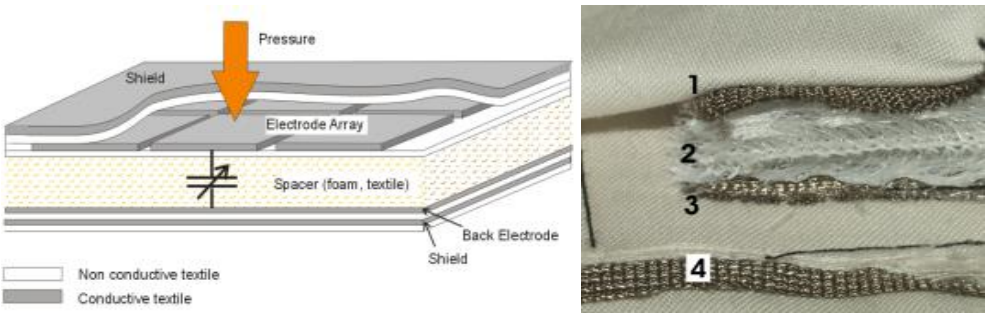

Figure 3.13 Scheme of the capacitive pressure sensor (top and bottom electrode of conductive textile (1, 3), compressible spacer fabric (2), and shielding layer (4)) [21]

Meyer evaluated the sensor by monitoring muscle activity, see Fig. 3.14. The periodic expansion and contraction cycles of biceps and triceps were monitored. As reported by the

authors, system has some disadvantages including uneven pressure distribution around arm caused by the friction between band and the skin [21].

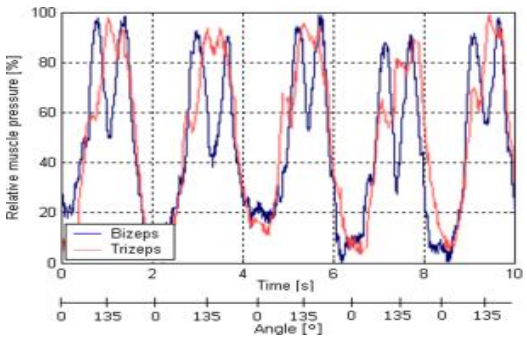

Figure 3.14 Muscle activity of biceps and triceps [21]

Textile based capacitive sensors have been proposed for health monitoring by many authors. Kang *et al.*, designed a capacitive fabric sensor for health monitoring as shown in Fig. 3.15. The sensor has been built by using stretchable and non-stretchable fabrics with conductive silver ink printed electrodes in a parallel-plate configuration which behaves as a capacitor. The sensor has been evaluated for monitoring repeated expansion and contraction cycles in breathing. Since system functions as a capacitive sensor, any change in the position of electrodes in the y axis during breathing leads to change in active area of the electrodes and capacitance. Breathing cycles can be monitored from this change [13].

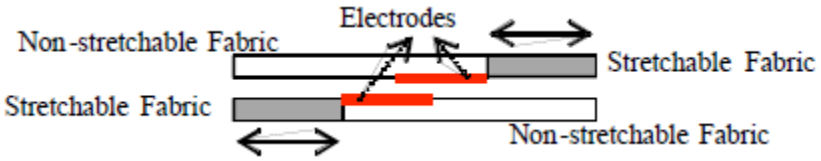

Figure 3.15 Schematic diagrams for the active electrodes [13]

Another textile based capacitive sensor with the same mechanism in ref. [13] for health monitoring has been proposed by Meritt *et al.* In addition to previous study, system was designed in the form of a belt, consists of silver ink printed electrodes, fabric, hook and loop fastener, and rubber, and conducting elastic material (see Fig. 3.16). Depending on the replacement of the parallel electrodes during inhaling and exhaling capacitance of the system changes and this change can be used for continuous monitoring of breathing [19].

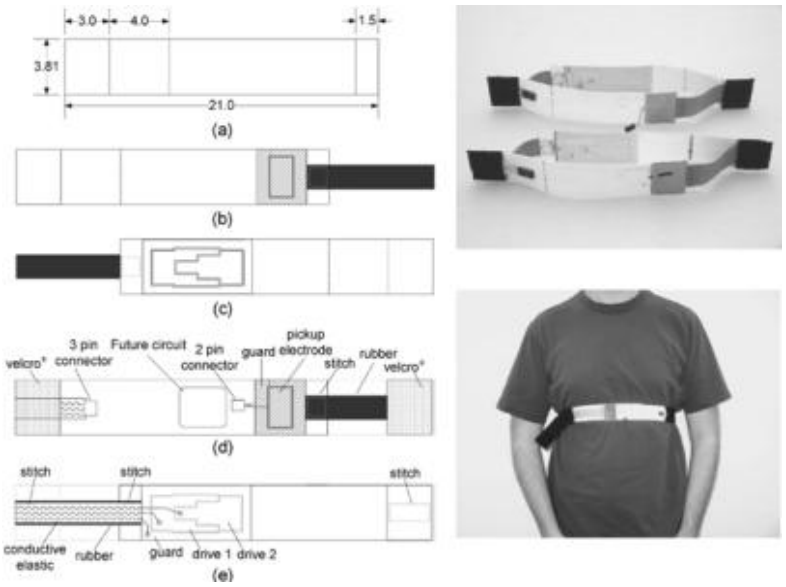

Figure 3.16 Capacitive sensory systems for respiration monitoring [19]

System was tested under different respiration rates to monitor respiration effort and compared with a spirometer (an apparatus for measuring the volume of air inspired and expired by the lungs). The data presented in Fig. 3.17 shows the best fit for deep breathing and panting [19].

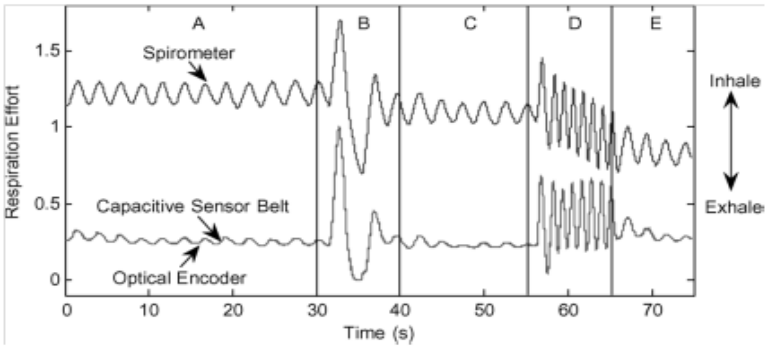

Figure 3.17 Respiration graph A: 30 s normal breathing, B: 10 s deep breath, C: 15 s normal breathing, D: 10 s panting, E: 20 s normal breathing [19]

One of the recent applications of a textile based capacitive sensor is in sweat-rate determination. To determine the sweat-rate, capacitive moisture sensors are used. If the sweat reaches to the sensor and penetrates into the dielectric, dielectric constant will change (increase) because of difference in polarizability of sweat. Change in dielectric constant directly affects the capacitance of the sensor. Coyle *et al.*, used capacitive moisture sensor consisting of hydrophilic films coated with a layer of gold and is integrated between net-like fabrics (88 wt% polyamide, 12 wt% elastane) as shown in Fig. 3.18

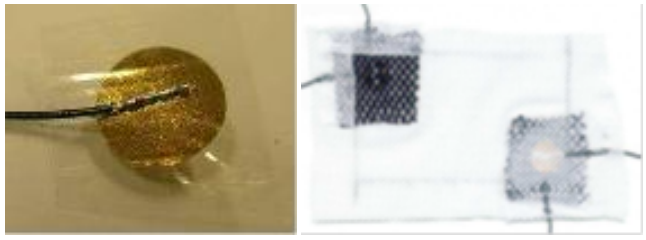

Figure 3.18 Humidity sensor and humidity sensors integrated to textiles [50]

Figure 3.19 Sweat monitoring belt [50]

Sweat-rate measurement during any type of exercise is a useful tool. As shown in Fig. 3.19, integrated sensors were found effective in terms of the measurement of sweat rate especially in the first 30 minutes of activity. However, long time monitoring such as whole day does not seem to be possible with this system (see Fig. 3.20) [50].

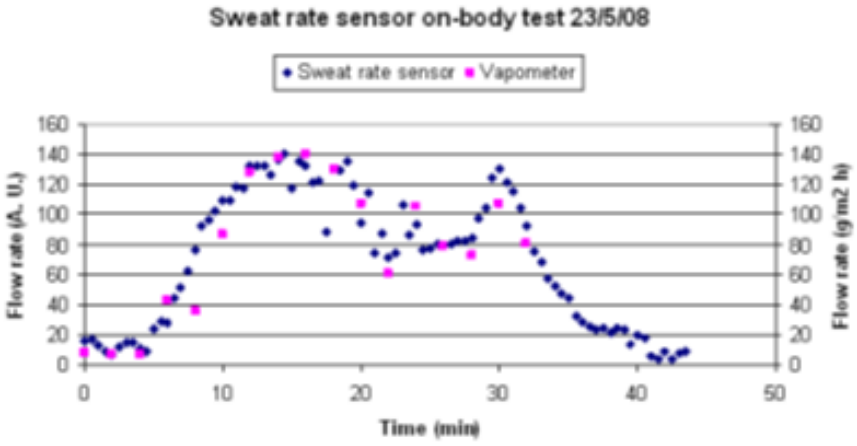

Figure 3.20 Response of textile sweat rate sensor compared to commercial vapometer [50]

One of the latest studies about capacitive textile sensors is reported by Cheng *et al.* [49]. The device consists of one electrode, and a flexible textile patch. The human body functions as the dielectric and earth (or ground) as the other electrode (see Fig. 3.21).

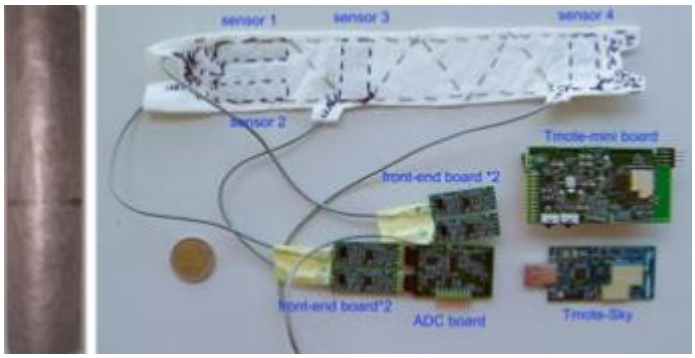

Figure 3.21 Sensory system [49]

The system measures the capacitive change in the body depending on the movement of a particular part of the body due to an action.

Figure 3.22 Three different placements of the sensory system (chest, wrist and neck) [49]

The sensor has been shown to be effective in following body posture, arm movement, chewing, swallowing, speaking, and head motions as shown in Figs. 3.22, 3.23and 3.24 [49].

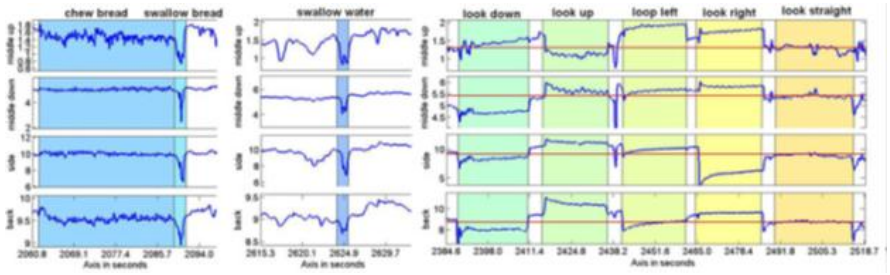

Figure 3.23 Signals from the neck electrodes left: chewing a piece of bread and swallowing, middle: swallowing 15ml of water, right: different head positions [49]

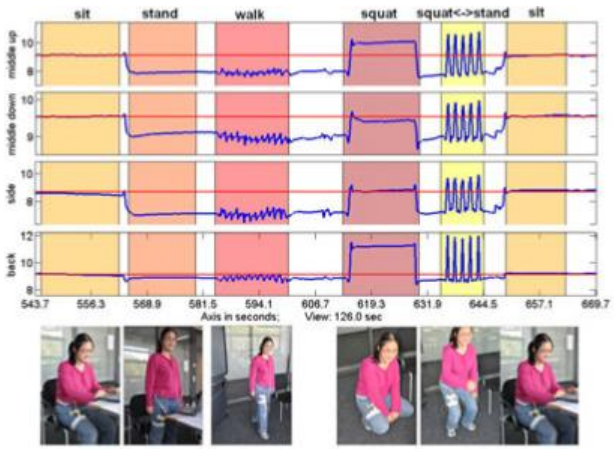

Figure 3.24 Signals from upper leg electrodes (front middle, front up, side and back) during a modes of locomotion experiment (left), signals from lower arm and wrist electrodes during a movement sequence (right) [49]

3.3.2 Textile Based Inductive Sensors

As mentioned earlier, inductive sensors are used for determination of position, proximity in order to detect metallic materials in a non-contact mode [10,32]. Basically they consist of inductive coils and emit electromagnetic field. If any metallic material approaches to the inductive coil, it affects the amplitude of the field produced by the sensor [10,32]. By analyzing the change in electromagnetic field and inductance position and proximity of the target system can be monitored. Although they are widely used in industry, their textile based derivations are limited [22,51]. As in industrial ones, textile based inductive sensors can be fabricated by formation of inductive coils with the help of knitting [51], stitching, or printing [22]. Different materials can be used including copper wires [51] or magnetic wires [22], and they can be used for respiration monitoring, motion capturing [22,51]. One of the main focuses in textile based inductive sensors is to produce inductive coils. As seen in Fig. 3.25,

different types and configurations of spirals can be designed including single, transformer-type and autotransformer-type differential sensor. Kang *et al.*, reported some alternatives for the basic layouts of textile based inductive sensors as shown in Fig. 3.25. In all these alternatives, the one which shows the highest inductive change under the same conditions should be preferred. In addition to that, electrical stability of the conducting materials needs to be considered [22].

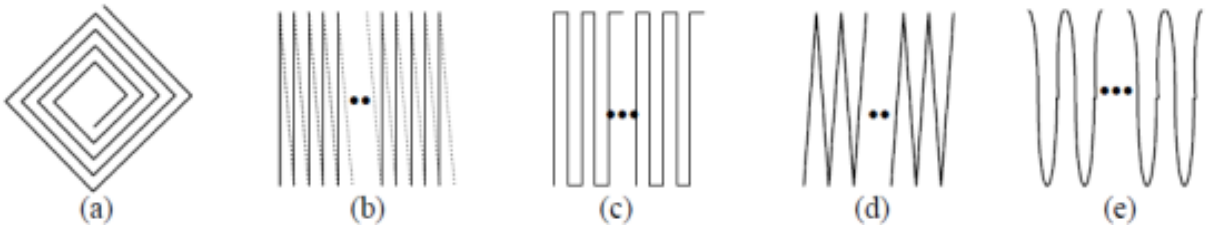

Figure 3.25 Basic geometric layout of the conductor for magnetic induction in single-plate sensor. (a) spiral, (b) solenoid type (conductors on both sides), (c) meander type, (d) zigzag type, and (e) sinusoid type [22]

Wijesiriwardana *et al.*, designed an inductive tranducer with Cu wire, elastomeric fibers (Lycra) and nonconductive fibers by knitting in the form of coils, as shown in Fig. 3.26 [51].

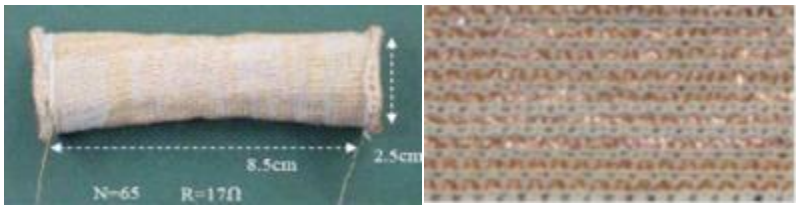

Figure 3.26 Knitted coils [51]

Knitted coils were used for the determination of strain and displacement. To determine the strain, wearable coils were located around the chest and variation was monitored during breathing was recorded, as shown in Fig. 3.27. The change in inductance was measured by inductive plethysmography technique and converted into voltage [51].

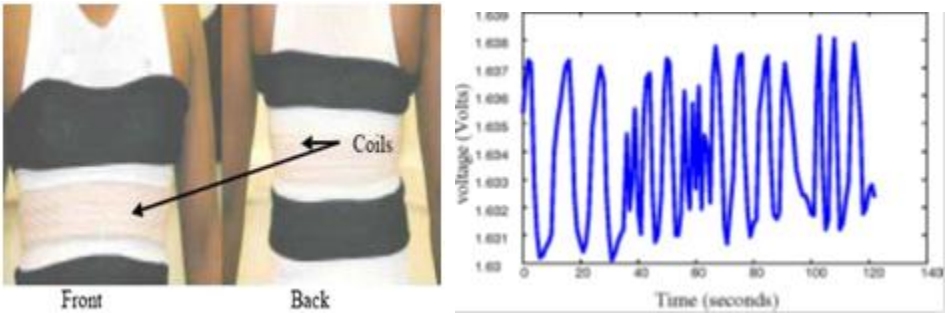

Figure 3.27 (a) Respiratory monitoring system made by knitted coils and (b) voltage change during breathing [51]

Coils were also used for measurement of the angular displacement of the elbow as shown in Fig. 3.28. In addition to that, fingers and calves were reported to be some other potential parts of the body on which they can be worn [51].

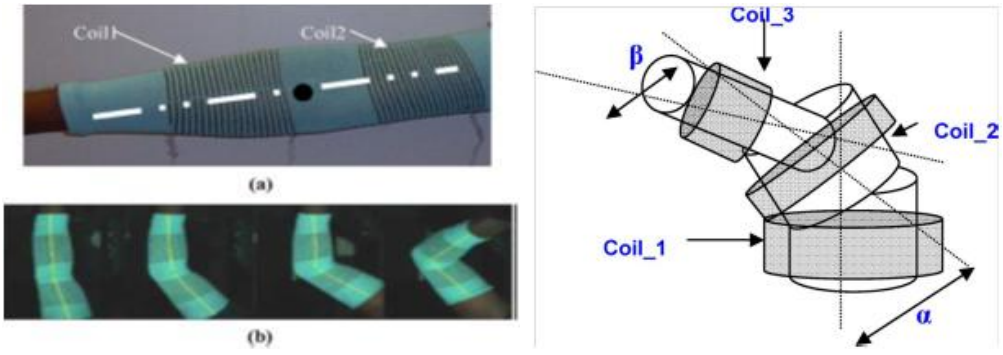

Figure 3.28 Sleeve arrangements (a) elbow straight position (b) different angular positions of the coils (c) angular displacements [51]

System successfully showed the change in angular rotation as shown in Fig. 3.29. However, sensitivity and repeatability of the system can be needs to be improved.

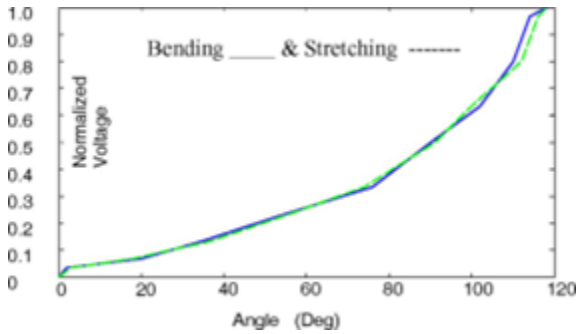

Figure 3.29 Normalized induced voltage of the coil-2 when coil-1 maintaining a constant voltage value [51]

Kang *et al.* designed inductive textile sensors by using nonwoven fabric and magnetic wires which were stitched onto the nonwoven fabric as shown in Fig. 3.30 [22].

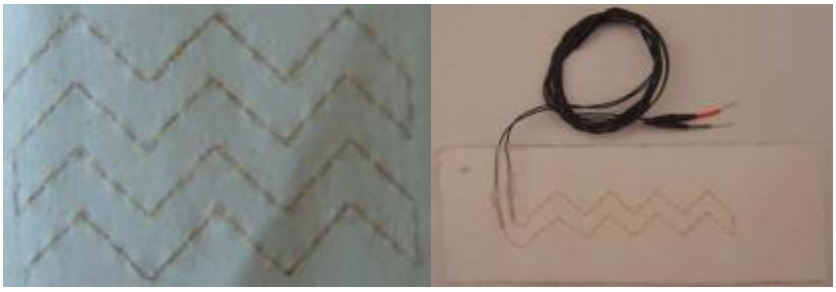

Figure 3.30 Inductive sensors with (a) four lines of zigzag pattern and (b) two lines of zigzag pattern [22]

In the study, inductive sensing was obtained by the change in the location of the wires under strain. Since system responded to low magnitude of strain, it was found effective in terms of determination of respiration signals as shown in Fig. 3.31 [22].

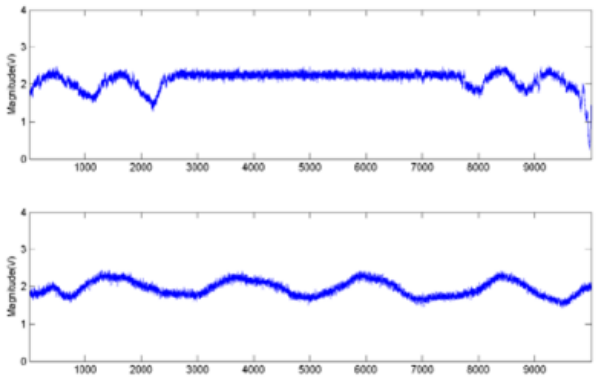

Figure 3.31 Simulated breathing signals during 4 seconds by stretching and relaxing the sensor by hand [22]

3.3.3 Textile Based Piezoelectric Sensors

Piezoelectric sensors may be ideal for textiles because of their ability to monitor the change in force, pressure or strain with the help of generated electrical potential with repeatable and reliable outcomes. Other advantages are simple structure, low cost, and low power consumption. Poly(vinylidenefluoride) (PVDF), may be the most common material used in the development of piezoelectric sensors is found in film form and can be easily integrated into e-textiles. However, interface, environmental factors, capacitive coupling between body and piezoelectric material and type of the connections are important criteria for the optimal efficiency of the piezoelectric sensors [52-57]. Textile based piezoeletric sensors have been

reported for applications, such as finger motion monitoring [52], gait analysis [53], strain sensing [54], cardio respiratory monitoring [55], heart rate monitoring [56], and pressure sensing [57].

Edmission *et al.* designed an electronic glove with the aim of using it as a functional keyboard. In order to sense flex and tap motions of the hands piezoelectric films were used. In the study, firstly kinetic activity and relative motions of the fingers were analyzed and some standard typing kinematics was determined. Depending on this, positions of the piezoelectric films were determined, as shown in Fig. 3.32. Two different piezoelectric films were used. Each sensor was connected to an A/D converter and signals generated during flexion and tapping were processed by the developed software [52].

Figure 3.32 Sensor arrangement and e-glove [52]

As seen from Fig. 3.33, according to outcomes, movement of the fingers could be monitored by monitoring voltage change during movement. In addition to that, direction of movement affects the magnitude and behavior of the response [52].

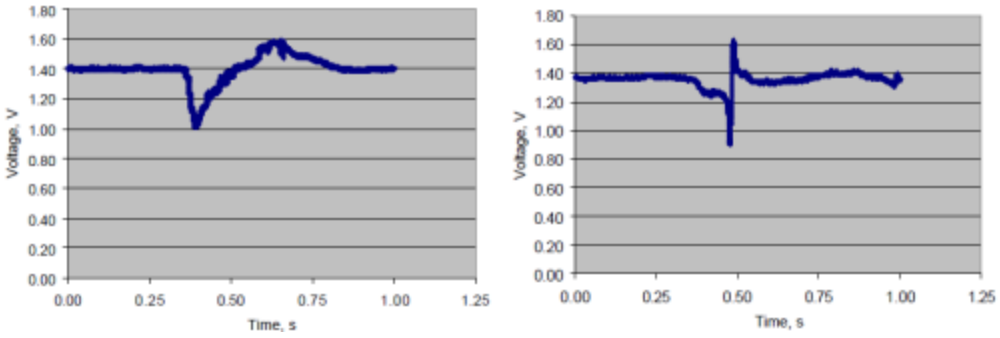

Figure 3.33 Voltage response of flex and tap [52]

Laxminarayana and Jalili reported nanocomposite electrospun webs of CNT/PVDF solution [54] to fabricate piezoelectric sensors. They prepared different nanocomposite fibrous sensors with filler ratio varying between from 0.01 to 0.05 wt% as shown in Fig. 3.34.

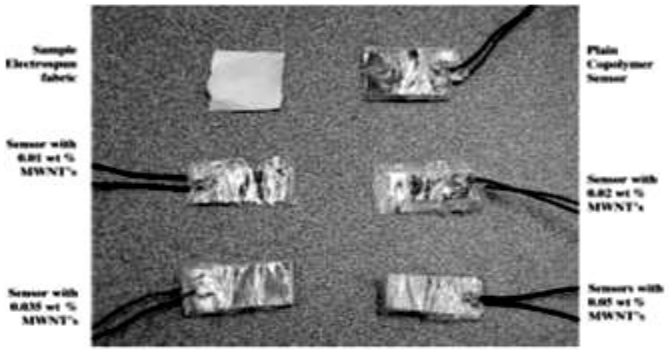

Figure 3.34 Electrospun sensors with different CNT content [54]

In order to test the voltage generated from strain, samples were sandwiched with PZT (lead zirconate titanate) actuator. When voltage is applied to the actuator, both actuator and nanofiber webs bend and the nanofiber webs generate voltage. As shown in Fig. 3.35, strain sensing ability of the CNT (0.05 wt%) filled composites increased about 35 fold. This

improvement was assumed to be caused not only by piezoelectric properties of CNF and PVDF but also by electrospinning. Electrospinning is a way for the formation of nanofibers under high voltages which enhances the dipole alignment in PVDF [54].

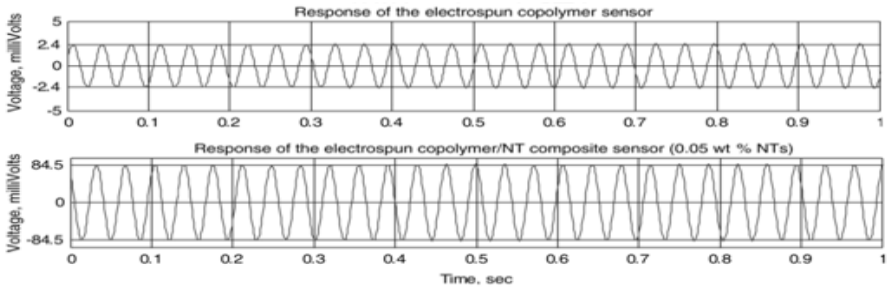

Figure 3.35 Comparison between plain copolymer sensor and CNT-based sensors, PZT input: 160 V at 175 rad second^{-1} PVDF [54]

Choi *et al.*, developed a piezoelectric sensory system for monitoring cardio-respiratory signals during sleeping. The system is designed in the form of a waist belt consisting of conducting fabrics (copper coated knitted fabric) as electrodes for electro cardiogram (ECG), PVDF film as a sensor for monitoring the respiratory behavior, signal acquisition circuits and a universal serial bus (USB) for communication.

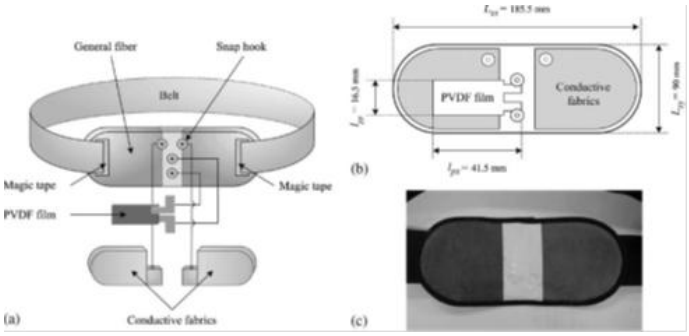

Figure 3.36 Sketch of the sensory system [55]

In order to compare the reliability of the system, commercial ECG and pneumography sensor systems were used. The system was found to be superior to the commercial sensors in monitoring the heartbeat and respiratory cycle after data extraction [55].

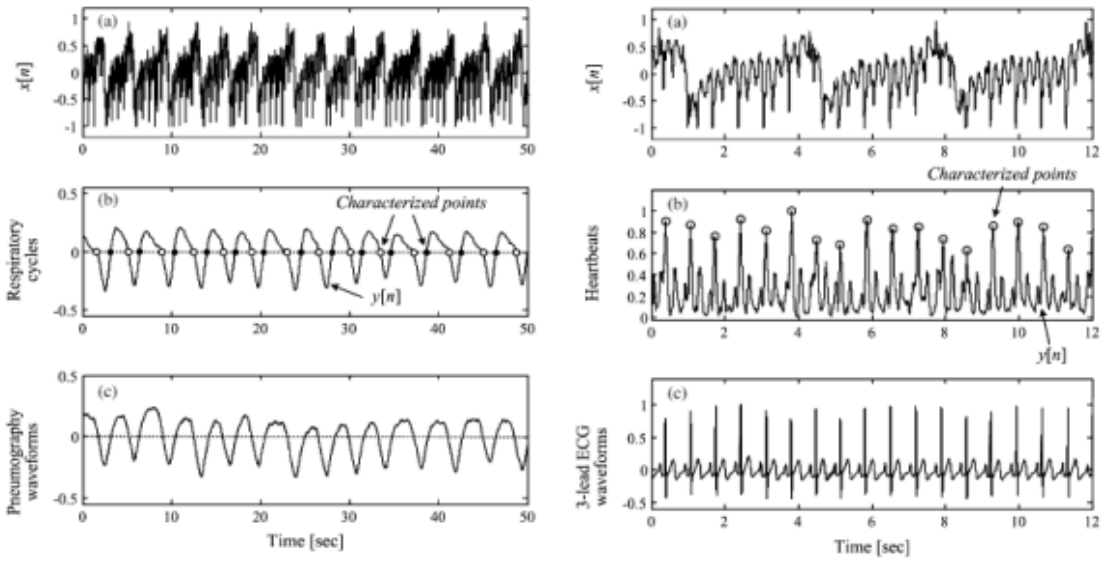

Figure 3.37 Extraction of respiratory cycle information from PVDF film sensor signals, (a) the original signal from PVDF film sensor, (b) the extracted respiratory cycle waveform and (c) the signal from the pneumography sensor for comparison (left). Extraction of heartbeats information from PVDF film sensor signals, (a) the original PVDF film sensor signal, (b) the extracted heartbeats information and (c) 3-lead ECG sensor signal (right) [55]

Another promising application of these sensors is in the automotive industry. Drean *et al.*, developed a car-seat with piezoelectric sensors intended to determine applied pressure [57]. The PVDF pressure gauges were located between outer fabric and foam. They were connected to an amplifier and impedance phase analyzer. Changes in phase angle as a function of pressure are shown in Fig. 3.39 for different laminate compositions.

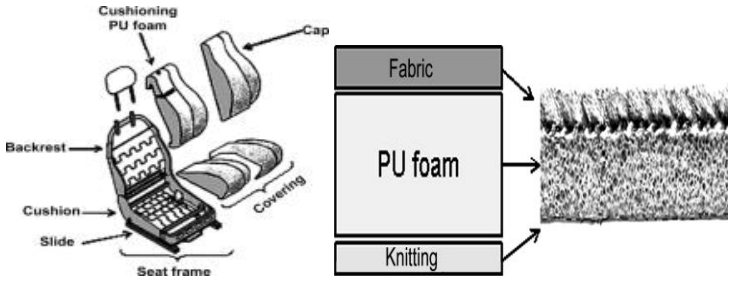

Figure 3.38 Car seat structure and fabric structure for cap components [57]

Although all three systems had different values, they showed linear behavior. This indicates that, these structures are good alternatives for sensory applications [57].

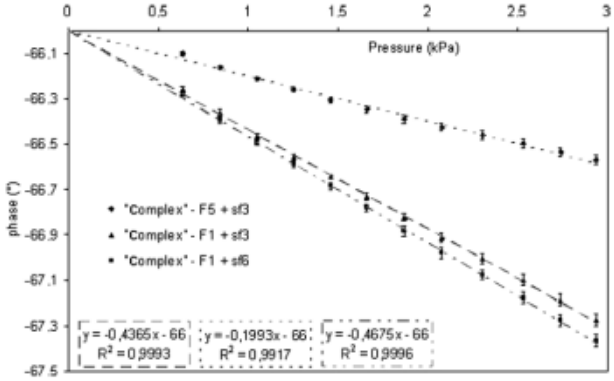

Figure 3.39 Change in phase angle as a function of pressure for different laminates [57]

Gait stability is one of the most important problems for motion impaired people. Lui *et al.*, developed a textile based monitoring system with the ability of storing angular velocity, vertical acceleration and piezoelectric data in order to monitor and evaluate the local dynamic stability of a motion impaired user to prevent falls. As designated in Fig. 3.40, system consists of various electronics including sensors, printed circuit boards, microcontrollers and communication devices. Piezoelectric sensors were integrated to the

heel in order to provide data for the heel contact. Data was transferred to a processer with the help of an electronic toll collection system and a Bluetooth. Tests were carried out with the help of different groups of people including four healthy elderly, four motion-impaired elderly and five healthy young individuals and showed the validity of the system in terms of evaluation of the local dynamic stability [58].

Figure 3.40 E-textile pants [58]

3.3.4 Textile Based Optical Sensors

Optical sensors offer potential alternatives to the textile based sensors discussed thus far, primarily because of superior structural properties including lightness and excellent optical properties even under harsh conditions [38,39]. Also, they are readily available in fiber form [59-61], and therefore can be easily be incorporated into textiles in different forms including woven [62,63], knitted [64] or nonwoven fabrics using different techniques [63,64]. However, fabric formation by knitting or weaving may lead to mechanical bending and decrease in the degree of light transmission. In order to minimize these effects, more flexible optical fibers or different fabric structures are preferred for textile based optical sensors [62,64]. Macro-bending [61,64,65], Bragg grating [61,65] and time reflectometry sensors [65] are common textile based optical sensors reported in the literature. Regardless of type of the optical fiber, they can be used as pressure [62] and strain sensors based on the change in intensity, phase, polarization, wavelength, spectral distribution of the transferred light after exposure to strain or pressure [61,64,65].

Rothmaier *et al.*, developed a textile based fiber optic sensor. In the study flexible optical fibers were produced and integrated into a woven fabric during weaving as shown in Fig. 3.41. Fabric sensors were tested for their pressure sensing ability. When pressure is applied, change in the dimensions of the optical fibers lead to change in transmitted light intensity. By monitoring this magnitude of the applied pressure was monitored for one fabric structure. On the other hand, the system was not found effective for the pressure mapping applications [62].

Figure 3.41 Atlas woven fabric by flexible optical fibers and cotton

Dhawan *et al.*, developed different textile based optical sensors in the form of woven, knitted and nonwoven fabrics by using silica and plastic optical fibers. For the woven fabric, optical fiber was incorporated during weaving. As shown in Fig. 3.42, sensory system was found effective in the determination of bending behavior of the fabric [64].

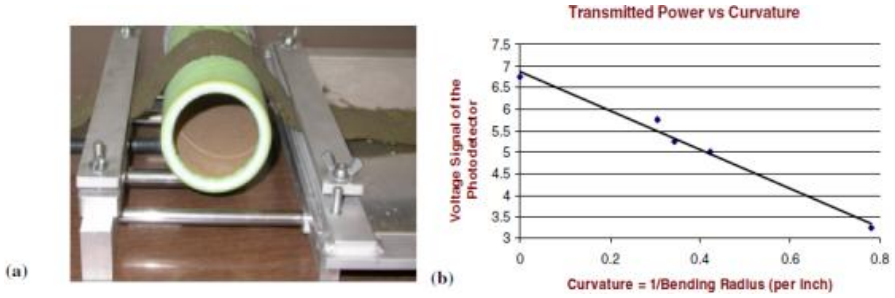

Figure 3.42 (a) Woven optical sensor under bending process and (b) response of the system as a function of transmitted power & curvature of fabric [64]

Optical fibers have also been integrated into knitted fabrics and evaluated for their strain sensing ability. The system was found to measure strain quite effectively (see Fig. 3.43 and 3.44).

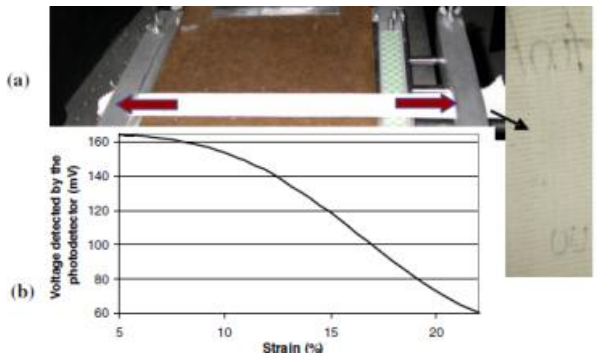

Figure 3.43 (a) Knitted optical sensor under strain (b) response of the system as a function of transmitted power and strain [64]

Figure 3.44 Chest band and strain sensor located at elbow/knee [64]

Another interesting application of textile based optical sensors is in health monitoring applications. De Jonckheere *et al.*, developed textile based sensors for health monitoring during Magnetic Resonance Imaging (MRI) [61]. Since metallic materials can affect the quality of the signal during the MRI process, optical fiber sensors have been used to follow the respiration. The proposed sensory system mainly consists of two parts as shown in Fig. 3.45.

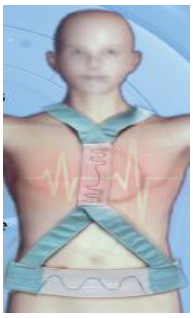

Figure 3.45 Sensory system [61]

The first part is designed for the monitoring of abdominal movement. Optical fiber is integrated into an elastic textile by a crochet process. Abdominal movement lead to stretching of the textile and change in the position of the optical fiber. As shown in Fig. 3.46, abdominal movement was successfully monitored [61].

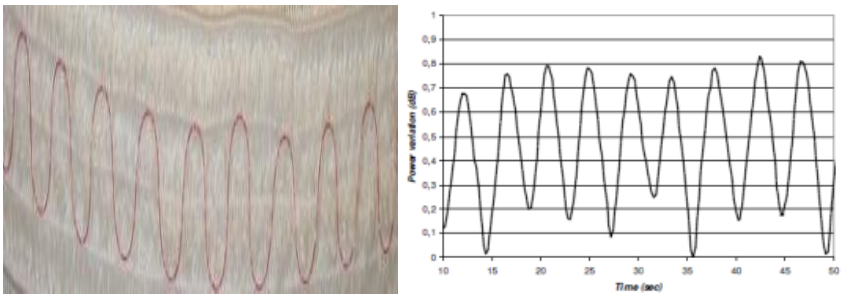

Figure 3.46 Optical fiber embedded textile sensor and corresponding cycle of power variation [61]

Since this sensor was not found adequate for the monitoring of thoracic movements, different optical fiber was stitched onto an elastic textile. Fiber Bragg Grating (FBG) is a special optical fiber with higher strain sensitivity. The sensor was able to monitor the thoracic movement, see Fig. 3.47.

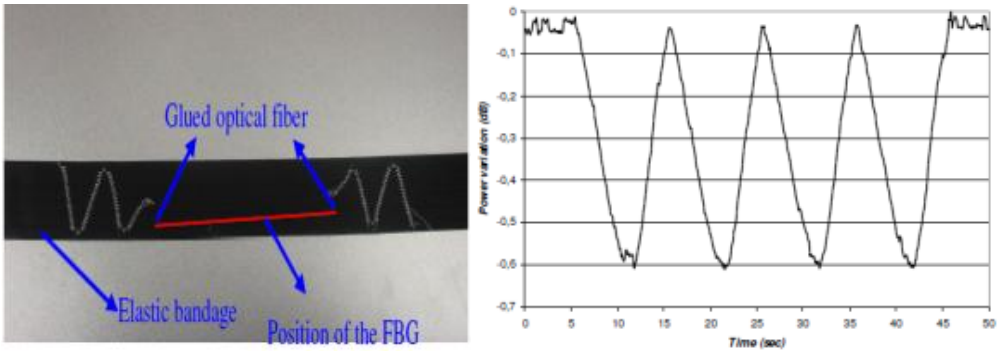

Figure 3.47 FBG stitched textile sensor and cycle of power variation [61]

Grillet *et al.*, developed textile based optical sensors including a macro-bending sensor, a Bragg grating sensor, and a time reflectometry sensor. All three sensors are strain sensors and used for the monitoring of the abdominal movement. Sensors were found effective in terms of determination of strain between 0 and 3% [65].

3.3.5 Textile Based Chemical Sensors

Recently, textile based chemical sensors have also been reported. Almost all textile systems summarized above are physical sensors and are used for determination of physical variables; however chemical sensors have different sensing mechanism and they are used for the converting chemical information to measureable signals [41,42].

Since textile based chemical sensing is a very new area, they are still at the level of design, optimization and validation. Textile based chemical sensors are generally used as biochemical sensors for the determination of body fluids such as sweat and used for the determination of sweating-rate and sweat pH and components of sweat [30,50,66], wound healing [67].

These sensors have been fabricated using different materials including polyamide/lycra, polyester/lycra fabrics with additional layers including pH sensitive dyes, and hydrogels. Although there are different sensing mechanism for traditional chemical sensors [41,42], textile based chemical sensors is a very new area and generally mechanism based on colorimetric changes. Coyle *et al.*, developed a textile based pH sensor by using pH sensitive dyes with various absorption behaviors. In the study, change in pH was aimed to be monitored by color change of the dyes. As shown in Fig. 3.48, system consists of a sweat collection system, LED light source, photo detector and pH sensitive dye (Bromothymol blue, pH 6-7.6) which is fixed on fabric.

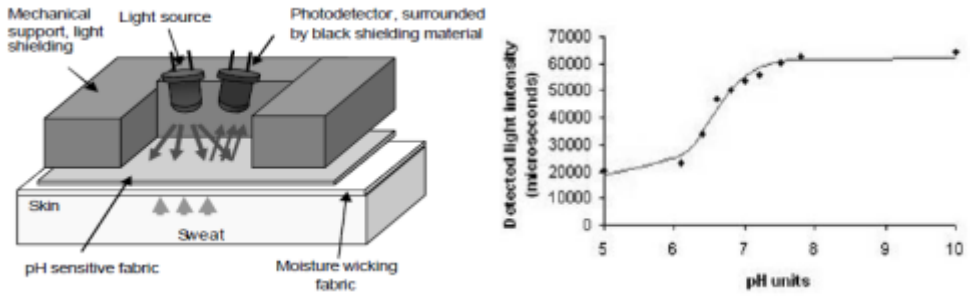

Figure 3.48 (a) Textile based pH sensor and (b) outcome as a function of light intensity *vs.* pH [20]

After sweat wicks to the pH sensitive dye, color starts to change from yellow to blue and the amount of the absorbed light coming from LED light source increases. This leads to decrease in the measured light intensity at the light detector. As shown in Fig. 3.49, change in pH was measured as a function of light intensity [20]. The sensory system was modified by using a different fluid transfer system by inserting additional sodium and conductivity sensors as

shown in Fig. 3.49. Fluid transport system consists of a polyamide/lycra ® fabric as a base material which is printed with a hydrophobic layer in order to obtain fluid transport channel. Effective sensing area was circumscribed by a polyurethane film and super absorbent material, was located at the end of the transport channel to store the sweat [30]. The sensing mechanism was same as the previous study [20,30].

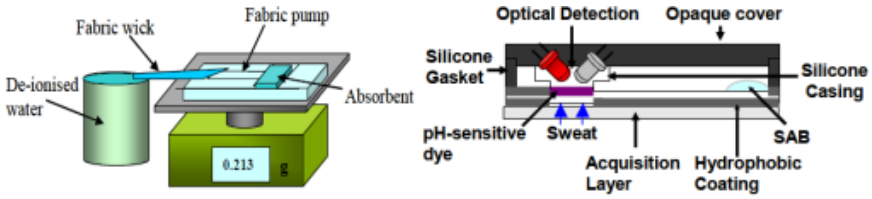

Figure 3.49 (a) Fluid handling system and (b) pH sensor and optical detection system [30]

As shown in Fig. 3.50, initial outcomes were reported to reflect the pH of the sweat during exercise [30].

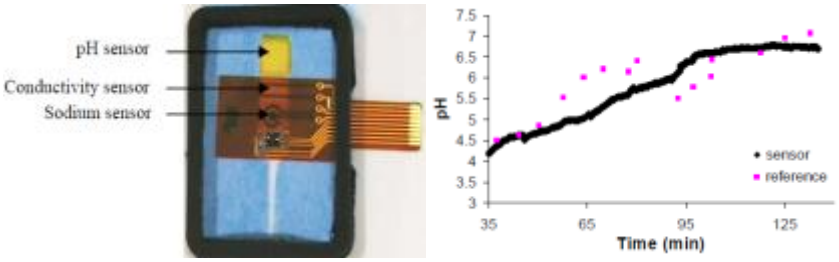

Figure 3.50 pH, conductivity and sodium sensors and outcomes of pH sensor during exercise [30]

Sodium activity and conductivity measurements were carried out in a number of studies [30,66]. However, it was not validated by another system; as shown in Fig. 3.51, response of the system was found successful [30,66].

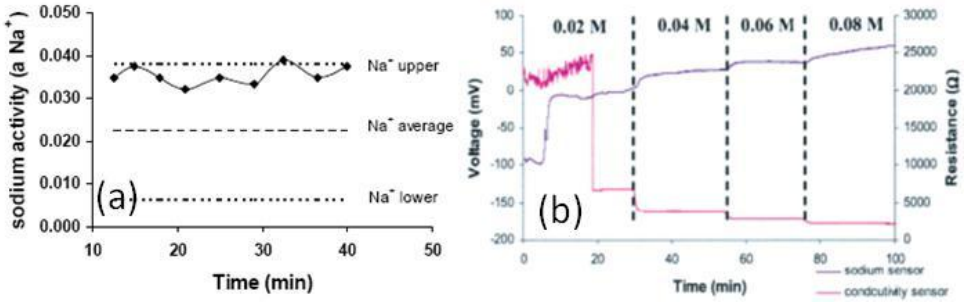

Figure 3.51 (a) Sodium activity during exercise trial [66] (b) sodium activity and change in conductivity during in vitro trials [30]

In addition to monitoring of body fluids, textile based structures have also been used for detection of blood proteins such as albumin. Shim *et al.* coated cotton yarns with single-walled carbon nanotubes (SWNTs). CNTs were dispersed in poly(sodium 4-styrene sulfonate) (PSS)-water solution containing anti-albumin and coating was carried out by dipping cotton yarn into these solutions. Mechanism of the sensing is shown in Fig. 3.52. When chemical sensor interacts with the albumin, albumins react with anti-albumins. Removal or rearrangement of anti-albumins leads to decrease in the tunneling distance of SWCNTs and increase in conductivity. Through the help of increase in conductivity, albumin concentration can be calculated. As reported, very low concentrations (119 nM) can be monitored with high sensitivity and selectivity [68].

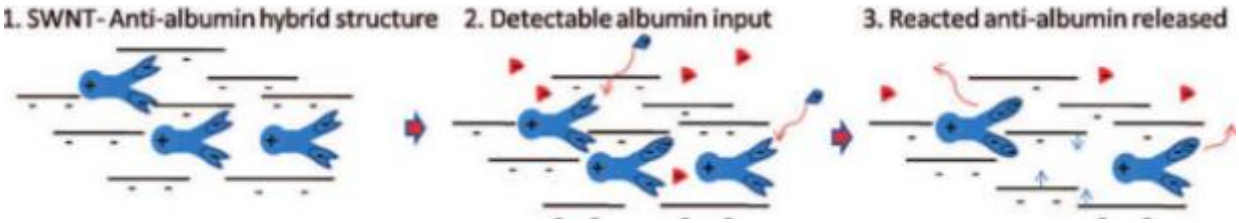

Figure 3.52 Chemical sensing mechanism of CNT/ anti albumin coated cotton yarns [68]

3.3.6 Textile Based Piezoresistive Sensors

Textile based piezoresistive sensors (TBPS) have wide range of applications including;

- strain monitoring [69-71],
- gas sensing [72],
- temperature sensing [69],
- pressure sensing [73],
- body-posture monitoring with:
- gloves [69,74],
- sleeve [71],
- leotard [71],
- knee pad [71],
- knee sleeve [6],
- bra (breast motion monitoring) [75],
- health monitoring (vital signals, respiration),
- rehabilitation.

Various materials including composites in a number of forms have been used for TBPS as applications. These include, inherently conducting polymers, conductive filler loaded composites, conducting yarns, and knitted fabrics. However most of the systems function according to the principle of strain sensors. Regardless of the type and form of the sensory material, when any type of external stimulus is applied, mainly two possible mechanisms occur. First one is the breakdown of the conducting junctions; second is the reformation of the new conducting network [76,77]. If the dominant behavior is the breakdown of electrical networks, resistance will increase; this behavior is referred as positive piezoresistance. On the other hand, if formation of new conducting network is dominant, resistance will decrease and this phenomenon is referred as negative piezoresistance. Dominant mechanism depends on many structural and external factors such as polymer type, filler type, concentration, geometry [77], filler orientation-dispersion [78], amplitude, direction and type of external factor [77].

Initial studies on TBPSs started with the coating of textile surfaces with inherently conducting polymers. Recently, intrinsically conducting polymers (ICPs) have become important alternative for many applications which require conductivity, because of their flexible, relatively lightweight structure. Polypyrrole (PPy) is the common conducting polymer in the literature for TBPSs because of its high conductivity, non-toxicity and ease of processing [6,69-73,75,79-83]. And also, poly(3, 4 – ethylenedioxythiophene) - poly(4-styrenesulfonate) (PEDOT-PSS) was also reported [84].

Most important contributions in the area of TBPS were made by De Rossi's group from University of Pisa, Italy. In their preliminary studies, they used coated Lycra fabrics with

PPy layer applied through epitaxial deposition. The fabric showed negative piezoresistivity with the gauge factor around 12.5- 13.25. The decrease in the resistance was attributed to the change in fabric geometry under strain which lead to increase in the total conducting area in contact between loops [69-71]. In the study, a sensing glove with PPy coated elastic fabrics on the finger-tips, was developed. In the data presented in Fig. 3.53 shows variation in resistance with movement of the fingers [69]. However, PPy coated sensors were reported to show some disadvantages such as high setting and response times and also coating process is relatively difficult when compared with traditional printing and coating methods [70].

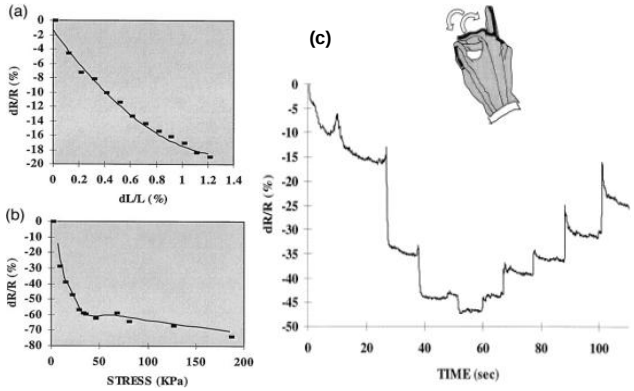

Figure 3.53 Piezoresistive behavior of the (a) PPy coated fabric and (b) sensing glove (c) time dependent behavior of sensing glove [69]

De Rossi *et al.*, also investigated the thermal behavior of sensors under different temperatures. PPy coated lycra fabrics samples showed negative piezoresistivity with the temperature coefficient (TCR) of resistance between -0.03 and -0.05°C^{-1} [69].

In addition to strain and thermal induced piezoresistivity, Scilingo *et al.*, reported pressure induced piezoresistive behavior of PPy coated fabrics. As shown in Fig. 3.54, increased pressures lead to decrease in the resistance [70].

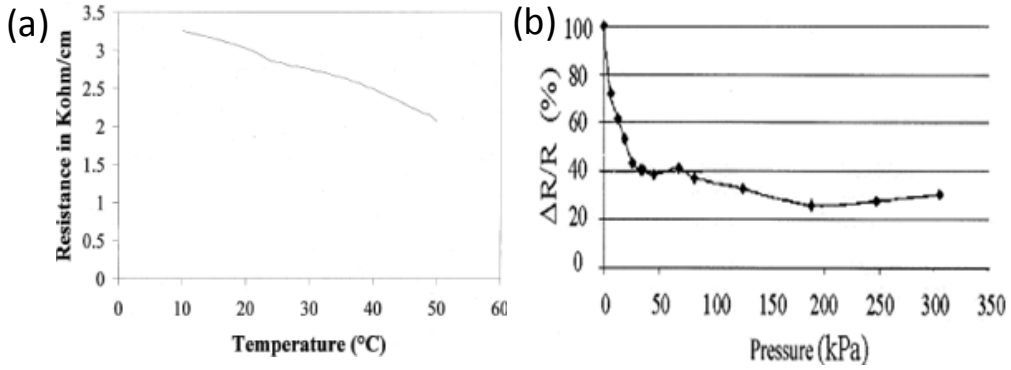

Figure 3.54 (a) Resistance change as a function of temperature (b) percent variation of resistance as a function of pressure for PPy-Lycra/cotton [70]

In another study, carried by De Rossi's group [4], cyclic behavior of the PPy coated fabrics was investigated. As seen in Fig. 3.55, the applied strain is not totally recoverable, there is a noticeable hysteresis between loading (stretching) and unloading (shortening) cycles. Since one sensor output is not enough for mapping the action, they have studied different topologies and sensor sets with a proper algorithm in order to optimize the system and showed the system's ability to map the human movements [4].

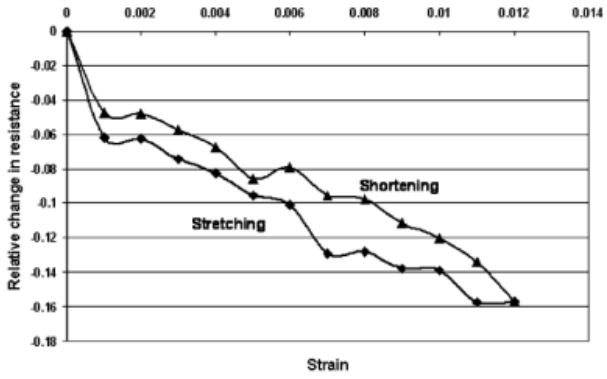

Figure 3.55 Cycling behavior of PPy coated fabric [4]

Generally, negative piezoresistance was reported for PPy coated textiles [6,69-71,81]; however, Kim *et al.*, observed positive piezoresistance for PPy/PET/Spandex fabric composites as shown in Fig. 3.56. Polymerization technique was also found to have significant influence in terms of the total PPy wt%, resistivity, and mechanical properties of the fabric and piezoresistive behavior of the sample. Different methods might lead to different amount of deposited layer on the fibers with different surface morphology and resistance values [83].

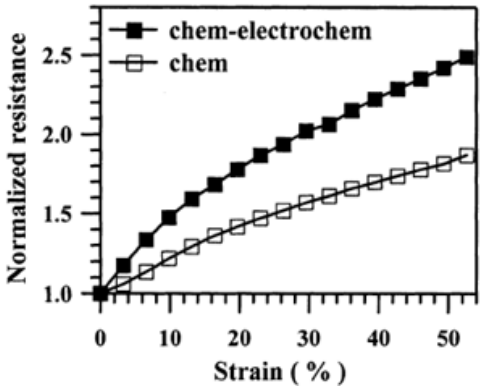

Figure 3.56 Piezoresistive behavior of the PPy/PET/Spandex fabric [83]

As mentioned previously, PPy coated textile sensors have some drawbacks including low stability and aging [81]. To understand the basic mechanism of degradation, Li *et al.*, prepared PPy-coated Nylon (83 wt%)/Lycra (17 wt%) fabrics by both chemical vapor deposition (CVD) and solution polymerization (SP). As shown in Fig. 3.57, CVD lead to a thinner and more homogeneous coating and higher sensitivity when compared with SP. This behavior was assumed to be caused by the thin layer coating of PPy which does not affect the recoverability of elastic fabric. They have also annealed the samples and obtained more stable sensing behavior against strain, temperature and humidity which is very promising for textile based sensors [79,80].

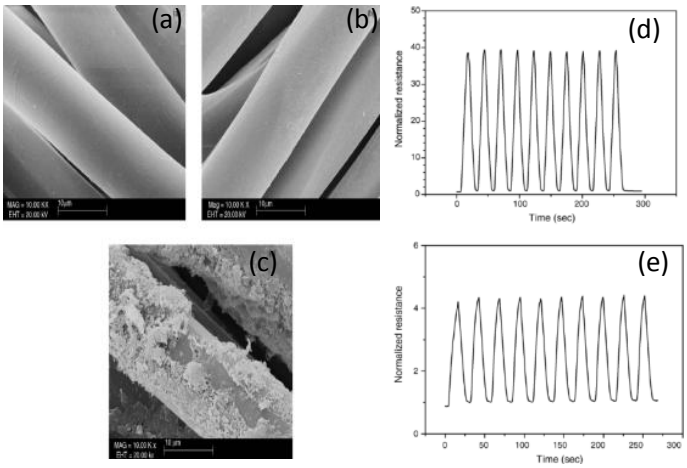

Figure 3.57 SEM images of (a) pristine fabrics and PPy-coated fabrics prepared (b) by CVD at low temperature and (c) by solution polymerization. (d) the conductivity changes with strain of PPy-coated fabrics prepared by CVD and (e) solution polymerization (deformation = 50%) [79]

Dunne *et al.*, developed a pressure-sensitive torso garment consisting pressure sensors which are mainly PPy coated polyurethane foams.

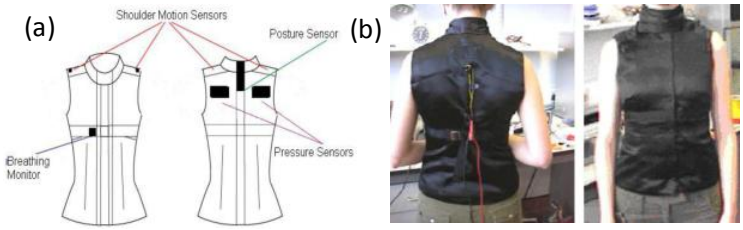

Figure 3.58 (a) Garment structure and sensor layout and (b) prototype pressure-sensitive torso garment [73]

As shown in Fig.3.58, sensors were located at six different positions with the aim of detecting vital signals and body movement including breathing, shoulder movement, neck movement, and shoulder-blade pressure [73].

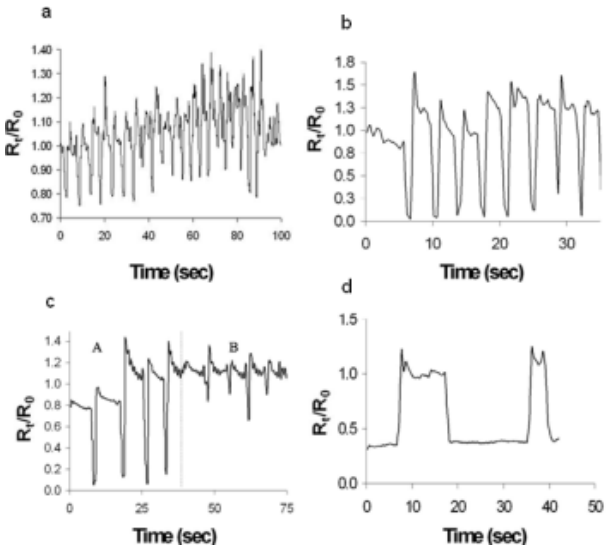

Figure 3.59 (a) Relative resistance response (R_t/R_0) to deep breathing, (b) resistance response to shoulder lift, (c) resistance response to neck movement, and (d) resistance response to constant scapula pressure [73]

As presented in Fig. 3.59, preliminary results showed that the system can be of use barring a few concerns related to aging of PPy, hysteresis, and thermal stability [73].

Campbell *et al.*, fabricated PPy coated fabrics for monitoring vertical beast displacement during exercise [75]. In this system, a PPy coated fabric sensor (nylon (80 wt%)/lycra (20 wt%)) was attached onto the brassiere with a 20% pre-strain, see Fig. 3.60. The prestrain was necessary to obtain data in the linear range of the sensor fabric. In addition to the sensors, infrared emitting diodes (IRED) were integrated in to the garment in order to determine the variation in sensor length and vertical breast movement. Meanwhile a commercial motion analysis system (OPTOTRAKs 3020) was used to validate the fabric sensor output. As shown in Fig. 3.60, the system was found effective for the determination of the beast displacement during running at 10 km h^{-1}.

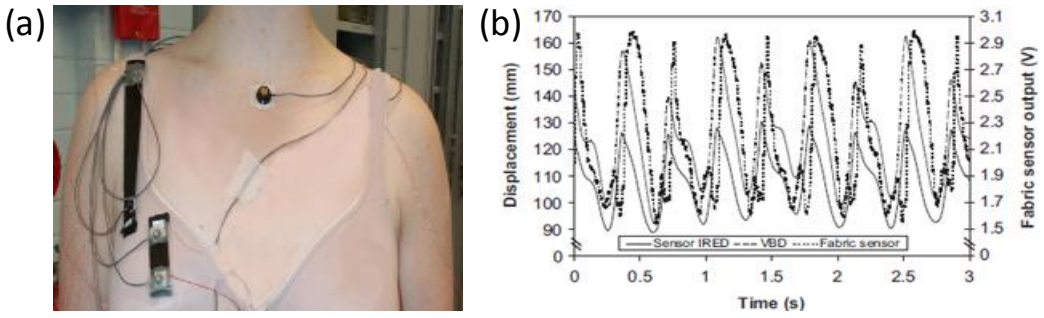

Figure 3.60 (a)Sensor attached brasserie (b) voltage change as a function of time and displacement data from IRED (10km h^{-1}) [75]

Another interesting application of TBPS in athletics was reported by Munro *et al.*, [6]. Monitoring the athletes' motion/body movement during training is of importance to minimize possible injuries. Munro *et al.*, developed a wearable knee sleeve consisting PPy-

coated nylon-lycra fabric sensor to monitor the anterior cruciate ligament movement as shown in Fig. 3.61. The system mainly aims to determine knee flexion angle and warns the users with an audio signal about the right landing position. Initial data on the fabric-sensor showed negative piezoresistance with gauge factors ranging between −0.1 and −10.0 (0–70% strain) as shown in Fig. 3.61, sample 1 showed the highest linearity and range of strain [6].

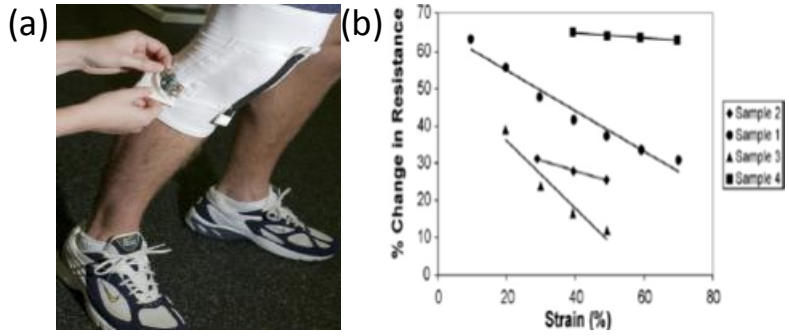

Figure 3.61 (a) The intelligent knee sleeve and (b) piezoresistive behavior of different fabric based sensors under strain [6]

After optimizing the sensor, different individuals were asked to perform four different landing positions with the sensorized wearable knee sleeve. The system was validated with the traditional methods used for this application and the comparison is shown in Fig. 3.62. The authors noted that the system is not very efficient for small changes in flexion angle, and has to be prestrained (*i.e.*, 10%) before the application. Sweating might also affect the resistance of the sensor [6].

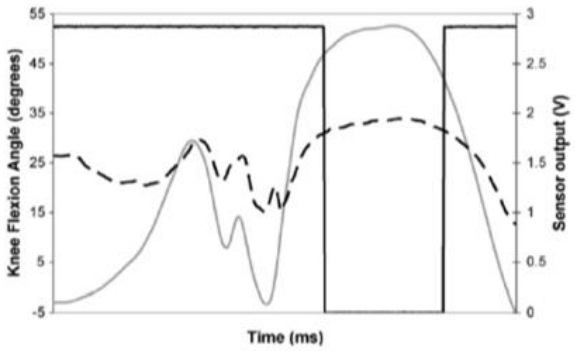

Figure 3.62 Example of intelligent knee sleeve raw sensor and audible output (audible onset (–); sensor strain output (– – –)) and knee flexion angle calculated (-) for the deep hop movement [6]

In addition to strain sensors, Kincal *et al.*, studied the gas sensing ability of PPy coated fabrics through the change in conductivity [72]. PPy coated fabrics were tested in order to determine their piezoresistive behavior under different gases. Samples were exposed to different mixture of gases such as NH_3/HCl and NH_3/CO_2. While NH_3/HCl exposure leads to nearly one order of magnitude change in conductivity, the sensor behavior was not found repeatable. On the other hand tests carried out with NH_3/CO_2 were found to be more stable with lower change in conductivity [72].

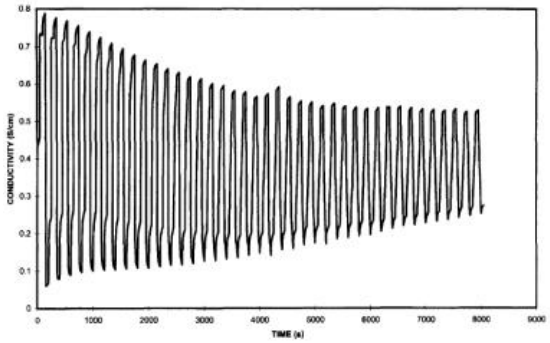

Figure 3.63 Conductivity change for PPY-4 during cycling with $HC1/N_2/NH_3/N_2$ [72]

Textiles coated with conducting elastomer composites have many advantages over ICPs, including high flexibility, stability and ease of application. In most of these studies, carbon or graphite is preferred as the conductive phase in the composite.

Scilingo *et al.*, fabricated piezoresistive textile sensors by coating an elastic fabric (86 wt% polyester and 14 wt% lycra) with carbon filled rubber [85]. In order to detect respiration, the sensors were located around rib cage and abdomen as shown in Fig. 3.64.

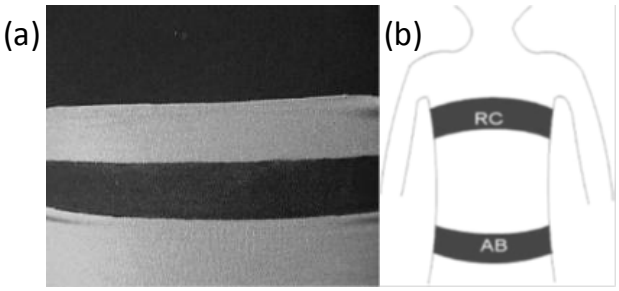

Figure 3.64 (a) Piezoresistive sensors (b) located at rib cage (RC) and the abdomen (AB) [85]

To monitor movement, sensors were located on the right elbow joint. The system was compared to commercial sensors and found to be effective for movement monitoring. As shown in Fig. 3.65, the output of the textile sensor, showed similar pattern compared to the commercial one [85].

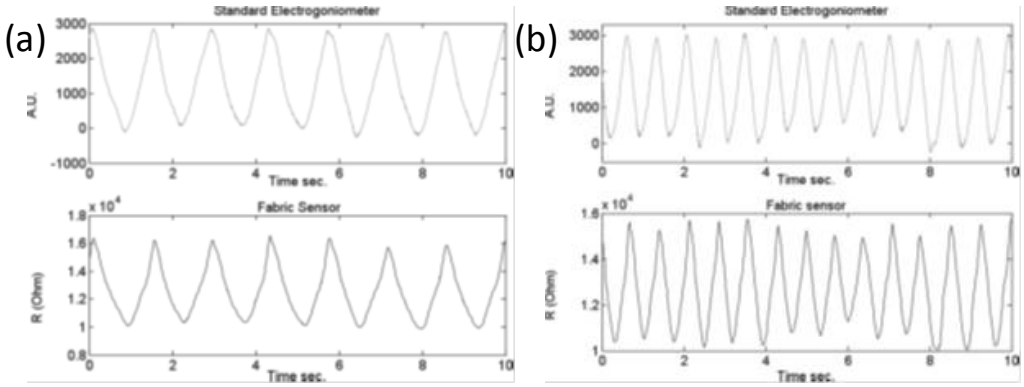

Figure 3.65 Signal obtained from electrogoniometer (upper) and fabric sensor (lower) during (a) slow movement (b) fast movement of the arm [85]

Tognetti *et al.*, reported a sensing garment for post-stroke rehabilitation called upper limb kinesthetic garment (ULKG) [86]. The ULKG is an elastic garment mainly consisting of arrays of conducting silicone elastomer (Elastosil) in various patterns and can be used for the gesture, posture and movement monitoring, see Fig. 3.66.

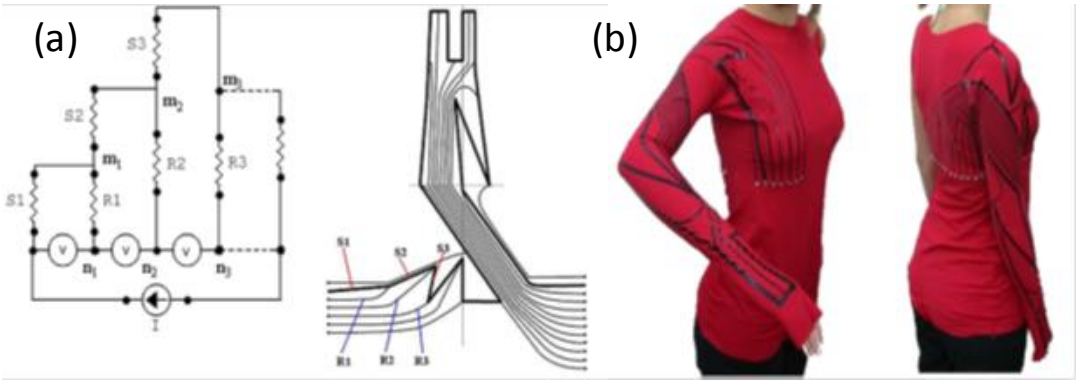

Figure 3.66 (a) The electronic acquisition scheme (on the left) and the mask (b) The UKLG [86]

Figure 3.67 Posture recognition trials performed by the user and represented by the avatar on the right [86]

Paradiso *et al.*, reported a smart health monitoring system using different textile based sensors [12].

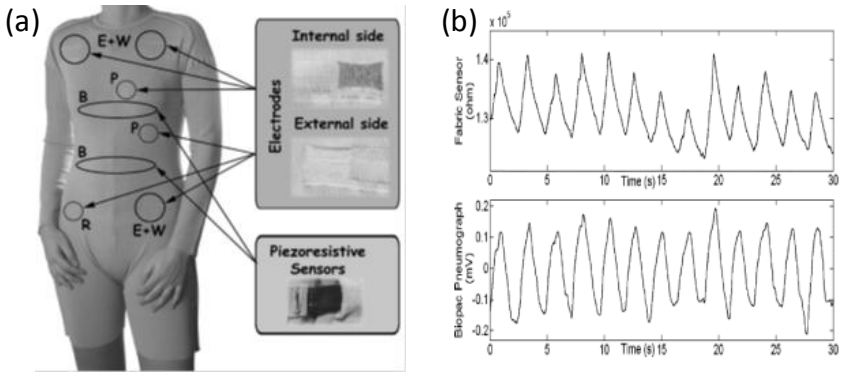

Figure 3.68 (a) Prototype model (b) respiration signal derived from piezoresistive fabric (upper) and biopac pneumograph (lower) [12]

Piezoresistive textile sensors, fabricated from carbon filled silicone coated elastic fabric, were located around chest and abdomen and used for respiration monitoring, see Fig. 3.68. The system was found effective for detecting respiration signals and compared well with a commercial system [12].

Lorussi *et al.*, developed a sensing glove for acquiring finger movements to be used in rehabilitation. The sensing glove is fashioned out of a fabric coated by conductive silicone and showed resistance value of 1 kΩ cm^{-1} and gauge factor of 2.8. The glove has a special pattern, while bold tracks function as sensors, thin tracks function as signal carriers [87].

Although the sensing glove, reported by Lorussi *et al.* [87], has many advantages such as comfort and wearability; resistance change did not show linear behavior and quick response it showed slow nonlinear behavior. This problem was addressed by post-processing of data [87].

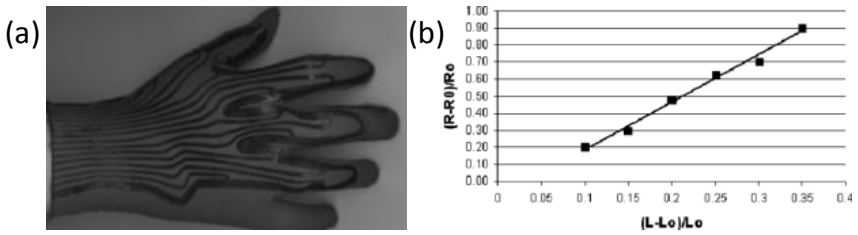

Figure 3.69 (a) Sensorized glove. (b) behavior of the relative variation of resistance of sensor against the relative strain [87]

Another interesting study was carried out by Tesconi *et al.* [88]. They designed a sensing band for monitoring knee flexion of patients who are suffering from venous ulcers. As shown in Fig. 3.70, the lower limb sensing garment consists of printed conductive elastomer arrays.

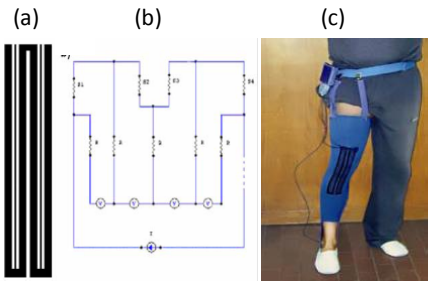

Figure 3.70 (a) The mask used for the sensors (b) the equivalent electric scheme (c) overall prototype consisting of a knee band KB, sensorized shoe and an "on body unit" [88]

In addition to this, sensing shoe was used for determination of the gait cycle [88]. The data obtained from knee flexion sturdy is shown in Fig. 3.71.

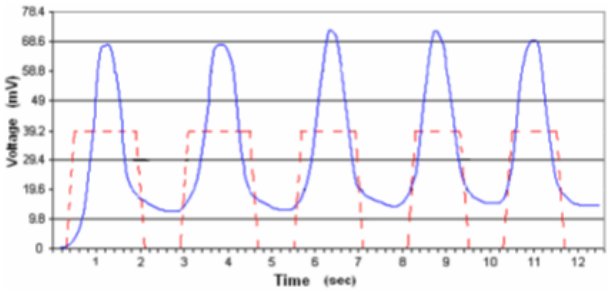

Figure 3.71 Flexion-extension of the central sensor of KB (continuous curve) and signal coming from the shoe sensor (dashed curve) which marks the gait cycle [88]

In addition to silicone, other polymers can also be used as a matrix for the conducting composites. Cochrane *et al.*, reported a piezoresistive sensor made of a nylon fabric printed with a Styrene-Butadiene-Styrene (SBS) co-polymer filled with highly structured carbon black powder [17].

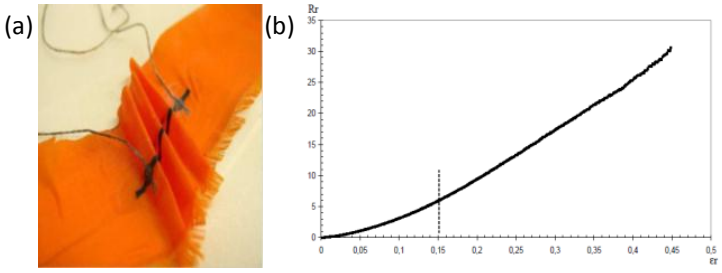

Figure 3.72 (a) Piezoresistive fabric sensor and (b) its piezoresistive behavior [17]

The fabric sensor showed positive piezoresistive response with a gauge factor of 80 [17]. Tesconi *et al.*, designed a smart garment for monitoring movement of lower limbs [89]. The sensing garment consists of an array of printed sensors (graphite/ silicon) to monitor knee and hip position during rowing, see Fig. 3.73.

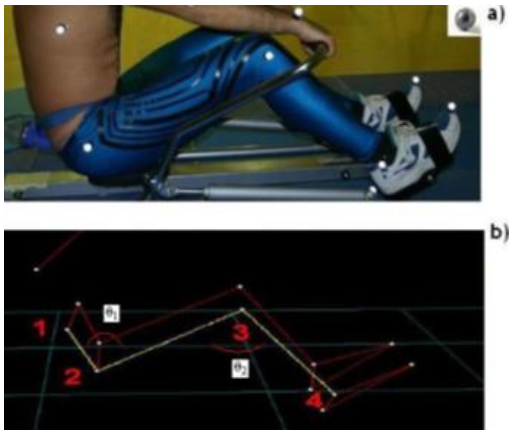

Figure 3.73 (a) The arrangement of the marker on body of the athlete (b) the model obtained by using experimental set-up [89]

The sensing garment was compared to a commercial system in measuring the flexion-extension angles during knee movement. The measured change in resistance was interpreted into kinematic output with the help of computational algorithms; see Fig. 3.74 [89].

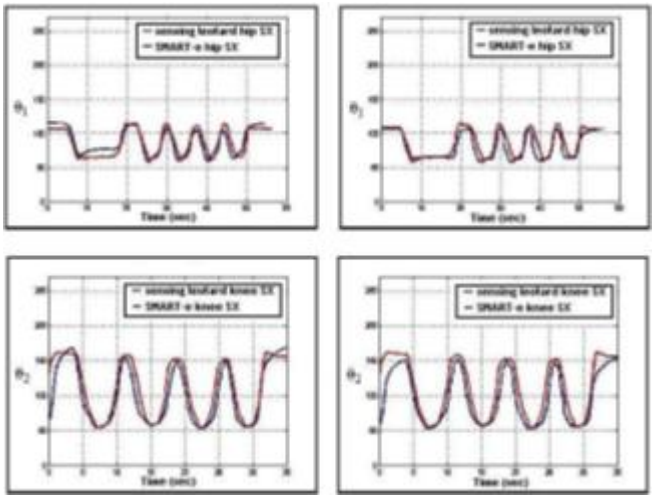

Figure 3.74 Flexion-extension angles of the hip (θ1) and knee (θ2) of the left leg in two different trials. The red line is the SMART-e output, while the blue one represents the sensing garment response [89]

In addition to strain sensor, conducting silicone has been used as a pressure sensor [90].

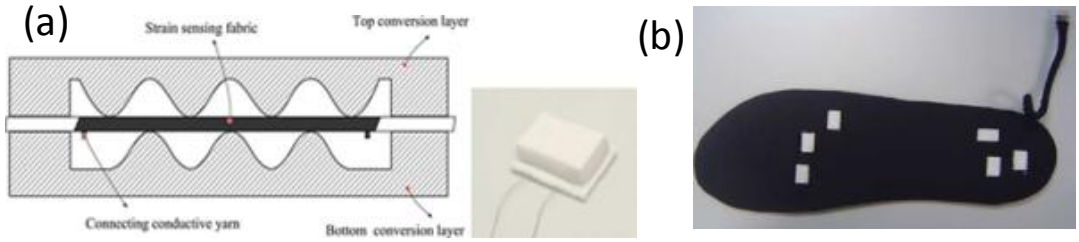

Figure 3.75 (a) Schematic diagram of the pressure sensor and sensor packages, (b) integrated textile sensors on insole [90]

Shu *et al.*, reported a carbon black filled silicone coated fabric pressure sensor for monitoring applied foot pressure during walking [90]. Six sensors were located on the insole of a shoe as shown in Fig. 3.75. In order to evaluate the performance, sensors were exposed to different pressures between 10-800 kPa. The sensors were characterized as stable after 100,000 cycles.

The sensors also showed high resistance to changes in the humidity because they were packaged in silicone rubber [90].

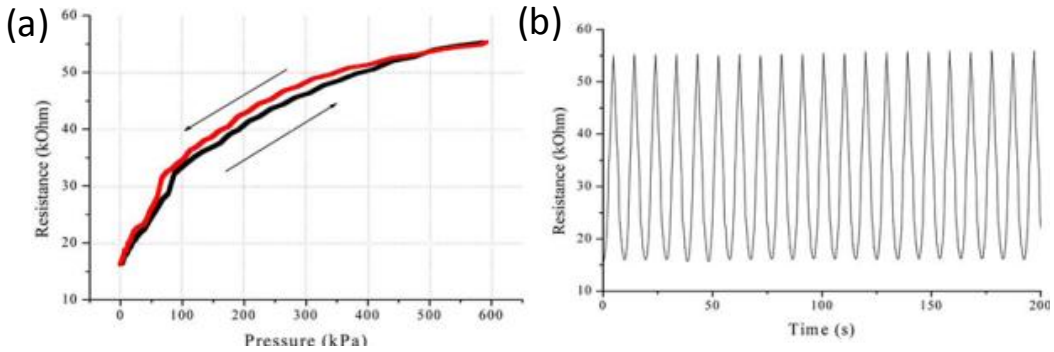

Figure 3.76 Piezoresistive behavior of pressure sensors as a function of (a) pressure and (b) time [90]

Knitted fabrics are formed by interlacement of yarn loops as shown in Fig. 3.77. Knitted fabrics are commonly used method in textile fabric manufacturing for apparel and are desirable in some applications because of their low stiffness and resulting comfort.

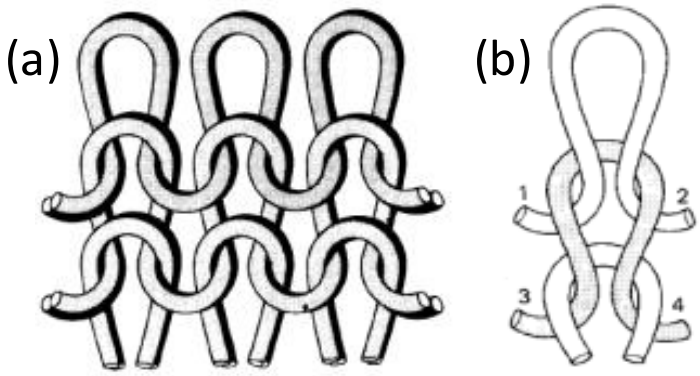

Figure 3.77 (a) Weft knitted fabric and (b) the knitted stitch [91]

The knit fabric structure is formed by overlapped loops and if conducting yarns are used, movement of these loops is the main factor for their piezoresistive response [92]. Different fibers can be used for knitted sensors including carbon and steel [16]. However, to increase the cyclic stability of the fabric, elastic conductive fibers are better alternatives. Since fabric structure directly affects electromechanical properties of the textile sensor, before the design of the knitted sensor, fiber type, yarn properties, loop geometry, fabric deformation-recovery behavior and pattern of the conductive path in the fabric should be taken into consideration. Integration of conductive yarns in a knit structure can be different based on the direction of the applied strain in an application, see Fig. 3.78 [14,16,26,92,93].

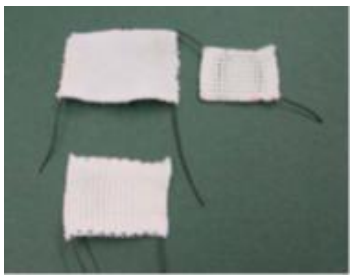

Figure 3.78 Textile sensors from knitted fabric [92]

One of the first studies on using knit fabrics as sensors was carried out by Wijesiriwardana *et al.* [92]. They developed a knitted strain gauge by using conductive elastomeric fibers as shown in Fig. 3.79 and evaluated its response to applied strain.

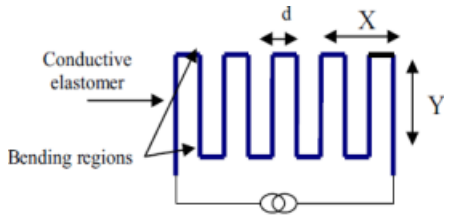

Figure 3.79 Electroconductive fiber path

While deformation in the Y direction resulted in increase in resistance, deformation in the X direction showed decrease in resistance. This difference in response is attributed to the mechanical anisotropy of loop deformation.

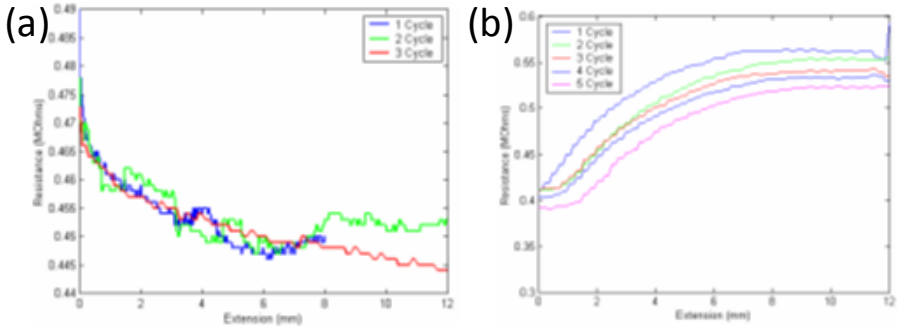

Figure 3.80 (a) Resistance change in wale direction (b) resistance change in course direction [92]

When a simple knit structure (*i.e.*, single jersey) is deformed in the Y direction, the loop shape changes to a slender shape in which the length to width ratio increases. This deformation characteristic is postulated to result in the decrease in resistance. On the other hand, when the applied strain is in X direction, the conducting paths in the fabric structure comes closer and is thought to lower overall electrical resistance of the structure [92].

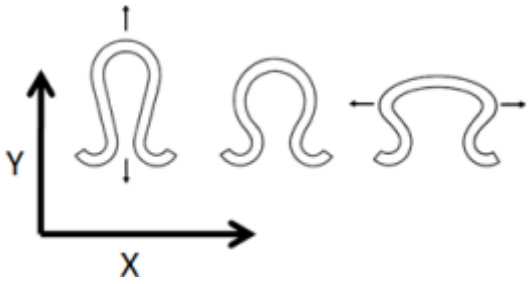

Figure 3.81 Loop extension and recovery in different directions [91]

Paradiso *et al.*, reported knitted piezoresistive sensors with the ability of monitoring vital signs and movement [94]. The knitted piezoresistive sensors fabricated using conductive yarns were located around abdomen and chest for respiration monitoring and on arms in order to monitor movement [94].

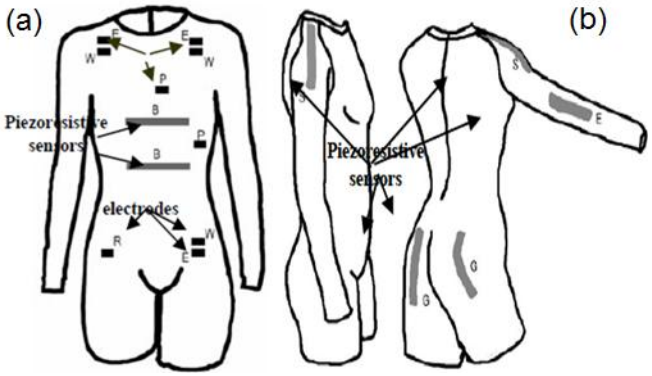

Figure 3.82 Prototype model [94]

The sensor system was able to monitor the basal condition respiration designated as Th-R and Ab-R in Fig. 3.82. While movement sensors did not show any change during basal condition, the elbow sensors' response was noticeable in the case of flexion and extension (Fig. 3.83) [94].

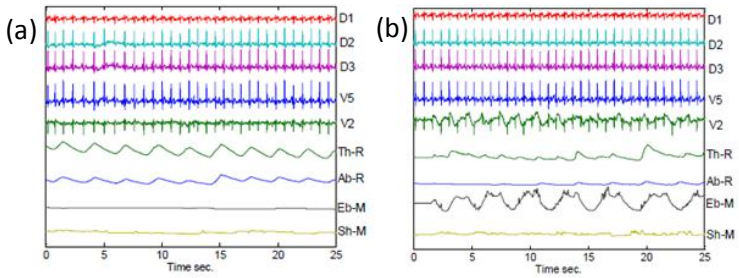

Figure 3.83 (a) Signals in basal condition, D1, D2, D3 Einthoven leads I, II, III. V2, V5: standard precordial leads V2 and V5. Th-R, Ab-R: respiration sensors on thoracic and abdominal position respectively. Sh-M, Eb-M: movement sensors on the left shoulder and elbow, respectively (b) Signals obtained during flex-extension of the left elbow [94]

In the another study Paradisio *et al.*, reported use of knitted sensors fabricated using commercial conducting yarns (PAC by Europa NCT, Poland) and located on shoulders and elbows to monitor movement, see Fig. 3.84 [24].

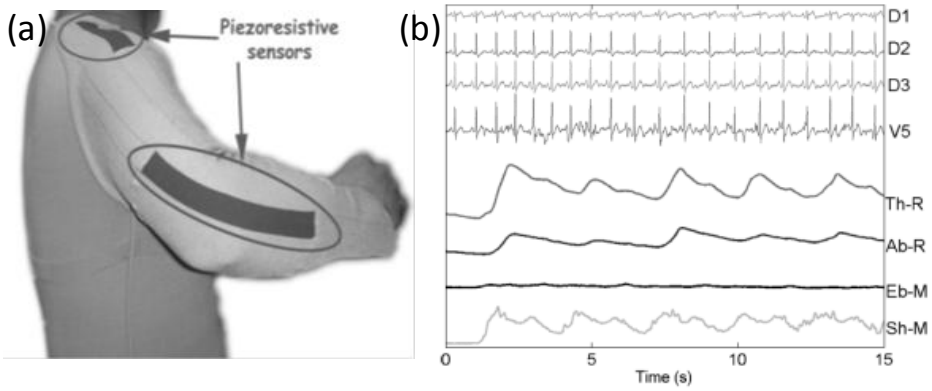

Figure 3.84 (a) Movement sensors located on shoulder and elbow (b) signals obtained during abduction-adduction of the left shoulder, D1, D2, D3 Einthoven leads I, II, III. V2, V5: standard precordial leads V2 and V5. Th-R, Ab-R: respiration sensors in thoracic and abdominal positions, respectively. Sh-M, Eb-M movement sensors on the left shoulder and elbow, respectively [24]

Loriga *et al.*, developed a sensing t-shirt by incorporating conducting yarns (Belltron®9R1), into the fabric structure during knitting by intarsia technique. The sensors are located at abdominal and thoracic regions for respiration monitoring, see Fig. 3.85 [25,95,95].

Figure 3.85 Knitted sensing t-shirt for monitoring abdominal and thoracic respiration [25,95]

In order to evaluate the efficiency of the system, the output from the knitted sensor is compared to that from a commercial system, see Fig. 3.86. Both systems showed similar behavior, although the thoracic and abdominal knitted sensors showed similar trends, the magnitude of change was noted to be different and is thought to have caused by different deformation ratio of the fabric sensors at different locations [25,95].

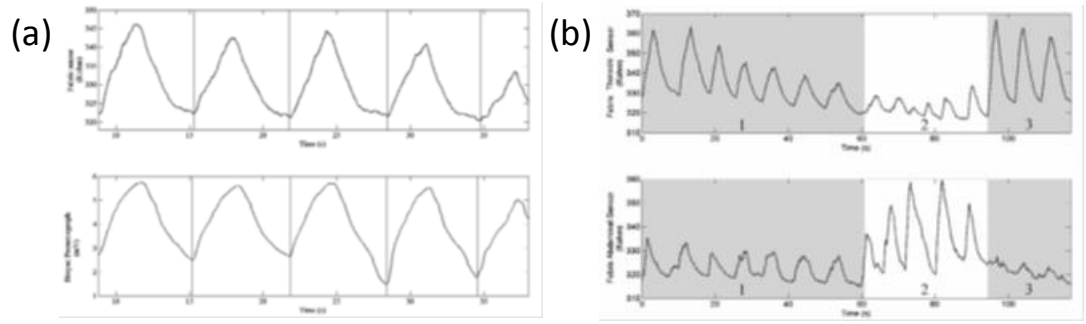

Figure 3.86 (a) Signals obtained from piezoresistive fabric sensor (upper) and Biopac pneumograph (lower) during normal respiration (b) comparison of thoracic (upper) and abdominal (lower) respiration signal by fabric sensors (1-normal, 2- predominantly abdominal, 3-thoracic repiration) [25,95]

Zhang *et al.*, produced tubular and flat warp knitted fabric from stainless steel and carbon fibers in order to use as strain sensors as shown in Fig. 3.87. They have investigated the effect of fiber type, structure, testing speed and temperature on the piezoresistive behavior of the knit structures [16].

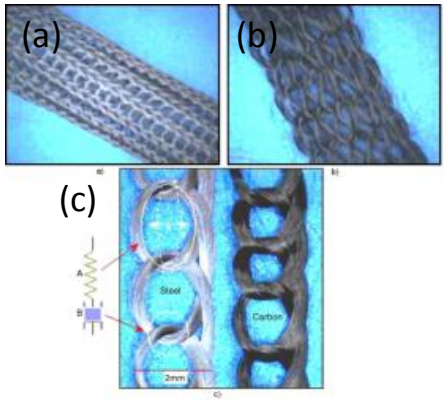

Figure 3.87 Tubular knitted fabric (a) steel (b) carbon and (c) single warp steel and carbon knitted fabric [16]

As seen in Fig. 3.88, both carbon and steel fabrics showed negative piezoresistance. However, carbon fabrics showed higher stability than of steel. The flat knitted warp sensor showed better stability when compared to tubular fabrics. It was also reported that, higher testing speed lead to lower hysteresis with higher recoverability.

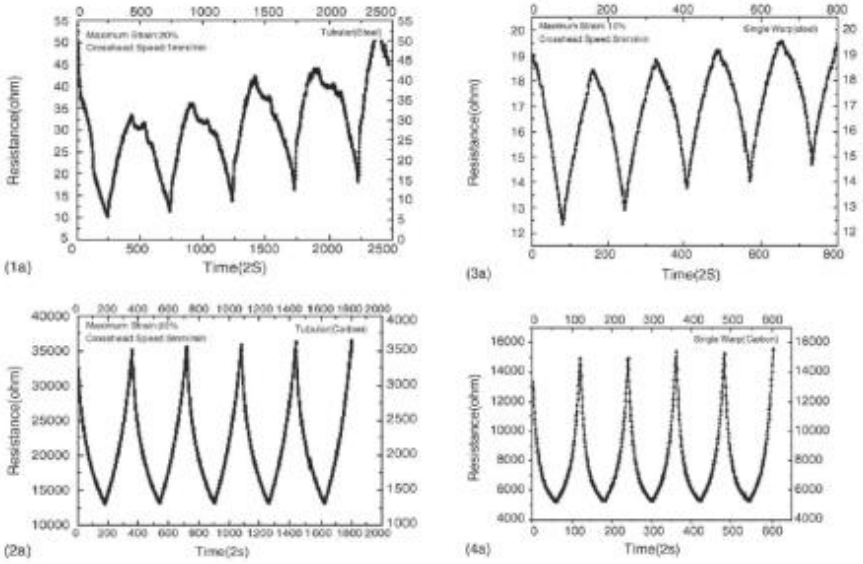

Figure 3.88 Piezoresistive response of (1a) tubular steel (2a) tubular carbon (3a) single warp steel (4a) single warp carbon

Since carbon fibers have high thermal stability, they have also been investigated under varying temperature. The knitted sensors showed similar behavior in the temperatures range of 20-200°C, see Fig. 3.89. However, resistance decreased at higher temperature.

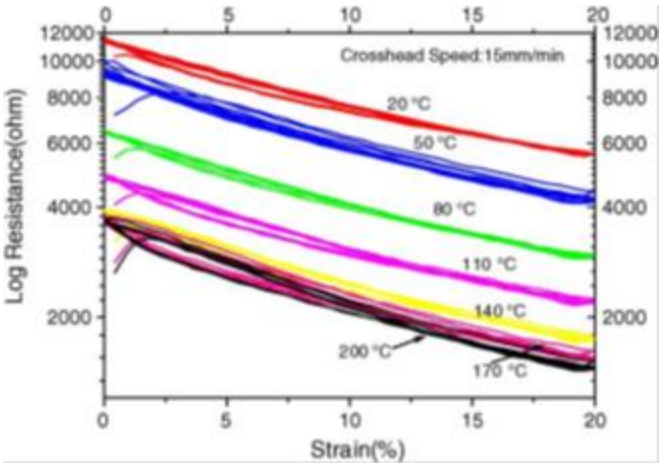

Figure 3.89 Piezoresistive respond under different temperature and strain [16]

Pacelli *et al.*, fabricated knitted sensors using conducting yarn and investigated the effect of elastic recovery on sensing performance. The base fabric of the sensors contained elastomeric yarn, spandex, of three different mass linear densities (designated as Ny60, Ny 59 and Ny 58 in Fig. 3.90). All three sensors showed positive and linear piezoresistive behavior in the range of 8-55% strain. Fig. 3.90 (b) presents the signals obtained from the knitted sensor and that from a commercial electrogoniometer. Although output values are different they showed similar pattern during the movement of the elbow [14].

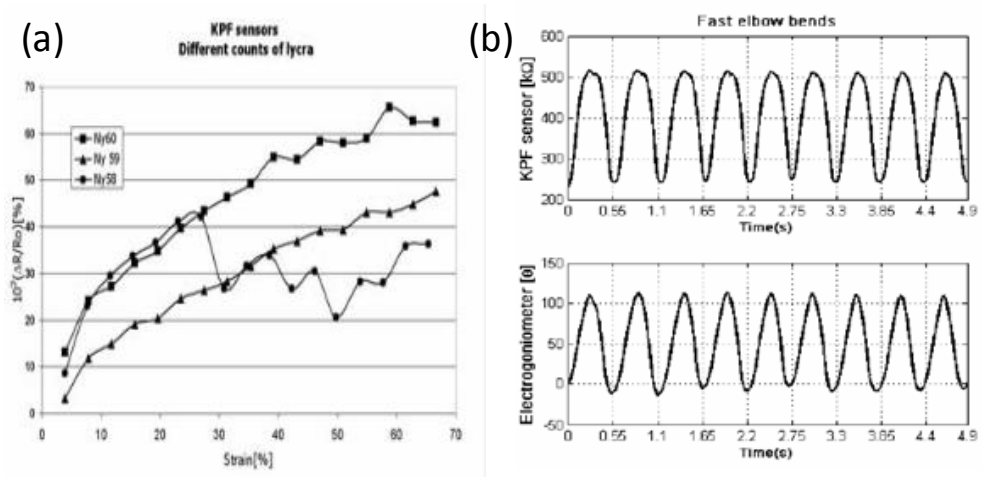

Figure 3.90 (a) Piezoresistive behavior of knitted sensors fabricated from different spandex fibers (b) Signal obtained from knitted sensor (upper) and electrogoniometer (lower) during fast elbow bends [14]

Huang *et al.*, developed a knitted respiration belt for babies in order to prevent Sudden Infant Death Syndrome (SIDS). As shown in Fig. 3.91, system consists of basal and conducting yarns. In this instance, the sensors are constructed from a conductive yarn (carbon coated Resistat F901) wrapped polyester yarn and elastomeric fibers. Unlike the previous systems, the conducting yarns are spaced in intervals. Evaluation of the belt was carried out using an artificial lung and the system was found effective for the respiration monitoring between ranges of number of breath per minute (BPM) [93,96].

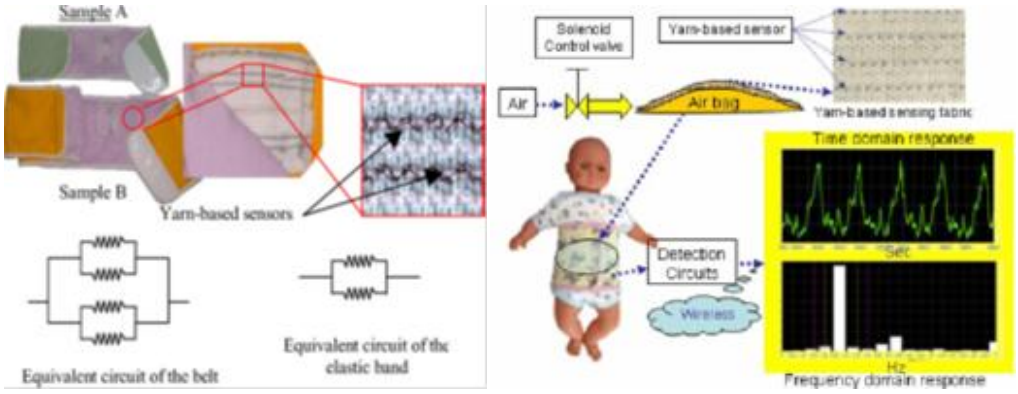

Figure 3.91 Respiration monitoring system [93,96]

Yarns, fabricated from different raw materials by different methods are the basic components of fabrics. Recent developments in materials and manufacturing technologies have facilitated growth of functional yarns particularly suited for use in sensors for e-textile applications [97]. Yarn based sensors have been reported for strain and posture monitoring [98-100]. Different materials including, carbon loaded elastomer [97,99], carbon coated fibers [93,96,101], silver coated fibers, and stainless steel fibers [100] have been used for the development of yarn based sensors. The sensors have been fabricated in the form of single filaments [97,99] or twisted yarns [93,96,101] have been used alone [93,97,101] or have been incorporated in various forms of textiles [98,99]. Unlike in traditional yarns, sensing yarns are required to have superior elasticity in addition to electrical conductivity. Elasticity can be an inherent property [97,99] of the conductive component or can be enhanced by the addition of elastic fibers into the yarn structure [93,96,101]. While for conducting filaments, mechanism of the piezoresistance is governed primarily by the material properties [97,99], in composite/twisted yarns every component and the structure influence the electromechanical behavior of the yarn [93,96,101].

Gibbs *et al.*, developed sensing pants with the ability of determining joint angles. The sensing elements are arrays of conductive textile fibers located around three different joints, see Fig. 3.92 [98].

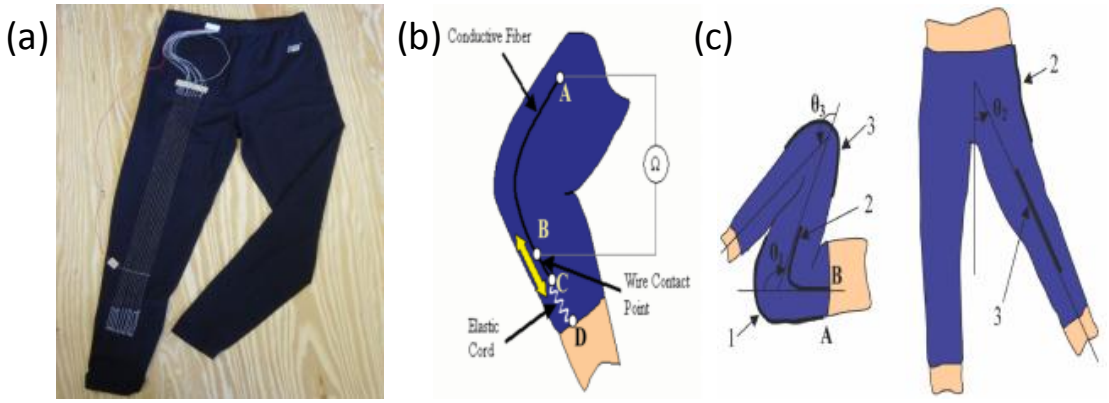

Figure 3.92 (a) Sensing pants (b) schematic of sensor (c) location of sensor arrays and basic angles used in the study [98]

The sensing mechanism based on the deformation of the fiber and the resulting change in resistance shown in Fig. 3.93 has been correlated with the change in the angle of joint [98].

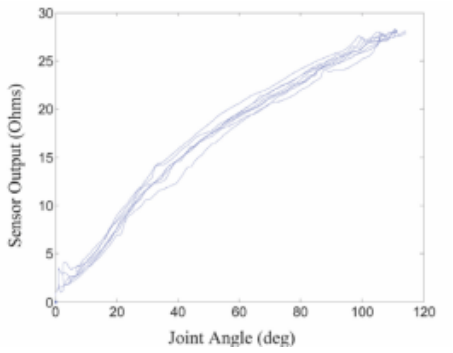

Figure 3.93 Resistance change as a function of knee flexion angle [98]

Mattmann *et al.*, fabricated piezoresistive fibers, with a gauge factor of 20, from carbon loaded thermoplastic elastomer (SEBS-block copolymers) as presented in Fig. 3.94. In the study, electromechanical properties of fiber and fiber attached to a fabric were evaluated [97].

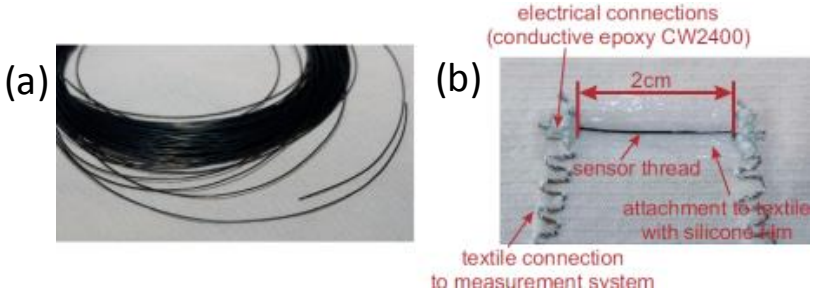

Figure 3.94 (a) Piezoresistive thread (b) piezoresistive thread attached onto the fabric [97]

The highest linearity of the piezoresistive response in the range of 0-100% strain was obtained from a 50 wt% carbon loaded composite and was chosen as the sensor thread for this study [97].

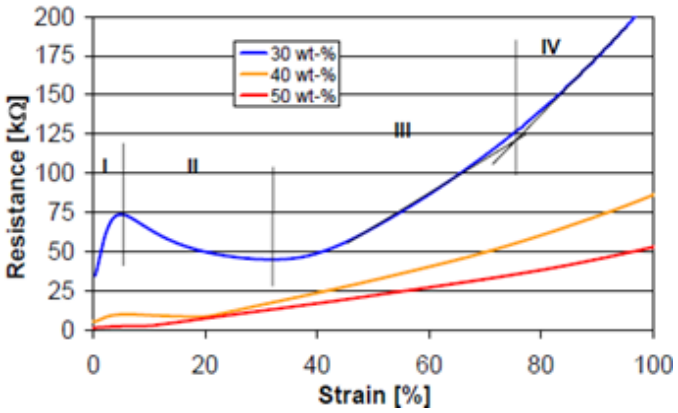

Figure 3.95 Piezoresistive behavior of fibers at different filler loading as a function of strain [97]

In the second part of the study, they attached the sensor threads onto a fabric and tested the effect of strain, testing speed and aging. As seen in Fig. 3.95, the resistance increased with the application of strain, however, the stability of the sensor was found to depend on the level of pre-cycling. If the samples cycled once to 80% strain, the following cycles showed stability regardless of the magnitude of the strain. In addition, the testing speed was found to have no significant effect on the piezoresistive response [97].

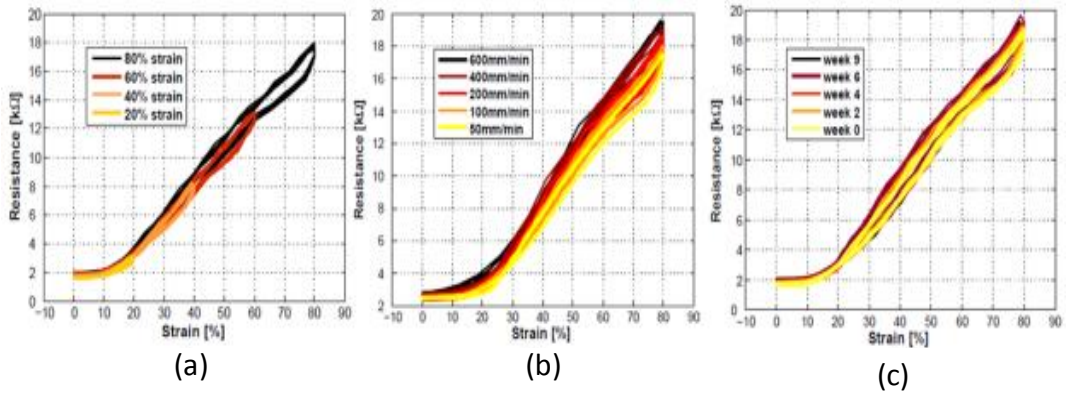

Figure 3.96 Piezoresistive behavior as a function of strain (a) at different maximum strain (b) at different testing speed (c) aging behavior [97]

By using these piezoresistive threads, Mattmann *et al.*, designed a sensing garment in order to monitor upper body posture, see Fig. 3.97. Piezoresistive threads were placed at 21 different locations throughout the garment using silicone film adhesive. The silicon film, used for attachment, also helped minimize the unrecovered strain [99].

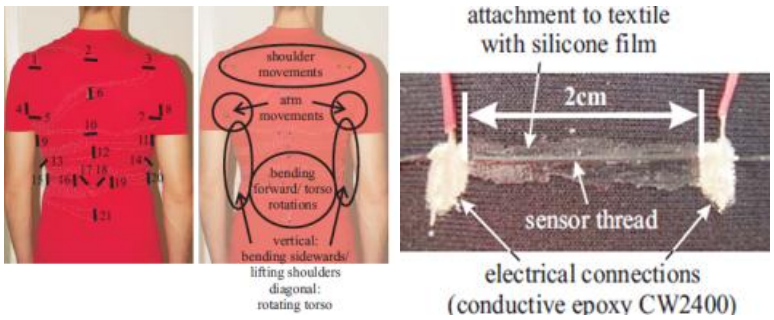

Figure 3.97 Sensing garment and attachment of sensor threads [99]

Fig. 3.98 shows an example of posture recorded using the SEBS yarn strain change as a function of time and rotational angle. It is evident that the sensor was able to record increased rotational angle and speed of movements. However, the system was not able to monitor similar postures and some positions in which upper body position did not change such as sitting and standing [99].

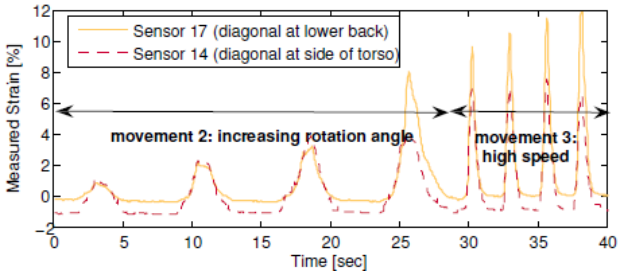

Figure 3.98 Strain change *vs.* movement speed and rotational angle [99]

In another interesting approach, Huang *et al.*, fabricated sensor yarns by using carbon coated fiber, elastic and polyester fibers by single or double wrapping with different levels of twist [93].

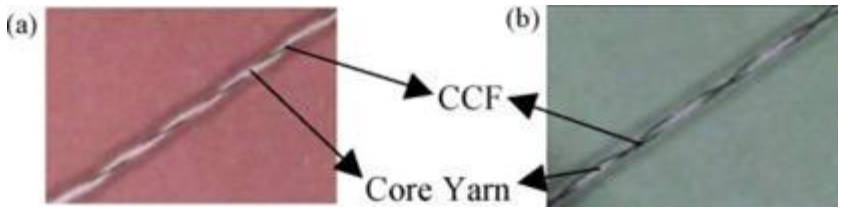

Figure 3.99 Piezoresistive yarn-based sensors (a) single wrapping (b) double wrapping [93]

For obvious reasons, single wrapped yarns showed higher resistance than double wrapped. Both yarns showed positive piezoresistance under strain but double wrapped yarn showed higher linear response with lower sensitivity [93].

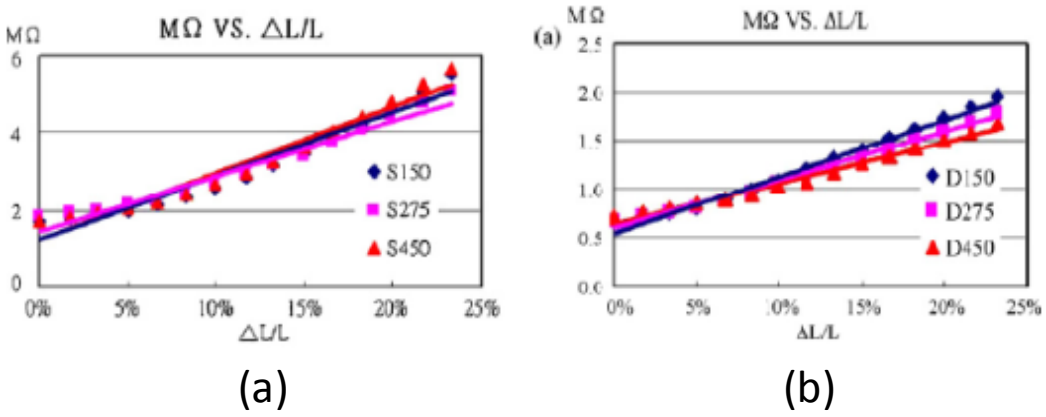

Figure 3.100 Piezoresistive response of (a) single wrapping yarns (b) double wrapping yarns [93]

This was attributed to less slippage in the structure in case of double wrapping under strain caused from synergistic effect of longitudinal and lateral forces. Higher level of twist was not found to have any influence on the piezoresistive behavior of yarns [93].

In another study carried out by Huang *et al.*, effect of different types of core and conductive yarns and level of twist were investigated. Two different polyester fibers

(56dtex/144filaments and 56dtex/48filaments) and two different conductive fibers (Resistat F901, Merge S022 (24dtex)-CCF 24 and Resistat F901, Merge D044 (49dtex)-CCF 49) and spandex were used. As shown in Fig. 3.101, polyester yarn with higher number of filaments in cross-section (56dtex/144filaments), lead to higher piezoresistive response. This was attributed to higher deformation rate and reduced distributed force for coarser yarns [101].

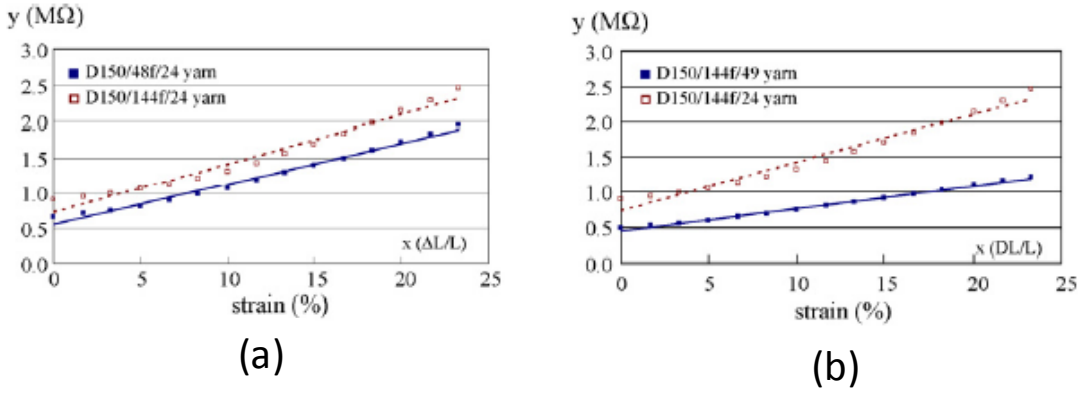

Figure 3.101 Effect of type of (a) core yarn and (b) conductive yarn on piezoresistive response [101]

Fig. 3.101 (b) shows the effect of conductive yarn type on piezoresistive behavior. As can be seen, CCF 49 showed lower gauge factor and higher linearity which was assumed to be caused from higher stiffness. Higher stiffness enables fiber to carry higher load under same strain and this leads to less deformation and lower change in resistance. In addition to material type, effect of twist number was also investigated. Although there is no significant difference was reported for CCF 49, twist number was found as an important criterion for CCF 24. Increased number of twist resulted with lower sensitivity because of its restrictive effect on conductive fibers. Although sensor yarns seem promising they have some

disadvantages such as requirement of preload before measurement. This was reported to be caused by the crimp of the yarn which is directly related with the addition of spandex fiber into the structure [101].

Conclusions

This review study provides detailed overview about the basic concepts textile based sensors that have attracted considerable scientific and commercial interest because of their potential for health monitoring, posture monitoring, and rehabilitation and so on. Textile-based sensing has become an active area of research in the emerging field of e-textiles in recent years. Although textile based sensors can be broadly categorized into capacitive, inductive, optical, chemical, piezoelectric and piezoresistive; much of the work has been focused on piezoresistive sensor. While, with the inductive sensors, the coils need to be integrated into the sensor which make them less comfortable and limit their usage. Capacitive sensors also have issues related to repeatability and stability. Similarly, the optical sensors are expensive and their properties might change while they are integrated into the fabric and hence are not reliable, while, the piezoelectric sensors are relatively expensive and have limited scope of applications. By contrast, printed piezoresistive sensors that are resistant to environmental conditions, besides being conformable to the body shape. Hence, from among the multitude of sensors discussed, the printable strain sensors using piezoresistive materials offer wide range of applications.

References

[1] Dittmar A, Axisa F, Delhomme G, Gehin C. New concepts and technologies in home care and ambulatory monitoring. Stud Health Technol Inform 2004;108:9-35.

[2] Lymberis A. Wearable ehealth systems for personalised health management : state of the art and future challenges. Amsterdam ; Washington, D. C.: IOS Press, 2004.

[3] Linz T, Vieroth R, Dils C, Koch M, Braun T, Becker K et al. Embroidered interconnections and encapsulation for electronics in textiles for wearable electronics applications. Smart Textiles 2009;60:85-94.

[4] Lorussi F, Rocchia W, Scilingo EP, Tognetti A, De Rossi D. Wearable, redundant fabric-based sensor arrays for reconstruction of body segment posture. IEEE Sens J 2004;4:807-18.

[5] Bartalesi R, Lorussi F, Tesconi M, Tognetti A, Zupone G, De Rossi D. Wearable kinesthetic system for capturing and classifying upper limb gesture. Los Alamitos, CA USA: IEEE Computer Soc, 2005.

[6] Munro BJ, Campbell TE, Wallace GG, Steele JR. The intelligent knee sleeve: a wearable biofeedback device. Sens Actuator B-Chem 2008;131:541-7.

[7] Zhang, X., Tao, X. Smart textiles: passive smart. Textile Asia 2001:45-49.

[8] Zhang, X., Tao, X. Smart textiles: active smart. Textile Asia 2001:49-52.

[9] Zhang, X., Tao, X. Smart textiles: very smart. Textile Asia 2001:35-37.

[10] Fraden J. Handbook of modern sensors : physics, designs, and applications. New York: AIP Press/Springer, 2004.

[11] Sergio M, Manaresi N, Nicolini M, Gennaretti D, Tartagni M, Guerrieri R. A textile-based capacitive pressure sensor. Sens Lett 2004;2:153-60.

[12] Paradiso R, Loriga G, Taccini N. A wearable health care system based on knitted integrated sensors. IEEE T Inf Technol Biomed 2005;9:337-44.

[13] Kang T, Merritt C, Karaguzel B, Wilson J, Franzon P, Pourdeyhimi B et al. Sensors on textile substrates for home-based healthcare monitoring. New York; USA: IEEE, 2006.

[14] Pacelli M, Caldani L, Paradiso R. Textile piezoresistive sensors for biomechanical variables monitoring. New York, USA: IEEE, 2006.

[15] Jayaraman S, Kiekens P, Grancaric AM. Intelligent textiles for personal protection and safety. Washington, D.C.: IOS Press, 2006.

[16] Zhang H, Tao XM, Yu TX, Wang SY. Conductive knitted fabric as large-strain gauge under high temperature. Sens Actuator A-Phys 2006;126:129-40.

[17] Cochrane C, Koncar V, Lewandowski M, Dufour C. Design and development of a flexible strain sensor for textile structures based on a conductive polymer composite. Sensors 2007;7:473-92.

[18] Lobodzinski SS, Laks MM. Comfortable textile-based electrocardiogram systems for very long-term monitoring. Cardiol J 2008;15:477-80.

[19] Merritt CR, Nagle HT, Grant E. Textile-Based Capacitive Sensors for Respiration Monitoring. IEEE Sens J 2009;9:71-8.

[20] Coyle S, Wu Y, Lau K, Brady S, Wallace G, Diamond D. Bio-sensing textiles - Wearable chemical biosensors for health monitoring. 4th International Workshop on Wearable and Implantable Body Sensor Networks (Bsn 2007) 2007;13:35-9.

[21] Meyer J, Lukowicz P, Troester G. Textile pressure sensor for muscle activity and motion detection. Los Alamitos, CA, USA: IEEE Computer Soc, 2006.

[22] Kang TH. Textile-embedded sensors for wearable physiological monitoring systems. Ph.D. Dissertation, Raleigh, NC, USA, 2006.

[23] Paradiso R, Gemignani A, Scilingo EP, De Rossi D. Knitted bioclothes for cardiopulmonary monitoring. Proceedings of the 25th Annual International Conference of the IEEE Engineering in Medicine and Biology Society, Vols 1-4 - a New Beginning for Human Health 2003;25:3720-3.

[24] Paradiso R, Belloc C, Loriga G, Taccini N. Wearable healthcare systems, new frontiers of e-textile. Stud Health Technol Inform 2005;117:9-16.

[25] Paradiso R, De Rossi D. Advances in textile technologies for unobtrusive monitoring of vital parameters and movements. New York, USA: IEEE, 2006.

[26] Pacelli M, Loriga G, Paradiso R. Flat knitted sensors for respiration monitoring. New York, USA: IEEE, 2007.

[27] Dobkin BH, Dorsch A. The Promise of mHealth: daily activity monitoring and outcome assessments by wearable sensors. Neurorehabil Neural Repair 2011;25:788-98.

[28] Lanata A, Scilingo EP, De Rossi D. A multimodal transducer for cardiopulmonary activity monitoring in emergency. IEEE T Inf Technol Biomed 2010;14:817-25.

[29] Coyle S, Lau K, Moyna N, O'Gorman D, Diamond D, Di Francesco F et al. BIOTEX-biosensing textiles for personalised healthcare management. IEEE T Inf Technol Biomed 2010;14:364-70.

[30] Morris D, Schazmann B, Wu Y, Fay C, Beirne S, Slater C et al. Wearable technology for the real-time analysis of sweat during exercise. New York, USA: IEEE, 2008.

[31] Webster JG. Measurement, instrumentation, and sensors handbook. CRC Press published in cooperation with IEEE Press, 1999.

[32] Wilson JS. Sensor technology handbook. 2005.

[33] Baxter LK. Capacitive sensors : design and applications. New York: IEEE Press, 1997.

[34] Gautschi G. Piezoelectric sensorics : force, strain, pressure, acceleration and acoustic emission sensors, materials and amplifiers. Berlin ; New York: Springer, 2002.

[35] Tandeske D. Pressure sensors : selection and application. New York: M. Dekker, 1991.

[36] Holden A. Crystals and crystal growing. Cambridge, Mass.: MIT Press, 1982.

[37] Harsányi G. Sensors in biomedical applications : fundamentals, technology & applications. Lancaster, Pa.: Technomic Pub. Co, 2000.

[38] Udd E. Fiber optic sensors : an introduction for engineers and scientists. New York: Wiley-Interscience, 2006, 1991.

[39] López-Higuera JM. Handbook of optical fibre sensing technology. New York: Wiley, 2002.

[40] Yu FTS. Fiber optic sensors. Boca Raton, FL: CRC Press, 2008.

[41] Flickinger MC. The encyclopedia of bioprocess technology : fermentation, biocatalysis, and bioseparation. New York: John Wiley, 1999.

[42] Hulanicki A, Glab S, Ingman F. Chemical sensors definitions and classification. Pure Appl Chem 1991;63:1247-50.

[43] Bao M. Micro mechanical transducers : pressure sensors, accelerometers, and gyroscopes. Amsterdam ; New York: Elsevier, 2000.

[44] Eickhoff M, Stutzmann M. Influence of crystal defects on the piezoresistive properties of 3C-SiC. J Appl Phys 2004;96:2878-88.

[45] Fernberg P, Nilsson G, Joffe R. Piezoresistive performance of long-fiber composites with carbon nanotube doped matrix. J Intell Mater Syst Struct 2009;20:1017-23.

[46] Thostenson ET, Chou T. Carbon nanotube networks: sensing of distributed strain and damage for life prediction and self healing. Adv Mater 2006;18:2837,+.

[47] Wijesiriwardana R, Mitcham K, Hurley W, Dias T. Capacitive fiber-meshed transducers for touch and proximity-sensing applications. IEEE Sens J 2005;5:989-94.

[48] Sergio M, Manaresi N, Campi F, Canegallo R, Tartagni M, Guerrieri R. A dynamically reconfigurable monolithic CMOS pressure sensor for smart fabric. IEEE J Solid State Circuits 2003;38:966-75.

[49] Cheng J, Amft O, Lukowicz P. Active capacitive sensing: exploring a new wearable sensing modality for activity recognition. Pervasive Computing, Proceedings 2010;6030:319-36.

[50] Morris D, Coyle S, Wu Y, Lau KT, Wallace G, Diamond D. Bio-sensing textile based patch with integrated optical detection system for sweat monitoring. Sensors Actuators B: Chem 2009;139:231-6.

[51] Wijesiriwardana R. Inductive fiber-meshed strain and displacement transducers for respiratory measuring systems and motion capturing systems. IEEE Sens J 2006;6:571-9.

[52] Edmison J, Jones M, Nakad Z, Martin T. Using piezoelectric materials for wearable electronic textiles. Los Alamitos, CA, USA: IEEE Computer Soc, 2002.

[53] Edmison J, Jones M, Lockhart T, Martin T. An e-textile system for motion analysis. Stud Health Technol Inform 2004;108:292-301.

[54] Laxminarayana K, Jalili N. Functional nanotube-based textiles: pathway to next generation fabrics with enhanced sensing capabilities. Text Res J 2005;75:670-80.

[55] Choi SJ, Jiang ZW. A novel wearable sensor device with conductive fabric and PVDF film for monitoring cardiorespiratory signals. Sens Actuator A-Phys 2006;128:317-26.

[56] Edmison J, Lehn D, Jones M, Martin T. E-textile based automatic activity diary for medical annotation and analysis. Los Alamitos, CA, USA: IEEE Computes Soc, 2006.

[57] Drean E, Schacher L, Bauer F, Adolphe D. A smart sensor for induced stress measurement in automotive textiles. J Text Inst 2007;98:523-31.

[58] Liu J, Lockhart TE, Jones M, Martin T. Local dynamic stability assessment of motion impaired elderly using electronic textile pants. IEEE Trans Autom Sci Eng 2008;5:696-702.

[59] El-Sherif MA, Yuan JM, MacDiarmid A. Fiber optic sensors and smart fabrics. J Intell Mater Syst Struct 2000;11:407-14.

[60] El-Sherif M, Fidanboylu K, El-Sherif D, Gafsi R, Yuan J, Richards K et al. A novel fiber optic system for measuring the dynamic structural behavior of parachutes. J Intell Mater Syst Struct 2000;11:351-9.

[61] De Jonckheere J, Narbonneau F, Kinet D, Zinke J, Paquet B, Depre A et al. Optical fibre sensors embedded into technical textile for a continuous monitoring of patients under magnetic resonance imaging. 2008 30th Annual International Conference of the IEEE Engineering in Medicine and Biology Society, Vols 1-8 2008:5266-9.

[62] Rothmaier M, Luong MP, Clemens F. Textile pressure sensor made of flexible plastic optical fibers. Sensors 2008;8:4318-29.

[63] Dhawan A, Muth JF, Kekas DJ, Ghosh TK. Optical nano-textile sensors based on the incorporation of semiconducting and metallic nanoparticles into optical fibers. Smart Nanotextiles 2006;920:121-6.

[64] Dhawan A, Ghosh TK, Muth JF. Incorporating optical fiber sensors into fabrics. MRS Proceedings 2005:870.

[65] Grillet A, Kinet D, Witt J, Schukar M, Krebber K, Pirotte F et al. Optical fiber sensors embedded into medical textiles for healthcare monitoring. IEEE Sens J 2008;8:1215-22.

[66] Morris D, Schazmann B, Wu Y, Coyle S, Brady S, Hayes J et al. Wearable sensors for monitoring sports performance and training. New York, USA: IEEE, 2008.

[67] Pasche S, Angeloni S, Ischer R, Liley M, Lupranoe J, Voirin G. Wearable biosensors for monitoring wound healing. Biomedical Applications of Smart Materials, Nanotechnology and Micro/nano Engineering 2009;57:80-7.

[68] Shim BS, Chen W, Doty C, Xu C, Kotov NA. Smart electronic yarns and wearable fabrics for human biomonitoring made by carbon nanotube coating with polyelectrolytes. Nano Lett 2008;8:4151-7.

[69] De Rossi D, Della Santa A, Mazzoldi A. Dressware: wearable hardware. Mater Sci Eng C-Biomimetic Supramol Syst 1999;7:31-5.

[70] Scilingo EP, Lorussi F, Mazzoldi A, De Rossi D. Strain-sensing fabrics for wearable kinaesthetic-like systems. IEEE Sens J 2003;3:460-7.

[71] Lorussi F, Scilingo E, Tesconi M, Tognetti A, De Rossi D. Wearable sensing garment for posture detection, rehabilitation and tele-medicine. Itab 2003: 4th International Ieee Embs Special Topic Conference on Information Technology Applications in Biomedicine, Conference Proceedings - New Solutions for New Challenges 2003:287-90.

[72] Kincal D, Kumar A, Child AD, Reynolds JR. Conductivity switching in polypyrrole-coated textile fabrics as gas sensors. Synth Met 1998;92:53-6.

[73] Dunne L, Brady S, Smyth B, Diamond D. Initial development and testing of a novel foam-based pressure sensor for wearable sensing. J Neuroeng Rehabil 2005;2:4.

[74] Lorussi F, Tognetti A, Tesconi M, Zupone G, Bartalesi R, De Rossi D. Electroactive fabrics for distributed, comfortable and interactive systems. Stud Health Technol Inform 2005;117:17-24.

[75] Campbell TE, Munro BJ, Wallace GG, Steele JR. Can fabric sensors monitor breast motion? J Biomech 2007;40:3056-9.

[76] Flandin L, Chang A, Nazarenko S, Hiltner A, Baer E. Effect of strain on the properties of an ethylene-octene elastomer with conductive carbon fillers. J Appl Polym Sci 2000;76:894-905.

[77] Zheng Q, Zhou JF, Song YH. Time-dependent uniaxial piezoresistive behavior of high-density polyethylene/short carbon fiber conductive composites. J Mater Res 2004;19:2625-34.

[78] Lu JR, Weng WG, Chen XF, Wu DJ, Wu CL, Chen GH. Piezoresistive materials from directed shear-induced assembly of graphite nanosheets in polyethylene. Adv Funct Mater 2005;15:1358-63.

[79] Li Y, Cheng XY, Leung MY, Tsang J, Tao XM, Yuen CWM. A flexible strain sensor from polypyrrole-coated fabrics. Synth Met 2005;155:89-94.

[80] Li Y, Leung MY, Tao XM, Cheng XY, Tsang J, Yuen CWM. Polypyrrole-coated conductive fabrics as a candidate for strain sensors. J Mater Sci 2005;40:4093-5.

[81] Wu J, Zhou D, Too CO, Wallace GG. Conducting polymer coated lycra. Synth Met 2005;155:698-701.

[82] Xue P, Tao XM, Tsang HY. In situ SEM studies on strain sensing mechanisms of PPy-coated electrically conducting fabrics. Appl Surf Sci 2007;253:3387-92.

[83] Kim HA, Kim MS, Chun SY, Park YH, Jeon BS, Lee JY et al. Characteristics of electrically conducting polymer-coated textiles. Mol Cryst Liquid Cryst 2003;405:161-9.

[84] Calvert P, Patra P, Lo T, Chen CH, Sawhney A, Agrawal A. Piezoresistive sensors for smart textiles - art. no. 65241I. Electroactive Polymer Actuators and Devices (Eapad) 2007 2007;6524:I5241-.

[85] Scilingo EP, Gemignani A, Paradiso R, Taccini N, Ghelarducci B, De Rossi D. Performance evaluation of sensing fabrics for monitoring physiological and biomechanical variables. IEEE T Inf Technol Biomed 2005;9:345-52.

[86] Tognetti A, Lorussi F, Bartalesi R, Quaglini S, Tesconi M, Zupone G et al. Wearable kinesthetic system for capturing and classifying upper limb gesture in post-stroke rehabilitation. Journal of NeuroEngineering and Rehabilitation 2005;2:8.

[87] Lorussi F, Scilingo EP, Tesconi M, Tognetti A, De Rossi D. Strain sensing fabric for hand posture and gesture monitoring. IEEE T Inf Technol Biomed 2005;9:372-81.

[88] Tesconi M, Scilingo EP, Barba P, De Rossi D. Wearable kinesthetic system for joint knee flexion- extension monitoring in gait analysis. New York, USA: IEEE, 2006.

[89] Tesconi M, Tognetti A, Scilingo EP, Zupone G, Carbonaro N, De Rossi D et al. Wearable sensorized system for analyzing the lower limb movement during rowing activity. New York, USA: IEEE, 2007.

[90] Shu L, Hua T, Wang Y, Li Q, Feng DD, Tao X. In-shoe plantar pressure measurement and analysis system based on fabric pressure sensing array. IEEE T Inf Technol Biomed 2010;14:767-75.

[91] Spencer DJ. Knitting technology: a comprehensive handbook and practical guide. Lancaster, Pa.; Cambridge, Eng.: Technomic; Woodhead, 2001.

[92] Wijesiriwardana R, Dias T, Mukhopadhyay S. Resistive fibre-meshed transducers. Los Alamitos, CA, USA: IEEE Computer Soc, 2003.

[93] Huang C, Shen C, Tang C, Chang S. A wearable yarn-based piezo-resistive sensor. Sensor Actuat A-Phys 2008;141:396-403.

[94] Taccini N, Loriga G, Dittmar A, Paradiso R. Knitted bioclothes for health monitoring. Proceedings of the 26th Annual International Conference of the Ieee Engineering in Medicine and Biology Society, Vols 1-7 2004;26:2165-8.

[95] Loriga G, Taccini N, De Rossi D, Paradiso R. Textile sensing interfaces for cardiopulmonary signs monitoring. 2005 27th Annual International Conference of the IEEE Engineering in Medicine and Biology Society, Vols 1-7 2005:7349-52.

[96] Huang C, Tang C, Shen C. A wearable textile for monitoring respiration, using a yarn-based sensor. Los Alamitos, CA, USA: IEEE Computer Soc, 2006.

[97] Mattmann C, Clemens F, Troester G. Sensor for measuring strain in textile. Sensors 2008;8:3719-32.

[98] Gibbs P, Asada HH. Wearable conductive fiber sensors for multi-axis human joint angle measurements. J Neuroeng Rehabil 2005;2:7.

[99] Mattmann C, Amft O, Harms H, Troester G. Recognizing upper body postures using textile strain sensors. Los Alamitos, CA, USA: IEEE Computer Soc, 2007.

[100] Soleimani M, Ogucu E. Electromechanical properties of wearable strain gauge transducers. Electron Lett 2008;44:1236-7.

[101] Huang C, Tang C, Lee M, Chang S. Parametric design of yarn-based piezoresistive sensors for smart textiles. Sensor Actuat A-Phys 2008;148:10-5.

CHAPTER 4. MECHANICAL BEHAVIOR OF CARBON NANOFIBER FILLED PLASTICIZED POLYVINYL CHLORIDE

Abstract

In the present study, we examine a conductive plastisol (plasticized polyvinyl chloride) composite for printing on textile fabrics as a sensory layer. Vapor grown carbon nanofibers (VGCNFs) at various concentration levels were dispersed in a plastisol matrix to create the composite. Microscopic analysis showed homogeneous dispersion of CNFs without any dominant filler orientation throughout the composites with good filler-matrix interface and absence of any pores or voids. Morphological and mechanical properties were studied as a function of filler, matrix, and plasticizer contents for three different molecular weights of PVC. Mechanical properties were found to be affected by CNF, DOS content and matrix molecular weight. PVC based polymer composites are promising materials for conductive coatings and piezoresistive sensors because of their lightweight and flexible structures.

4.1 Introduction

Polymer nanocomposites (PNCs) are relatively new and promising class of materials with at least one nanoscale component. Nanofillers with relatively high surface area and aspect ratio used in these composites may have profound effects on the mechanical, electrical, and thermal properties even at very low concentrations. For PNCs, different kinds of nanoparticles can be used in the form of fibers, tubes, or spheres in order to obtain desired

properties in combination with any of thermoplastic, thermosetting, or elastomer resins [1,2]. Recently, there has been increasing interest in nanocomposites filled with carbon nanofibers due to their high surface area and aspect ratio, superior electrical [3], thermal [4], mechanical [5] properties and lower cost (compared with carbon nanotubes). PVC has been of importance to the industry for many years with a wide range of applications from construction sector to toys and medical industry to textiles because of its desirable properties including strength, lightweight, durability, and ease of processing at relatively low cost. Plastisol is a multiphase, paste-like composition obtained by the suspension of PVC resin in a suitable plasticizer. Compositions of plastisol are commercially available as printing paste for textiles with tunable print properties [6-8]. Functionalization of plastisol with the addition of conductive fillers such as CNFs can be a good way of fabricating lightweight, conformable flexible sensory materials that are compatible with electronic textile products including body-worn sensors.

Here, an elastic conductive and solvent-free nanocomposite plastisol paste, formulated from PVC and other additives has been investigated for its morphological and mechanical properties in the form of films. The goal is to use this nanocomposite for printing on textiles to develop various e-textile components including sensors.

4.2 Materials and Methods

The PVC resins used for plastisol preparation are commercially available Solvin 367, 372, and 376 from Solvay Corporation (Brussels, Belgium). These resins are referred to as PVC-41, PVC-50, and PVC-60, where the postscripts denote the number-average molecular

weight of the resin in kg mol^{-1}. Bis(2-ethylhexyl) sebacate (dioctyl sebacate) (DOS, Fisher Chemicals) was used as the plasticizer and poxidized soybean oil (ESO) (Spectrum Chemicals Mfg Corp.) was used as the thermal stabilizer. Vapor grown carbon nanofibers (VGCNF, Showa Denko Corporation) with surface area of 13 m^2 g^{-1}, and nominal fiber diameter of 150 nm with aspect ratio ranging from 100 to 150 were used as fillers. For potential application of the plastisol composite in screen printing on textile fabrics, a bonding agent, designated as Binder 2001 and sold by Nazdar SourceOne, was also used.

Composite samples with well dispersed CNF were prepared in a high shear mixer (Mazerustar KK-50S). ESO and DOS were mixed for 10 sec. and CNF was added and mixed further for 60 sec. which was followed by addition and mixing of PVC. In the last step binder was added to the mixture and mixed further for 60 sec. CNF containing plastisol paste was compression molded into 0.5 mm thick films in a laboratory type hydraulic press with heated platens at 140°C for 30 min.

Composites with four levels of PVC/DOS ratios (50/50, 45/55, 40/60, 35/65), and eight levels of filler concentrations from 0 to 8 wt% were prepared with ESO (5 wt% of PVC) and binder (20 wt% of PVC+DOS).

To investigate the level of CNF dispersion, orientation, surface morphology, and filler-matrix adhesion characteristics, the composite specimens were examined in a JEOL-6400F field emission scanning electron microscope (FESEM) under low-voltage (1 kV) without any coating on the surface.

Stress–strain behavior of the composite films was characterized by following ASTM test method 1708 on a universal load frame (MTS 3G). For each composite type, 5 specimens

were tested for load-extension behavior. The load-extension values were subsequently converted to engineering-stress and true-strain. For the strain cycling tests, (25mm x 80mm) composite specimens were prepared and tested on a MTS 3G load-frame with a gauge length of 50 mm. Samples were cycled to pre-yield strain of 20% at 4.4 mm min^{-1}. The strain value which intercepts stress value at 0 MPa was determined as unrecovered strain.

To understand the viscoelastic response of the composites dynamic mechanical analysis (DMA) was conducted with a dynamic mechanical analyzer from TA Instruments. The tests were performed in tension mode in a temperature range from -140 to 40°C with heating rate of 3°C min^{-1} at a frequency of 1 Hz, and a strain amplitude of 15 μm. The gauge length was 15-16 mm with specimen width of 0.65 mm. Glass transition temperature (T_g) of the samples was determined from the peak of tan δ.

4.3 Results and Discussion

4.3.1 Morphology

In order to understand the dispersion and orientation of fibers and surface morphology, we have taken images from cross-section, edge and surface of the samples, cryo-fractured in liquid nitrogen. Cross-sectional and edge images presented in Fig. 4.1 show well dispersed CNF in the plasticized PVC without any dominant orientation and/or fiber clusters even at high concentrations for all three matrixes. For all samples no pores, pulled out CNFs, or matrix discontinuity were observed. The good matrix-filler interaction is probably due to well dispersed fibers (high-shear mixing), decreased surface tension of the polymer by the addition of plasticizer, high temperature processing (melt processing), and nanoscale surface

roughness of the CNF particles. High shear mixing is a one-step, easy and effective way of dispersing nanofillers in a polymeric matrix and lowering the matrix viscosity by which the matrix-filler interaction is enhanced [9]. In addition, plasticizers are known to lower the surface tension of the polymer and increase the penetration ratio between two phases [10]. Nano-scale surface roughness of the CNFs may also have led to mechanical interlocking with the matrix in order to have higher adhesion and make the interface stronger [11].

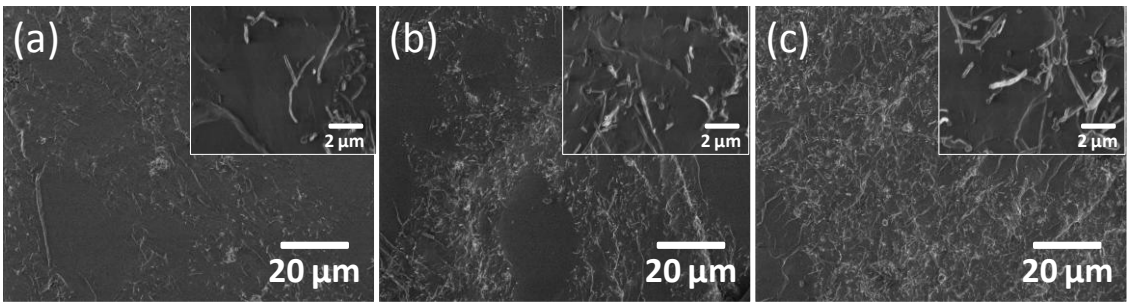

Figure 4.1 Cross-section images of 50/50 PVC-60/DOS at (a) 2% (b) 5% and (c) 8% CNF (wt%) inset showing the magnified images of the samples

4.3.2 Mechanical Behavior

Mechanical properties of composites are of significance not only for providing insights into the structure in terms of filler dispersion and morphology but also for determination of their performance limits and mechanical compatibility with other materials. Typical stress-strain behavior of the PVC-CNF composites (PVC-50, 50/50 PVC/DOS) for various CNF content is presented in Fig. 4.2.

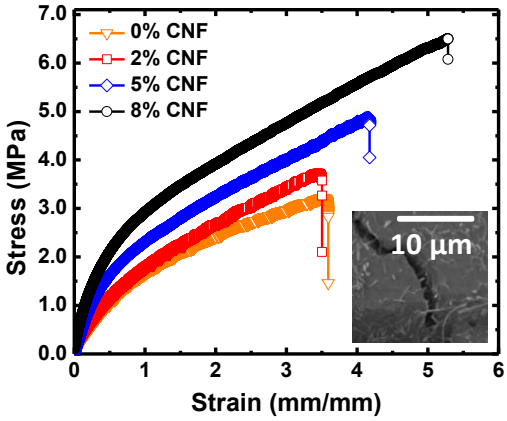

Figure 4.2 Stress-strain behavior PVC-50 (50/50 PVC/DOS) as a function of CNF (wt %) content Inset: SEM image of the cracked composite represents reinforcing and bridging effect of CNFs in PVC matrix

Tensile strength of the composites as a function of CNF (wt%) content, PVC/DOS ratio, and molecular weight of PVC is presented in Fig. 4.3. It is obvious that the composite strength increased with increasing CNF content for all PVC molecular weights and PVC ratios as the load bearing capacity of the polymeric system is increased by transferring the stress from matrix to the fibers. It has been known for many years that, with the incorporation of filler into a polymeric system, mechanical properties change due to high modulus of fillers and strong interactions between polymeric matrix and particles [5,11-17]. Mechanism of reinforcement in composites depends critically on filler and polymeric matrix. During the application of continuously increasing load, at some point plastic deformation occurs and matrix cannot withstand the stress. This process is followed by micro crack formation. With increasing load, micro cracks can propagate to the interface between fiber and matrix. The role of the nanofibers becomes important at that point by providing substantial bridging to matrix and strength to composite. As a result, load bearing capacity of the composite

increases, micro crack formation is prevented/minimized to some degree and behavior of the breakage changes from fracture mode to crack propagation [18,19].

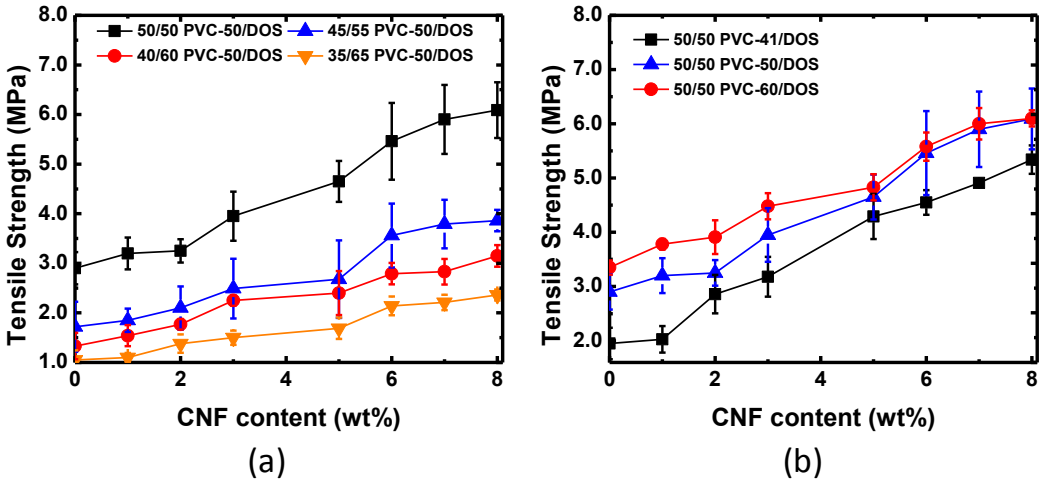

Figure 4.3 Variation of tensile strength of plastisol composites with various CNF content and PVC/DOS ratios for (a) PVC-50 (b) comparison of tensile strength for various PVC matrixes for 50/50 PVC/DOS ratio

Since the contribution of the CNFs in the reinforcing mechanism is dictated by the fiber/matrix interface, transfer of the load from matrix to the filler depends on the bonding at the interface which determines the interfacial strength and overall properties of the composite. As known strong interface shows modified bulk polymer properties which are better than bulk polymer [11-14]. Although this effect is seen for almost all types of fillers; in the case of nanofillers, enhancement is more pronounced because of their high aspect ratio and surface area. High aspect ratio and surface area lead to increase in total contact area between filler and matrix which directly alters interface (altered polymer rate) throughout the composite and enhances mechanical properties [11-13,20-22]. Good filler/polymer interphase

with high adhesion of polymer to the filler regardless of the CNF concentration is evidenced in the cross-sectional images presented in Fig. 4.1.

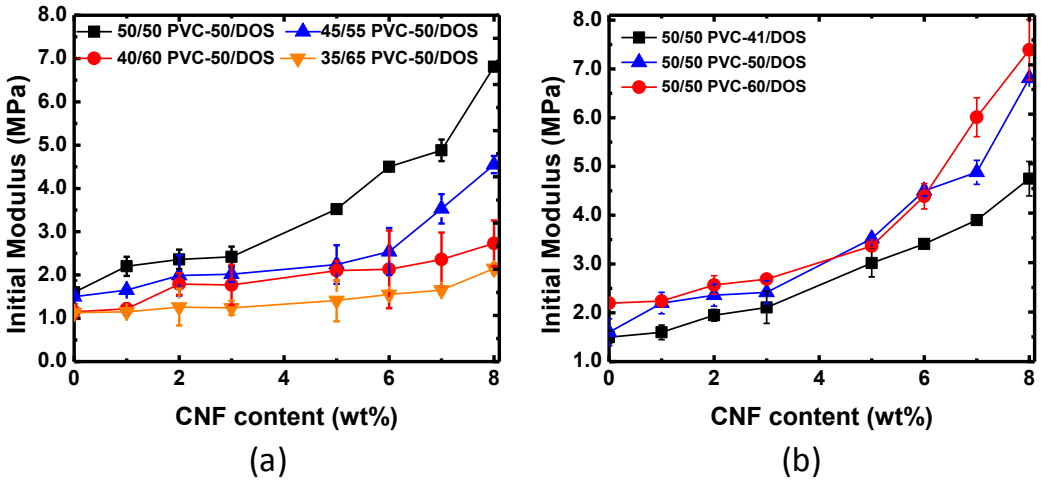

Figure 4.4 Variation of initial modulus of plastisol composites with various CNF content and PVC/DOS ratios for (a) PVC-41 (b) comparison of initial modulus for various PVC matrixes for 50/50 PVC/DOS ratio

It is also apparent from Fig. 4.3 that with increasing amount of DOS, the tensile strength decreased gradually, most likely due to the plasticizing effect of DOS. Plasticizers are known to penetrate into the amorphous regions [11-13,20-22] of the polymer, and lower the intermolecular forces (cohesion), and entanglement ratio in the polymer by increasing the free volume, thereby making the movement of chains easier, resulting in lowered mechanical properties [7,10,23]. Among the different compositions of the plastisol, highest tensile strength was observed for 50/50 PVC/DOS at 8 wt% VGCNF which indicated an optimum composition for highest continuity of the matrix and sufficient matrix-filler contact that enhanced stress transfer from matrix to filler. Amongst the three different molecular weights

of PVC, PVC-60 showed the highest tensile strength (Fig. 4.3b) supporting our hypothesis of enhanced polymer chain entanglements and lower free volume caused by lower number of chain ends. In line with these observations, initial modulus data presented in Fig. 4.4 show similar trends. The increase in initial modulus is more pronounced for composites with least plasticizer content, possibly indicating higher level of plasticization resulting in weaker matrix and CNF-matrix interface. While the highest value for PVC-41 was found around 5 MPa; for PVC-61 same composition showed initial modulus around 7.5 MPa.

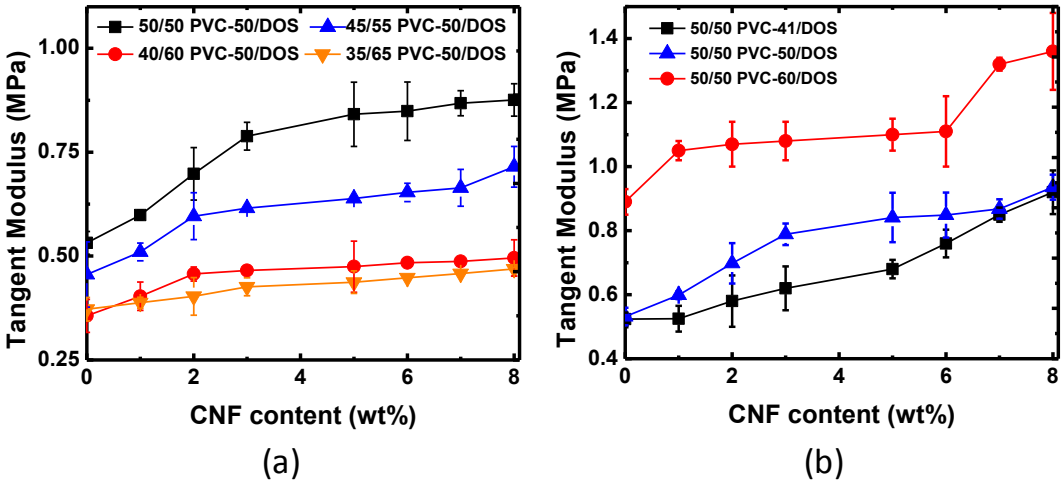

Figure 4.5 Variation of tangent modulus of plastisol composites with various CNF content and PVC/DOS ratios for (a) PVC-50 (b) comparison of tangent modulus for various PVC matrixes for 50/50 PVC/DOS ratio

Close examination of the composite stress-strain curves presented in Fig. 4.2 show almost bilinear behavior. Apart from the initial Hookean region, a second linear region is seen between ~150-300% strain. The second region, characterized by the tangent modulus at 250% strain, the modulus increased with increasing CNF content. Higher molecular weight

and lower DOS content also lead to higher modulus at this point. However the increase in the tangent modulus is not as distinctive as in initial modulus. It seems, the filler reinforcement effect is more significant in the Hookean region compared to that at higher strains.

Yield stress is the stress at which yield occurs and after that plastic deformation starts which is useful piece of information for determination of mechanical limits of the polymeric systems. As we did not observe yield point because of high level of plasticizer [24], yield stress was calculated based on the yield point at which deviation started from linear response on the stress-strain curve. As given in Fig. 4.6, results are parallel with the initial modulus outcomes that, yield stress is increasing with the addition of CNF and higher molecular weight and lower DOS content gives higher yield stress values.

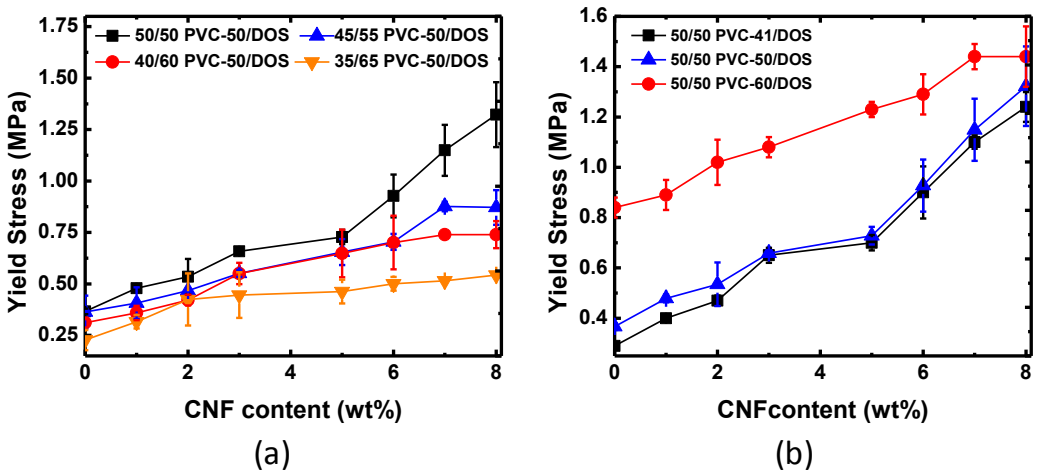

Figure 4.6 Variation of yield stress of plastisol composites with various CNF content and PVC/DOS ratios for (a) PVC-50 (b) comparison of yield stress for various PVC matrixes for 50/50 PVC/DOS ratio

Dimensional stability of a material is a measure of its ability to retain the shape under various conditions including stress, temperature and humidity. Mechanical strain cycling is a useful tool to determine its dimensional stability and potential response under cyclic loading condition [7,10,23].

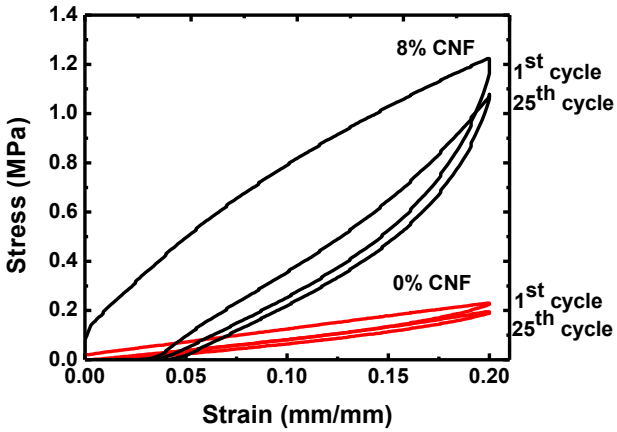

Figure 4.7 Stress-strain behavior of 50/50 PVC-50/DOS composites (0 % and 8% wt CNF)

Fig. 4.7 shows the stress–strain responses of the 1st and 25th extension cycles of the plastisol/CNF composites with 0 and 8 % CNF (wt%) performed at 20% strain amplitude. Stress softening is observed for all samples regardless of the composition of the composites. Elastomers, in general, and elastomeric composites, in particular, are known to show lower maximum stress value compared to the first cycle when stretched repeatedly to a constant maximum strain. This is a well-known phenomenon referred to as "Mullins Effect" [25-28]. Although further softening can be observed in the subsequent cycles, the magnitude is relatively lower than the first softening [25,26,29]. The primary manifestation of Mullins effect is in the reduced level of stress in the polymer during recovery relative to that observed

during extension. This behavior gives rise to hysteresis in polymers and polymer composites. In general, composites consist of three basic phases namely matrix, filler, and interface. Each of these phases may respond differently to the applied stresses. Polymer chains might slide on each other, change their orientation, or chain rupture might occur in the polymer-filler interface (Fig.4.11) [25,26]. Since CNFs are very rigid, they can retain their shape and show high dimensional stability under small strain. On the other hand, their relative distance and spatial location can change under stress due to rigid body translation and rotation leading to distortions between polymer-polymer and filler-polymer interphase. While some of these changes are reversible, some of them are not, see Fig. 4.8. As a result of irreversible changes, which are basically breakage/rupture of filler-polymer interactions and/or disruption of filler network, composites show different mechanical behavior in the following cycles [27,28,30-32].

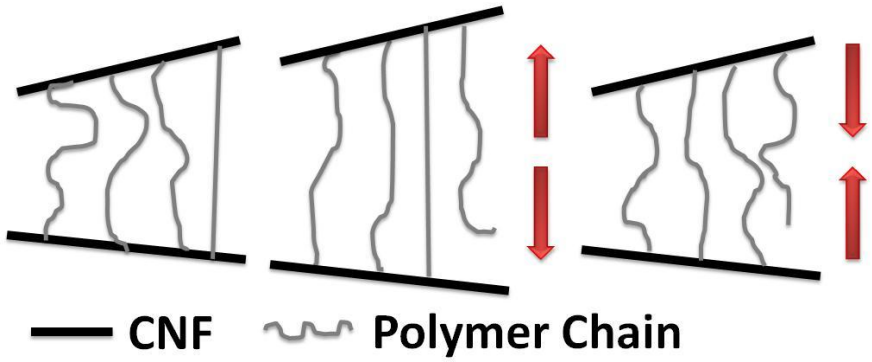

Figure 4.8 Schematic showing polymer-filler interaction in a composite under stress

The unrecovered strain during unloading cycles as a function of number of cycles for various filler concentrations of 50/50 PVC-50/DOS composition are shown in Fig 4.9. All

compositions show stress softening and reach a steady state after a few (ca. 4) cycles. However, the softening is more pronounced for higher CNF content and the relative change between cycles increases with increasing filler concentration. Since CNFs are rigid elements in the composite structure, the recoverability of the composite is directly related to the response of the polymer chains during unloading cycle. In case of higher filler concentrations, polymer chains experience higher levels of constraints due to the CNFs and require more time for recovery [25,33]. While the total unrecovered strain is 0.046 (mm/mm) for 8 wt% CNF containing sample end of 25 cycles; it is 0.012 (mm/mm) for unfilled sample. The impact of filler concentration on the stress softening has been noted previously in the literature [25-28,30-33].

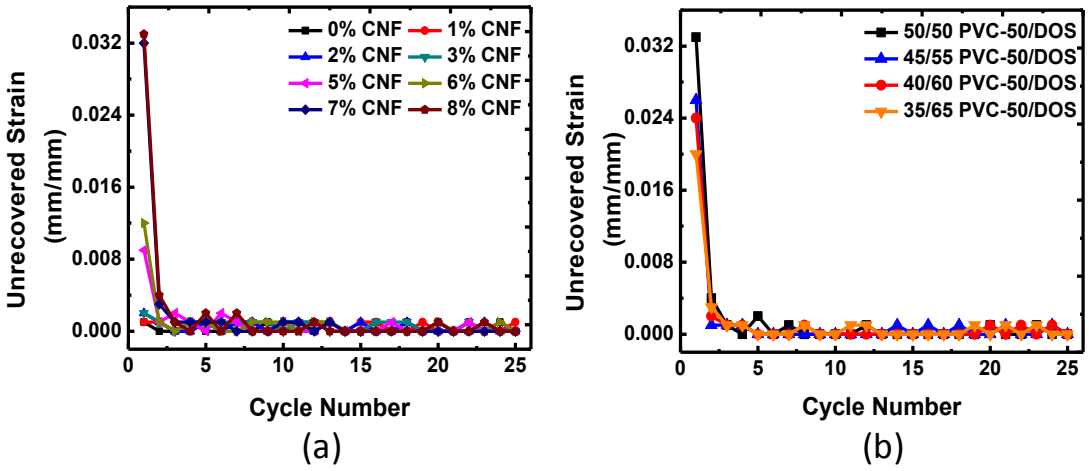

Figure 4.9 Effect of (a) filler concentration (b) plasticizer (DOS) content on unrecovered strain as a function number of cycles in strain cycling at 20% strain amplitude for 50/50 PVC-50/DOS composites

Fig. 4.9a shows the effect of filler concentration for PVC-50/DOS 50/50 composites on unrecovered strain. Higher filler concentration leads to higher unrecovered strain, especially. in the first few cycles which is of importance in terms of total unrecovered strain. Effect of plasticizer content on the response of the composites containing 8% CNF during strain cycling is shown in Fig 4.9b. In general, plastisol compositions with higher plasticizer content show lower levels of unrecovered strain during the few initial cycles. However, there is no significant difference between 45/55 and 40/60 PVC-50/DOS containing samples in terms of unrecovered strain. Their values were found to be between 50/50 and 35/65 PVC/DOS composites. Increased plasticizer content tends to reduce the restriction on polymer chains by increasing free volume and weakening interaction between filler and matrix. As a result of increased mobility of polymer chains, recovery time decreased and highly plasticized samples showed lower unrecovered strain.

Fig. 4.10 shows the effect of molecular weight on unrecovered strain for 8 wt% CNF containing PVC/DOS 50/50 composites. As previously mentioned, although filler content and PVC/DOS ratio were found to be important in determining hysteresis behavior, we did not observe any significant influence of PVC molecular weight on the unrecovered strain. Since the difference in molecular weights is not very significant, the effect was suppressed by plasticizer and filler at low level of strains.

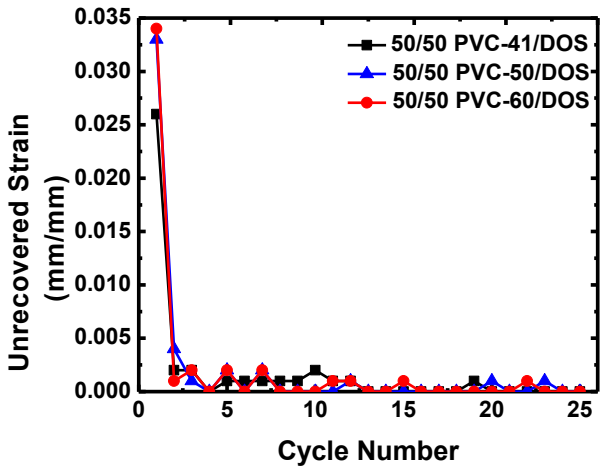

Figure 4.10 Unrecovered strain as a function of number of cycles in strain cycling at 20% strain amplitude for various plastisol composites having varying PVC molecular weights and 8% CNF

4.3.3 Dynamic Mechanical Analysis

Dynamic mechanical measurements (DMA) over a range of temperatures at constant frequency is a sensitive, useful tool in understanding the viscoelastic response of polymer composites, especially in determining the relaxation transitions and phase transitions including glass transition (T_g) and melting (T_m) temperatures. DMA measurements were performed on the virgin plastisol and composites with 2, 5, and 8 wt% CNF at different PVC/DOS ratios for different molecular weights of PVC. Fig. 4.11a shows the storage modulus and tan δ curves as a function of temperature for various CNF concentrations for 50/50 PVC-50/DOS obtained at a frequency of 1 Hz, and a strain amplitude of 15 μm with a ramp of 3ºC min^{-1}. All samples showed typical temperature dependent behavior of

thermoplastic polymers; higher storage modulus in glassy state and lower storage modulus at higher temperatures, especially in rubbery state.

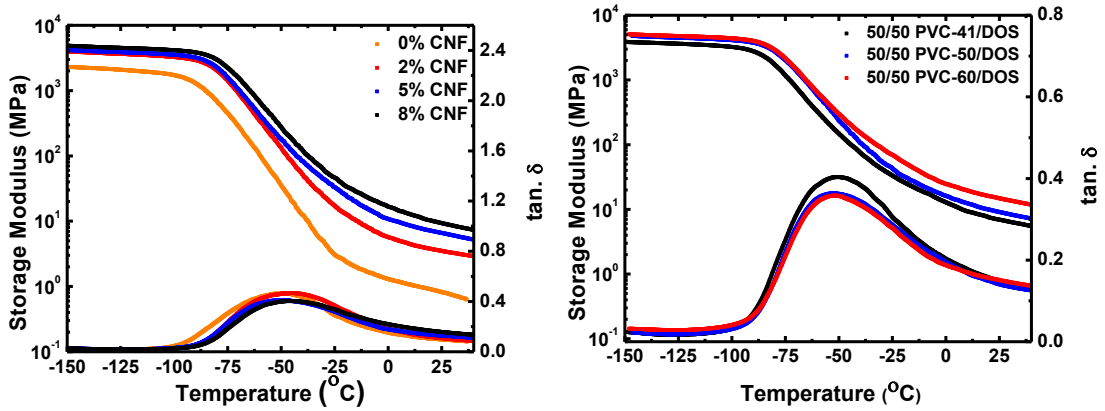

Figure 4.11 (a) Storage modulus and tan δ curves as a function of temperature for 50/50 PVC-50/DOS composites with 0, 2, 5, and 8 wt% CNF (b) storage modulus and tan δ curves as a function of temperature for 8 wt% CNF filled 50/50 PVC/DOS composites for various PVC molecular weights

Rapid decrease in storage modulus due to enhanced mobility of polymer chains was observed around -80ºC. Storage modulus increased significantly by the addition of CNFs and upward shift occurred in the rubbery plateau region. This behavior was attributed to reinforcing effect of well-dispersed high modulus nanofillers which was also reported for CNF and CNT filled composites [34-37]. In addition, filler concentration was found to affect the T_g which was determined from the maxima of tan δ curve. Increase in the filler concentration lead to increase in T_g (Fig. 4.12b), decrease in the magnitude of tan δ and shift in the peak value of tan δ of the composites [34-37]. This was attributed to the restriction of molecular mobility of the polymer chains by the addition of nanofillers (confinement effect of CNFs lead to

immobilization of polymer chains) [35,38]. Although addition of 2 wt% CNF caused around 5˚C change in T_g, further increase in filler concentration resulted in minor increase in T_g [36]. In addition to that, samples with CNFs showed broader tan δ curve which can be attributed to wider transition regime compared with neat plastisol. Similar response was obtained for all three molecular weights of PVC.

Effect of plasticizer content on storage modulus and tan δ is shown in Fig. 4.12. It is obvious that increasing amount of plasticizer, result in lower storage modulus and T_g most likely due to the plasticizing effect of DOS.

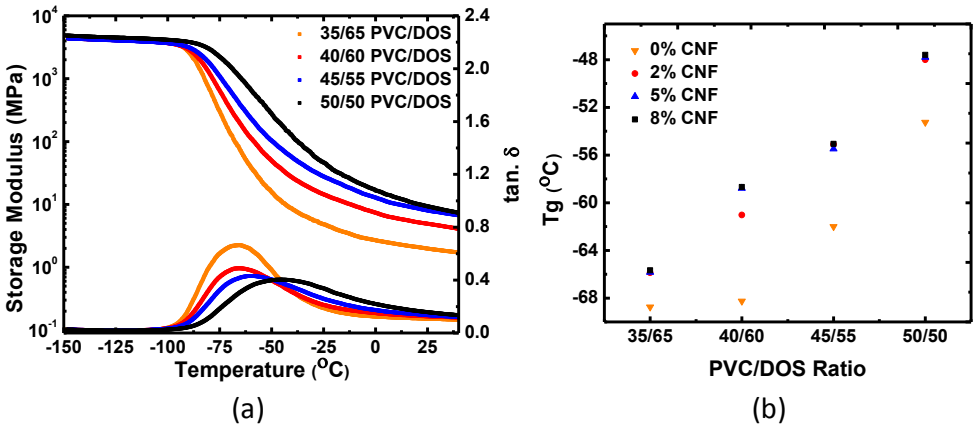

Figure 4.12 (a) Storage modulus and tan δ curves as a function of temperature for 8 wt% CNF filled 35/65, 40/60, 45/55 and 50/50 PVC-50/DOS composites, (b) T_g as a function of CNF (wt%) content and PVC-50/DOS ratio

As mentioned previously plasticizers penetrate into the amorphous regions of the polymer, and lower the intermolecular forces (cohesion) in the polymer, and entanglement ratio by increasing the free volume, thereby making the movement of chains easier [7,10,23] which lead to lower storage modulus and T_g. As shown in Fig. 4.12b among the four different

PVC/DOS ratios, lowest T_g was observed for 35/65 PVC/DOS due to higher plasticization effect.

Effect of molecular weight on storage modulus and tan δ is shown in Fig. 4.11b. As seen, higher molecular weight resulted in higher storage modulus which is probably caused by enhanced polymer chain entanglements and lower free volume caused from lower number of chain ends resulting into increased strength. However we did not observe significant change in T_g depending on PVC molecular weight for CNF filled composites at any PVC/DOS ratio. As a summary, T_g was found to be highly depended on PVC/DOS ratio. While addition of CNFs filler concentration was found to affect the T_g, increase in filler concentration showed slight effect on T_g. On the other hand, matrix molecular weight did not lead to significant shift in T_g.

Conclusions

CNF reinforced plastisol composites were prepared by incorporation of different levels of CNFs for three different molecular weights of PVC. Morphology and mechanical properties of composites were investigated. Mechanical properties were found to be affected by CNF, DOS content and matrix molecular weight. Fillers provide substantial bridging in the matrix and enhance strength by increasing load bearing capacity of the composite by preventing or minimizing crack formation. Good filler/polymer interphase was observed without any dominant filler orientation regardless of the CNF concentration throughout the composites even at high filler concentrations. T_g of the samples was found to be affected by PVC/DOS ratio and filler concentration. While higher plastisol content lead to lower T_g, higher filler

concentration resulted in higher T_g. CNF reinforced plastisol composites are alternative materials for conductive coatings and piezoresistive sensors because of their strong, lightweight and flexible structures.

References

[1] Koo JH. Polymer nanocomposites : processing, characterization, and applications. New York: McGraw-Hill, 2006.

[2] Advani SG. Processing and properties of nanocomposites. Singapore: World Scientific Publishing, 2007.

[3] Lozano K, Bonilla-Rios J, Barrera EV. A study on nanofiber-reinforced thermoplastic composites (II): Investigation of the mixing rheology and conduction properties. J Appl Polym Sci 2001;80:1162-72.

[4] Lozano K, Barrera EV. Nanofiber-reinforced thermoplastic composites. I. Thermoanalytical and mechanical analyses. J Appl Polym Sci 2001;79:125-33.

[5] Kuriger RJ, Alam MK, Anderson DP, Jacobsen RL. Processing and characterization of aligned vapor grown carbon fiber reinforced polypropylene. Composites Part A 2002;33:53-62.

[6] Nakajima N, Harrell ER. Rheology of PVC plastisol: Particle size distribution and viscoelastic properties. J Colloid Interface Sci 2001;238:105-15.

[7] Grossman RF. Handbook of vinyl formulating. Hoboken, N.J.: Wiley-Interscience, 2008.

[8] Cadogan DF, and Howick CJ. Plasticizers. John Wiley & Sons Inc., 2000.

[9] Andrews R, Jacques D, Minot M, Rantell T. Fabrication of carbon multiwall nanotube/polymer composites by shear mixing. Macromol Mater and Eng 2002;287:395-403.

[10] Wypych G. Handbook of plasticizers. Toronto; New York: ChemTec Pub.; William Andrew Pub, 2004.

[11] Palmeri MJ, Putz KW, Brinson LC. Sacrificial bonds in stacked-cup carbon nanofibers: biomimetic toughening mechanisms for composite systems. ACS Nano 2010;4:4256-64.

[12] Lipatov IS. Polymer reinforcement. Toronto-Scarborough: Chem Tec, 1995.

[13] Hull D. An introduction to composite materials. Cambridge England; New York: Cambridge University Press, 1996.

[14] Lee SM. Handbook of composite reinforcements. New York: VCH, 1993.

[15] Al-Saleh MH, Sundararaj U. A review of vapor grown carbon nanofiber/polymer conductive composites. Carbon 2009;47:2-22.

[16] Guth E. Theory of filler reinforcement. J Appl Phys 1945;16:20-5.

[17] Kurian T, De PP, Khastgir D, Tripathy DK, De SK, Peiffer DG. Reinforcement of epdm-based ionic thermoplastic elastomer by carbon-black. Polymer 1995;36:3875-84.

[18] Saito R. Physical properties of carbon nanotubes. London: Imperial College Press, 1998.

[19] Pierson HO. Handbook of carbon, graphite, diamond, and fullerenes: properties, processing, and applications. Park Ridge, NJ, USA: Noyes Publications, 1993.

[20] Ramanathan T, Abdala AA, Stankovich S, Dikin DA, Herrera-Alonso M, Piner RD et al. Functionalized graphene sheets for polymer nanocomposites. Nat Nanotechnol 2008;3:327-31.

[21] Manoharan MP, Sharma A, Desai AV, Haque MA, Bakis CE, Wang KW. The interfacial strength of carbon nanofiber epoxy composite using single fiber pullout experiments. Nanotechnology 2009;20:295701.

[22] Choi YK, Sugimoto K, Song SM, Gotoh Y, Ohkoshi Y, Endo M. Mechanical and physical properties of epoxy composites reinforced by vapor grown carbon nanofibers. Carbon 2005;43:2199-208.

[23] Van Oosterhout JT, Gilbert M. Interactions between PVC and binary or ternary blends of plasticizers. Part I. PVC/plasticizer compatibility. Polymer 2003;44:8081-94.

[24] Povolo F, Schwartz G, Hermida ÉB. Stress relaxation of PVC below the yield point. Journal of Polymer Science Part B: Polymer Physics 1996;34:1257-67.

[25] Mullins L. Effect of stretching on the properties of rubber 1948;21:281-300.

[26] Holt WL. Behaviour of rubber under repeated stresses. Industrial & Engineering Chemistry 1931;23:1471-5.

[27] Harwood JAC, Payne AR. Stress softening in natural rubber vulcanizates. Part III. Carbon black-filled vulcanizates. J Appl Polym Sci 1966;10:315-24.

[28] Harwood JAC, Mullins L, Payne AR. Stress softening in natural rubber vulcanizates. Part II. Stress softening effects in pure gum and filler loaded rubbers. J Appl Polym Sci 1965;9:3011-21.

[29] Wolff EG. Introduction to the dimensional stability of composite materials. Lancaster, PA: DEStech Publications, Inc, 2004.

[30] Bueche F. Molecular basis for the mullins effect. J Appl Polym Sci 1960;4:107-14.

[31] Kraus G, Childers CW, Rollmann KW. Stress softening in carbon black-reinforced vulcanizates. Strain rate and temperature effects. J Appl Polym Sci 1966;10:229-44.

[32] Diani J, Fayolle B, Gilormini P. A review on the Mullins effect. Eur Polym J 2009;45:601-12.

[33] Dorfmann A, Ogden RW. A constitutive model for the Mullins effect with permanent set in particle-reinforced rubber. Int J Solids Structures 2004;41:1855-78.

[34] Jin Z, Pramoda KP, Xu G, Goh SH. Dynamic mechanical behavior of melt-processed multi-walled carbon nanotube/poly(methyl methacrylate) composites. Chem Phys Lett 2001;337:43-7.

[35] Zeng J, Saltysiak B, Johnson WS, Schiraldi DA, Kumar S. Processing and properties of poly(methyl methacrylate)/carbon nano fiber composites. Compos Part B-Eng 2004;35:173-8.

[36] Green KJ, Dean DR, Vaidya UK, Nyairo E. Multiscale fiber reinforced composites based on a carbon nanofiber/epoxy nanophased polymer matrix: synthesis, mechanical, and thermomechanical behavior. Composites Part A 2009;40:1470-5.

[37] Siengchin S, Psarras GC, Karger-Kocsis J. POM/PU/carbon nanofiber composites produced by water-mediated melt compounding: structure, thermomechanical and dielectrical properties. J Appl Polym Sci 2010;117:1804-12.

[38] Bhattacharyya AR, Pötschke P, Häußler L, Fischer D. Reactive compatibilization of melt mixed PA6/SWNT composites: Mechanical properties and morphology. Macromol Chem Physic 2005;206:2084-95.

CHAPTER 5. ELECTRICAL CHARACTERIZATION of CARBON NANOFIBER FILLED PLASTICIZED POLYVINYL CHLORIDE

Abstract

In the present study, we investigated the electrical behavior of a conductive composite based on plasticized Poly(vinyl chloride) (PVC) in dioctylsebacate (DOS) and carbon nanofibers (CNFs). Microscopic analysis showed homogeneous dispersion of CNFs without any dominant filler orientation throughout the composites with good filler-matrix interface, absence of any pore or voids. Electrical properties were studied as a function of filler, matrix and plasticizer contents for three different molecular weights of PVC. Flexible conductive composites were found to show negative piezoresistive behavior under different levels of strain in the range of 2-16%. In addition, piezoresistive behavior was found to be affected by strain preconditioning, filler concentration and plastisol composition.

5.1 Introduction

Polymers are preferred for many applications because of their desirable properties, such as strength and toughness, lightweight, facile process ability, and environmental stability. Vast majority of the polymers are electrically insulating and are used extensively as electrical insulators. However, in many applications electrical conductivity is desirable, therefore, various conductive fillers including nanoparticles have been incorporated into their structure to engender conductivity. Polymeric nanocomposites filled with conducting nanoparticles have received great attention with regard to their functional structures. Vapor grown carbon

nanofibers (VGCNFs) are one of the common nanofillers used for nanocomposites, because of their high surface area, superior electrical [1], thermal [2], mechanical [3] properties and relatively lower cost (compared with carbon nanotubes). Carbon nanofibers (CNFs) are fibrous structures that grow spontaneously by autocatalytic chemical vapor deposition of organic gases on metal catalysts [4,5]. These fibrous structures consist of (stacked) graphitic outer layer which show different orientations to the fiber axis. Graphite is composed of parallel sheets of sp^2 bonded carbon atoms in crystalline lattices. sp^2 hybridized carbon atoms form hexagons by sigma and pi bonds. While sigma bonds provide strength to the graphite, pi bonds are responsible for electrical conductivity [6,7]. This form of carbon enhances mobility and interaction of loosely bound valence electrons between adjacent planes lead to good electrical conductivity [5,6]. CNFs can be used for many applications including electrostatic dissipation (ESD) [8], electromagnetic/radio frequency interference (EMI/RFI) protection [9], reinforced structures [3,10], to lithium-ion secondary batteries [11], electrochemical capacitors [12], hydrogen storage [13], and piezoresistive sensors [14-16].

Piezoresistance refers to the change in electrical resistance stemming from applied external forces. Piezoresistive effect has been observed for metals such as iron and nickel [17], and semiconductors such as germanium and silicon [17-20] as well as multi-component composite systems [14-16,21,22]. In general, piezoresistivity stems from changes in material dimensions as well as inherent changes in resistivity caused from lattice deformations. While for metals piezoresistive effect is caused by geometrical changes; for semiconductors it is dominated by crystal lattice degeneration and change in carrier mobility [20]. Mechanism of piezoresistance is somewhat different for conductive polymer composites. Since conductivity

is obtained through networks formed by conductive fillers, the network configuration determines its piezoresistive response. Unlike metals or semiconductors, neither geometrical nor structural deformation is the issue for conductive fillers (CB, CNF, CNT, *etc*.). The conductive fillers used in polymer composites are much stiffer than the matrix materials, at low level of strain they maintain their dimensional stability. However, their relative spatial location or orientation can change under stress due to displacement and/or rotation [14,21,22]. Changes in the conductive network configuration lead to change in electrical resistance, ultimately. By monitoring the change in resistance, magnitude of the applied stress/strain can be determined. In other words, the piezoresistive response of conductive polymer composites is primarily due to the breakdown of the filler junctions and/or reformation of the conducting network [14,21,22]. Dominant mechanism depends on many factors such as filler concentration, filler geometry, filler orientation and dispersion, and direction and amplitude of the applied stress [14,21,22]. Depending on the dominant mechanism, the observed piezoresistive behavior can be either positive (increase in resistance) or negative (decrease in resistance) [14,21,22] as a function of applied stress. Recent trend in the area of piezoresistive sensors is to design elastomeric structures which show good recoverability and repeatability.

In this work, we report the piezoresistive behavior of plasticized-PVC (plastisol)-CNF composites with the long-term goal of using the composite as sensory layers on fabrics. Plastisol is a multiphase, paste-like composition obtained by the suspension of PVC resin in a suitable plasticizer with other additives such as thermal stabilizers and fillers. It is the common synthetic print media for textiles for many years owing to its low cost, easy

processability (printability) and durability [23-25]. Conducting plastisol films were found to show homogeneous filler dispersion and excellent strain-dependent piezoresistive response. Sensitivity and stability of the piezoresistive behavior was found to critically depend on the preconditioning and magnitude of the applied strain, filler concentration and plastisol composition. In addition to these, effect of stress softening on electrical response was also examined.

Since conductive plastisols can easily be printed on textiles, they are promising candidates as flexible, lightweight, conformable sensory materials that are compatible with electronic textile (e-textile) products including body-worn sensors. They can be used for many applications including health monitoring and posture determination.

5.2 Materials and Methods

The PVC resins used for plastisol preparation were Solvin 367, 372, and 376 from Solvay Corporation, France. These resins are referred to as PVC-41, PVC-50, and PVC-60, where the postscript designation denotes the nominal number-average molecular weight of the resin in kg mol^{-1}. The plasticizer used was Bis(2-ethylhexyl) sebacate (dioctyl sebacate) (DOS) manufactured by Acros Organics and obtained from Fisher Chemicals. Epoxidized soybean oil (ESO) was used as thermal stabilizer and obtained from Spectrum Chemicals Mfg. Corp. The carbon filler was VGCNF obtained from the Showa Denko Corporation, Japan. Fibers had surface area of 13 m^2 g^{-1} and nominal fiber diameter of 150 nm with aspect ratio ranging from 100 to 150. In order to ensure adhesion between the conducting plastisol composite and

fabric substrates in future studies, a bonding agent commercially available as Binder 2001 (Nazdar SourceOne, USA) was also used.

In the first step in forming the composite, ESO and DOS were mixed for 10 sec. and CNF was added and mixed for 60 sec. which was followed by addition and mixing of PVC for further 60 sec. In the final step, the binder was added to that mixture and processed for 60 sec. In all cases the mixing was done in a high shear mixer (Mazerustar KK-50S). Then, CNF containing plastisol paste was compression molded into 0.5 mm thick films in a laboratory type hydraulic press with heated platens at 140°C for 30 min. The temperature was chosen to achieve complete melting of PVC to enhance the interaction between matrix and filler interface.

All of the experimental data being reported here were collected using the low, middle and high molecular weight PVC, earlier designated as PVC-41, PVC-50, and PVC-60, respectively. Composites with four levels of PVC/DOS ratios (50/50, 45/55, 40/60, 35/65), and ten levels of filler concentrations from 0 up to 10 wt% were prepared with ESO (5 wt% of PVC as generally used in the literature [23,25-27] and binder (20 wt% of PVC+DOS as recommended by the manufacturer) as the other additives. To investigate CNF dispersion, orientation, surface morphology, filler-matrix adhesion characteristics, composite specimens were examined with a JEOL-6400F field emission scanning electron microscope (FESEM) under low-voltage (1kV) without any coating on the surface.

Dimensional stability of a material is a measure of its ability to retain the shape under various conditions including stress, temperature and humidity. Mechanical strain cycling is a useful tool to determine its dimensional stability and potential response under cyclic loading

condition [26,28,29]. Since this material was proposed to be used as a strain sensor, mechanical properties under cyclic conditions need to be determined. For the strain cycling tests, (25mm x 80mm) composite specimens were prepared and tested on a MTS 3G load-frame with a gauge length of 50 mm. Samples were cycled to pre-yield strain of 16% strain at 4.4 mm min^{-1}. The strain value which intercepts stress value at 0 MPa was determined as unrecovered strain.

Volume resistivity of the composite films was determined by Keithley Model 6517B Electrometer and Model 8009 Resistivity Chamber in accordance with ASTM D-257 standard. Before making the electrical measurements, specimen thicknesses were determined using a precision thickness meter (Mitutoyo ID-C112E).

To determine the piezoresistive behavior of the films in longitudinal (parallel to the strain) direction, specimens, 80 mm long and 25 mm wide, were prepared by attaching four electrical leads, 1.3 mm apart, along the centerline of the sample parallel to the longitudinal direction. Electrical leads were attached to the samples by using small beads of plastisol composites with high carbon black content (20 wt%) prepared in our lab for this purpose. Test specimens were clamped on a specially made load-frame (Fig. 5.1) with the gauge-length set at 50 mm and cycled to 2, 4, 8, 12, and 16% strain amplitudes at a speed of 4.4 mm min^{-1}. Dynamic resistance measurement on these samples was carried out using a set-up consisting of a current source (Keithley 6221) and a nano-voltmeter (Keithley 2182A) under 1 μA input current. The set-up is controlled by a computer for automated data acquisition and control.

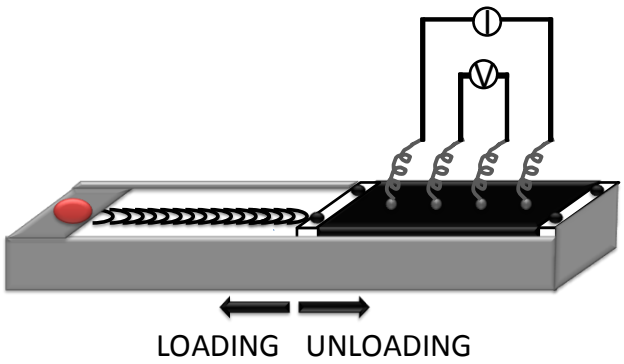

Figure 5.1 Piezoresistance measurement set-up.

5.3 Results and Discussion

5.3.1 Morphology

In order to analyze the dispersion and orientation of fibers and surface morphology, we have taken images from cross-section, edge and surface of the samples which were cryofractured in liquid nitrogen. Uniformly dispersed light and raised spots in cross-sectional images in Fig. 5.2 represent CNFs. The images (Fig. 5.2 inset) clearly show homogeneously dispersed CNFs in the plasticized PVC matrix without any dominant orientation and fiber clusters even at high concentrations. In addition, robust filler/polymer interphase is seen in high polymer-filler adhesion, regardless of the CNF concentration. The good adhesion is probably due to the well dispersed fibers, decreased surface tension of the polymer by the addition of plasticizer, high temperature processing (melt processing), and nano-scale surface roughness of the CNFs.

High shear mixing is an easy and effective way of dispersing nano-fillers in a polymeric matrix. High shear forces in mixing are generally thought to lead to thinning of matrix polymer (lowering of viscosity) causing enhanced interaction between matrix and fillers [30]. In addition to that, plasticizers lower the surface tension of the polymer and increase the penetration ratio between the two phases [26]. Additionally, high temperature processing can also result in better adsorption. Nano-scale surface roughness of the CNFs might also be effective in interlocking with the matrix resulting in higher adhesion and stronger interface [10].

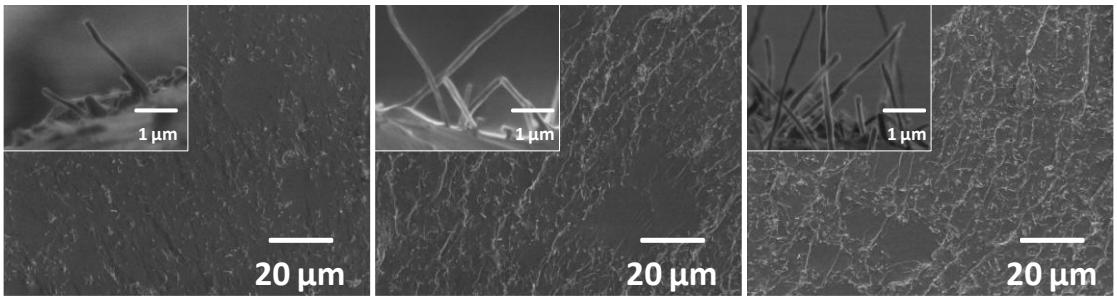

Figure 5.2 50/50 PVC-50/DOS at different CNF concentrations cross-section images (a) 2 wt% (b) 5 wt% and (c) 8 wt% CNF. Inset figures show the magnified edge images of the samples

5.3.2 Electrical Properties

5.3.2.1 Resistivity

The addition of conducting fillers into an insulating matrix enhances its electrical properties such as conductivity. Unlike inherently conducting materials, a percolation threshold must be

reached by the filler before the matrix becomes conductive. As the fraction of conducting phase of the composite increases the composite generally undergoes an insulator to conductor transition. This transition has been generally analyzed within the framework of effective media and percolation theories [31,32]. The clearly delineated transition from insulative to conductive behavior is referred to as the percolation threshold. This is the point at which conductive filler particles begin to form of a continuous conducting path across the composite and the resistivity of the composite drops precipitously by many orders of magnitude. From the structural perspective, percolation occurs when geometric features composed of large clusters (of size p) approach p_c, the critical cluster size. At small values of cluster size, flocs or individually separated particles exist and conduction throughout the material cannot take place. However, as p is increased, fraction of conducting phase of the composite, the physical cluster size increase, sufficiently large flocs starts to form a continuous network and connect opposite edges of the specimen which generally lead composite to undergo an insulator to conductor transition.

According to percolation theory, the bulk resistivity (ρ) of a percolating composite with volume concentration, ϕ, of the conducting phase follows a power law of the form [33-37]:

$$\rho \propto (\phi - \phi_c)^{-t} \quad \text{for} \quad \phi > \phi_c \qquad \text{Equation (5.1)}$$

where, ϕ_c is the percolation threshold, t is the critical exponent. For percolating systems the values of ϕ_c and critical exponent t can be obtained from the best linear fit of log (ρ) and log (ϕ-ϕ_c).

The value of the critical exponent t is thought to be material independent and for three-dimensional percolating systems the universal behavior is represented by t=2 [22,35,38,39]

However, conductive composites show t values in a wide range from 0.9 to 6.4 depending on the network structure and mechanism of conductance [22,35-41]. In two-dimensional systems the reported values of t lie between 1.4-1.5, and for three-dimensional systems, t values are assumed in the range of 1.5-2 [22,35,38,39]. The difference between 2D and 3D networks and non-universal behavior were basically attributed to filler type, filler geometry [22,35,38,39], matrix type [40], and processing conditions [41] all of which affect the tunneling behavior between conductive fillers [42-45].

The resistivity of plastisol composite films as a function of CNF content (wt%) and PVC/DOS ratio is shown in Fig. 5.3.

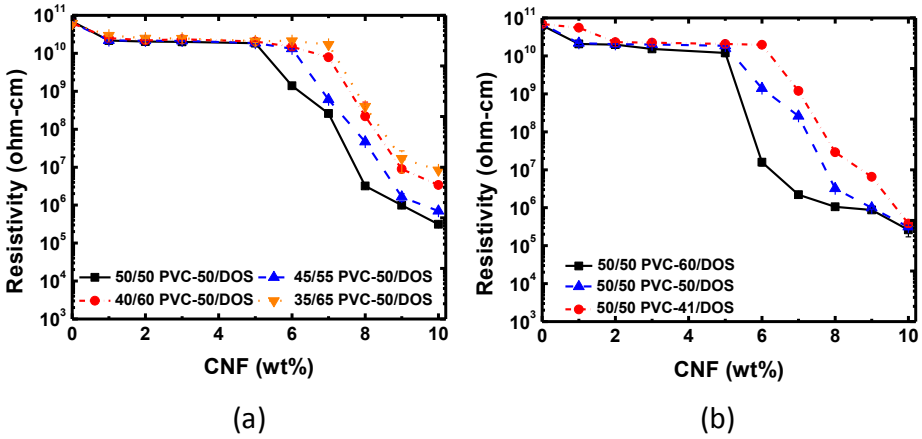

Figure 5.3 (a) Variation of resistivity of plastisol composite films as a function of CNF content and PVC-50/DOS ratios, (b) Effect of matrix type on resistivity

All four PVC/DOS compositions show transition from insulating to conducting regardless of the matrix molecular weight. In all cases, the composites tend to show higher percolation threshold for increasing plasticizer content and lower percolation threshold for higher

molecular weights of PVC. In order to confirm that and to explore the lattice dimensionality/structure, critical exponent (t) and percolation concentration (ϕ_c) were calculated from power law equation given in Eq. 1. Calculated values of ϕ_c and t for PVC-41, PVC-50, and PVC-60 at different PVC/DOS ratios are shown in Fig. 5.4 For the PVC/CNF composites being reported here the calculated values of the critical exponent t were found to be higher than 2 for all plastisol compositions (PVC/DOS). This is in line with previous results (2.38-3.21) obtained from VGCNF filled composites [35-37]. Deviation from universal behavior probably caused by the complex conduction mechanism due to high aspect ratio [35-37] of CNFs and higher contact resistance between fillers [46,47] caused by the presence of DOS.

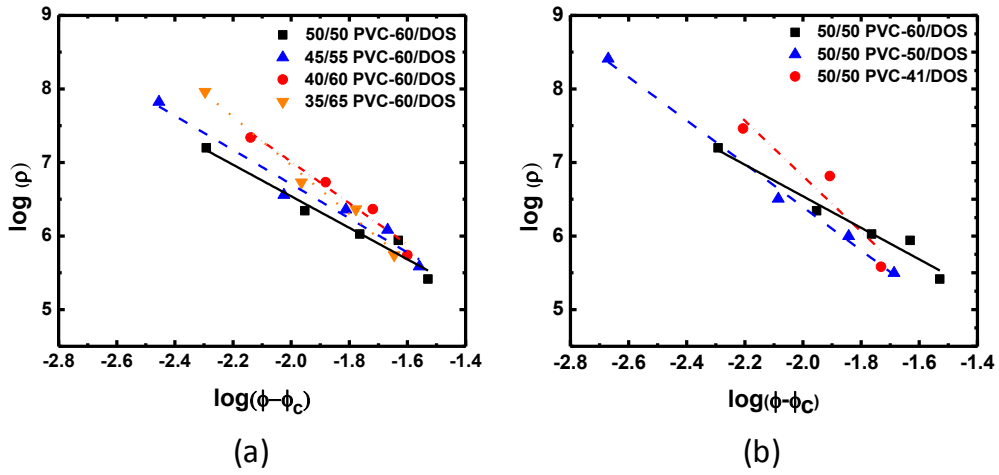

Figure 5.4 (a) Effect of PVC-60/DOS ratio and (b) matrix molecular weight on exponent t value

Fig. 5.4 a and Table 5.1 shows the log (ρ) *vs.* log (ϕ-ϕ_c) for different PVC/DOS ratios for PVC-60 and Fig 5.4b shows log (ρ) *vs.* log (ϕ-ϕ_c) values for 50/50 PVC/DOS, PVC-41, PVC-

50 and PVC-60. While increase in DOS content lead to increase in ϕ_c and exponent t; increase in molecular weight resulted in lower ϕ_c and exponent t. While 50/50 PVC-60/DOS had a ϕ_c value of 0.03, 35/65 PVC-60/DOS had ϕ_c value of 0.034 with corresponding t values 2.15 and 3.29, respectively. The difference between ϕ_c values and the critical exponent t were assumed to be caused by plasticizer content [48] and molecular weight of the PVC. PVC-DOS interaction is directly related with the polymer-plasticizer compatibility and is determined by their physical and chemical properties (molecular weight, polarity, *etc*.) [23,24,26,49]. DOS is an aliphatic CH_2 chain compound with two ester groups which makes it relatively non-polar, see Fig. 5.5a. The DOS molecule can interact with PVC with the help of the ester groups as shown in Fig. 5.5b [26,49-51].

Table 5.1 t, ϕ_c and R^2 values of samples

Composite	**t**	**ϕ_c**	**R^2**
50/50 PVC-41/DOS	3.77	0.041	0.9
50/50 PVC-50/DOS	2.94	0.039	0.99
50/50 PVC-60/DOS	2.15	0.03	0.96
45/55 PVC-60/DOS	2.32	0.031	0.96
40/60 PVC-60/DOS	2.82	0.0325	0.96
35/65 PVC-60/DOS	3.29	0.034	0.98

In case of high DOS content, as in Fig 5.6a, the excess DOS will either be absorbed by the filler, or migrate to the surface to form an insulating layer [51]. In either case, DOS can

modify the electrical conductivity of the CNFs, increase the contact resistance between fillers (charge transfer between fillers become more difficult) and lead to higher resistivity at a given filler concentration [52].

In a conducing composite, the mechanism of conductivity can change depending on the components of the system. Although CNFs seem to be the conducting phase in the composite, they also generate resistance to electron flow at the contact points as constriction resistance and tunneling resistance. The contribution of conducting phase to the overall conductivity is not only related to its inherent conductivity or its concentration but also the structure of the network and contact resistance between fillers [46,53].

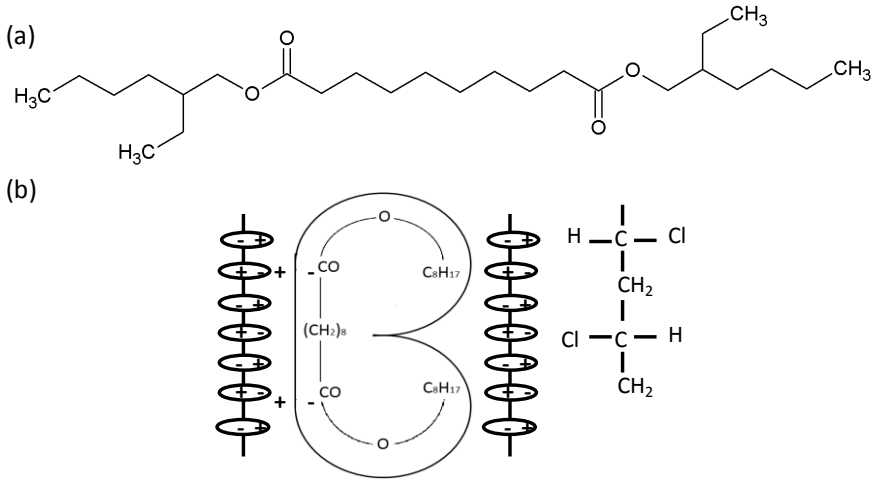

Figure 5.5 (a) Chemical structure of DOS and (b) PVC-DOS interaction [26,51]

In a system consisting of only polymer and filler, electron transfer can occur by direct contact between fillers and/or tunneling of electrons through a thin layer of polymer of the order of few angstroms. In the case of higher plasticizer content even if the filler-filler distances

remains constant, electron transfer might be hindered because of formation of additional insulating layer between filler-polymer and the mechanism of conductivity might become more complex [20,46,54].

In case of higher molecular weight of PVC-60, the accessible polar groups are higher. That leads to higher interaction with DOS and the amount of the plasticizer present at the fiber-matrix interface and on the surface is likely to be lower. The PVC-60, therefore, is likely to produce lower resistivity compared to the PVC-41 due to PVC-plasticizer interactions. In fact, PVC-60 has a lower t value of 2.15 compared to 2.94 for PVC-50 and 3.77 in case of PVC-41. On the other hand, for low molecular weight PVC-41, lower interaction might lead DOS molecules to be absorbed by CNF or migrate to the surface, shown schematically in Fig 5.6b.

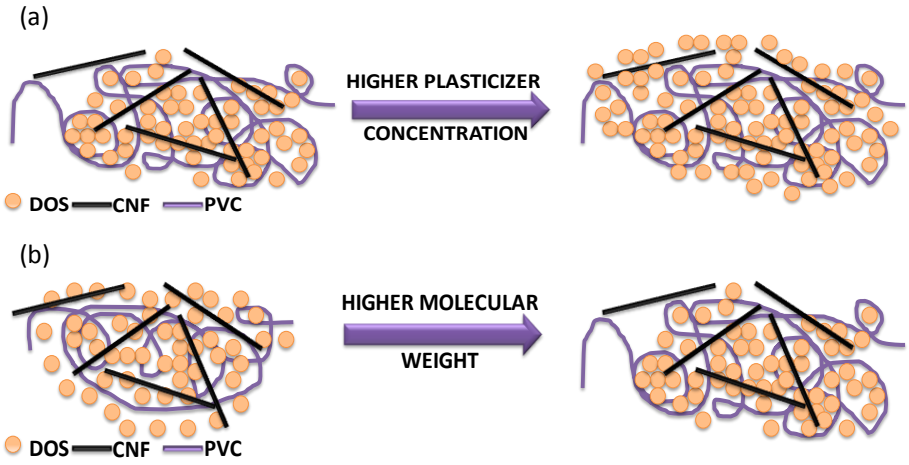

Figure 5.6 Potential effect of DOS ratio on morphology (a) effect of DOS ratio and (b) effect of molecular weight

5.3.2.2 Piezoresistance

Understanding of the piezoresistive behavior is a key to determine potential application of the PVC-CNF composite in sensing. Based on the percolation behavior of the composites presented in Fig. 5.3a, PVC-50 was chosen for further investigation for its piezoresistive behavior. In the study of piezoresistive behavior, influence of filler concentration and two levels of PVC/DOS ratio (50/50 and 35/65) were examined. CNF content of 8 and 9 wt% were chosen for their potential to be the most sensitive and stable response. Additionally, the conductivity values of these combinations were in the range of our four point conductivity measurement set up.

Ideally a piezoresistive sensor should show effective sensing behavior over a useful range of strain. In order to analyze this, piezoresistance studies were carried out with composite films at 2, 4, 8, 12, and 16% strain amplitudes. One of the most important observations made in this study is the effect of mechanical strain preconditioning, the repeated cyclic uniaxial straining of the specimen, on its piezoresistive response. Strain preconditioning creates a strain history which not only affects the subsequent mechanical behavior [55] but also electrical response. Our initial studies on the piezoresistive behavior of the composites suggested strong influence of the preconditioning amplitude. In general, the samples preconditioned at a higher strain level, produced consistent mechanical and electrical behavior below that strain level. Therefore, all of the samples reported in this study were preconditioned at 16% strain for 25 cycles.

In addition to piezoresistive response, other characteristics such as, dynamic response (repeatability and dynamic range, hysteresis), and aging behavior are also important for potential application of a material as sensor.

Dynamic response of a sensor is significant in terms of its ability to respond timely under the effect of stimulus. If a sensor does not respond at the required frequency, dynamic error might occur [56,57]. In all of the measurements reported here the strain-resistance relationship was monitored simultaneously as a function of time. Dynamic response is not only important for obtaining a continuous data but also important for evaluating cyclic stability of the sensory material.

Fig. 5.7 illustrates the change in electrical resistance of 8 wt% CNF containing 50/50 PVC/DOS plastisol film at 2, 4, 8, 12, and 16% strains. In case of lower strain amplitudes (in the range of 2-8%), electrical resistance dropped with increasing strain and subsequently increased during recovery. This behavior can be attributed to the reversible CNF network configuration caused by applied strain. For higher strain amplitudes (in the range of 12-16%), increasing strain resulted in decreasing resistance, however, beyond a certain strain threshold; a slight increase in resistance is noted with increasing strain. After several cycles, the electrical response stabilizes and subsequent cycles almost retrace the same trend except for the beginning and end of the cycles.

Although strain induced reduction in resistance (negative piezoresistance) has been reported elsewhere [21,22,58], to our knowledge this type of behavior is being reported for the first time for CNF containing composites.

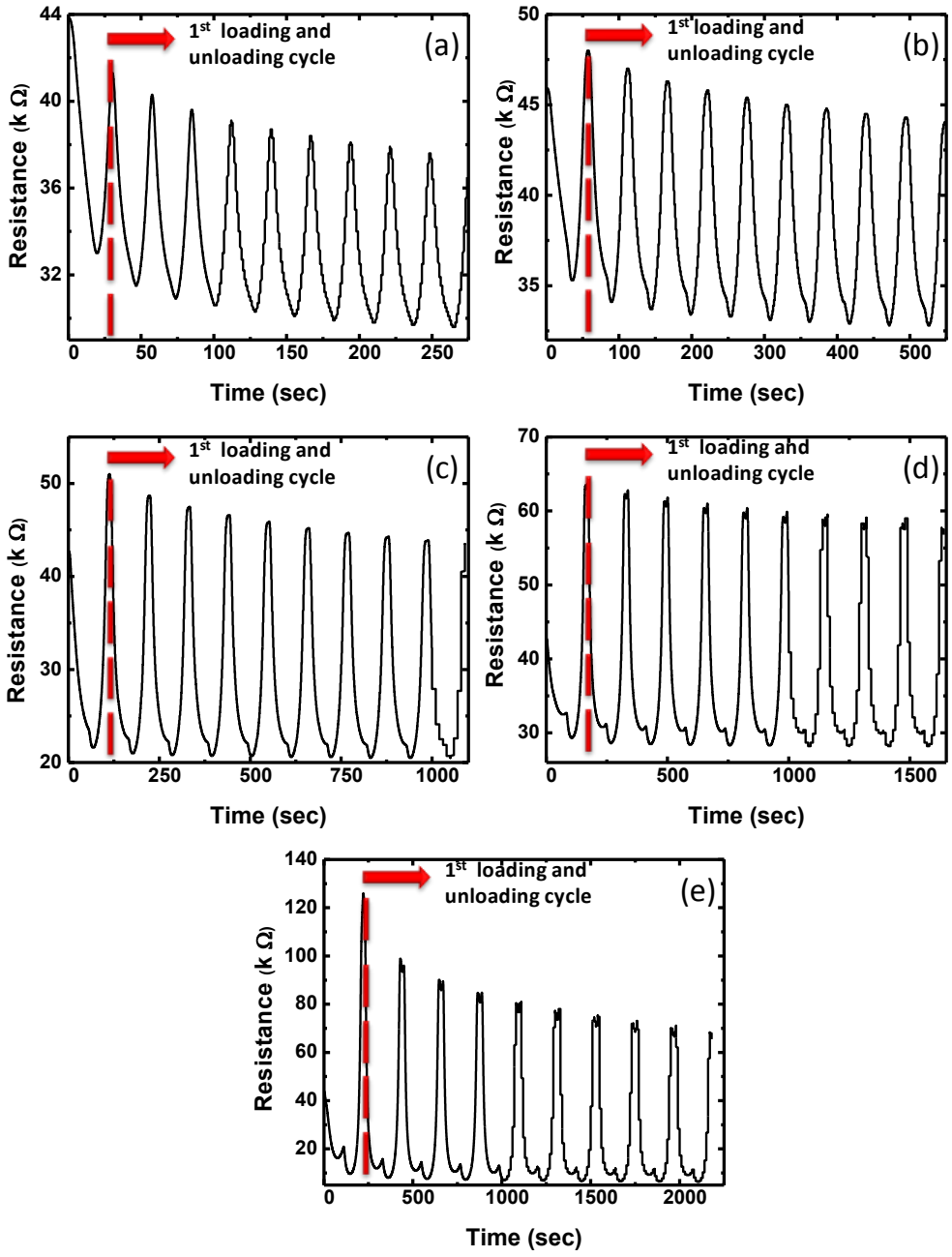

Figure 5.7 Dynamic piezoresistive behavior of 8 wt% CNF containing 50/50 PVC-50/DOS plastisol composite films as a function of time for 10 cycles at different levels of strain: (a) 2% (b) 4% (c) 8% (d) 12% and (e) 16%

CNFs are high aspect ratio, cylindrical fillers, as a result any strain induced rotation and/or reorientation would have more significant and somewhat different effect on CNF composites than composites containing spherical fillers, *i.e.* carbon black. Unlike spherical particles, any change in spatial orientation (due to rotation) of the CNFs is more likely to affect the conducting network configuration (density of the contact points) within the composite. At lower values of strain, fibers tend to reorient along the strain direction primarily through rotation resulting in relatively lower filler to filler distance and formation of new bridges, networks leading to lower electrical resistance (see Fig. 5.8). At higher values of strain, translation of particles predominates, resulting in greater inter-particle separation and higher resistance (see Fig. 5.8). The increase in resistance during unloading is primarily due to the restoration of the relative position of the CNF particles due to recovery of the matrix polymer. However, in almost all cases the zero-strain electrical resistance is higher than that at the end of the first cycle. This is caused by the deformation (highest stress softening occurs in the first cycle) occurred in the first loading cycle [55].

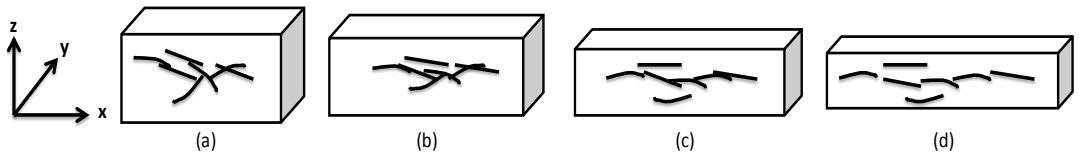

Figure 5.8 Mechanism of piezoresistance change in PVC/CNF composites (a) at zero strain (b) between zero strain and critical strain (c) critical strain (d) after critical strain

Hysteresis is another important parameter used for sensor characterization. Hysteresis is a phenomenon in which the response of a physical system to an external stimulus depends not

only on the present magnitude of the stimulus but also on the history. For piezoresistive strain sensors, it indicates the ability of a sensor to recover to its original behavior after repeated use. Since, hysteresis is an indicator of deviation from its original characteristics; its magnitude is of extreme important in terms of repeatability of the sensing function [56,57]. In our system, hysteresis behavior of electrical resistance was evaluated from resistance data during the loading-unloading cycles. Any deviation from the electrical resistance during the last loading cycle is assumed to be due to hysteresis. Based on this explanation, two characteristics of electrical resistance during loading-unloading cycles are noted as indicators of hysteresis; the change in resistance at the end of unloading cycle, and a measure of the plateau region at the beginning and end of cycles caused by the unrecovered strain as shown in Fig. 5.9. Since piezoresistance is an electro-mechanical phenomenon, mechanical response of the composite has significant impact not only on the polymer-polymer and filler-polymer interactions, but also configuration of filler network and electrical response. CNFs are very stiff material; they can retain their shape and show high dimensional stability under low level of strain. On the other hand, their relative distance and spatial location can change due to rigid body rotation and movement under stress caused by the deformation of the polymeric matrix (elongation along strain direction). Since filler spacial position under strain is controlled by the matrix polymer deformation, the ability of the polymer to recover from applied strain directly affects the mechanical and electrical response of the composite during the following cycles [21,22]. Although the samples showed good cyclic stability at low level of strains (in range of 2-8%); it showed a higher drop in resistance for 16% strain and

stabilized after higher number of cycles. This is assumed to be caused by stress softening of the composites under cyclic loading.

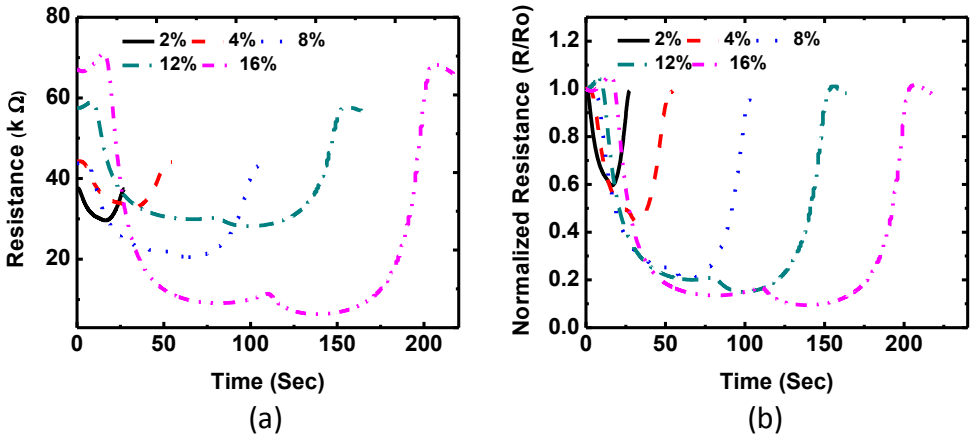

Figure 5.9 10th cycles of 8 wt% CNF containing 50/50 PVC-50/DOS plastisol composite films for different levels of strain amplitudes (a) change in resistance plotted a function of time, and (b) normalized resistance plotted as a function of time R_0 is the resistance value at zero strain

The level of unrecovered strain after mechanical cycling depends on the extent of stress softening and that in turn depend on the strain amplitude [59-61]. As seen in Fig. 5.10, the higher the maximum strain the higher the unrecovered strain (deformation). Effect of unrecovered strain on piezoresistive response is clearly manifested in the 10th cycle strain-resistance plot presented in Fig. 5.9. The resistance values plotted in Fig 5.9b is normalized by the initial resistance (R_o) at the beginning of the cycle. The small rise and fall in resistance at the beginning and end of the plot, respectively, represent the slack in the sample due to unrecoverable deformation in the sample representative of mechanical hysteresis. For obvious reasons, the highest hysteresis is observed in case of 16% and followed by 12%

strain amplitudes. Another notable feature of the behavior is the critical strain of transition at which the transition occurs from decreasing to increasing resistance as a function of strain. Strain amplitudes of 2, 4 and 8% did not show any transition, they showed continuous decrease in the resistance as a function of strain. While the critical strain of transition is 11.3% for 12% strained sample, it is 11.7% for 16% strain amplitude. Small shift in that value is assumed to be caused from higher deformation end of 16% strain cycle. Higher deformation leads to higher unrecovered strain and it requires more time for complete recovery which is a result of different time-dependent behavior of composites.

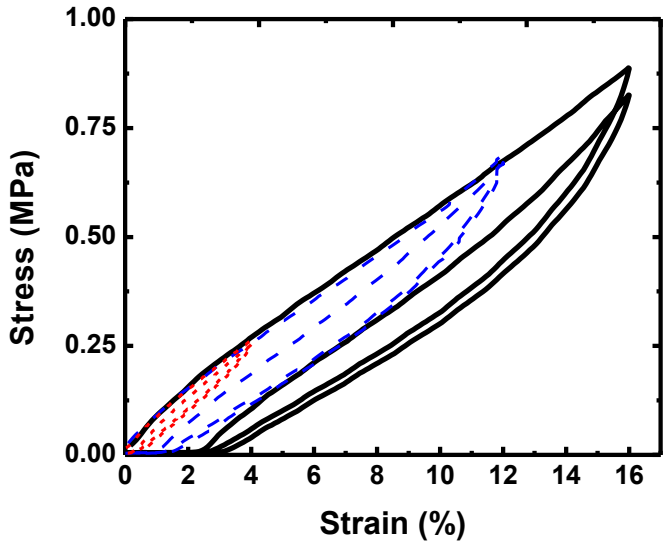

Figure 5.10 Cyclic tensile loading unloading curves for 8 wt% CNF containing 50/50 PVC-50/DOS plastisol composite film at 4%, 12%, and 16% strain (1stand 25th cycles)

Elastomers and elastomeric composites when subjected to cyclic loading shows significant stress softening or reduction in stress at a given level of strain on unloading compared with the stress on the initial loading on the first and successive cycles in strain cycling test of fixed

amplitude. This is a well-known phenomenon is referred to as Mullins effect [55,59,60] and has been attributed to various forms of network alteration in elastomers.

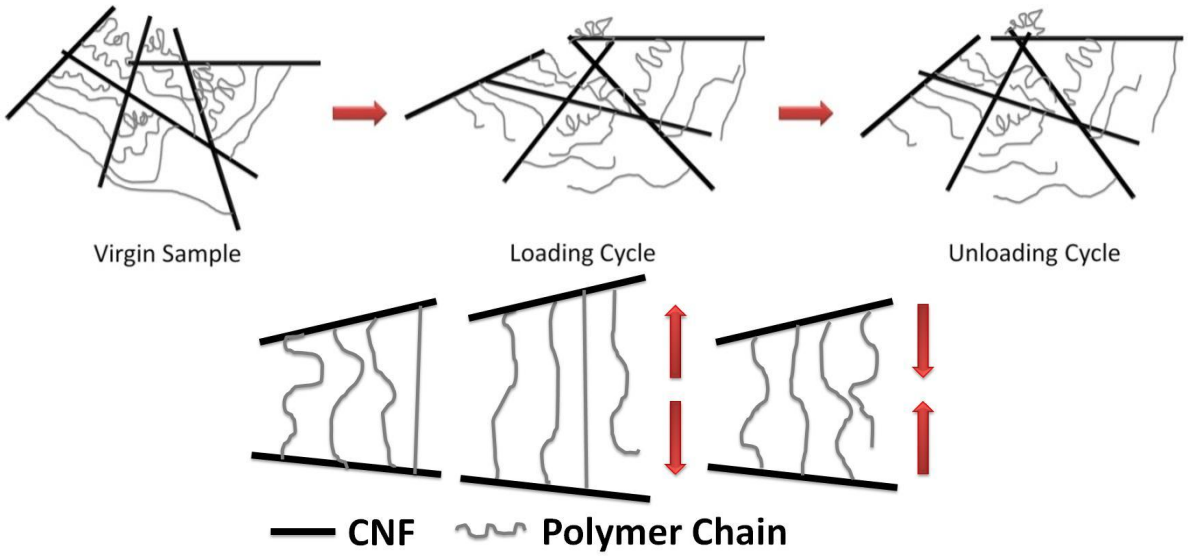

Figure 5.11 Polymer-filler interaction/stress softening during loading and unloading cycles (Mullins Effect)

During repeated loading-unloading cycles, polymer chains might slide on each other, change their orientation or chain rupture might occur in the polymer-filler interface (Fig. 5.11) [55,59,60]. While some of these changes are reversible some are not. As a result of the irreversible changes, mostly due to micro level distortions between polymer chains and damage at the filler-polymer interphase [62-66], composites show hysteresis in mechanical response. Although further softening can be observed in the subsequent cycles, the magnitude is relatively lower than the initial softening [55]. In case of higher strain amplitudes, the degree of stress softening is relatively higher. In the present case, (Fig. 5.10)

the highest stress softening, and the largest decrease in resistance during loading and highest increase in resistance at the end of first cycle was observed for 16% strained sample.

Another important point is the symmetry of resistance values recorded during loading-unloading cycles. Although, the response during loading and unloading cycles almost seem to mirror each other, the drop in resistance during recovery is slightly more than the during the loading cycle. This is most likely due to the Mullins effect discussed earlier. The lower stress at a given strain during unloading compared to the loading cycle results in lower restorative force during recovery. This behavior has been noticed consistently in all PVC/CNF composites.

A) Effect of filler concentration on piezoresistive response

Filler concentration in a composite is one of the most influencing parameters in determining the composite characteristics, including its piezoresistive response. Filler concentration directly affects the conductive network structure (number of contacts, density of the conductive network in unit volume) which is critical for the sensing behavior of the material. In the case of very low filler concentrations, conductive network can be broken-down under very low level of strain that makes it impossible to monitor the piezoresistive behavior at higher level of strains. On the other hand, at very high filler concentrations (far above the percolation threshold), because of the difficulty in disturbing/breaking-down the highly saturated filler network, it is very difficult to monitor the piezoresistive response at low level of strains. Starting from these observations, we have compared the piezoresistive response of 8 and 9 wt% CNF containing 50/50 PVC-50/DOS samples. Fig. 5.12 shows the effect of filler concentration on the piezoresistive behavior of PVC/CNF composites with 8 and 9 wt%

CNF at strain amplitudes of 2 and 16%. As obvious from the data both samples showed chance in resistance under strain but magnitude of sensitivity, which is represented by gauge factor, is different for each sample.

Gauge factor (K) is defined as the change in resistance of a sample (ΔR) under an external strain (ε) was calculated using the expression by considering the most linear part of the R *vs.* ε response:

$$K = \Delta R/\varepsilon R_0 \qquad \text{Equation (5.2)}$$

Here R_0 is the resistance of the sample at zero strain.

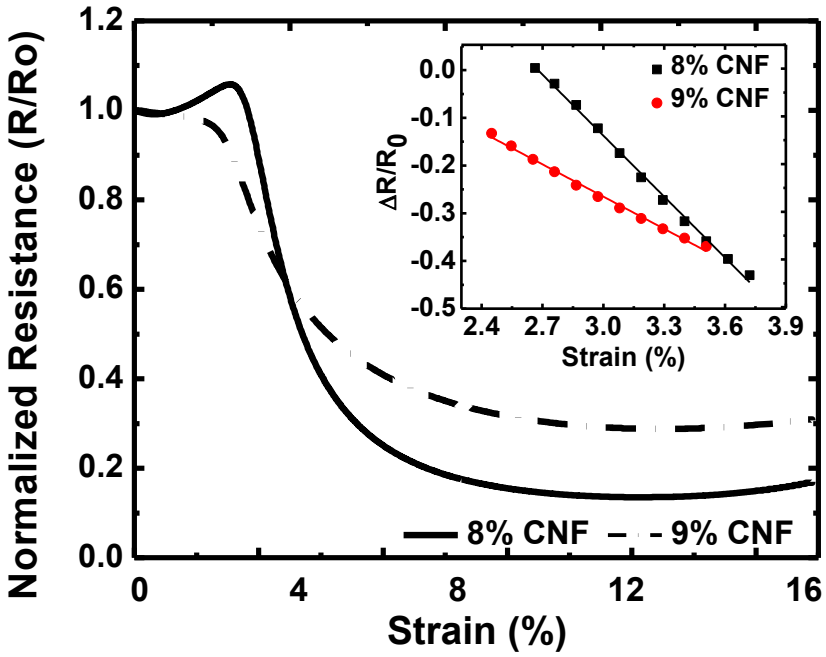

Figure 5.12 Normalized resistance of 10th loading cyles of 8% and 9% CNF containing 50/50 PVC-50/DOS containing samples. Inset figure shows the gauge factor for each sample

As given in Fig. 5.12, while 8 wt% CNF containing sample showed a K value of -42.63; 9 wt% CNF containing sample showed a value of -22.54. As obvious from these results piezoresistive response was found more sensitive at concentrations close to the percolation threshold and weaker for higher filler concentrations. Piezoresistive response of conductive polymer composites is primarily due to the breakdown of the filler junctions and/or reformation of the conducting network. In our case lower filler concentration was found to support the formation of the additional conductive paths in throughout the composite by change in filler orientation. On the other hand, since at higher concentration number of the conductive paths already higher (more saturated network), and resistivity of the system is lower, change in filler orientation did not lead to large-scale changes in the resistance. This relationship between filler concentration and piezoresistive response gives us chance to choose the filler concentration for desired sensory behavior.

B) Effect of PVC/DOS ratio on piezoresistive response

Matrix type is another important variable for the piezoesistive response, because it directly affects the processing conditions, filler-matrix interaction, interphase, filler dispersion and network configuration. However in our case, same polymer was used with different matrix/plasticizer ratio. Since we observed different electrical behavior and percolation threshold values depending on the PVC/DOS ratio in the previous part, we have investigated the effect of plasticizer (DOS) content on piezoresistive response. In order to discern the influence of the plasticizer (DOS) content of the composites on their piezoresistive behavior, an additional composition of 35/65 PVC/DOS matrix was evaluated. Fig. 5.13 shows the dependence of relative resistance of the composites. Although both samples showed negative

piezoresistance under strain, magnitude of the relative resistance chanced and critical strain of transition values were affected by composition of the composite. As given in Fig. 5.12 and Figure 5.13, while 50/50 PVC-50/DOS showed a K value of -22.54; 35/65 PVC-50/DOS sample showed a value of -44.36. As obvious from these results, 35/65 PVC-50/DOS composite showed higher sensitivity with almost no hysteresis when compared with 50/50 PVC/DOS. There are basically two reasons for this kind of response. First one is the higher flexibility and better recoverability of the composite which contains higher level of DOS. Increased plasticizer reduces the restriction of polymer chains by increasing free volume and weakening interaction between filler and matrix. As a result of increased mobility of polymer chains, fillers can rotate relatively easier even at lower levels of strain. The relative change in resistance for 35/65 PVC/DOS at 4% strain was higher than the one obtained for 50/50 PVC/DOS at 16% strain. This was also seen in transition values of critical strain. While 50/50 composite presented a transition value round 11.5%; 35/65 PVC-50/DOS showed a value of around 6%.

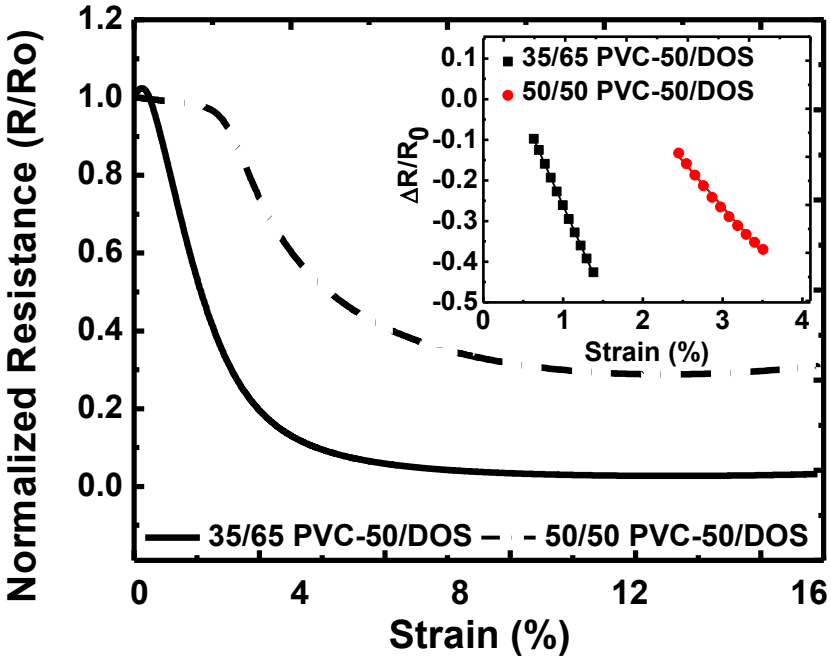

Figure 5.13 Normalized resistance of 10th loading cyles of 9 wt% CNF containing samples with the PVC-50/DOS ratios of 50/50 and 35/65. Inset figure shows the gauge factor for each sample

Other reason is the contact resistance between fillers. As previously mentioned, higher DOS content increases the contact resistance between fillers and lead to higher resistivity. In that case, even at lower strains chance in filler location is crucial for overcoming the contact resistance between fillers. Since zero strain resistance of 35/65 PVC/DOS relatively higher, movement and rotation of fillers lead to formation of new pathways and decreases the distance between fillers and electron movement from one filler to other enhances.

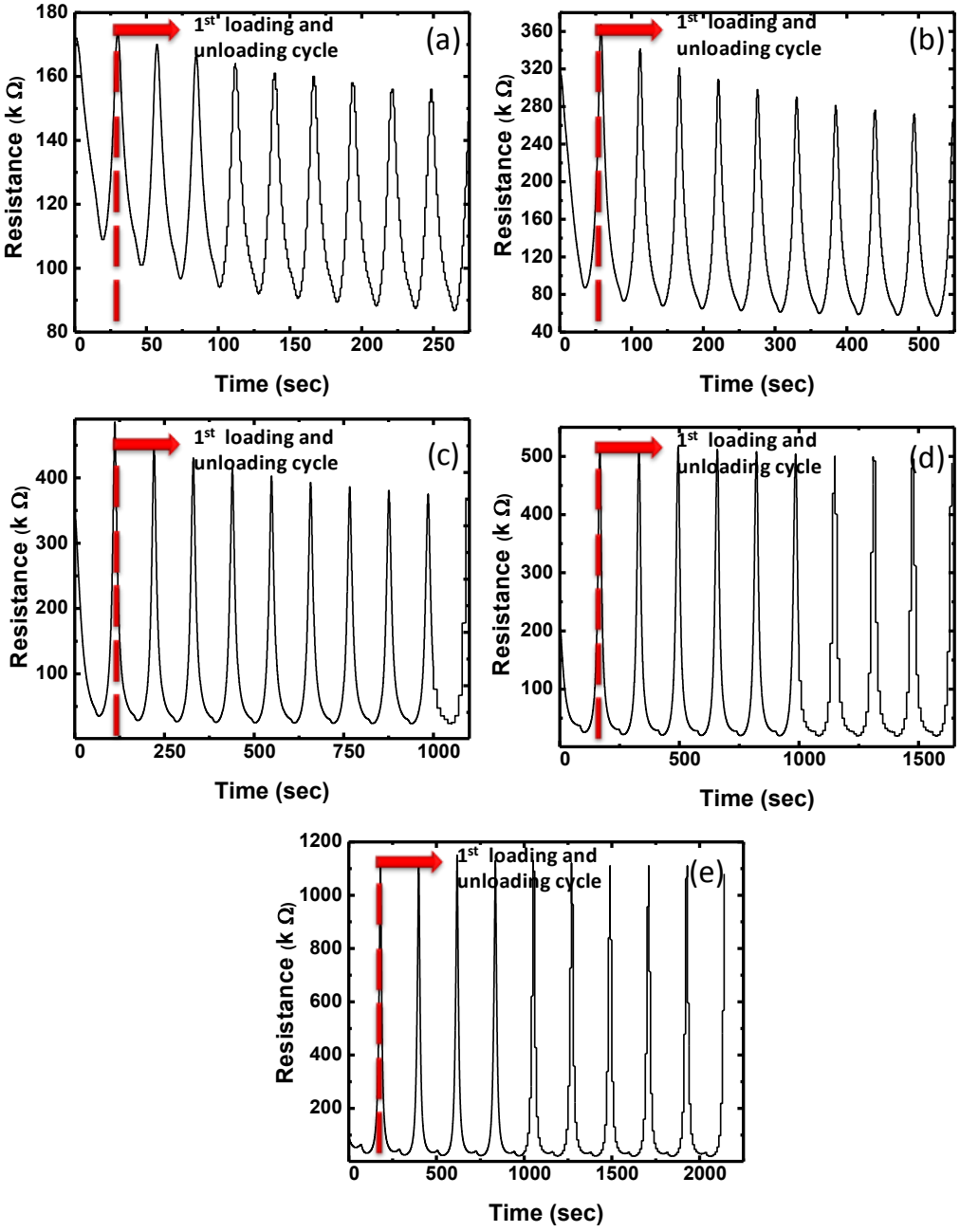

Figure 5.14 Dynamic piezoresistive behavior of 9 wt% CNF containing 35/65 PVC-50/DOS plastisol composite films as a function of time for different levels of strain (a) 2% (b) 4% (c) 8% (d) 12% and (e) 16%

The other point is the difference in cyclic symmetry and cyclic stability. As clearly seen from Fig. 5.14, 35/65 PVC/DOS showed almost no hysteresis with good cyclic stability and symmetry when compared with 50/50 PVC/DOS one. As previously mentioned hysteresis occurred in piezoresistive response was caused by mechanical hysteresis given unrecovered strain. While 50/50 PVC-50/DOS sample showed unrecovered strain value of 3.7% end of 10 cycles; 35/65 showed 2.2% which is an indication of better recoverability.

Conclusions

In this study, we have presented the fabrication of various conductive plastiosol composite films and their morphological, electrical and piezoresistive characterization. Homogeneous CNF distribution was achieved by high shear mixing for both low and high filler concentrations. Filler concentration, PVC/DOS ratio and molecular weight of PVC were found to affect the resistivity of the system. While increased DOS content was found to increase in resistivity, higher molecular weight resulted in lower resistivity. Samples were found to show negative piezoresistance at different levels of strain. Both filler concentration and PVC/DOS ratio was found significant in terms of piezoresistive response. Lower CNF content and higher DOS content lead to higher sensitivity in terms of piezoresistance.

As a summary we have shown that CNF filled conductive plastisols were able to detect the change in strain by monitoring the change in resistance. These materials can be used for many applications including printed sensors.

References

[1] Lozano K, Bonilla-Rios J, Barrera EV. A study on nanofiber-reinforced thermoplastic composites (II): Investigation of the mixing rheology and conduction properties. J Appl Polym Sci 2001;80:1162-72.

[2] Lozano K, Barrera EV. Nanofiber-reinforced thermoplastic composites. I. Thermoanalytical and mechanical analyses. J Appl Polym Sci 2001;79:125-33.

[3] Kuriger RJ, Alam MK, Anderson DP, Jacobsen RL. Processing and characterization of aligned vapor grown carbon fiber reinforced polypropylene. Composites Part A 2002;33:53-62.

[4] Tibbetts GG, Doll GL, Gorkiewicz DW, Moleski JJ, Perry TA, Dasch CJ et al. Physical properties of vapor-grown carbon-fibers. Carbon 1993;31:1039-47.

[5] Rodriguez NM. A Review of catalytically grown carbon nanofibers. J Mater Res 1993;8:3233-50.

[6] Pierson HO. Handbook of carbon, graphite, diamond, and fullerenes: properties, processing, and applications. Park Ridge, N.J., U.S.A.: Noyes Publications, 1993.

[7] Saito R. Physical properties of carbon nanotubes. London: Imperial College Press, 1998.

[8] Kumar S, Lively B, Sun LL, Li B, Zhong WH. Highly dispersed and electrically conductive polycarbonate/oxidized carbon nanofiber composites for electrostatic dissipation applications. Carbon 2010;48:3846-57.

[9] Tibbetts GG, Lake ML, Strong KL, Rice BP. A review of the fabrication and properties of vapor-grown carbon nanofiber/polymer composites. Composites Sci Technol 2007;67:1709-18.

[10] Palmeri MJ, Putz KW, Brinson LC. Sacrificial bonds in stacked-cup carbon nanofibers: Biomimetic toughening mechanisms for composite systems. ACS Nano 2010;4:4256-64.

[11] Yoon SH, Park CW, Yang HJ, Korai Y, Mochida I, Baker RTK et al. Novel carbon nanofibers of high graphitization as anodic materials for lithium ion secondary batteries. Carbon 2004;42:21-32.

[12] Tao XY, Zhang XB, Zhang L, Cheng JP, Liu F, Luo JH et al. Synthesis of multi-branched porous carbon nanofibers and their application in electrochemical double-layer capacitors. Carbon 2006;44:1425-8.

[13] Blackman JM, Patrick JW, Arenillas A, Shi W, Snape CE. Activation of carbon nanofibres for hydrogen storage. Carbon 2006;44:1376-85.

[14] Bao SP, Liang GD, Tjong SC. Effect of mechanical stretching on electrical conductivity and positive temperature coefficient characteristics of poly(vinylidene fluoride)/carbon nanofiber composites prepared by non-solvent precipitation. Carbon 2011;49:1758-68.

[15] Li L, Li J, Lukehart CM. Graphitic carbon nanofiber-poly(acrylate) polymer brushes as gas sensors. Sensor Actuat B-Chem 2008;130:783-8.

[16] Arlen MJ, Wang D, Jacobs JD, Justice R, Trionfi A, Hsu JWP et al. Thermal-electrical character of in situ synthesized polyimide-grafted carbon nanofiber composites. Macromolecules 2008;41:8053-62.

[17] Thomson W. On the electro-dynamic qualities of metals: Effects of magnetization on the electric conductivity of nickel and of iron. P R Soc London 1856;8:546-50.

[18] Smith CS. Piezoresistance effect in germanium and silicon. Phys Rev 1954;94:42-9.

[19] Barlian AA, Park WT, Mallon JR, Rastegar AJ, Pruitt BL. Review: semiconductor piezoresistance for microsystems. Proc IEEE 2009;97:513-52.

[20] Sun Y. Strain effect in semiconductors: theory and device applications. New York: Springer, 2009.

[21] Flandin L, Hiltner A, Baer E. Interrelationships between electrical and mechanical properties of a carbon black-filled ethylene-octene elastomer. Polymer 2001;42:827-38.

[22] Flandin L, Chang A, Nazarenko S, Hiltner A, Baer E. Effect of strain on the properties of an ethylene-octene elastomer with conductive carbon fillers. J Appl Polym Sci 2000;76:894-905.

[23] Wilkes CE. PVC handbook. Munich ; Cincinnati, Ohio: Hanser, 2005.

[24] Titow WV. PVC technology. London ; New York: Elsevier Applied Science, 1984.

[25] Nass LI. Encyclopedia of PVC. New York: Marcel Dekker, 1998.

[26] Wypych G. Handbook of plasticizers. Toronto; New York: ChemTec Pub; William Andrew Pub, 2004.

[27] Cadogan DF, and Howick CJ. Plasticizers. John Wiley & Sons Inc., 2000.

[28] Van Oosterhout JT, Gilbert M. Interactions between PVC and binary or ternary blends of plasticizers. Part I. PVC/plasticizer compatibility. Polymer 2003;44:8081-94.

[29] Grossman RF. Handbook of vinyl formulating. Hoboken, N.J.: Wiley-Interscience, 2008.

[30] Andrews R, Jacques D, Minot M, Rantell T. Fabrication of carbon multiwall nanotube/polymer composites by shear mixing. Macromol Mater Eng 2002;287:395-403.

[31] Kirkpatrick S. Percolation and conduction. Rev Mod Phys 1973;45:574-88.

[32] Stauffer D. Introduction to percolation theory. London; Washington, DC: Taylor & Francis, 1992.

[33] Psarras GC. Charge transport properties in carbon black/polymer composites. J Polym Sci Pol Phys 2007;45:2535-45.

[34] Vionnet-Menot S, Grimaldi C, Maeder T, Str\assler S, Ryser P. Tunneling-percolation origin of nonuniversality: Theory and experiments. Phys Rev B 2005;71:064201.

[35] Xu J, Donohoe JP, Pittman CU. Preparation, electrical and mechanical properties of vapor grown carbon fiber (VGCF)/vinyl ester composites. Composites Part A 2004;35:693-701.

[36] Ardanuy M, Rodríguez-Perez MA, Algaba I. Electrical conductivity and mechanical properties of vapor-grown carbon nanofibers/trifunctional epoxy composites prepared by direct mixing. Compos Part B-Eng 2011;42:675-81.

[37] Allaoui A, Hoa SV, Pugh MD. The electronic transport properties and microstructure of carbon nanofiber/epoxy composites. Composites Sci Technol 2008;68:410-6.

[38] Balberg I. A comprehensive picture of the electrical phenomena in carbon black–polymer composites. Carbon 2002;40:139-43.

[39] Kujawski M, Pearse JD, Smela E. Elastomers filled with exfoliated graphite as compliant electrodes. Carbon 2010;48:2409-17.

[40] Yu J, Zhang LQ, Rogunova M, Summers J, Hiltner A, Baer E. Conductivity of polyolefins filled with high-structure carbon black. J Appl Polym Sci 2005;98:1799-805.

[41] Hauptman N, Žveglič M, Maček M, Klanjšek Gunde M. Carbon based conductive photoresist. J Mater Sci 2009;44:4625-32.

[42] Blighe F, Hernandez Y, Blau W, Coleman J. Observation of percolation-like scaling far from the percolation threshold in high volume fraction, high conductivity polymer-nanotube composite films. Adv Mater 2007;19:4443-7.

[43] Grimaldi C, Balberg I. Tunneling and nonuniversality in continuum percolation systems. Phys Rev Lett 2006;96:066602.

[44] Balberg I. Tunneling and nonuniversal conductivity in composite materials. Phys Rev Lett 1987;59:1305-8.

[45] Chen G, Weng W, Wu D, Wu C. PMMA/graphite nanosheets composite and its conducting properties. Eur Polym J 2003;39:2329-35.

[46] Mamunya EP, Davidenko VV, Lebedev EV. Percolation conductivity of polymer composites filled with dispersed conductive filler. Polym Composite 1995;16:319-24.

[47] Kilbride BE, Coleman JN, Fraysse J, Fournet P, Cadek M, Drury A et al. Experimental observation of scaling laws for alternating current and direct current conductivity in polymer-carbon nanotube composite thin films. J Appl Phys 2002;92:4024-30.

[48] Ma X, Chang PR, Yu J, Lu P. Electrically conductive carbon black (CB)/glycerol plasticized-starch (GPS) composites prepared by microwave radiation. Starch - Stärke 2008;60:373-5.

[49] Marcilla A, Garcia S, Garcia-Quesada JC. Migrability of PVC plasticizers. Polym Test 2008;27:221-33.

[50] Messadi D, Taverdet JL, Vergnaud JM. Plasticizer migration from plasticized poly(vinyl chloride) into liquids. Effect of several parameters on the transfer. Industrial & Engineering Chemistry Product Research and Development 1983;22:142-6.

[51] Ehrenstein GW. Polymeric materials: structure, properties, applications. Carl Hanser Verlag, Munich, 2001.

[52] Dalmas F, Dendievel R, Chazeau L, Cavaillé J, Gauthier C. Carbon nanotube-filled polymer composites. Numerical simulation of electrical conductivity in three-dimensional entangled fibrous networks. Acta Materialia 2006;54:2923-31.

[53] Ruschau G, Yoshikawa S, Newnham R. Resistivities of conductive composites. J Appl Phys 1992;72:953.

[54] Sun J, Gerberich WW, Francis LF. Electrical and optical properties of ceramic/polymer nanocomposite coatings. J Polym Sci Pol Phys 2003;41:1744-61.

[55] Wolff EG. Introduction to the dimensional stability of composite materials. Lancaster, PA: DEStech Publications, Inc, 2004.

[56] Fraden J. Handbook of modern sensors: physics, designs, and applications. New York: AIP Press/Springer, 2004.

[57] Wilson JS. Sensor technology handbook. 2005.

[58] Yamaguchi K, Busfield JJC, Thomas AG. Electrical and mechanical behavior of filled elastomers. I. The effect of strain. Journal of Polymer Science Part B: Polymer Physics 2003;41:2079-89.

[59] Mullins L. Effect of stretching on the properties of rubber, Chem Technol 1948;21:281-300.

[60] Holt WL. Behaviour of rubber under repeated stresses. Ind Eng Chem 1931;23:1471-5.

[61] Dorfmann A, Ogden RW. A constitutive model for the Mullins effect with permanent set in particle-reinforced rubber. Int J Solids Structures 2004;41:1855-78.

[62] Bueche F. Molecular basis for the mullins effect. J Appl Polym Sci 1960;4:107-14.

[63] Harwood JAC, Mullins L, Payne AR. Stress softening in natural rubber vulcanizates. Part II. Stress softening effects in pure gum and filler loaded rubbers. J Appl Polym Sci 1965;9:3011-21.

[64] Harwood JAC, Payne AR. Stress softening in natural rubber vulcanizates. Part III. Carbon black-filled vulcanizates. J Appl Polym Sci 1966;10:315-24.

[65] Kraus G, Childers CW, Rollmann KW. Stress softening in carbon black-reinforced vulcanizates. Strain rate and temperature effects. J Appl Polym Sci 1966;10:229-44.

[66] Diani J, Fayolle B, Gilormini P. A review on the Mullins effect. Eur Polym J 2009;45:601-12.

CHAPTER 6. PIEZORESISTIVE FABRIC BASED SENSORS

Abstract

In this study, we demonstrate fabrication of piezoresistive sensors on textile fabrics through application of a screen-printed conductive nanocomposite layer of plasticized poly(vinyl chloride) (PVC), and carbon nanofiber (CNF). CNFs at various concentration levels were dispersed in a plastisol matrix to achieve the piezoresistive sensing layer on the fabric. Microscopic analysis showed homogeneous dispersion of CNFs without any dominant filler orientation throughout the conductive layer with good filler-matrix interface. It was also shown that conductive layer presented good adhesion to the fabric even after repeated cycles. The PVC/CNF nanocomposite printed fabrics were found to exhibit significant sensitivity to applied strain and magnitude of sensitivity was found to depend on magnitude of strain and filler concentration.

6.1 Introduction

Recent efforts in integrating electronic functionality in fibers and textiles have led to an entirely new field of research and product development dubbed as electronic textiles or e-textiles. Electronic textiles are functional textiles which offer aesthetic appearance as conventional textiles with the additional electronic functionality. Although research in the field of e-textiles started at the end of 1960s; the most important contributions have been made in the last two decades parallel with the advances in polymer-based flexible electronics

and optics. In addition, design and development of functional polymers and fibers have played a significant role in this development. Electronic textiles include wearable-instrumented garments capable of sensing fundamental signals related to physiological and mechanical activities, including vital signs, of a human body with no discomfort to the subject. In a broader sense e-textiles is can be extended to any textile products and may be crucial to many future applications including biomedicine, rehabilitation, and haptic interfaces.

Textiles (garments and others products) constitute an obvious choice as multifunctional platforms because of many reasons, including, flexibility, lightweight, conformability, *etc.* However, off-the-shelf electronic systems are often not ideal for integration in textiles because of their incompatible properties such as bulk, rigidity, *etc.* and associated problems with wearability and lack of durability to washing, perspiration, *etc.* In its simplest form, E-textiles can only have sensory elements which can only sense the changes in the environment. Others may have the ability to sense and react. The third generation of the E-textiles has the ability of sense, react and adapt to the environment [1-3]. Depending on the type and function of adapted/integrated electrical-electronic system, E-textiles may be capable of sensing, data processing, actuation, and energy storage or generation.

Integrated sensing capability with flexibility and environmental stability is a key element for future e-textile products. Sensors are transducers that are capable of converting mechanical, chemical, optical, and other forms of stimuli into electrical signals. In other words, sensors are able to measure and convert the quantity of physical variable into an electrical signal. Depending on the system, common physical variable or stimulus (measurand) can be in the

form of force, temperature, length, strain, pressure, time, resistance, capacity, frequency, velocity, acceleration; and output signal can be voltage or current [4,5]. Like in the traditional electronic sensors, ideal textile based sensors should be able to provide an interface between user and the electronic system by converting any type of physiological or environmental measurand into electrical signal [6-14]. Such sensors can be readily used in many applications such as sports [12], medicine-rehabilitation [15], and protection [16].

Textile based sensors can be classified in a number of ways based on application (health monitoring, pressure, strain sensors) or type of material (knitted, woven, printed fabric, *etc*.). However, in a fundamental sense, the most useful classification can be based on the principle of sensing. The most common principles of sensing implemented in textiles are capacitive [8,17-20], inductive [18,21,22], piezoelectric [23,24], optical [10,25-28], chemical/biochemical [9,12,13] and piezoresistive [29-32]. In all these, textile based piezoresistive sensors (TBPS) have wide range of applications including; strain monitoring [33], gas sensing [34], temperature sensing [15,35], pressure sensing [36,37] body-posture monitoring [38-40] health monitoring (vital signals, respiration) and rehabilitation [29,38,41].

Piezoresistivity is a material property where the bulk resistivity of the material is altered by applied deformation. The piezoresistive effect has been observed for semiconductors such as germanium and silicon [42] as well as multicomponent composite systems [43]. The piezoresistive response of polymer composites with conductive fillers has been attributed, primarily, to the breakdown of the filler-filler junctions and/or reformation of the conducting network. Dominant mechanism depends on many factors such as filler concentration [44,45], filler geometry and orientation [46,47] and direction and amplitude of the applied stress [48].

Depending on the dominant mechanism, the observed piezoresistive behavior due to applied tensile strain can be either positive (increase in resistance) or negative (decrease in resistance).

Various materials and composites in a number of forms have been used for TBPS. These include, inherently conducting polymers (ICPs) [34,49-51], conductive polymer composites (CPCs), conducting yarns [11,52,53], and knitted fabrics [54] made from conductive yarns. Initial studies in the area of TBPS started with simply coating of textile surfaces with ICPs, primarily because of their good electrical conductivity and flexiblity. Polypyrrole (PPy) is the most often used conducting polymer reported in the literature for textile based sensors because of its high conductivity, and non-toxicity [33,34,49-51]. However, PPy has the disadvantages of instability in air, aging tendency, high response times with poor repeatability [34,35]. It is also reported that coating with PPy is relatively difficult and time consuming when compared with traditional printing and coating methods [35]. On the other hand, textiles coated with CPCs have many advantages over ICPs, including higher flexibility, stability, ease of application, low cost and compatibility, accuracy with good repeatability [14]. The aim of this work is to develop a flexible, lightweight and strain sensitive textile based sensor for E-textile applications. Potential applications of the proposed sensor include physiological monitoring and rehabilitation.

In this work, we report printed sensors using elastic, conductive, and solvent-free nanocomposite plastisol paste, developed mainly from PVC, and CNFs. The conducting plastisol composite layer was found to show homogeneous filler dispersion and good adhesion to the fabric. The printed fabrics showed strain-dependent negative piezoresistive

response. Sensitivity and stability of the piezoresistance was found to be dependent on the preconditioning and magnitude of the applied strain and filler concentration.

6.2 Materials and Methods

The PVC resin used for plastisol preparation is Solvin 372 from Solvay Corporation. The resin was referred to as PVC-50, where the postscript designation denotes the number-average molecular weight of the resin in kg mol^{-1}. The plasticizer used is Bis(2-ethylhexyl) sebacate (dioctyl sebacate) (DOS) manufactured by Acros Organics and obtained from Fisher Chemicals. Epoxidized soybean oil (ESO) is used as thermal stabilizer and obtained from Spectrum Chemicals Mfg Corp. Vapor grown carbon nanofibers (VGCNF) used as conducting filler is obtained from the Showa Denko Corporation. The VGCNF had surface area of 13 m^2 g^{-1} and nominal fiber diameter of 150 nm with aspect ratio ranging from 100 to 150. In order to ensure adhesion between the conducting plastisol composite and the fabric substrate, a bonding agent, designated as Binder 2001 and sold by Nazdar SourceOne, is also used.

Based on our previous studies plastisol with 50/50 PVC/DOS ratio was deemed ideal for printing on fabrics. Composites with 50/50 level of PVC/DOS ratio and five levels of filler concentrations from 3 up to 7 wt% were prepared with binder (20 wt% of PVC+DOS as recommended by the manufacturer) as the other additive 5 wt% (of PVC) of ESO and 20 wt% of PVC+DOS as the other additive. In preparing the composite printing paste all mixing was done in a high shear mixer (Mazerustar KK-50S). In the first step of composite preparation, appropriate amount of ESO and DOS were mixed for 10 sec. and CNF was

added and mixed further for 60 sec. This was followed by addition and mixing of PVC for another 60 sec. In the last step, the binder was added to the mixture and processed further for 60 sec. Screen printing of the plastisol composite on fabrics (single jersey knitted, 92% Polyester, 8% Spandex, 345 gr m^{-2}) were carried out by hand with flat printing screen with the mesh number of 60 (60 mesh in 1 inch). Post printing curing of the conductive plastisol is necessary to gel and fuse the material for producing uniform, rubbery printed layers. Curing was carried out in a Mathis Laboratory type dryer at 140°C for 30 minutes. The temperature was chosen to achieve complete melting of PVC to enhance the interaction between matrix-filler and paste-fabric interface. For the preparation of the films, CNF containing plastisol paste was then compression molded into 0.5 mm thick films in a laboratory type hydraulic press with heated platens at 140°C for 30 minutes.

To investigate CNF dispersion, orientation, surface morphology of printed layer, filler-matrix and composite-fabric adhesion characteristics, the printed fabrics were examined with a JEOL-6400F field emission scanning electron microscope (FESEM) under low-voltage (1kV) without any surface coating.

Volume resistivity of the composite films was determined by Keithley Model 6517B Electrometer and Model 8009 Resistivity Chamber in accordance with ASTM D-257 standard. Since printed fabrics have two layers as printed layer and fabric, same instrument is not proper for resistivity measurements of printed fabrics. Resistance measurement of the printed fabrics was carried out using a four- probe set-up consisting of a current source (Keithley 6221) and a nano-voltmeter (Keithley 2182A) under 1 µA input current. The set-up

is controlled by a computer for automated data acquisition and voltage scans. Resistivity of the samples was calculated from the following formula:

$$\rho = RA/L \qquad \text{Equation (6.1)}$$

Before making the electrical measurements, specimen thicknesses were determined using a precision thickness meter (Mitutoyo ID-C112E).

To determine the piezoresistive behavior of the printed fabrics, specimens, 80 mm long and 25 mm wide, were prepared by attaching four electrical leads, 1.3 mm apart, along the centerline of the sample parallel to the longitudinal direction (parallel to the direction of applied strain). Electrical leads were attached using small beads of plastisol composites with high carbon black content (20 wt%) prepared in our lab for this purpose. Specimens were clamped on a load frame (Fig. 6.1) with the gauge length set at 50 mm and cycled to 2, 4, 8, 12, 16% strain amplitudes at a speed of 4.4 mm min^{-1}. Dynamic resistance measurement on these samples was carried out using the same four-probe set up used for resistance measurements.

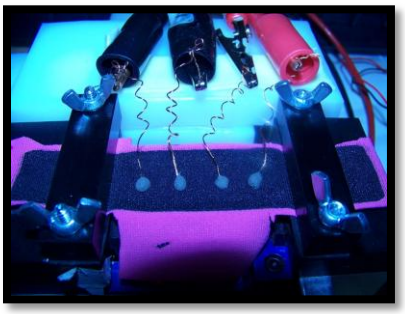

Figure 6.1 Piezoresistance measurement set-up

Since we have observed the effect of mechanical strain preconditioning, the repeated cyclic uniaxial straining of the specimen, on its piezoresistive response for conductive composites, all of the samples reported in this study were, therefore, preconditioned at 16% strain for 25 cycles. For the strain cycling tests, (25mm x 80mm) composite specimens were prepared and tested on a MTS 3G load-frame with a gauge length of 50 mm. Samples were cycled to pre-yield strain of 16% strain at 4.4 mm min^{-1}. The strain value which intercepts stress value at 0 MPa was determined as unrecovered strain.

6.3 Results and Discussion

6.3.1 Morphology

In order to analyze the dispersion and orientation of CNFs in the plastisol composite, and to discern the surface morphology of the printed layer as well as plastisol-fabric adhesion we examined cyrofractured (in liquid nitrogen) cross-sections and surfaces of the test samples.

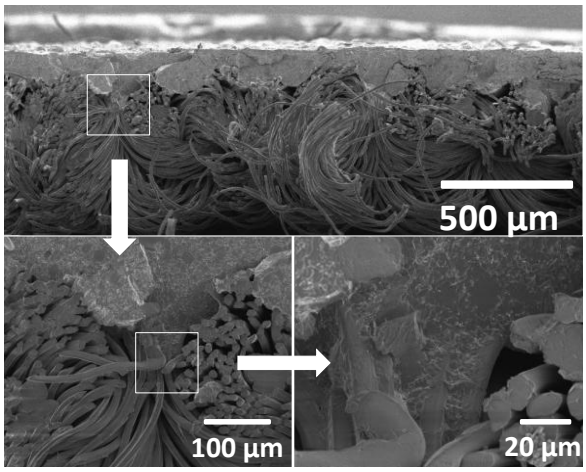

Figure 6.2 SEM images of 6% CNF containing 50/50 PVC-50/DOS plastisol printed fabric at different magnifications

Uniformly distributed light and raised spots representing the CNF particles in Fig. 6.2 and Fig. 6.3 clearly show the uniform dispersion of fillers without any dominant orientation and particle clusters. It is also obvious from Fig. 6.3c and d, that the filler/polymer interphase is robust with high matrix/filler adhesion. The good adhesion between CNFs and plastisol is probably due to, decreased surface tension of the plasticized polymer matrix, high temperature processing (melt processing), and the nanoscale surface roughness of CNF particles. In addition, printed plastisol layers in Fig. 6.2, 6.3c and d) do not show any surface cracks or delamination as evidence of good adhesion to the fabric even after mechanical cycling.

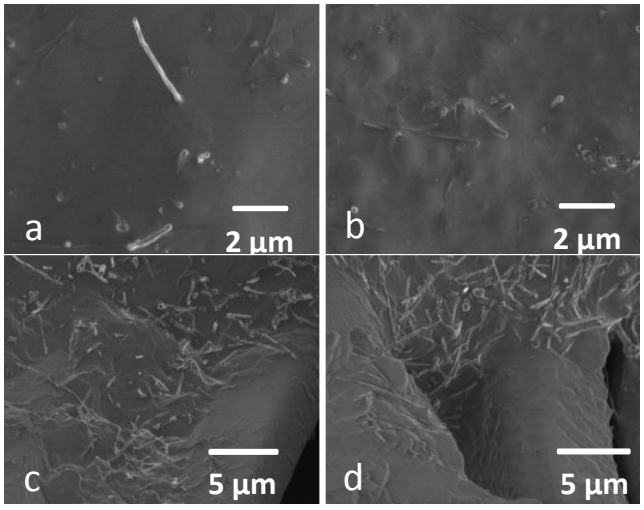

Figure 6.3 SEM images of 6% CNF containing 50/50 PVC-50/DOS plastisol printed fabric (a) surface before cycling (b) surface after 200 cycles (c) cross-section before cycling and (d) cross-section after 200 cycles

6.3.2 Electrical properties

6.3.2.1 Resistivity

The addition of conducting fillers into an insulating matrix enhances its electrical properties, *i.e.*, conductivity [55-57]. Unlike inherently conducting materials, a percolation threshold must be reached by the filler before the matrix becomes conductive. Percolation threshold is the point at which conductive filler particles begin to form of a continuous conducting path across the composite and the resistivity of the composite drops precipitously by many orders of magnitude. The resistivity of printed fabrics as a function of CNF content (wt%) is shown in Fig. 6.4.

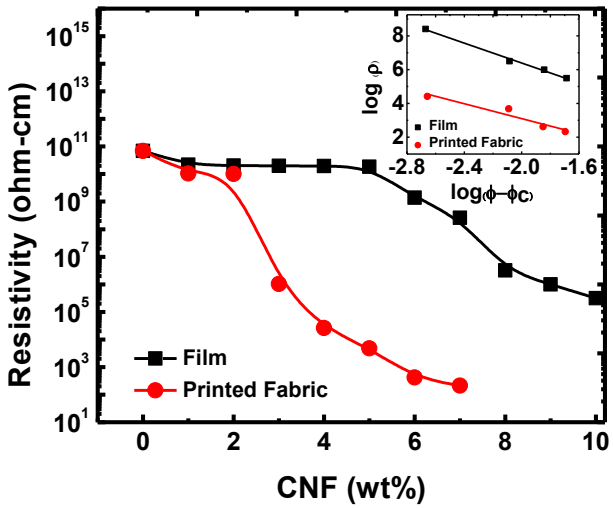

Figure 6.4 Variation of resistivity of composite films and printed fabrics as a function of CNF content. Inset figure shows the on exponent t values of film and printed fabric

As shown in Fig. 6.4, resistivity of both composite film and printed fabric showed transition from insulating to conducting by increasing the filler content. However, percolation threshold of printed fabric seems to be lower than composite film. In order to determine the percolation threshold according to the classical percolation theory and to have an idea about the lattice dimensionality/structure/strength of the percolating network, critical exponent was calculated (by using the resistivity values) below the percolation threshold with a power law equation [58,59] as follows which was well agreed in the literature [55,56,60-62]:

$$\rho \propto (\phi - \phi_c)^{-t} \text{ for } \phi > \phi_c \qquad \text{Equation (6.2)}$$

ρ is the resistivity of the printed layer, ϕ is the volume fraction of the filler, ϕ_c is the percolation threshold, and t is the dc transport critical exponent. The occurring linear relationship between log (ρ) *vs*. log (ϕ-ϕ_c) allowed us to calculate the ϕ_c and t. Different ϕ_c values were used in order to obtain best fit and highest R^2 values.

Table 6.1 t, ϕ_c and R^2 values of samples

Material	**t**	**ϕ_c**	**R^2**
Composite Film	2.94	0.039 (~7 wt %)	0.99
Printed Fabric	2.20	0.021(~3.5 wt %)	0.92

As given in Table 6.1, percolation behavior of the printed composite layer was found to be significantly different from the composite films. While composite film showed a ϕ_c value of 0.039 (~7 wt %) and t value of 2.94, printed fabric showed a ϕ_c value of 0.021 (~3.5 wt %)

and t value of 2.20. In our previous studies, we have observed the negative effect of DOS on resistivity. Based on this observation, we have investigated the plasticizer-fabric interaction. While polar plasticizers have strong interactions with polymeric matrix and lower potential for migration from the matrix to the fabric; non-polar solvents show poor interaction and higher migration tendency [24, 36]. DOS is a non-polar plasticizer and its migration from plastisol to fabric seems possible, especially for the composites with higher levels of plasticizer. The lower percolation threshold for printed fabric is likely caused by plasticizer migration from the matrix plastisol to the fabric. In order to investigate this, fabric samples were extracted in acetone and dried followed by printing (on part of it) and curing. Non-printed part of the fabric at the boundary of the printed area was removed and boiled in acetone for 30 minutes for extraction of DOS. Acetone was evaporated and FT-IR spectrum of the extract was obtained.

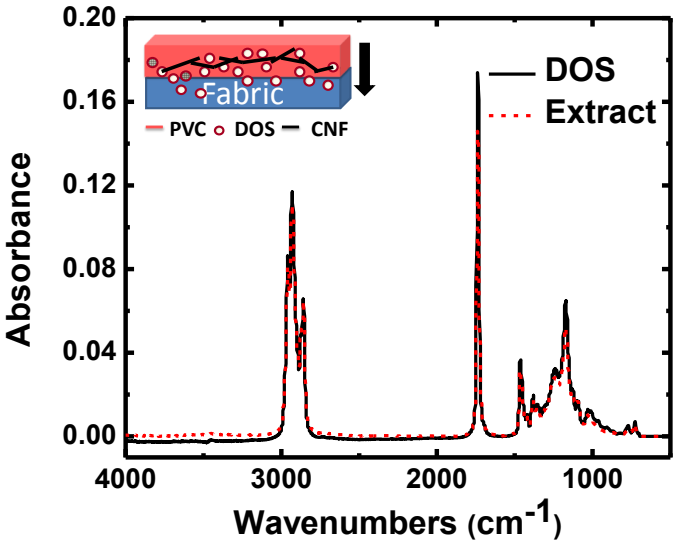

Figure 6.5 FT-IR spectrum of DOS (black) and extract (red). Inner figure represents the DOS migration from plastisol to fabric

FT-IR spectra of pure DOS and the extract presented in Fig. 6.5 completely overlap each other. It is obvious that the plasticizer has migrated to the fabric during printing and/or the curing process. DOS is an aliphatic CH_2 chain with two ester groups which makes it relatively non-polar, see Fig. 6.6a. The DOS molecule can interact with PVC with the help of the ester groups as shown in Fig. 6.6b [63-66]. Because of relatively non-polar structure, all DOS molecules might not interact with PVC and easily accessible smooth fiber surfaces (see Fig. 6.2) likely to allow wicking of DOS into the fabric structure and away from the composite. Decreased DOS will also decrease the contact resistance between fillers and increase the conductivity of the network.

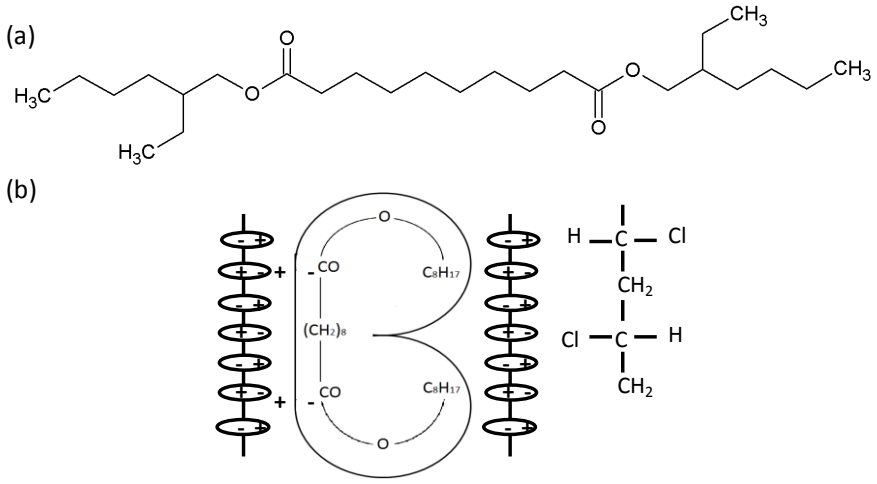

Figure 6.6 (a) Chemical structure of DOS (b) PVC-DOS interaction [63,66]

Mechanism of conductivity in a material and in particular in a composite can change depending on the components of the system. Although CNFs seem to be the conducting phase in the PVC/CNF plastisol, they also may give rise to resistance to electron flow at the

contact points as constriction resistance and tunneling resistance. The contribution of conducting phase to the overall conductivity is not only related with its inherent conductivity or its concentration but also the structure of the network and contact resistance between the fillers [67,68]. In a system consisting of only polymer and filler, electron transfer can occur by direct contact of fillers and/or tunneling of electrons through a thin layer of polymer in the order of few angstroms. In the case of higher plasticizer content, even if the filler-filler distances kept constant, electron transfer might be hindered by the formation of an additional insulating layer at the filler-polymer interphase and the mechanism of conductivity might become more complex [67,69,70]. On the other hand, in the case of printing, migration of DOS from plastisol to the fabric decreases contact resistance between fillers and enhances the electrical conductivity and lowers the percolation threshold of the system.

In addition to ϕ_c value, we have observed change in t value for printed films. As given in the literature, conductive composites show t values in a wide range from 0.9 to 6.4 depending on the network structure and mechanism of conductance [55,56,62,71-75]. While two dimensional systems were found to show t values between 1.4-1.5, three dimensional systems were reported to have 1.5-2. As a common terminology, t=2 accepted as a universal behavior and deviation from this (t>2) described as non-universal behavior. The difference between 2D and 3D networks and non-universal behavior were basically attributed to filler type, filler geometry [62,72,74,75], matrix type [71], processing conditions [73] all of which affect the tunneling between conductive fillers [76-79]. Deviation from universal behavior (t=2) and complex conduction mechanism probably caused by high aspect ratio [55,56,62] of CNFs and high contact resistance between fillers [67,80]. Although, t value of the printed

layer was higher than 2 which is in agreement with previous results (2.38-3.21) obtained from VGCNF filled composites [55,56,62], it was lower than what we obtained for composite films which is also caused from the migration of DOS from the plastisol structure during printing or curing.

6.3.2.2 Piezoresistance

Ideally a piezoresistive sensor should show effective sensing behavior over a practical range of strain. In order to analyze this, piezoresistance studies were carried out with printed fabrics at 2, 4, 8, 12, and 16% strain amplitudes. Our initial studies on the piezoresistive behavior of the printed fabrics suggested strong influence of mechanical preconditioning of the samples to a higher strain for consistent behavior within the strain range of interest. All of the samples reported in this study were, therefore, preconditioned at 16% strain for 25 cycles prior to evaluation of their piezoresisitive behavior.

The piezoresisitve behavior reported here is limited to fabrics printed with 5, 6, and 7 wt% CNF containing plastisol composites. The choice is primarily based on our initial studies on percolation behavior of the PVC/CNF composites and printed fabrics, as well as the viscosity of the printing paste required for screen printing.

The piezoresistive response of the printed fabrics was investigated as a function of strain amplitude ranging from 2% to 16%. Figs. 6.8, 6.9, and 6.10 show change in electrical resistance as a function of time during 10 loading and unloading cycles at various strain amplitudes for different filler concentrations. In all cases, all fabric sensors showed drop in resistance with applied strain, a response dubbed as negative piezoresistance in the literature.

In all cases of lower strain amplitudes (in the range of 2-8%), electrical resistance dropped continuously with increasing strain, and the resistance increased during recovery. The drop in resistance can be attributed to the reversible change in CNF network configuration in which the rotation as well as translation of cylindrical CNF particles due to applied strain resulted in more CNF particles being brought to the sample-plane. The potential result is greater number of percolating pathways through the composite and there by lower electrical resistance. For higher strain amplitudes (in the range 12-16%), increasing strain resulted in initial lowering of resistance, however, beyond a certain strain small increase in resistance is noted with increasing strain. The rise in resistance at greater applied strain is a result of translation dominated particle movement at higher strain that results in overall damage to the percolating network. Although strain induced negative piezoresistance has been reported elsewhere for carbon black filled composites [46,81,82] and CNT-coated yarns [83], to our knowledge, this type of behavior is being reported for the first time for conductive (CNF filled) plastisol printed fabrics. CNFs are high aspect ratio, cylindrical fillers, as a result any strain induced rotation and/or reorientation would have more significant and somewhat different effect on CNF composites than composites containing spherical fillers, *i.e.* carbon black. Unlike spherical particles, any change in spatial orientation (due to rotation) of the CNFs is more likely to affect the conducting network configuration (density of the contact points) within the composite.

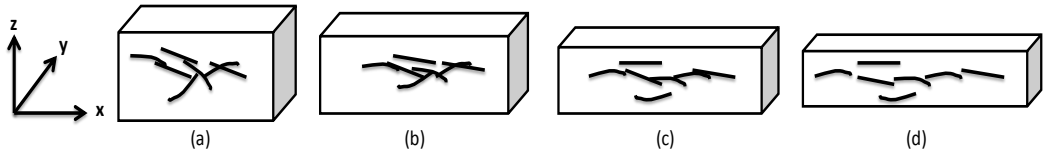

Figure 6.7 Mechanism of piezoresistance change in PVC/CNF composites (a) zero strain (b) between zero strain and critical strain (c) critical strain (d) after critical strain

As shown in Fig. 6.7, at lower values of strain, fibers tend to reorient along the strain direction primarily through rotation resulting in lower filler to filler relative distance and formation of new bridges, networks leading to lower electrical resistance. At higher values of strain (after critical strain), translation of particles predominates, resulting in greater inter-particle separation and higher resistance (see Fig. 6.7). The increase in resistance during unloading was a result of relaxation and recovery of the polymeric matrix, which stimulates CNFs to return to their original position. The resistance-strain relationships of PVC/CNF composite printed fabrics shown in Figs. 6.8, 6.9, and 6.10, are generally stable, repeatable, and show almost no hysteresis. This behavior is markedly different from that of composite films reported earlier.

The difference is most likely caused by the structural characteristics of the highly elastic knitted fabric and the flexible printed layer. Printed fabrics can be considered as laminates with three components namely, the printed layer (plastisol composite), the fabric, and may be more importantly the interphase, see Fig 6.2. The properties of each of these directly affect electrical, mechanical, morphological properties of the system. The interphase is formed by the penetration of plastisol composite into the fabric structure and functions to bind the yarns in the fabric and restricts their mobility. Particularly, in case of relatively more deformable

knit fabrics the formation of this interphase enhances the mechanical properties of the fabric significantly.

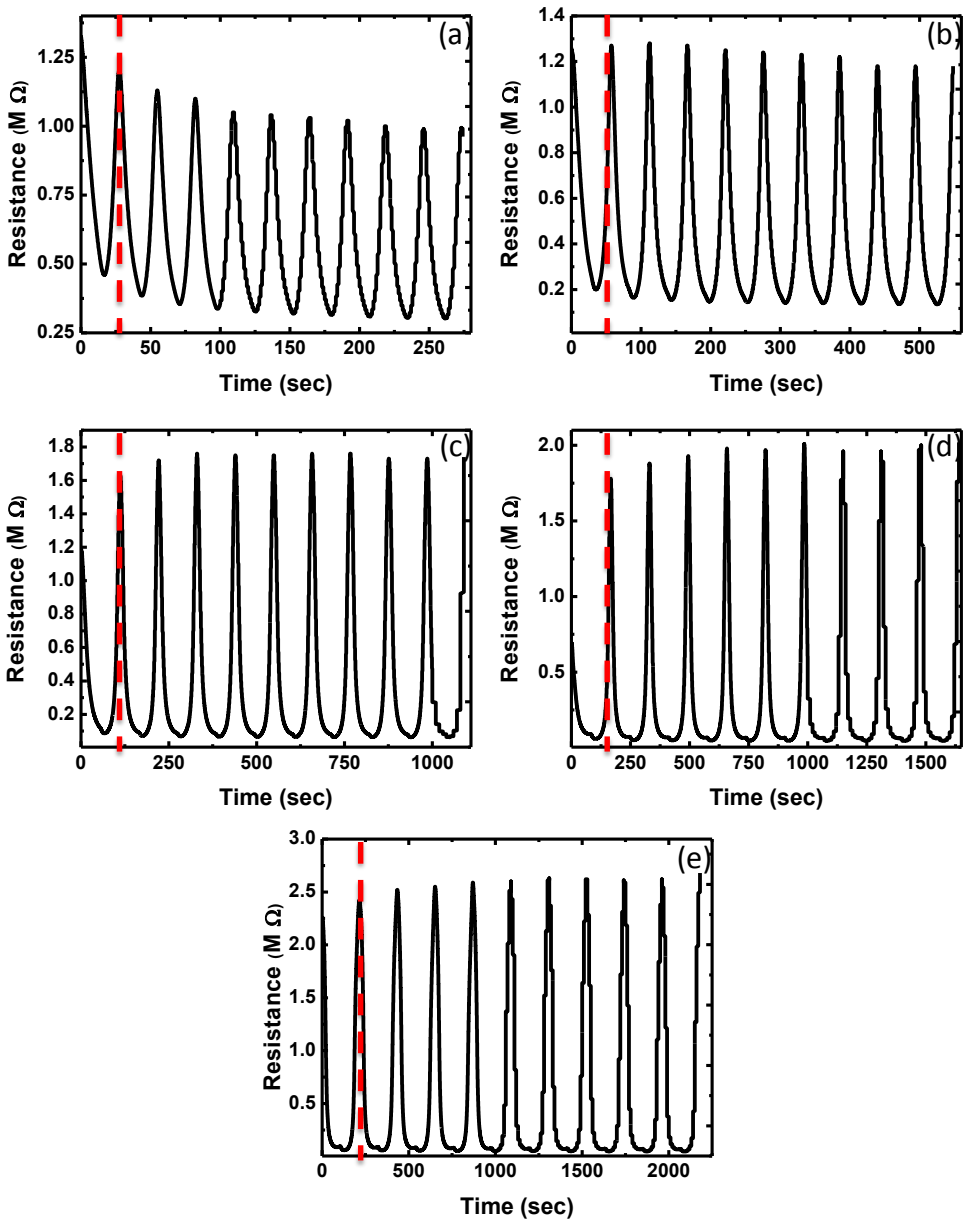

Figure 6.8 Dynamic piezoresistive behavior of 5 wt% CNF containing 50/50 PVC/DOS plastisol printed fabric as a function of time for different levels of strain (a) 2% (b) 4% (c) 8% (d) 12% and (e) 16% (red dashed lines represents the end of 1st loading and unloading cycle)

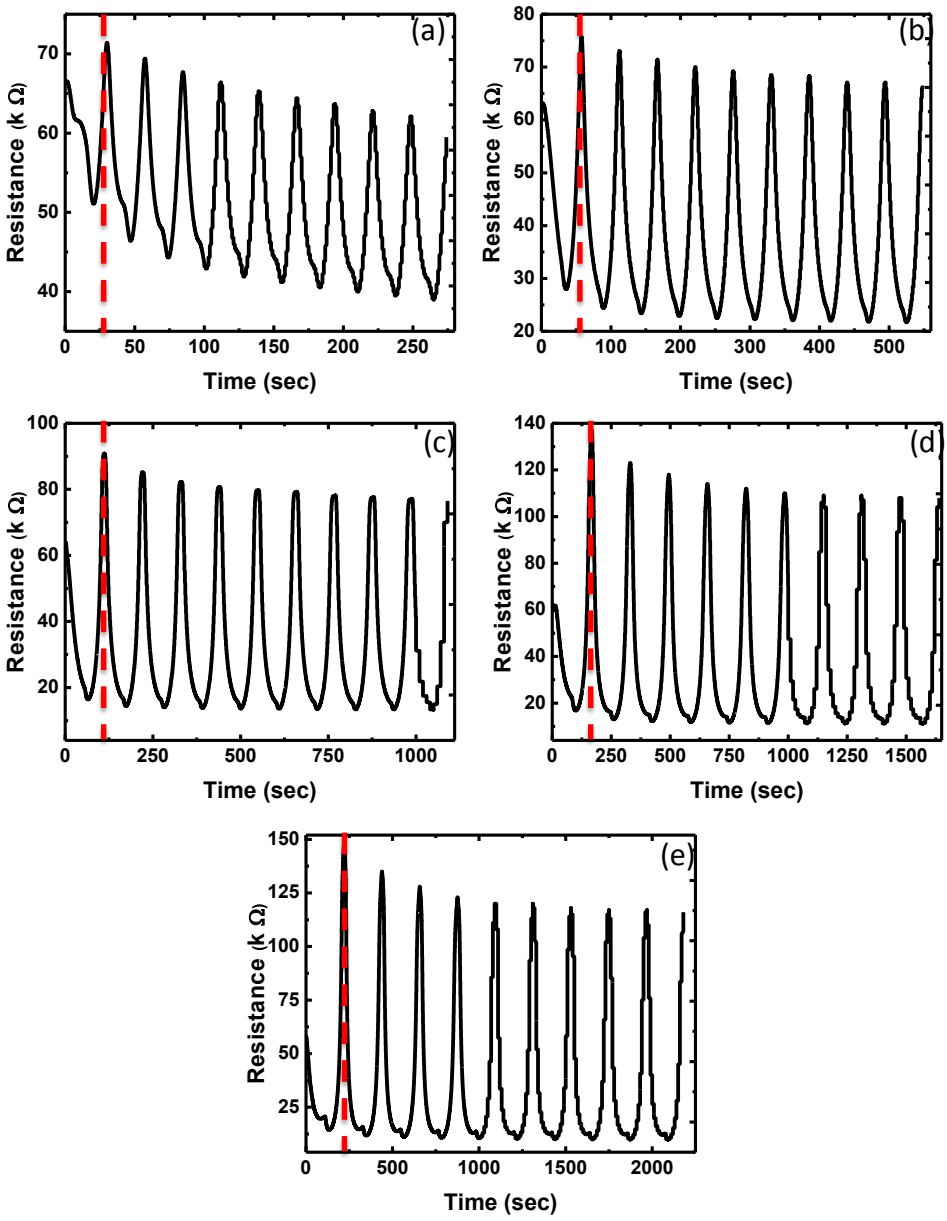

Figure 6.9 Dynamic piezoresistive behavior of 6 wt% CNF containing 50/50 PVC/DOS plastisol printed fabric as a function of time for different levels of strain (a) 2% (b) 4% (c) 8% (d) 12% and (e) 16% (red lines represents end of 1st loading and unloading cycle)

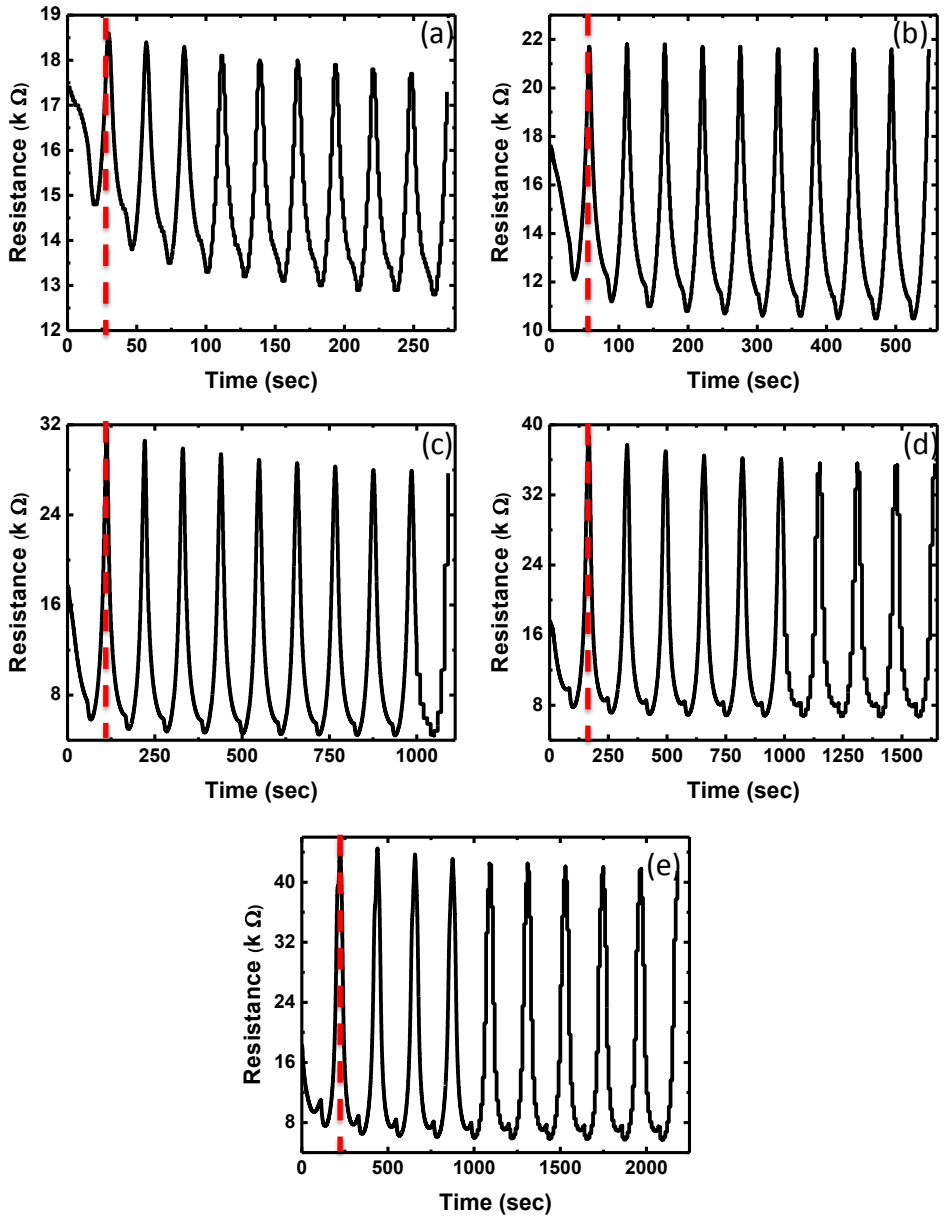

Figure 6.10 Piezoresistive behavior of 7 wt% CNF containing 50/50 PVC/DOS plastisol printed fabric as a function of time for different levels of strain (a) 2% (b) 4% (c) 8% (d) 12% and (e) 16% (red lines represents end of 1st loading and unloading cycle)

Fig. 6.11 shows the effect of filler concentration and strain amplitude on strain sensitivity (normalized resistance) and cyclic symmetry of the printed fabrics.

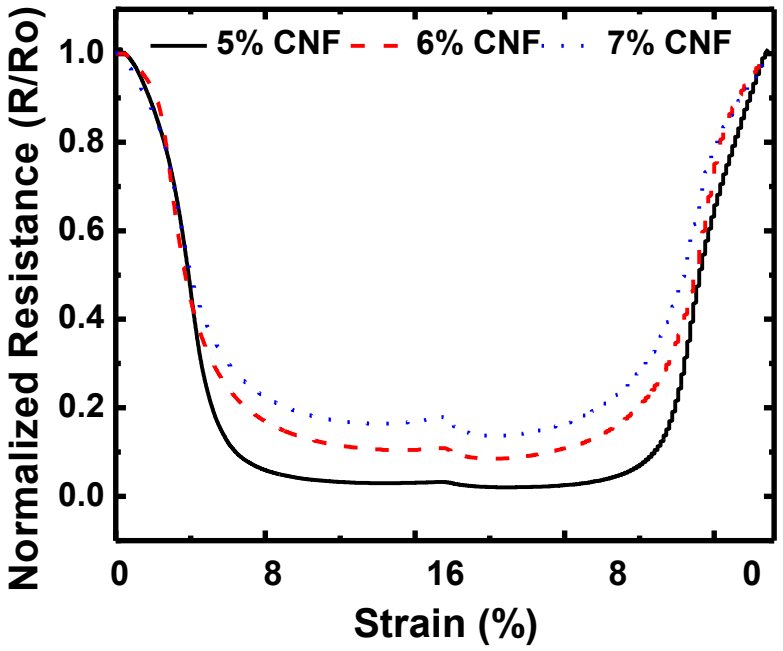

Figure 6.11 Normalized resistance values of printed fabrics with 5, 6, and 7 wt% CNF containing plastisol as a function of strain (10^{th} loading and unloading cycles)

As obvious from the data, both samples showed chance in resistance under strain with very good cyclic symmetry but magnitude of sensitivity which is represented by gauge factor, is different for each sample. Gauge factor (K) is defined as the change in resistance of a sample (ΔR) under an external strain (ε) was calculated using the expression by considering the most linear part of the R *vs.* ε response:

$$K = \Delta R/\varepsilon R_0 \qquad \text{Equation (6.3)}$$

Here R_0 is the resistance of the sample at zero strain.

As given in Fig. 6.11, while 5% CNF containing sample showed a K value of -31.51; 6 wt% CNF containing sample has a value of -11.8 and 7 wt% CNF containing sample has a value

of -8.3. As obvious from these results piezoresistive response was found more sensitive at concentrations close to the percolation threshold and weaker for higher filler concentrations.

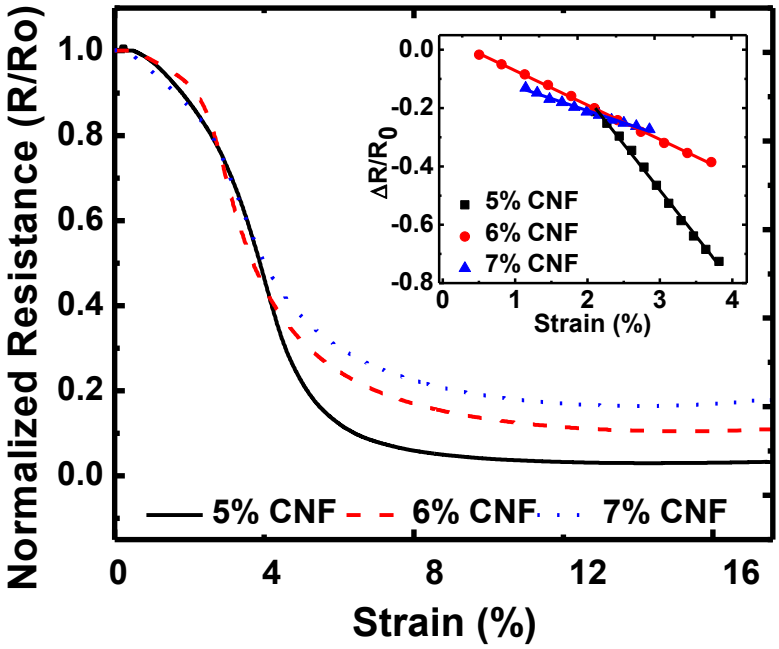

Figure 6.12 Normalized resistance of 10th loading cyles of 5, 6, and 7 wt% CNF containing samples. Inset figure shows the gauge factor for each sample (10th loading and unloading cycles)

Piezoresistive response of conductive polymer composites is primarily due to the breakdown of the filler junctions and/or reformation of the conducting network. In our case, lower filler concentration was found to support the formation of the additional conductive paths in throughout the composite by change in filler orientation. On the other hand, at higher concentrations number of the conductive paths already higher (more saturated network), and resistivity of the system is lower, change in filler orientation did not lead to large-scale

changes in the resistance. This relationship between filler concentration and piezoresistive response gives us chance to choose the filler concentration for desired sensory behavior.

Conclusions

In this study, we have presented the fabrication of piezoresistive fabric based sensors and their morphological, electrical and piezoresistive characterization. Homogeneous CNF distribution was achieved by high shear mixing for both low and high filler concentrations. Samples were found to show negative piezoresistance at different levels of strain. Strain level and filler concentration were found to affect the piezoresistive behavior and sensitivity of the printed sensors. Lower CNF content and higher strain level resulted in more sensitive piezoresisive response. As a summary, we have shown that printed fabrics with CNF filled conductive plastisols were able to detect the change in strain by monitoring the change in resistance with perfect cycling stability. These materials can be used for many applications including strain gauges and rehabilitation purposes.

References

[1] Zhang, X., Tao, X. Smart textiles: passive smart. Textile Asia 2001:45-49.

[2] Zhang, X., Tao, X. Smart textiles: active smart. Textile Asia 2001:49-52.

[3] Zhang, X., Tao, X. Smart textiles: very smart. Textile Asia 2001:35-37.

[4] Wilson JS. Sensor technology handbook. 2005.

[5] Fraden J. Handbook of modern sensors : physics, designs, and applications. New York: AIP Press/Springer, 2004.

[6] Coyle S, Lau K, Moyna N, O'Gorman D, Diamond D, Di Francesco F et al. BIOTEX-Biosensing textiles for personalized healthcare management. IEEE T Inf Technol Biomed 2010;14:364-70.

[7] Mitchell E, Coyle S, O'Connor NE, Diamond D, Ward T. Breathing feedback system with wearable textile sensors. Body Sensor Networks (BSN), 2010 International Conference on 2010:56-61.

[8] Merritt CR, Nagle HT, Grant E. Textile-based capacitive sensors for respiration monitoring. IEEE Sens J 2009;9:71-8.

[9] Morris D, Coyle S, Wu Y, Lau KT, Wallace G, Diamond D. Bio-sensing textile based patch with integrated optical detection system for sweat monitoring. Sensor Actuats B-Chem 2009;139:231-6.

[10] De Jonckheere J, Narbonneau F, Kinet D, Zinke J, Paquet B, Depre A et al. Optical fibre sensors embedded into technical textile for a continuous monitoring of patients under magnetic resonance imaging. 2008 30th Annual International Conference of the IEEE Engineering in Medicine and Biology Society, Vols 1-8 2008:5266-9.

[11] Huang C, Shen C, Tang C, Chang S. A wearable yarn-based piezo-resistive sensor. Sensor Actuat A-Phys 2008;141:396-403.

[12] Morris D, Schazmann B, Wu Y, Coyle S, Brady S, Hayes J et al. Wearable sensors for monitoring sports performance and training. New York, USA: IEEE, 2008.

[13] Morris D, Schazmann B, Wu Y, Fay C, Beirne S, Slater C et al. Wearable technology for the real-time analysis of sweat during exercise. New York, USA: IEEE, 2008.

[14] Cochrane C, Koncar V, Lewandowski M, Dufour C. Design and development of a flexible strain sensor for textile structures based on a conductive polymer composite. Sensors 2007;7:473-92.

[15] Lorussi F, Scilingo E, Tesconi M, Tognetti A, De Rossi D. Wearable sensing garment for posture detection, rehabilitation and tele-medicine. Itab 2003: 4th International Ieee Embs Special Topic Conference on Information Technology Applications in Biomedicine, Conference Proceedings - New Solutions for New Challenges 2003:287-90.

[16] Jayaraman S, Kiekens P, Grancaric AM. Intelligent textiles for personal protection and safety. Amsterdam; Washington DC: IOS Press, 2006.

[17] Cheng J, Amft O, Lukowicz P. Active capacitive sensing: exploring a new wearable sensing modality for activity recognition. Pervasive Computing, Proceedings 2010;6030:319-36.

[18] Wijesiriwardana R, Mitcham K, Hurley W, Dias T. Capacitive fiber-meshed transducers for touch and proximity-sensing applications. IEEE Sens J 2005;5:989-94.

[19] Sergio M, Manaresi N, Nicolini M, Gennaretti D, Tartagni M, Guerrieri R. A textile-based capacitive pressure sensor. Sens Lett 2004;2:153-60.

[20] Baxter LK. Capacitive sensors : design and applications. New York: IEEE Press, 1997.

[21] Wijesiriwardana R. Inductive fiber-meshed strain and displacement transducers for respiratory measuring systems and motion capturing systems. IEEE Sens J 2006;6:571-9.

[22] Wijesiriwardana R, Dias T, Mukhopadhyay S. Resistive fibre-meshed transducers. Los Alamitos, CA, USA, IEEE Computer Soc, 2003.

[23] Edmison J, Jones M, Nakad Z, Martin T. Using piezoelectric materials for wearable electronic textiles. Los Alamitos, CA,USA: IEEE Computer Soc, 2002.

[24] Gautschi G. Piezoelectric sensorics: force, strain, pressure, acceleration and acoustic emission sensors, materials and amplifiers. Berlin; New York: Springer, 2002.

[25] Grillet A, Kinet D, Witt J, Schukar M, Krebber K, Pirotte F et al. Optical fiber sensors embedded into medical textiles for healthcare monitoring. IEEE Sens J 2008;8:1215-22.

[26] Rothmaier M, Luong MP, Clemens F. Textile pressure sensor made of flexible plastic optical fibers. Sensors 2008;8:4318-29.

[27] Dhawan A, Muth JF, Kekas DJ, Ghosh TK. Optical nano-textile sensors based on the incorporation of semiconducting and metallic nanoparticles into optical fibers. Smart Nanotextiles 2006;920:121-6.

[28] Dhawan A, Ghosh TK, Muth JF. Incorporating optical fiber sensors into fabrics. MRS Proceedings 2005:870.

[29] Pacelli M, Caldani L, Paradiso R. Textile piezoresistive sensors for biomechanical variables monitoring. New York, USA: IEEE, 2006.

[30] Bartalesi R, Lorussi F, Tesconi M, Tognetti A, Zupone G, De Rossi D. Wearable kinesthetic system for capturing and classifying upper limb gesture. Los Alamitos, CA, USA: IEEE Computer Soc, 2005.

[31] Lorussi F, Scilingo EP, Tesconi M, Tognetti A, De Rossi D. Strain sensing fabric for hand posture and gesture monitoring. IEEE T Inf Technol Biomed 2005;9:372-81.

[32] Paradiso R, Loriga G, Taccini N. A wearable health care system based on knitted integrated sensors. IEEE T Inf Technol Biomed 2005;9:337-44.

[33] Munro BJ, Campbell TE, Wallace GG, Steele JR. The intelligent knee sleeve: a wearable biofeedback device. Sens Actuator B-Chem 2008;131:541-7.

[34] Kincal D, Kumar A, Child AD, Reynolds JR. Conductivity switching in polypyrrole-coated textile fabrics as gas sensors. Synth Met 1998;92:53-6.

[35] Scilingo EP, Lorussi F, Mazzoldi A, De Rossi D. Strain-sensing fabrics for wearable kinaesthetic-like systems. IEEE Sens J 2003;3:460-7.

[36] Shu L, Hua T, Wang Y, Li Q, Feng DD, Tao X. In-shoe plantar pressure measurement and analysis system based on fabric pressure sensing array. IEEE T Inf Technol Biomed 2010;14:767-75.

[37] Dunne L, Brady S, Smyth B, Diamond D. Initial development and testing of a novel foam-based pressure sensor for wearable sensing. J Neuroeng Rehabil 2005;2:4.

[38] Tognetti A, Lorussi F, Bartalesi R, Quaglini S, Tesconi M, Zupone G et al. Wearable kinesthetic system for capturing and classifying upper limb gesture in post-stroke rehabilitation. J Neuroeng Rehabil 2005;2:8.

[39] Tesconi M, Tognetti A, Scilingo EP, Zupone G, Carbonaro N, De Rossi D et al. Wearable sensorized system for analyzing the lower limb movement during rowing activity. New York, USA: IEEE, 2007.

[40] Tesconi M, Scilingo EP, Barba P, De Rossi D. Wearable kinesthetic system for joint knee flexion- extension monitoring in gait analysis. New York, USA: IEEE, 2006.

[41] Gibbs P, Asada HH. Wearable conductive fiber sensors for multi-axis human joint angle measurements. J Neuroeng Rehabil 2005;2:7.

[42] Smith CS. Piezoresistance effect in germanium and silicon. Phys Rev 1954;94:42-9.

[43] Lu J, Lu M, Bermak A, Lee Y. Study of piezoresistance effect of carbon nanotube-PDMS composite materials for nanosensors. New York, USA: IEEE, 2007.

[44] Zhang XW, Pan Y, Zheng Q, Yi XS. Piezoresistance of conductor filled insulator composites. Polym Int 2001;50:229-36.

[45] Luheng W, Tianhuai D, Peng W. Influence of carbon black concentration on piezoresistivity for carbon-black-filled silicone rubber composite. Carbon 2009;47:3151-7.

[46] Flandin L, Chang A, Nazarenko S, Hiltner A, Baer E. Effect of strain on the properties of an ethylene-octene elastomer with conductive carbon fillers. J Appl Polym Sci 2000;76:894-905.

[47] Zheng Q, Zhou JF, Song YH. Time-dependent uniaxial piezoresistive behavior of high-density polyethylene/short carbon fiber conductive composites. J Mater Res 2004;19:2625-34.

[48] Huang JC, Wu CL. Processability, mechanical properties, and electrical conductivities of carbon black-filled ethylene-vinyl acetate copolymers. Adv Polym Technol 2000;19:132-9.

[49] Xue P, Tao XM, Tsang HY. In situ SEM studies on strain sensing mechanisms of PPy-coated electrically conducting fabrics. Appl Surf Sci 2007;253:3387-92.

[50] Brady S, Diamond D, Lau KT. Inherently conducting polymer modified polyurethane smart foam for pressure sensing. Sens Actuator A-Phys 2005;119:398-404.

[51] Li Y, Cheng XY, Leung MY, Tsang J, Tao XM, Yuen CWM. A flexible strain sensor from polypyrrole-coated fabrics. Synth Met 2005;155:89-94.

[52] Huang C, Tang C, Lee M, Chang S. Parametric design of yarn-based piezoresistive sensors for smart textiles. Sensor Actuat A-Phys 2008;148:10-5.

[53] Huang C, Tang C, Shen C. A wearable textile for monitoring respiration, using a yarn-based sensor. Los Alamitos, CA, USA: IEEE Computer Soc, 2006.

[54] Taccini N, Loriga G, Dittmar A, Paradiso R. Knitted bioclothes for health monitoring. Proceedings of the 26th Annual International Conference of the Ieee Engineering in Medicine and Biology Society, Vols 1-7 2004;26:2165-8.

[55] Allaoui A, Hoa SV, Pugh MD. The electronic transport properties and microstructure of carbon nanofiber/epoxy composites. Composites Sci Technol 2008;68:410-6.

[56] Ardanuy M, Rodríguez-Perez MA, Algaba I. Electrical conductivity and mechanical properties of vapor-grown carbon nanofibers/trifunctional epoxy composites prepared by direct mixing. Compos Part B-Eng 2011;42:675-81.

[57] Arlen MJ, Wang D, Jacobs JD, Justice R, Trionfi A, Hsu JWP et al. Thermal-electrical character of in situ synthesized polyimide-grafted carbon nanofiber composites. Macromolecules 2008;41:8053-62.

[58] Kirkpatrick S. Percolation and conduction. Rev Mod Phys 1973;45:574-88.

[59] Stauffer D. Introduction to percolation theory. London; Washington DC: Taylor & Francis, 1992.

[60] Psarras GC. Charge transport properties in carbon black/polymer composites. J Polym Sci Pol Phys 2007;45:2535-45.

[61] Vionnet-Menot S, Grimaldi C, Maeder T, Strassler S, Ryser P. Tunneling-percolation origin of nonuniversality: Theory and experiments. Phys Rev B 2005;71:064201.

[62] Xu J, Donohoe JP, Pittman CU. Preparation, electrical and mechanical properties of vapor grown carbon fiber (VGCF)/vinyl ester composites. Composites Part A 2004;35:693-701.

[63] Wypych G. Handbook of plasticizers. Toronto; New York: ChemTec Pub; William Andrew Pub, 2004.

[64] Marcilla A, Garcia S, Garcia-Quesada JC. Migrability of PVC plasticizers. Polym Test 2008;27:221-33.

[65] Messadi D, Taverdet JL, Vergnaud JM. Plasticizer migration from plasticized poly(vinyl chloride) into liquids. Effect of several parameters on the transfer. Ind Eng Chem Prod RD 1983;22:142-6.

[66] Ehrenstein GW. Polymeric materials: structure, properties, applications. Carl Hanser Verlag, Munich, 2001.

[67] Mamunya EP, Davidenko VV, Lebedev EV. Percolation conductivity of polymer composites filled with dispersed conductive filler. Polymer Composites 1995;16:319-24.

[68] Ruschau G, Yoshikawa S, Newnham R. Resistivities of conductive composites. J Appl Phys 1992;72:953.

[69] Sun Y. Strain effect in semiconductors: theory and device applications. New York: Springer, 2009.

[70] Sun J, Gerberich WW, Francis LF. Electrical and optical properties of ceramic/polymer nanocomposite coatings. J Polym Sci Pol Phys 2003;41:1744-61.

[71] Yu J, Zhang LQ, Rogunova M, Summers J, Hiltner A, Baer E. Conductivity of polyolefins filled with high-structure carbon black. J Appl Polym Sci 2005;98:1799-805.

[72] Balberg I. A comprehensive picture of the electrical phenomena in carbon black–polymer composites. Carbon 2002;40:139-43.

[73] Hauptman N, Žveglič M, Maček M, Klanjšek Gunde M. Carbon based conductive photoresist. J Mater Sci 2009;44:4625-32.

[74] Flandin L, Chang A, Nazarenko S, Hiltner A, Baer E. Effect of strain on the properties of an ethylene-octene elastomer with conductive carbon fillers. J Appl Polym Sci 2000;76:894-905.

[75] Kujawski M, Pearse JD, Smela E. Elastomers filled with exfoliated graphite as compliant electrodes. Carbon 2010;48:2409-17.

[76] Blighe F, Hernandez Y, Blau W, Coleman J. Observation of percolation-like scaling far from the percolation threshold in high volume fraction, high conductivity polymer-nanotube composite films. Adv Mater 2007;19:4443-7.

[77] Grimaldi C, Balberg I. Tunneling and nonuniversality in continuum percolation systems. Phys Rev Lett 2006;96:066602.

[78] Balberg I. Tunneling and nonuniversal conductivity in composite materials. Phys Rev Lett 1987;59:1305-8.

[79] Chen G, Weng W, Wu D, Wu C. PMMA/graphite nanosheets composite and its conducting properties. Eur Polym J 2003;39:2329-35.

[80] Kilbride BE, Coleman JN, Fraysse J, Fournet P, Cadek M, Drury A et al. Experimental observation of scaling laws for alternating current and direct current conductivity in polymer-carbon nanotube composite thin films. J Appl Phys 2002;92:4024-30.

[81] Flandin L, Hiltner A, Baer E. Interrelationships between electrical and mechanical properties of a carbon black-filled ethylene-octene elastomer. Polymer 2001;42:827-38.

[82] Yamaguchi K, Busfield JJC, Thomas AG. Electrical and mechanical behavior of filled elastomers. I. The effect of strain. J Polym Sci Pol Phys 2003;41:2079-89.

[83] Kang TJ, Choi A, Kim D, Jin K, Seo DK, Jeong DH et al. Electromechanical properties of CNT-coated cotton yarn for electronic textile applications. Smart Mater Struct 2011;20:015004.

CHAPTER 7. CONCLUSIONS & FUTURE SUGGESTIONS

Carbon nanofiber (CNF) filled plastisol (plasticized polyvinyl chloride) composites were developed by incorporation of different levels of filler for three different molecular weights of PVC to be used as a printing media for textile based sensors. Morphological, mechanical and electrical properties of composites were investigated. Good filler/polymer interphase was observed without any dominant filler orientation regardless of the CNF concentration throughout the composites even at high filler concentrations. Mechanical properties such as tensile strength and elastic modulus were found to be affected by filler, plasticizer content and matrix molecular weight. While, increase in filler ratio and molecular weight of polymer matrix lead to enhance in mechanical properties; increase in plasticizer ratio was found to negatively affect the mechanical properties. Same variables were also found to affect the electrical and piezoresistive response of the composites. While increased plasticizer content was found to increase the resistivity, higher molecular weight resulted in lower resistivity. Although all conductive plastisols were found to show negative piezoresistance at different levels of strain from 2 to 16%, samples with lower CNF content and higher DOS content lead to higher piezoresistive sensitivity with the gauges factors around -42to -44. In addition to characterization of composites, conductive plastisol was used as printing media for textiles to be used as piezoresistive strain sensors. Printed fabrics showed relatively lower percolation threshold compared with composite films. This difference was showed to be caused by plasticizer migration from plastisol to fabric during printing and curing. Similar with plastisol composites, printed fabrics showed negative piezoresistance under different levels of strain

changing from 2-16% and lower filler concentration showed higher gauge factor compared with higher filler concentrations. 5, 6 and 7% CNF containing printed samples showed gauge factors of -31.51, -11.18 and -8.3 respectively. However printed fabrics resulted in higher cyclic stability compared with composites. The difference is most likely caused by the structural characteristics of the highly elastic knitted fabric and the flexible printed layer. Printed fabrics can be considered as laminates with three components namely, the printed layer (plastisol composite), the fabric, and may be more importantly the interphase. The properties of each of these directly affect electrical, mechanical, morphological properties of the system. The interphase is formed by the penetration of plastisol composite into the fabric structure and functions to bind the yarns in the fabric and restricts their mobility. Particularly, in case of relatively more deformable knit fabrics the formation of this interphase enhances the mechanical properties and recoverability of the fabric significantly.

The key material parameters that determine performance of conductive piezoresistive composites are their filler, plastisol and matrix composition. Different sensor materials with different sensing limits can be obtained by tuning the plastisol composition. In addition to strain sensors, these materials are promising materials for pressure, temperature and gas sensors. Research in that area might be useful for development of multifunctional textile sensors.